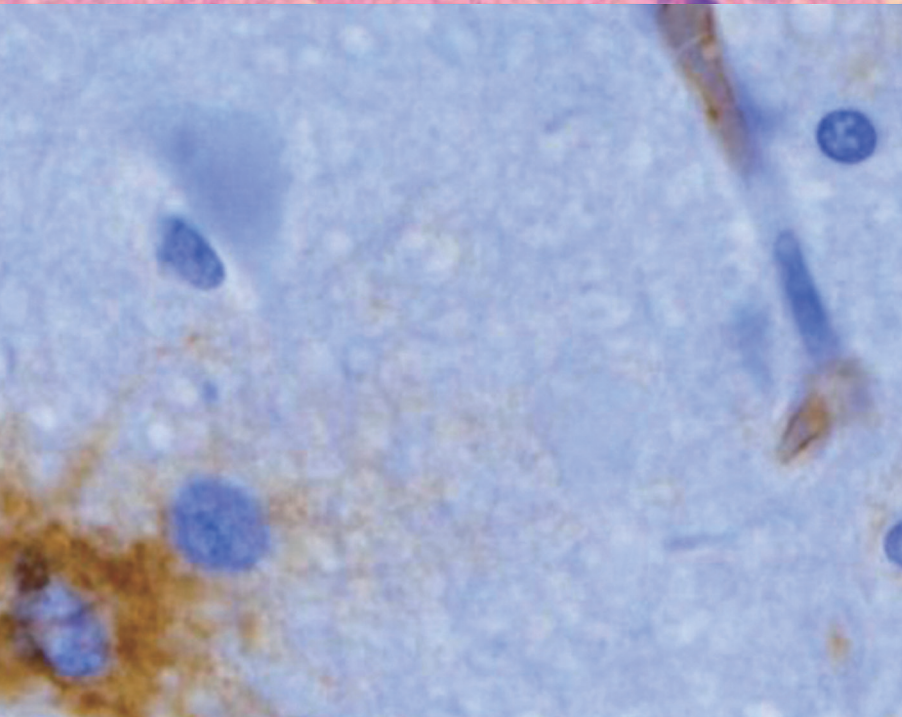


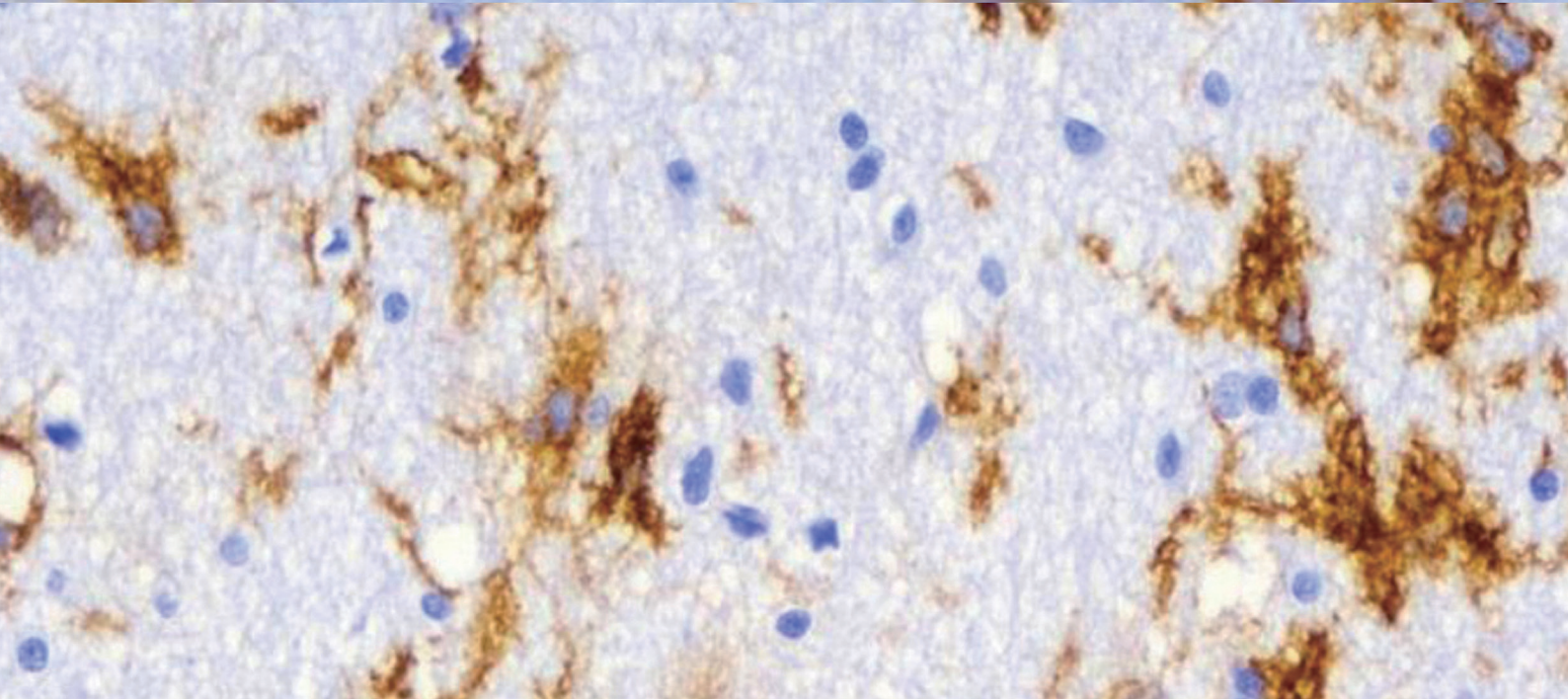
JPTM

Journal of Pathology
and Translational Medicine

November 2015
Vol. 49 / No. 6
jpatholm.org
pISSN: 2383-7837
eISSN: 2383-7845



*In Memory of Professor
Je Geun Chi, a Great Mentor
and Pathologist*



Aims & Scope

The *Journal of Pathology and Translational Medicine* is an open venue for the rapid publication of major achievements in various fields of pathology, cytopathology, and biomedical and translational research. The Journal aims to share new insights into the molecular and cellular mechanisms of human diseases and to report major advances in both experimental and clinical medicine, with a particular emphasis on translational research. The investigations of human cells and tissues using high-dimensional biology techniques such as genomics and proteomics will be given a high priority. Articles on stem cell biology are also welcome. The categories of manuscript include original articles, review and perspective articles, case studies, brief case reports, and letters to the editor.

Subscription Information

To subscribe to this journal, please contact the Korean Society of Pathologists/the Korean Society for Cytopathology. Full text PDF files are also available at the official website (<http://jpatholm.org>). *Journal of Pathology and Translational Medicine* is indexed by PubMed, PubMed Central, Scopus, KoreaMed, KoMCI, WRPIM and CrossRef. Circulation number per issue is 700.

Editors-in-Chief

Hong, Soon Won, M.D. (*Yonsei University, Korea*)

Kim, Chong Jai, M.D. (*University of Ulsan, Korea*)

Associate Editors

Choi, Yoon Jung, M.D. (*National Health Insurance Service, Ilsan Hospital, Korea*)

Han, Jee Young, M.D. (*Inha University, Korea*)

Editorial Board

Ali, Syed Z. (*Johns Hopkins Hospital, U.S.A.*)

Avila-Casado, Maria del Carmen (*University of Toronto, Toronto General Hospital UHN, Canada*)

Cho, Kyung-Ja (*University of Ulsan, Korea*)

Choi, Yeong-Jin (*Catholic University, Korea*)

Chung, Jin-Haeng (*Seoul National University, Korea*)

Gong, Gyung Yub (*University of Ulsan, Korea*)

Grignon, David J. (*Indiana University, U.S.A.*)

Ha, Seung Yeon (*Gachon University, Korea*)

Jang, Se Jin (*University of Ulsan, Korea*)

Jeong, Jin Sook (*Dong-A University, Korea*)

Kang, Gyeong Hoon (*Seoul National University, Korea*)

Katoh, Ryohei (*University of Yamaguchi, Japan*)

Kerr, Keith M. (*Aberdeen University Medical School, U.K.*)

Kim, Aeree (*Korea University, Korea*)

Kim, Kyoung Mee (*Sungkyunkwan University, Korea*)

Kim, Kyu Rae (*University of Ulsan, Korea*)

Kim, Se Hoon (*Yonsei University, Korea*)

Kim, Seok-Hyung (*Sungkyunkwan University, Korea*)

Kim, Woo Ho (*Seoul National University, Korea*)

Kim, Youn Wha (*Kyung Hee University, Korea*)

Ko, Young Hyeoh (*Sungkyunkwan University, Korea*)

Koo, Ja Seung (*Yonsei University, Korea*)

Lee, C. Soon (*University of Western Sydney, Australia*)

Lee, Hye Seung (*Seoul National University, Korea*)

Lee, Kyung Han (*Sungkyunkwan University, Korea*)

Lee, Sug Hyung (*Catholic University, Korea*)

Lim, Beom Jin (*Yonsei University, Korea*)

Moon, Woo Sung (*Chonbuk University, Korea*)

Park, Chan-Sik (*University of Ulsan, Korea*)

Park, Sanghui (*Ewha Womans University, Korea*)

Park, So Yeon (*Seoul National University, Korea*)

Park, Young Nyun (*Yonsei University, Korea*)

Ro, Jae Y. (*Cornell University, The Methodist Hospital, U.S.A.*)

Romero, Roberto (*National Institute of Child Health and Human Development, U.S.A.*)

Schmitt, Fernando (*IPATIMUP [Institute of Molecular Pathology and Immunology of the University of Porto], Portugal*)

Shin, Eunah (*Cha University, Korea*)

Sung, Chang Ohk (*University of Ulsan, Korea*)

Tan, Puay Hoon (*National University of Singapore, Singapore*)

Than, Nandor Gabor (*Semmelweis University, Hungary*)

Tse, Gary M. (*Prince of Wales Hospital, Hongkong*)

Vielh, Philippe (*International Academy of Cytology Gustave Roussy Cancer Campus Grand Paris, France*)

Wildman, Derek (*University of Illinois, U.S.A.*)

Yatabe, Yasushi (*Aichi Cancer Center, Japan*)

Yoon, Bo Hyun (*Seoul National University, Korea*)

Yoon, Sun Och (*Yonsei University, Korea*)

Statistics Editors

Kim, Dong Wook (*National Health Insurance Service Ilsan Hospital, Korea*)

Yoo, Hanna (*Yonsei University, Korea*)

Manuscript Editor

Chang, Soo-Hee (*InfoLumi Co., Korea*)

Contact the Korean Society of Pathologists/the Korean Society for Cytopathology

Publishers: Changsuk Kang, MD, So Young Jin, MD

Editors-in-Chief: Soon Won Hong, MD, Chong Jai Kim, MD

Published by the Korean Society of Pathologists/the Korean Society for Cytopathology

Editorial Office

Room 1209 Gwanghwamun Officia, 92 Saemunan-ro, Jongno-gu,

Seoul 110-999, Korea/#406 Lilla Swami Bldg, 68 Dongsan-ro,

Seocho-gu, Seoul 03186, Korea

Tel: +82-2-795-3094/+82-2-593-6943

Fax: +82-2-790-6635/+82-2-593-6944

E-mail: office@jpatholm.org

Printed by ML communications Co., Ltd.

Jungang Bldg. 18-8 Wonhyo-ro 89-gil, Yongsan-gu, Seoul 04314, Korea

Tel: +82-2-717-5511 Fax: +82-2-717-5515 E-mail: ml@smileml.com

Manuscript Editing by InfoLumi Co.

210-202, 421 Pangyo-ro, Bundang-gu, Seongnam 13522, Korea

Tel: +82-70-8839-8800 E-mail: infolumi.chang@gmail.com

Front cover image: The histology and CD34 immunoreactivity of focal cortical dysplasia (FCD) in the peritumoral cortex. p445.

© Copyright 2015 by the Korean Society of Pathologists/the Korean Society for Cytopathology

© Journal of Pathology and Translational Medicine is an Open Access journal under the terms of the Creative Commons Attribution Non-Commercial License (<http://creativecommons.org/licenses/by-nc/3.0>).

© This paper meets the requirements of KS X ISO 9706, ISO 9706-1994 and ANSI/NISO Z.39.48-1992 (Permanence of Paper).

This journal was supported by the Korean Federation of Science and Technology Societies Grant funded by the Korean Government.

CONTENTS

EDITORIAL

- 425 In Memory of Professor Je Geun Chi, a Great Mentor and Pathologist
Chong Jai Kim

REVIEWS

- 427 The Continuing Value of Ultrastructural Observation in Central Nervous System Neoplasms in Children
Na Rae Kim, Sung-Hye Park
- 438 Dysembryoplastic Neuroepithelial Tumors
Yeon-Lim Suh
- 450 Neuroendocrine Tumors of the Female Reproductive Tract: A Literature Review
Yi Kyeong Chun
- 462 Acute Atherosclerosis of the Uterine Spiral Arteries: Clinicopathologic Implications
Joo-Yeon Kim, Yeon Mee Kim

ORIGINAL ARTICLES

- 472 Therapeutic Effects of Umbilical Cord Blood Derived Mesenchymal Stem Cell-Conditioned Medium on Pulmonary Arterial Hypertension in Rats
Jae Chul Lee, Choong Ik Cha, Dong-Sik Kim, Soo Young Choe
- 481 Analysis of Mutations in Epidermal Growth Factor Receptor Gene in Korean Patients with Non-small Cell Lung Cancer: Summary of a Nationwide Survey
Sang Hwa Lee, Wan Seop Kim, Yoo Duk Choi, Jeong Wook Seo, Joung Ho Han, Mi Jin Kim, Lucia Kim, Geon Kook Lee, Chang Hun Lee, Mee Hye Oh, Gou Young Kim, Sun Hee Sung, Kyo Young Lee, Sun Hee Chang, Mee Sook Rho, Han Kyeom Kim, Soon Hee Jung, Se Jin Jang, The Cardiopulmonary Pathology Study Group of Korean Society of Pathologists
- 489 Chronic Placental Inflammation in Twin Pregnancies
Heejin Bang, Go Eun Bae, Ha Young Park, Yeon Mee Kim, Suk-Joo Choi, Soo-young Oh, Cheong-Rae Roh, Jung-Sun Kim
- 497 Tongue Growth during Prenatal Development in Korean Fetuses and Embryos
Soo Jeong Hong, Bong Geun Cha, Yeon Sook Kim, Suk Keun Lee, Je Geun Chi

-
- 511 **Comprehensive Cytomorphologic Analysis of Pulmonary Adenoid Cystic Carcinoma: Comparison to Small Cell Carcinoma and Non-pulmonary Adenoid Cystic Carcinoma**
Seokhwi Kim, Jinah Chu, Hojoong Kim, Jounggho Han

CASE REPORTS

- 520 **Mediastinal Glomus Tumor: A Case Report and Literature Review**
Si-Hyong Jang, Hyun Deuk Cho, Ji-Hye Lee, Hyun Ju Lee, Hae Yoen Jung, Kyung-Ju Kim, Sung Sik Cho, Mee-Hye Oh
- 525 **CD30-Positive T-Cell Lymphoproliferative Disease of the Oral Mucosa in Children: A Manifestation of Epstein-Barr Virus-Associated T-Lymphoproliferative Disorder**
Mineui Hong, Young Hyeoh Ko
- 531 **Intrahepatic Cholangiocarcinoma with Ductal Plate Malformation-like Feature Associated with Bile Duct Adenoma**
Ah-Young Kwon, Hye Jin Lee, Hee Jung An, Haeyoun Kang, Jin-Hyung Heo, Gwangil Kim
- 535 **Apocrine Carcinoma of the Axilla Associated with Extramammary Paget's Disease: A Case Report and Review of the Literature**
Hye Ra Jung, Sun Young Kwon, Daegu Son

CORRESPONDENCE

- 538 **Erratum: WHO Grade IV Gliofibroma: A Grading Label Denoting Malignancy for an Otherwise Commonly Misinterpreted Neoplasm**

Instructions for Authors for *Journal of Pathology and Translational Medicine* are available at <http://jpatholm.org/authors/authors.php>

In Memory of Professor Je Geun Chi, a Great Mentor and Pathologist

Chong Jai Kim

Editor-in-Chief
Journal of Pathology and Translational Medicine

The introduction of modern medicine in Korea goes hand in hand with the establishment of medical schools during the Japanese colonial period. Since then, medicine in the Republic of Korea has been greatly improved by the introduction of medical systems of the United States. Accordingly, pathology in Korea began as a basic academic discipline, but made a major shift to hospital-based surgical pathology after the Korean War. Most Korean institutions continue to practice joint operations between clinical service and experimental research. In this context, the quality of medical faculty and training has been and will continue to be a key to ensuring the quality and global competitiveness of Korean pathologists. A unique combination of residency training and graduate school education in Korea inevitably led to a stronger mentoring system compared to that in other countries. The outstanding achievements and performances of Korean scholars in surgical and experimental pathology would not have been possible without the contribution and support of great mentors.

Professor Je Geun Chi was the founder of neuropathology and pediatric pathology, and he was an enormous contributor to the development of modern pathology in Korea. He received his medical degree from Seoul National University College of Medicine in 1962. He then went on to pathology residency and subsequent neuropathology fellowship training at the Boston Children's Hospital, Beth Israel Hospital, and Harvard Medical School. He joined the Harvard faculty in 1975. He then came back to Korea in 1976 and became a faculty member at Seoul National University. He published more than 800 articles in

international journals. He served as the president of the Korean Society of Pathologists in 1996, the Korean Academy of Medical Science in 1999, and the National Academy of Medicine of Korea in 2004. After retirement, he expanded his work on magnetic resonance imaging neuroanatomy at Neuroscience Research Institute of Gachon University, and he published 7.0 Tesla MRI Brain Atlas with Professor Zang-Hee Cho.

Professor Chi was a great mentor to many of the leading pathologists in Korea today. His unique strength as a pathologist was in human embryogenesis and fetal development. The depth of his understanding of human development clearly distinguished him from other pathologists. Neurogenesis is one of the most dynamic and fascinating parts of human development, and this would partly explain Professor Chi's enthusiasm for neuropathology and pediatric pathology. Unfortunately, he passed away on November 26, 2014. In memory of him, the November issue of the *Journal of Pathology and Translational Medicine*, formerly the *Korean Journal of Pathology* published since 1967, includes reviews and original articles written by several of his mentees, who are now leaders and great mentors in their respective fields. Their articles will provide the readers with topical and important information in the fields of neuropathology and pediatric pathology.

Dr. Yeon-Lim Suh wrote a review article on dysembryoplastic neuroepithelial tumor (DNT). The article is a great summary of the characteristics of three forms of DNT. Dr. Suk Keun Lee wrote an article on prenatal tongue development. The article is meaningful in that it is based on the collection of Professor Chi, on which Dr. Lee had been working closely with Professor Chi for decades. Drs. Sung-Hye Park and Na Rae Kim contributed an article describing the importance of ultrastructural examination in the evaluation of childhood brain tumors. Professor Chi advocated the importance of ultrastructural examination in pa-

Corresponding Author

Chong Jai Kim, MD, PhD
Department of Pathology, Asan Medical Center, University of Ulsan College of Medicine, 88 Olympic-ro 43-gil, Songpa-gu, Seoul 05505, Korea
Tel: +82-2-3010-4516, Fax: +82-2-472-7898, E-mail: ckim@amc.seoul.kr



Fig. 1. Professor Chi (on the left) celebrates his 77th birthday with his mentees.

thology practice and research. Dr. Yi Kyeong Chun wrote a review article on neuroendocrine tumors of the female reproductive tract. The article is a comprehensive summary of neuroendocrine tumor pathology in the female reproductive tract. Dr. Yeon Mee Kim described the pathological features of acute atherosclerosis in spiral arteries, introducing its clinical significance and relationship with poor placentation in human pregnancy. Dr. Jung-

Sun Kim described the incidence and significance of chronic chorioamnionitis (maternal anti-fetal cellular rejection) in twin gestations. The clinical significance of chronic chorioamnionitis is becoming more appreciated in maternal and fetal medicine.

The term 'mentor' originates from the Greek mythology the *Odyssey*. Mentor was a great, trusted counselor of Odysseus' son Telemachus. Professor Chi was a great teacher, friend, counselor, and writer. He left his beloved family, friends, and mentees behind (Fig. 1). He was a dedicated pathologist who left behind a tremendous legacy in the field. His views on pathology are available online (http://navercast.naver.com/contents.nhn?rid=83&contents_id=41771).

The editors of the *Journal of Pathology and Translational Medicine* deeply miss the great mentorship of Professor Chi and would like to express special thanks to the mentees of Professor Chi for their special contributions to the November issue.

Conflicts of Interest

No potential conflict of interest relevant to this article was reported.

The Continuing Value of Ultrastructural Observation in Central Nervous System Neoplasms in Children

Na Rae Kim · Sung-Hye Park¹

Department of Pathology, Gachon University Gil Medical Center, Incheon; ¹Department of Pathology, Seoul National University College of Medicine, Seoul, Korea

Received: September 15, 2015

Accepted: September 19, 2015

Corresponding Author

Na Rae Kim, MD
Department of Pathology, Gachon University Gil Medical Center, 21 Namdong-daero 774 beon-gil, Namdong-gu, Incheon 21565, Korea
Tel: +82-32-460-3847
Fax: +82-32-460-2394
E-mail: clara_nrk@gilhospital.com

Central nervous system (CNS) neoplasms are the second most common childhood malignancy after leukemia and the most common solid organ neoplasm in children. Diagnostic dilemmas with small specimens from CNS neoplasms are often the result of multifactorial etiologies such as frozen or fixation artifact, biopsy size, or lack of knowledge about rare or unfamiliar entities. Since the late 1950s, ultrastructural examination has been used in the diagnosis of CNS neoplasms, though it has largely been replaced by immunohistochemical and molecular cytogenetic studies. Nowadays, pathologic diagnosis of CNS neoplasms is achieved through intraoperative cytology, light microscopy, immunohistochemistry, and molecular cytogenetic results. However, the utility of electron microscopy (EM) in the final diagnosis of CNS neoplasms and investigation of its pathogenetic origin remains critical. Here, we reviewed the distinguishing ultrastructural features of pediatric CNS neoplasms and emphasize the continuing value of EM in the diagnosis of CNS neoplasms.

Key Words: Microscopy, electron; Central nervous system; Neoplasms; Childhood

The general incidence of pediatric central nervous system (CNS) neoplasms is as follows: the most common type is astrocytomas including pilocytic astrocytomas, fibrillary astrocytomas, or brain stem gliomas (46%–48%); followed by medulloblastomas (40%–45%); ependymomas (8%–10%); and others, including germ cell tumors, gangliogliomas, sellar craniopharyngiomas, etc. (2%–5%).^{1,2} Commonly encountered CNS neoplasms in adults, such as oligodendrogliomas, high-grade astrocytic tumors, or meningiomas, are relatively uncommon in children, except for meningiomas with or without neurofibromatosis syndrome or meningioangiomas or CNS lymphomas in immunocompromised children with acquired immunodeficiency syndrome or Wiskott-Aldrich syndrome.³⁻⁵ Treatments for adults differ from those for children due to the unpredictable clinical course and a the greater hazardous effect of aggressive treatments such as radiation on the developing brain. Similar to differences in primary CNS neoplasms between children and adults, metastatic CNS neoplasms in children commonly originate from neuroblastoma, embryonal rhabdomyosarcoma, Wilms tumor, or malignant melanoma arising from neurocutaneous melanosis, whereas cerebral metastatic tumors in adults typically originate from lung, breast, or colon cancers, renal cell carcinoma, or malignant melanomas.^{6,7}

Regarding incidence, the spectrum of pediatric CNS neoplasms varies, from primitive embryonal tumors to highly differentiated tumors such as meningioma, schwannoma, or glioblastoma.⁸ The former group is represented by small round cell tumors, i.e., undifferentiated or poorly differentiated tumors. The 2007 World Health Organization (WHO) classification of CNS neoplasms included angiocentric glioma, papillary glioneuronal tumor (PGNT), rosette-forming glioneuronal tumor of the fourth ventricle, papillary tumor of the pineal region (PTPR), pituicytoma, and spindle cell oncocytoma of the adenohypophysis, which are rarely encountered in either children or adults.⁹

The role of electron microscopy (EM) in diagnostic pathology has declined over recent decades due to major advancements in immunohistochemistry, flow cytometry, and molecular cytogenetic analysis, thereby eliminating the need for EM. However, its role in the neuropathology field includes identification of etiologic agents or cellular stored materials or for use as an ancillary method for CNS neoplasms for which light microscopy or immunohistochemistry are inconclusive and ambiguous.^{10,11} Although benignity and malignancy cannot be distinguished by EM, pediatric CNS neoplasms require the integration of comprehensive data from light microscopic examination with immunohistochemical, EM, and molecular cytogenetic studies.

Actually, starting with the 2000 WHO classification of CNS neoplasms, genetic profiles have been incorporated as an additional tool used in the definition of brain tumors because molecular cytogenetic evaluation has both diagnostic and predictive utility.¹² For example, emerging data from cytogenetic and molecular genetic analyses suggest that some molecular cytogenetic alterations such as isocitrate dehydrogenase-1 (IDH-1) or 1p19q loss of heterozygosity (LOH) provide both diagnostic and prognostic data on CNS neoplasms though IDH-1 mutation or 1p19q LOH are rarely found in pediatric oligodendrogliomas, compared to 40%–80% of adult cases.^{4,13,14} IDH-1 mutation-specific immunohistochemistry is diagnostically helpful in recognizing diffuse tumor infiltration of astrocytoma or oligodendroglioma and to distinguishing WHO grade I pilocytic astrocytomas from diffuse astrocytomas as well as astrocytic and oligodendroglial tumors from ependymomas or oligodendrogliomas from other glioneuronal tumors with clear-cell morphology.¹⁴ However, it has diagnostic limitations in terms of specificity or sensitivity, and further evaluation of other diagnostic tools might be needed.

Here, we review the ultrastructural findings and categorize the EM findings of pediatric CNS neoplasms based on light microscopic morphology as follows: spindle cell tumors, round cell tumors including oligodendroglioma and oligodendroglioma-like tumors, papillary tumors, rhabdoid cell tumors, and pleomorphic cell tumors. Although not uncommonly encountered in pediatric CNS neoplasms, germ cell neoplasms showing characteristic light microscopic findings such as germinoma, teratoma, choriocarcinoma, embryonal carcinoma, or endodermal sinus tumor will not be described in this review.

SPINDLE CELL TUMORS OF THE CENTRAL NERVOUS SYSTEM

First, the spindle cell category includes the following entities: meningioma, schwannoma, ependymoma, and astrocytoma including pilocytic astrocytoma, and pilomyxoid astrocytoma. Among these, ependymoma and pilocytic astrocytoma are common in children, while meningioma or schwannoma are not common. Rather, meningioma associated with meningioangiomas has been reported mainly in childhood.⁵ Previous reports on meningioma arising in meningioangiomas describe entrapped neurons in the infiltrating meningioma.¹⁵ Ultrastructural findings of meningioma show its meningotheial arachnoidal cell nature, i.e., epithelial and mesenchymal nature; connective tissue fibers and basal lamina are not usually seen among

tumor cells within the syncytium (Fig. 1A). Elongated interdigitating cell processes filled with copious amounts of intracytoplasmic intermediate filaments show an interdigitating and jigsaw pattern, corresponding to the whorls of enwrapping meningioma tumor cells under light microscopy. The epithelial nature, such as well-formed desmosomes, is a characteristic ultrastructural feature. The extracellular space of meningioma sometimes contains fine granular materials, mimicking basal lamina. Meningiomas also show basement membrane separating the syncytium from the fibrous septum or the perivascular connective tissue.¹⁶ Rhabdoid or chordoid meningioma can have a thick continuous basal lamina.¹⁷⁻¹⁹ Schwannoma, also called neurilemmoma, neuroma, or neurinoma, is relatively rare in the brain with or without cranial nerve-relation. Intracerebral schwannomas not related to cranial nerves are rare, and most cases occur in the first two decades of life.²⁰ Schwannoma can be diagnosed in children who might be associated with neurofibromatosis type 2, while intracerebral schwannomas have a weak relationship with neurofibromatosis type 2. The ultrastructure of schwannoma is almost exclusively cells with characteristics of differentiated Schwann cells of a neuroectodermal origin. Numerous finger-like cytoplasmic processes are lined by continuous basal lamina with occasional duplication (Fig. 1B). Closely apposed stacks of plasma membrane, i.e., reminiscent of myelin lamellae, are characteristic of schwannoma. Compared to normal collagen fibers of 64-nm periodicity, so-called Luse bodies show more widely spaced collagen fibers with up to 150-nm periodicity and are frequently found in schwannoma. The tumor cells themselves are composed of cigar-shaped or elliptical nuclei containing one or two small nucleoli and rare nuclear bodies. The cytoplasm contains well-developed Golgi complexes, scattered mitochondria, short segments of rough endoplasmic reticulum (RERs), small numbers of ribosomes, and scattered polysomes. Absence of pinocytotic vesicles always happens in schwannoma. Microfilaments, microtubules, and small vesicles are often found, but few mitochondria and ribosomes are found. These ultrastructural characteristics of schwannoma provide diagnostic clues, particularly regarding small cell changes in schwannoma or small cell malignant peripheral nerve sheath tumors.^{21,22} Ependymoma occurs mainly in the ventricular system, and infratentorial ependymomas occur predominantly in children, although development of ependymomas can occur at any age.²³⁻²⁵ Ultrastructural findings of a well-developed ependymal tumor, which is likely derived from ependymal cells lining the CNS ventricular system, show both epithelial and astrocytic features, and the tumor cells of grade I and II ependymal tumors resemble typi-

cal ependymocytes, while anaplastic ependymomas are poorly differentiated with minimal evidence of such ependymal differentiation. Ependymal differentiation includes well-developed junctions, such as zonula adherens or occludens, villous projections, and cilia in a 9+2 arrangement of microtubules (Fig. 1C). The centriole or blepharoplast is located in the basis of the cilia; in the cytoplasm, microtubules or glial filaments are present in the perikaryal area or cytoplasmic processes. Basal lamina is observed in the ependymoma and around blood vessels but not around tumor cells.²⁶ However, all of the above-mentioned findings are not specific for ependymomas; these ultrastructural

findings are shared by angiocentric glioma, i.e., monomorphous angiocentric neuroepithelial tumor, composed of bipolar spindle cells and epithelioid round cells although the occurrence of angiocentric glioma has not yet been reported in children.⁹ Angiocentric glioma is composed of infiltrating round, monopolar epithelioid cells arranged in a perivascular arrangement and bipolar spindle-shaped glial cells. Epithelioid monopolar cells showing microlumina filled with numerous microvilli and some cilia with a 9+2 or abnormal 10+2 configuration. Intermediate junctions of complex interdigitating membranes and basal lamina have also been observed.²⁷ Ependymomas and angiocen-

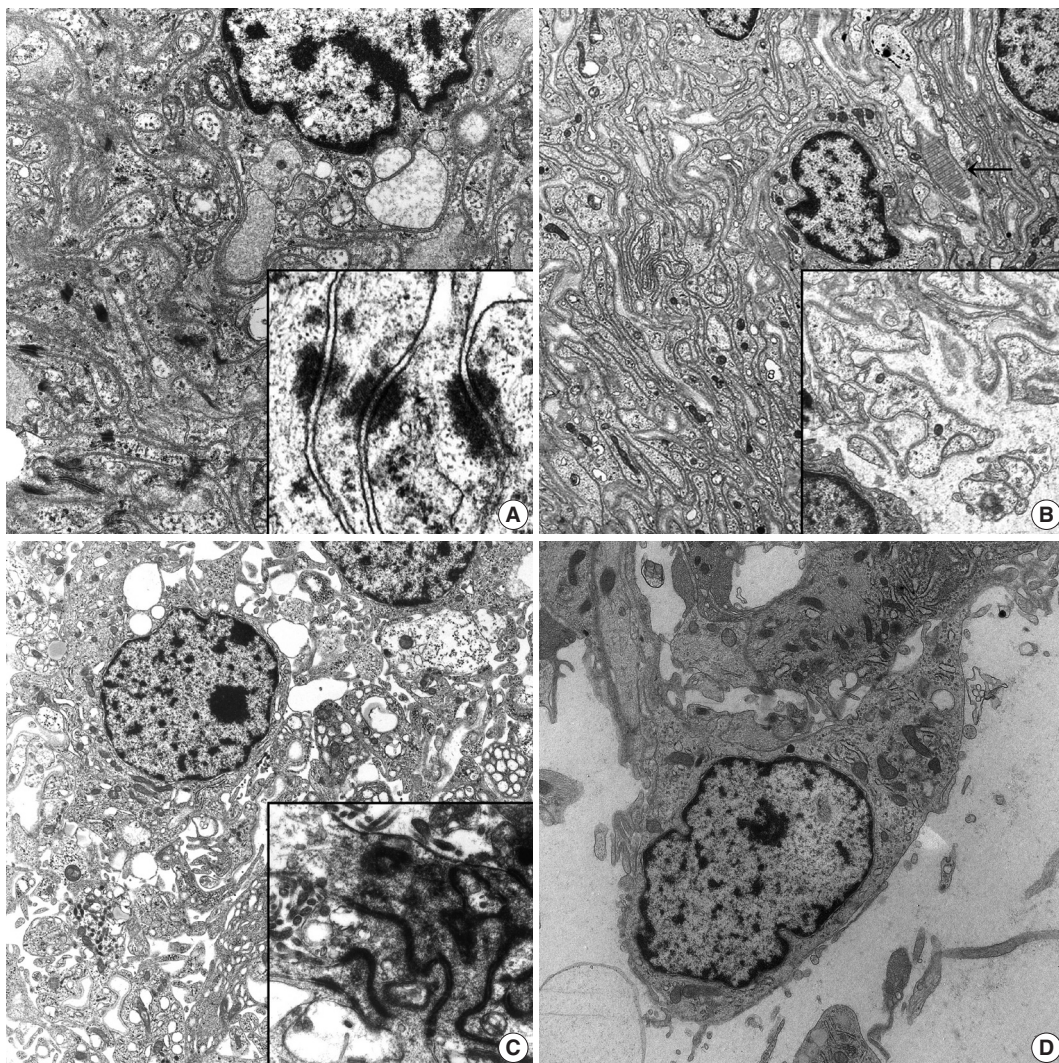


Fig. 1. (A) Meningioma shows closely apposed oval- to spindle-shaped tumor cells having interdigitating cell processes lined by well-formed desmosomes ($\times 8,000$). Inset indicates tonofibrils attached to the desmosomal plaques ($\times 30,000$). (B) Schwannoma shows abundant reduplicated continuous basal lamina surrounding the interdigitating cell processes ($\times 3,500$). Note the extracellular long-spacing collagen (arrow) and high power view of reduplicated basal lamina (inset, $\times 6,500$). (C) Ependymoma reveals spindle cells with numerous cytoplasmic processes filled with bundles of intermediate filaments ($\times 4,000$). Inset shows well-formed zonula occludens with surface microvilli ($\times 15,000$). (D) Pilomyxoid astrocytoma shows bipolar cells with surface microvilli and cilia in the electron-lucent extracellular space ($\times 9,000$). Note some intracellular microlumen.
(Continued to the next page)

tric glioma share molecular cytogenetic alterations, as indicated by shared ultrastructural features.²⁸ These findings suggest that angiocentric glioma belongs to a lineage of ependymal tumors.

Pilocytic astrocytoma is a commonly encountered CNS tumor in children, and the most common site of occurrence is the sellar region. In contrast, pituitary adenoma, meningioma, and metastatic carcinoma are common tumors in adults but are rarely encountered in children.¹ Pilocytic astrocytoma and pilomyxoid astrocytoma share pathogenetic and clinicopathologic features; *BRAF* oncogene activation through *KIAA1549-BRAF* fusion most commonly found in pilocytic astrocytoma has also

been described in pilomyxoid astrocytoma.^{29,30} As with light microscopy, irregularly shaped, amorphous, granular electron-dense Rosenthal fibers are commonly found in pilocytic astrocytoma under EM.³¹ These Rosenthal fibers are closely located in the glial intermediate filaments.³² Pilomyxoid astrocytoma showing a monomorphic histologic appearance more commonly occurs in infants and young children compared with pilocytic astrocytoma.³³ Ultrastructurally, pilomyxoid astrocytomas have two morphologically distinct cell types;³⁴ one is spindle cells showing neurite-like features, and the other is spindle cells showing overt astrocytic morphology (Fig. 1D). Despite shared

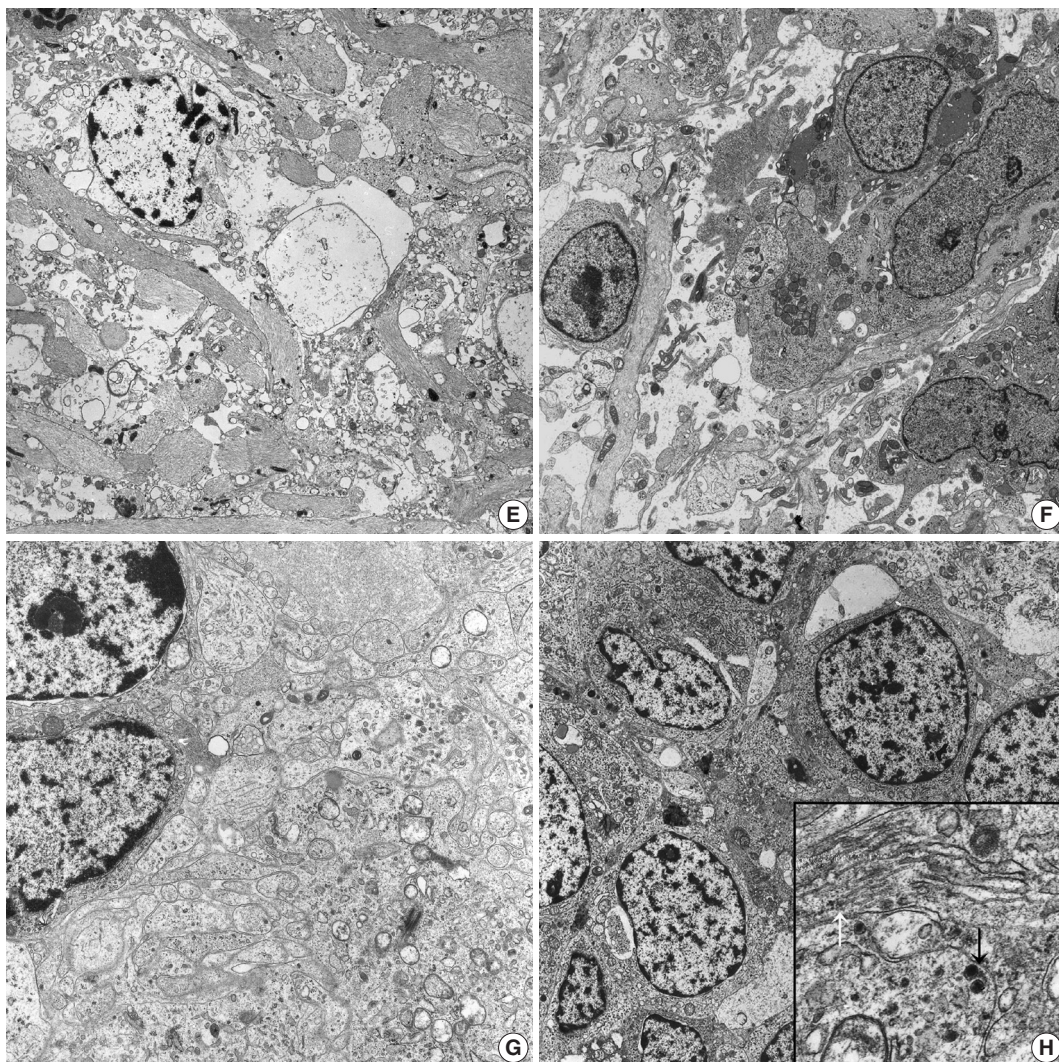


Fig. 1. (Continued from the previous page) (E) Astrocytoma shows loosely scattered round to oval cells having numerous long cytoplasmic processes filled with bundles of glial filaments and scarce other organelles ($\times 2,500$). (F) Glioblastoma shows many pleomorphic spindle and oval cells with numerous cytoplasmic processes containing bundles of intermediate filaments with surface microvilli-like differentiation ($\times 2,500$). (G) Medulloblastoma shows that loosely arranged oval-shaped tumor cells project cytoplasmic processes forming rosettes filled with glial filaments and dense core granules indicating neuroglial differentiation ($\times 9,000$). (H) Neuroblastoma reveals that closely packed polygonal to spherical tumor cells have numerous, thin, electron-lucent cell processes forming an interlacing meshwork between groups of cell bodies ($\times 9,000$). Inset shows longitudinally-oriented 20 nm microtubules (white arrow) and dense core granules (black arrow, $\times 15,000$). (Continued to the next page)

histologic and molecular cytogenetic findings, pilomyxoid astrocytoma relating to pilocytic astrocytoma and other glioneuronal tumors remain undefined and controversial. With progression of WHO grade in astrocytic tumors, there are sparser glial filaments and more irregular microvillus-like cell projections in anaplastic astrocytoma or glioblastoma, compared to diffuse astrocytoma (Fig. 1E, F). Pediatric glioblastomas are rarely encountered.³⁵⁻³⁷ Excluding components of gliosarcoma, pediatric brain sarcomas are rare. However, various types of primary intracranial sarcomas can occur in the absence of radiation history.^{38,39} Although rare cases of rhabdomyosarcoma or chondrosar-

coma have also been described, most reported cases in children are fibrosarcomas.⁴⁰ Proliferation of spindle cells resembling meningioma on immunohistochemistry and light microscopy but with a classical herring-bone pattern suggests fibrosarcoma. Fibrosarcoma is composed of fibroblast-like spindle cells with well-developed, abundant dilated RERs and prominent Golgi complexes.⁴¹ Small patches of basal lamina materials lining some tumor cell surfaces are observed in rare cases. Features of myoid differentiation have not been observed.

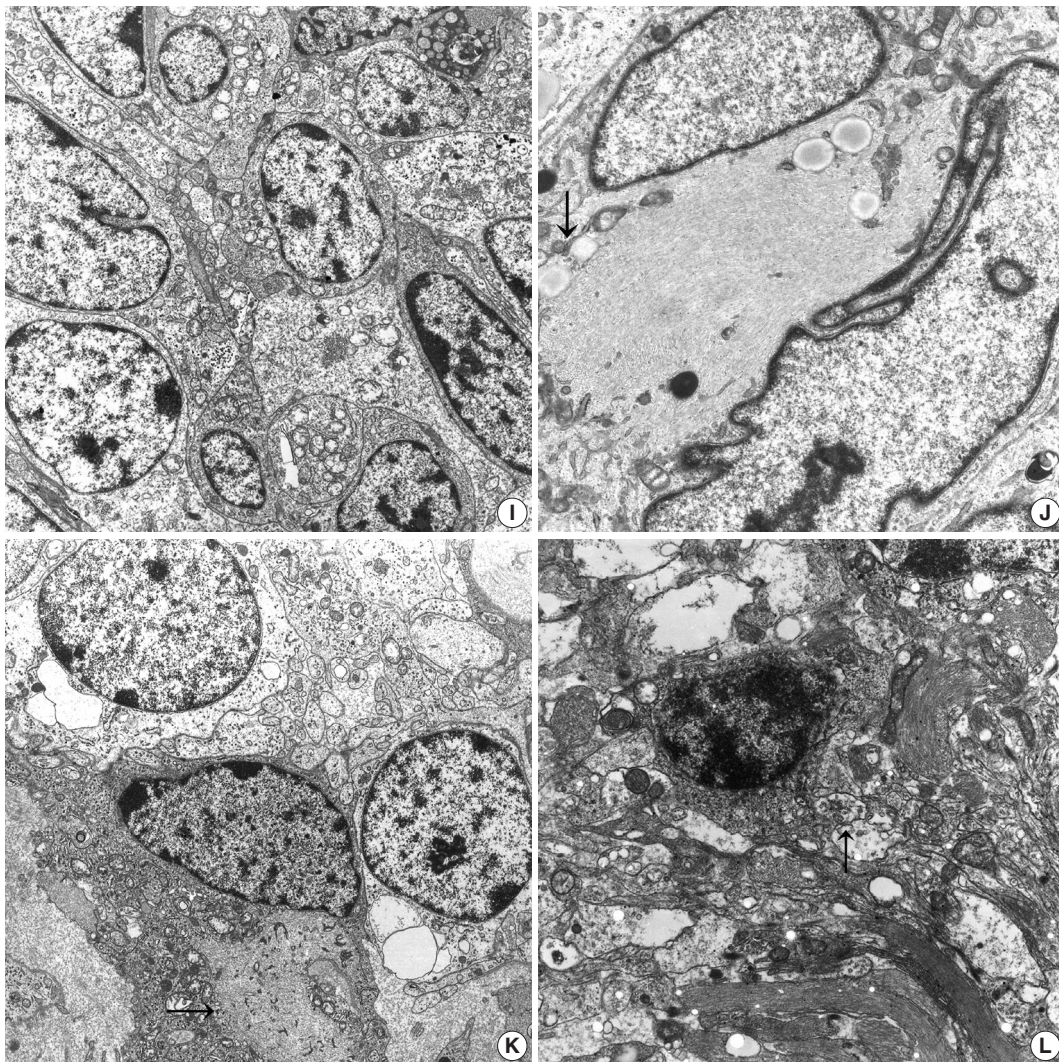


Fig. 1. (Continued from the previous page) (I) Primitive neuroectodermal tumor reveals round to closely apposed oval-shaped tumor cells with abundant cytoplasmic processes containing sparse organelles including glycogen particles, mitochondria, and some microtubules ($\times 8,000$). (J) Atypical teratoid and rhabdoid tumor reveals paranuclear aggregates of intermediate filaments (arrow) compressing the heterochromatic nuclei ($\times 15,000$). (K) Oligodendroglioma presents tumor cells with uniform round nuclei and sparse cytoplasmic organelles as well as some irregularly shaped cell processes (arrow) containing occasional globoid collections of intermediate filaments ($\times 3,500$). (L) Neurocytoma reveals round tumor cells with a moderate amount of cytoplasm and numerous long thin cell processes containing microtubules, few electron dense core granules and secretory vesicles (arrow), and glial intermediate filaments ($\times 8,000$). (Continued to the next page)

SMALL ROUND CELL CATEGORY OF PEDIATRIC CENTRAL NERVOUS SYSTEM TUMORS

In this group, small round cell pediatric CNS tumors include medulloblastoma, CNS primitive neuroectodermal tumor (PNET)/embryonal tumor with abundant neuropils and true rosettes, atypical teratoid and rhabdoid tumor (AT/RT), and neuroblastoma.^{2,42-48} Medulloblastoma is a common malignant primary brain tumor in children, categorized as a PNET of the cerebellum, i.e., an undifferentiated tumor exhibiting classic un-

differentiated multipotent tumor cells showing myoblastic, neuronal, glial, and melanotic differentiation observed under light microscopy, immunohistochemistry, and EM.⁴⁸ A broad spectrum of neural differentiation has been identified in nearly all cases of medulloblastoma.⁴⁹ Therefore, there is a spectrum in which the most undifferentiated area might have large undifferentiated cells compared to more differentiated areas exhibiting neuroblastic differentiation. Ultrastructurally, medulloblastoma is composed of primitive cells having a high nuclear-cytoplasmic ratio, and those cells that lack distinguishing ultrastructur-

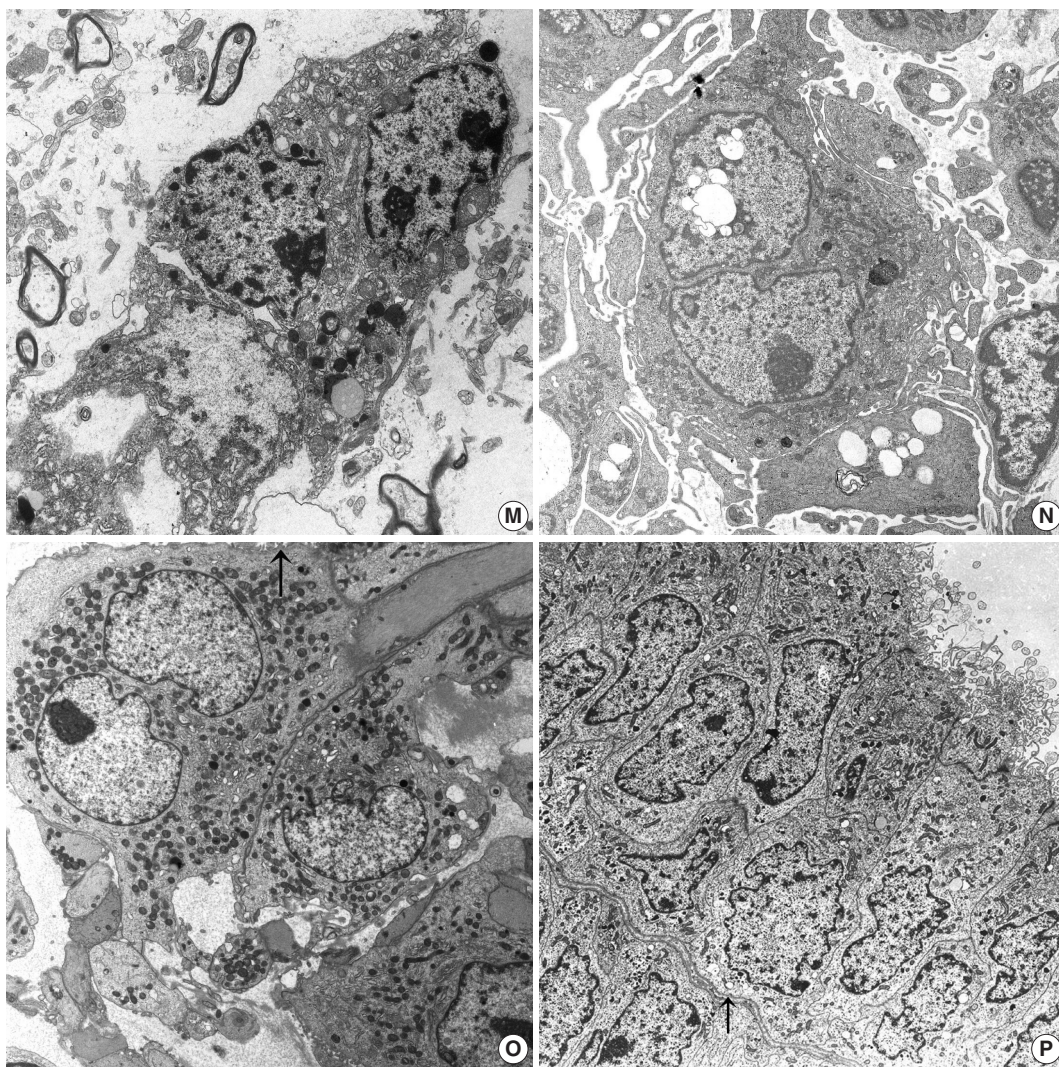


Fig. 1. (Continued from the previous page) (M) Dysembryoplastic neuroepithelial tumor reveals oligodendroglial-like cells with elongated bulbous cell processes forming a neuropil-like structure filled with intermediate filaments in electron-lucent mucoid extracellular spaces ($\times 7,000$). (N) Papillary tumor of the pineal region reveals polygonal-shaped tumor cells having short-villous cell surfaces and cytoplasm having abundant rough endoplasmic reticulum with distended cisternae and vacuoles ($\times 3,500$). (O) Chordoid glioma of the third ventricle reveals tumor cells with cytoplasmic processes filled with intermediate glial filaments and surrounded by basal lamina ($\times 7,000$). Note the numerous surface microvilli (arrow). (P) Choroid plexus papilloma shows ovoid to polygonal tumor cells arranged in glandular patterns joined by well-formed junctional complexes and a continuous basal lamina (arrow) surrounding these glandular structures ($\times 1,500$). Note the apical portion of tumor cells lined by numerous microvilli and cilia composed of 9+2 microtubules.

al findings such as tightly packed poorly differentiated oval to polygonal tumor cells with large nuclei; Rosenthal fibers, i.e., astrocytic differentiation; or neuronal differentiation such as rudimentary synaptic junctions or dense core granules (Fig. 1G). The central acellular area is composed of centrally projected broad cell processes, forming Homer-Wright rosettes. These central acellular rosettes composed of cytoplasmic processes are found in other tumors such as neuroblastoma, neurocytoma, and ependymoma.^{25,50,51} Glial intermediate filaments fill the cell processes in an ependymoma or medulloblastoma with glial differentiation, while microtubules are found in tumors of neuronal differentiation such as neurocytoma or neuroblastoma (Fig. 1H).^{49,51,52}

PNET was originally described as an undifferentiated neuroepithelial tumor with mesenchymal differentiation and now encompasses tumors showing pluripotentiality toward neuronal, astrocytic, and other cell lines such as those of a mesenchymal lineage (Fig. 1I). However, this entity might be a confusing and controversial factor in the diagnosis and classification of pediatric embryonal tumors. Some cases of PNET mimicking AT/RT have been reported.⁵³ AT/RT, which occurs mainly in children under the age of 3 years and is associated with frequent recurrence, is a malignant rhabdoid tumor (MRT), i.e., a CNS counterpart of renal MRT, belonging to rhabdoid tumor predisposition syndrome. Mutation or deletion of SMARCB1/INI-1/hSNF5/BAF47-tumor-suppressor gene located on chromosome band 22q11.2 inactivates the tumor suppressor gene, resulting in subsequent negative immunostaining in AT/RT but not in other rhabdoid phenotypes of CNS neoplasms, although mutations of INI-1 in some choroid plexus carcinomas have been reported.^{47,53,54} Immunohistochemistry for INI-1 is actually superior to EM or small biopsy of light microscopy because ultrastructural descriptions of AT/RT are few and lack specific CNS cell components of glial or neuronal lineage (Fig. 1J). Histologically, AT/RT shows various mixed histologies of epithelial, mesenchymal, rhabdoid, and primitive neuroepithelial components, suggesting an origin of immature and pluripotent neuroectodermal cells capable of differentiating along multiple lineages, as demonstrated by EM.⁵⁵

OLIGODENDROGLIOMA AND OLIGODENDROGLIOMA-LIKE TUMORS

Oligodendroglioma-like tumors, i.e., oligodendroglioma-mimickers, include oligodendroglioma, dysembryoplastic neuroepithelial tumor (DNT), neurocytoma, clear cell ependymoma

(CCE), ganglioglioma, and gangliocytoma.^{25,56-58} Oligodendroglioma is composed of closely apposed round-shaped tumor cells with euchromatic round nuclei and cytoplasm containing some microtubules and few glial filaments (Fig. 1K). Short broad cell processes might be seen within the tumor cells. Cell junctions or surface microvilli are not found in oligodendroglioma.^{25,59} Among oligodendroglioma-mimickers, neurocytomas have distinct immunohistochemical and ultrastructural characteristics compared with oligodendrogliomas.^{50,51,60} Both can have microtubules, but the former exhibit neuronal differentiation such as synaptic vesicles or dense core granules. Central and extraventricular neurocytoma has been reported as ependymoma of the foramen of Monro or intraventricular oligodendroglioma due to mimicry of oligodendroglioma-like cells under light microscopy.⁶⁰ Characteristic immunohistochemical findings of rosette-like acellular fibrillary areas stained with neuronal markers such as synaptophysin or NeuN might not be identified in extraventricular neurocytomas.⁶¹ Ultrastructurally, neurocytoma has numerous thin neuritic processes filled with dense core granules and microtubules with or without synapses (Fig. 1L). DNT consists of neoplastic oligodendroglial-like cells (OLCs) and elongated processes forming a neuropil-like structure in the mucinous extracellular area.⁵⁸ Ultrastructurally, OLCs have round to oval or elongated nuclei and scanty cytoplasm filled with electron-lucent synaptic vesicles, whereas elongated tumor cells have abundant cellular processes containing scanty microtubules and dense-core granules (Fig. 1M). OLCs of DNT can be distinguished from astrocytes by the lack of glial intermediate filaments and from neuronal cells by the presence of microtubules. Some cells of DNT have cytoplasmic ribosome-lamellae complexes, also found in lymphoid neoplasms or glioblastomas.^{62,63} These structures have been regarded as astrocytic differentiation but remain elusive. CCE resembling oligodendroglioma and neurocytic tumor under light microscopy can be distinguished from the latter using EM, which shows intracytoplasmic lumen lined by microvilli, complex cell junctions, and cilia. The clear cell morphology of CCE is caused by organelle-free areas of the cytoplasm with edema and vacuolization.^{64,65}

Ganglioglioma and gangliocytoma are composed of several types of tumor cells; neuronal tumor cells have dense core granules, diagnostically salient features, and synaptic junctions. Spherical protein bodies are found in gangliogliomas.⁵⁶ Multi-vesicular bodies, abundant autophagic vacuoles, and dense core vesicles are seen in neoplastic neuronal cells of ganglioglioma and gangliocytomas.⁶⁶

PAPILLARY TUMORS OF THE CENTRAL NERVOUS SYSTEM

Papillary tumors of the CNS observable under light microscopy include PGNT, tumors of the suprasellar area such as PTPR, pituitary adenoma of papillary configuration, or chordoid glioma of the third ventricle.⁶⁷⁻⁶⁹ PGNTs can occur at any age, and pediatric cases have been reported.⁶⁷ Ultrastructurally, either astrocytic or neuronal differentiation and poorly differentiated or uncommitted primitive cells are found in PGNT.^{52,69} PTPR was recently added to the 2007 WHO classification as a rare neuroepithelial tumor of papillary appearance arising in the pineal area.^{45,46} This tumor has been named papillary pineocytoma or choroid plexus papilloma due to papillary features and epithelial morphology showing immunopositivity for pancytokeratin and ependymal differentiation. Pediatric occurrence of PTPR is rare. Specialized ependymal cells of the subcommissural organ (SCO) are considered the origin of PTPR because of ultrastructural findings of divergent differentiation of epithelial, ependymal, and neuroendocrine cells. On EM, clear and dark epithelioid cells have an ovoid nuclei and abundant cytoplasm filled with abundant organelles including RERs, dense core vesicles, microtubules, numerous clear and coated vesicles, mitochondria, and intermediate filaments.⁷⁰ Abundant microvilli and less frequent cilia are found at the apical pole (Fig. 1N). Well-formed junctional complexes are found at the apical portion, and the basal portion is surrounded by a basement membrane. Chordoid glioma of the third ventricle is characterized by clusters and cords of epithelioid cells in a mucinous chordoid matrix. It is a slowly growing glial tumor occurring mainly in adults, although rare cases of pediatric choroid glioma have been reported.^{68,71} Chordoid glioma and PTPR share an anatomic location, i.e., circumventricular organ occurrence and subsequent shared ultrastructural findings; secretory vesicles as well as cilia, microvilli, and junctional complexes such as hemidesmosomes, are suggestive of the origin of modified specialized ependymal, i.e., tanyocytes of the SCO such as lamina terminalis (Fig. 1O).^{68,69} Choroid plexus papilloma shows cuboidal-shaped tumor cells with apical-basal orientation with varying sizes of apical club-like or roundish microvilli filled with glycogen particles and rare cilia with a 9+2 arrangement of microtubules (Fig. 1P).^{25,72,73} The neoplastic cells contain numerous free ribosomes, glycogen granules, and RERs. Elongated junctional complexes were occasionally seen near the apical ends. The basal portions of the tumor cells are lined with a continuous basal lamina. These apical cilia or glycogen particles are

more often seen in infantile choroid plexus papillomas than in those of older age.⁷²

RHABDOID CELL TUMORS

Rhabdoid cells are designated as large cells with eccentrically located nuclei and well-demarcated abundant, eosinophilic globular inclusions with characteristic immunoreactivity for vimentin, keratin, and epithelial membrane antigen, which ultrastructurally correspond to paranuclear whorls of intermediate filaments. These rhabdoid changes can appear in various neoplasms from diverse organ sites.^{54,73-75} In the CNS, most rhabdoid tumors occur in the infratentorial posterior fossa of very young children. Histological diagnosis of an MRT depends on identification of characteristic rhabdoid choroid plexus carcinoma, an extremely rare variant of choroid plexus carcinoma, belonging to choroid plexus tumor; however, carcinoma can lose its papillary pattern, and this ill-defined growth pattern with small foci of epithelial differentiation can make diagnosis challenging and mimic AT/RT due to overlapping morphological, immunohistochemical, and ultrastructural features, except for INI-1 expression.^{54,55,74} Like other MRT, EM shows the typical rhabdoid cells with paranuclear whorls or bundles of intermediate filaments as well as reminiscent retention of choroid plexus differentiation.⁷³ These rhabdoid features can be seen in rhabdoid meningioma, ependymoma, glioma, or germ cell tumors and even in metastatic rhabdoid melanoma.^{19,75,76}

PLEOMORPHIC CELL TUMORS

CNS tumors showing pleomorphic features under light microscopy include pleomorphic xanthoastrocytoma (PXA), glioblastoma, AT/RT, or undifferentiated primitive tumors.^{63,77,78} Tumors such as AT/RT or undifferentiated primitive tumors were previously discussed in the section on small round cell tumors. PXA that is prevalent in children belongs to an astrocytic lineage and appears as irregularly-shaped heterochromatic nuclei and abundant cytoplasm filled with lysosomes, lipid droplets, and glial filaments.⁶³ Ultrastructurally, PXA is composed of two types of cells; spindle-shaped astrocytic cells and bizarre giant cells filled with glial filaments and lipid droplets; the astrocytic tumor undergoes neuronal differentiation. Basal lamina surrounds the individual tumor cells or in groups, in contrast to other astrocytic tumors. Cytoplasmic lysosomes and ribosome-lamellae complexes are predominant in PXA, as in DNT, lymphoid leukemia and glioblastoma.^{62,63}

CONCLUSION

Despite declining usage, EM retains its diagnostic usefulness in neuropathology, particularly in distinguishing histological look-alikes, poorly differentiated or undifferentiated CNS neoplasms. When there is an overlap in the immunohistochemical profiles between CNS tumors, ultrastructural examination serves to confirm the concrete diagnosis even if the components of surrounding non-neoplastic cells may be misinterpreted as those of the tumor cells.

In this article, we summarized and reviewed diagnostic ultrastructural findings of CNS neoplasms commonly found in children.

Conflicts of Interest

No potential conflict of interest relevant to this article was reported.

Acknowledgments

The authors are very grateful to Professor Je G. Chi, who passed away last winter. He was a great mentor and friend to all of us. This work is dedicated to his memory.

REFERENCES

1. Pappathoma P, Thomopoulos TP, Karalexi MA, *et al.* Childhood central nervous system tumours: incidence and time trends in 13 Southern and Eastern European cancer registries. *Eur J Cancer* 2015; 51: 1444-55.
2. Schmidt LS, Schmiegelow K, Lahteenmaki P, *et al.* Incidence of childhood central nervous system tumors in the Nordic countries. *Pediatr Blood Cancer* 2011; 56: 65-9.
3. Gerstner ER, Batchelor TT. Primary central nervous system lymphoma. *Arch Neurol* 2010; 67: 291-7.
4. Zhang C, Bao Z, Zhang W, Jiang T. Progress on molecular biomarkers and classification of malignant gliomas. *Front Med* 2013; 7: 150-6.
5. Kim NR, Cho SJ, Suh YL. Allelic loss on chromosomes 1p32, 9p21, 13q14, 16q22, 17p, and 22q12 in meningiomas associated with meningioangiomas and pure meningioangiomas. *J Neurooncol* 2009; 94: 425-30.
6. Ahsan J, Hashmi SN, Muhammad I, *et al.* Spectrum of central nervous system tumours: a single center histopathological review of 761 cases over 5 years. *J Ayub Med Coll Abbottabad* 2015; 27: 81-4.
7. Pastuszek Ż, Tomczykiewicz K, Piusińska-Macoch R, Stępień A, Kordowska J. The occurrence of tumors of the central nervous system in a clinical observation. *Pol Merkur Lekarski* 2015; 38: 88-92.
8. Hicks J, Mierau GW. The spectrum of pediatric tumors in infancy, childhood, and adolescence: a comprehensive review with emphasis on special techniques in diagnosis. *Ultrastruct Pathol* 2005; 29: 175-202.
9. Louis DN, Ohgaki H, Wiestler OD, Cavenee WK. WHO classification of tumours of the central nervous system. 4th ed. Lyon: IARC Press, 2007.
10. Langford LA. Central nervous system neoplasms: indications for electron microscopy. *Ultrastruct Pathol* 1996; 20: 35-46.
11. Uematsu Y. The role of electron microscopy in the diagnosis of surgical pathology in the central nervous system. *Med Mol Morphol* 2006; 39: 127-35.
12. Kleihues P, Cavenee WK. World Health Organization classification of tumours of pathology and genetics of tumours of the nervous system. 3rd ed. Lyon: IARC Press, 2000.
13. Speirs CK, Simpson JR, Robinson CG, *et al.* Impact of 1p/19q codeletion and histology on outcomes of anaplastic gliomas treated with radiation therapy and temozolomide. *Int J Radiat Oncol Biol Phys* 2015; 91: 268-76.
14. Mur P, Mollejo M, Hernández-Iglesias T, *et al.* Molecular classification defines 4 prognostically distinct glioma groups irrespective of diagnosis and grade. *J Neuropathol Exp Neurol* 2015; 74: 241-9.
15. Giangaspero F, Guiducci A, Lenz FA, Mastronardi L, Burger PC. Meningioma with meningioangiomas: a condition mimicking invasive meningiomas in children and young adults: report of two cases and review of the literature. *Am J Surg Pathol* 1999; 23: 872-5.
16. Kepes J. Electron microscopic studies of meningiomas. *Am J Pathol* 1961; 39: 499-510.
17. Donato G, Ferraro G, Signorelli F, *et al.* Chordoid meningioma: case report and literature review. *Ultrastruct Pathol* 2006; 30: 309-14.
18. Couce ME, Aker FV, Scheithauer BW. Chordoid meningioma: a clinicopathologic study of 42 cases. *Am J Surg Pathol* 2000; 24: 899-905.
19. Buccoliero AM, Castiglione F, Rossi Degl'Innocenti D, *et al.* Pediatric rhabdoid meningioma: a morphological, immunohistochemical, ultrastructural and molecular case study. *Neuropathology* 2011; 31: 59-65.
20. Srinivas R, Krupashankar D, Shasi V. Intracerebral schwannoma in a 16-year-old girl: a case report and review of the literature. *Case Rep Neurol Med* 2013; 2013: 171494.
21. Peydró-Olaya A, Llombart-Bosch A, Carda-Batalla C, Lopez-Guerrero JA. Electron microscopy and other ancillary techniques in the diagnosis of small round cell tumors. *Semin Diagn Pathol* 2003; 20: 25-45.
22. Kim NR, Ha SY, Cho HY. Utility of transmission electron microsc-

- py in small round cell tumors. *J Pathol Transl Med* 2015; 49: 93-101.
23. Mrazk RE. The Big Eye in the 21st century: the role of electron microscopy in modern diagnostic neuropathology. *J Neuropathol Exp Neurol* 2002; 61: 1027-39.
 24. Langford LA, Barré GM. Tanycytic ependymoma. *Ultrastruct Pathol* 1997; 21: 135-42.
 25. Scheithauer BW, Bruner JM. Central nervous system tumors. *Clin Lab Med* 1987; 7: 157-79.
 26. Baloyannis SJ, Baloyannis IS. The fine structure of ependymomas. *CNS Oncol* 2014; 3: 49-59.
 27. Miyata H, Ryufuku M, Kubota Y, Ochiai T, Niimura K, Hori T. Adult-onset angiocentric glioma of epithelioid cell-predominant type of the mesial temporal lobe suggestive of a rare but distinct clinicopathological subset within a spectrum of angiocentric cortical ependymal tumors. *Neuropathology* 2012; 32: 479-91.
 28. Preusser M, Hoischen A, Novak K, *et al.* Angiocentric glioma: report of clinico-pathologic and genetic findings in 8 cases. *Am J Surg Pathol* 2007; 31: 1709-18.
 29. de Chadarevian JP, Halligan GE, Reddy G, *et al.* Glioneuronal phenotype in a diencephalic pilomyxoid astrocytoma. *Pediatr Dev Pathol* 2006; 9: 480-7.
 30. Horbinski C, Nikiforova MN, Hagenkord JM, Hamilton RL, Pollack IF. Interplay among BRAF, p16, p53, and MIB1 in pediatric low-grade gliomas. *Neuro Oncol* 2012; 14: 777-89.
 31. Liberski PP. The ultrastructure of glial tumors of astrocytic lineage: a review. *Folia Neuropathol* 1998; 36: 161-77.
 32. Wippold FJ 2nd, Perry A, Lennerz J. Neuropathology for the neuroradiologist: Rosenthal fibers. *AJNR Am J Neuroradiol* 2006; 27: 958-61.
 33. Paraskevopoulos D, Patsalas I, Karkavelas G, Foroglou N, Magras I, Selviaridis P. Pilomyxoid astrocytoma of the cervical spinal cord in a child with rapid progression into glioblastoma: case report and literature review. *Childs Nerv Syst* 2011; 27: 313-21.
 34. Fuller CE, Frankel B, Smith M, *et al.* Suprasellar monomorphous pilomyxoid neoplasm: an ultrastructural analysis. *Clin Neuropathol* 2001; 20: 256-62.
 35. Kim NR, Wang KC, Bang JS, *et al.* Glioblastomatous transformation of ganglioglioma: case report with reference to molecular genetic and flow cytometric analysis. *Pathol Int* 2003; 53: 874-82.
 36. Broniscer A, Baker SJ, West AN, *et al.* Clinical and molecular characteristics of malignant transformation of low-grade glioma in children. *J Clin Oncol* 2007; 25: 682-9.
 37. Brodbelt A, Greenberg D, Winters T, *et al.* Glioblastoma in England: 2007-2011. *Eur J Cancer* 2015; 51: 533-42.
 38. Lee S, Kim NR, Chung DH, Yee GT, Cho HY. Squash cytology of a dural-based high-grade chondrosarcoma may mimic that of glioblastoma in the central nervous system. *Acta Cytol* 2015; 59: 219-24.
 39. Lopes MB, Lanzino G, Cloft HJ, Winston DC, Vance ML, Laws ER Jr. Primary fibrosarcoma of the sella unrelated to previous radiation therapy. *Mod Pathol* 1998; 11: 579-84.
 40. Okeda R, Mochizuki T, Terao E, Matsutani M. The origin of intracranial fibrosarcoma. *Acta Neuropathol* 1980; 52: 223-30.
 41. Franchi A, Santucci M. The contribution of electron microscopy to the characterization of soft tissue fibrosarcomas. *Ultrastruct Pathol* 2013; 37: 9-14.
 42. Könnecke HK, Rushing EJ, Neidert MC, *et al.* Heterogeneous appearance of central nervous system involvement in malignant mixed Müllerian tumors. *J Neurol Surg A Cent Eur Neurosurg* 2015 Jul 27 [Epub]. <http://dx.doi.org/10.1055/s-0035-1558412>.
 43. Müller K, Diez B, Muggeri A, *et al.* What's in a name? Intracranial peripheral primitive neuroectodermal tumors and CNS primitive neuroectodermal tumors are not the same. *Strahlenther Onkol* 2013; 189: 372-9.
 44. Majumdar K, Batra VV, Tyagi I, Sharma A. Embryonal tumor with abundant neuropil and true rosettes with melanotic (retinal) differentiation. *Fetal Pediatr Pathol* 2013; 32: 429-36.
 45. Fèvre Montange M, Vasiljevic A, Bergemer Fouquet AM, *et al.* Histopathologic and ultrastructural features and claudin expression in papillary tumors of the pineal region: a multicenter analysis. *Am J Surg Pathol* 2012; 36: 916-28.
 46. Abela L, Rushing EJ, Ares C, *et al.* Pediatric papillary tumors of the pineal region: to observe or to treat following gross total resection? *Childs Nerv Syst* 2013; 29: 307-10.
 47. Perry A, Fuller CE, Judkins AR, Dehner LP, Biegel JA. INI1 expression is retained in composite rhabdoid tumors, including rhabdoid meningiomas. *Mod Pathol* 2005; 18: 951-8.
 48. Sakata H, Kanamori M, Watanabe M, Kumabe T, Tominaga T. Medulloblastoma demonstrating multipotent differentiation: case report. *Brain Tumor Pathol* 2008; 25: 39-43.
 49. Weeks DA, Malott RL, Goin L, Mierau GW. Ultrastructural spectrum of medulloblastoma with immunocytochemical correlations. *Ultrastruct Pathol* 2003; 27: 101-7.
 50. Hassoun J, Gambarelli D, Grisoli F, *et al.* Central neurocytoma. An electron-microscopic study of two cases. *Acta Neuropathol* 1982; 56: 151-6.
 51. Iida M, Tsujimoto S, Nakayama H, Yagishita S. Ultrastructural study of neuronal and related tumors in the ventricles. *Brain Tumor Pathol* 2008; 25: 19-23.
 52. Bouvier-Labit C, Daniel L, Dufour H, Grisoli F, Figarella-Branger D. Papillary glioneuronal tumour: clinicopathological and biochemical study of one case with 7-year follow up. *Acta Neuropathol* 2000; 99: 321-6.

53. Miller S, Ward JH, Rogers HA, Lowe J, Grundy RG. Loss of INI1 protein expression defines a subgroup of aggressive central nervous system primitive neuroectodermal tumors. *Brain Pathol* 2013; 23: 19-27.
54. Judkins AR, Burger PC, Hamilton RL, *et al.* INI1 protein expression distinguishes atypical teratoid/rhabdoid tumor from choroid plexus carcinoma. *J Neuropathol Exp Neurol* 2005; 64: 391-7.
55. Antonelli M, Cenacchi G, Modena P, Morra I, Forni M, Giangaspero F. Ultrastructural evidence of ependymal differentiation in a genetically proven atypical teratoid/rhabdoid tumor. *Childs Nerv Syst* 2009; 25: 1627-31.
56. Issidorides MR, Havaki S, Chrysanthou-Piterou M, Arvanitis DL. Ultrastructural identification of protein bodies, cellular markers of human catecholamine neurons, in a temporal lobe ganglioglioma. *Ultrastruct Pathol* 2000; 24: 399-405.
57. Kawano N, Yada K, Aihara M, Yagishita S. Oligodendroglia-like cells (clear cells) in ependymoma. *Acta Neuropathol* 1983; 62: 141-4.
58. Biernat W, Liberski PP, Kordek R, Zakrzewski K, Polis L, Budka H. Dysembryoplastic neuroectodermal tumor: an ultrastructural study of six cases. *Ultrastruct Pathol* 2001; 25: 455-67.
59. Luse SA. Electron microscopic observations of the central nervous system. *J Biophys Biochem Cytol* 1956; 2: 531-42.
60. Zulch KJ, Schmid EE. The ependymoma of the side ventricles at the foramen Monro. *Arch Psychiatr Nervenkr Z Gesamte Neurol Psychiatr* 1955; 193: 214-28.
61. Mut M, Guler-Tezel G, Lopes MB, Bilginer B, Ziyal I, Ozcan OE. Challenging diagnosis: oligodendrogloma versus extraventricular neurocytoma. *Clin Neuropathol* 2005; 24: 225-9.
62. Rosner MC, Golomb HM. Ribosome-lamella complex in hairy cell leukemia. Ultrastructure and distribution. *Lab Invest* 1980; 42: 236-47.
63. Hirose T, Giannini C, Scheithauer BW. Ultrastructural features of pleomorphic xanthoastrocytoma: a comparative study with glioblastoma multiforme. *Ultrastruct Pathol* 2001; 25: 469-78.
64. Jain D, Sharma MC, Arora R, Sarkar C, Suri V. Clear cell ependymoma: a mimicker of oligodendrogloma: report of three cases. *Neuropathology* 2008; 28: 366-71.
65. Min KW, Scheithauer BW. Clear cell ependymoma: a mimic of oligodendrogloma: clinicopathologic and ultrastructural considerations. *Am J Surg Pathol* 1997; 21: 820-6.
66. Sikorska B, Papierz W, Zakrzewski K, Fiks T, Polis L, Liberski PP. Ultrastructural heterogeneity of gangliogliomas. *Ultrastruct Pathol* 2007; 31: 9-14.
67. Barnes NP, Pollock JR, Harding B, Hayward RD. Papillary glioneuronal tumour in a 4-year-old. *Pediatr Neurosurg* 2002; 36: 266-70.
68. Suh YL, Kim NR, Kim JH, Park SH. Suprasellar chordoid glioma combined with Rathke's cleft cyst. *Pathol Int* 2003; 53: 780-5.
69. Myung JK, Byeon SJ, Kim B, *et al.* Papillary glioneuronal tumors: a review of clinicopathologic and molecular genetic studies. *Am J Surg Pathol* 2011; 35: 1794-805.
70. Cykowski MD, Wartchow EP, Mierau GW, Stolzenberg ED, Gummerlock MK, Fung KM. Papillary tumor of the pineal region: ultrastructural study of a case. *Ultrastruct Pathol* 2012; 36: 68-77.
71. Castellano-Sanchez AA, Schemankewitz E, Mazewski C, Brat DJ. Pediatric chordoid glioma with chondroid metaplasia. *Pediatr Dev Pathol* 2001; 4: 564-7.
72. Nakashima N, Goto K, Tsukidate K, Sobue M, Toida M, Takeuchi J. Choroid plexus papilloma: light and electron microscopic study. *Virchows Arch A Pathol Anat Histopathol* 1983; 400: 201-11.
73. Tena-Suck ML, Gómez-Amador JL, Ortiz-Plata A, Salina-Lara C, Rembao-Bojórquez D, Vega-Orozco R. Rhabdoid choroid plexus carcinoma: a rare histological type. *Arq Neuropsiquiatr* 2007; 65: 705-9.
74. Las Heras F, Pritzker KP. Adult variant of atypical teratoid/rhabdoid tumor: immunohistochemical and ultrastructural confirmation of a rare tumor in the sella tursica. *Pathol Res Pract* 2010; 206: 788-91.
75. Jay V, Edwards V, Halliday W, Rutka J, Lau R. "Polyphenotypic" tumors in the central nervous system: problems in nosology and classification. *Pediatr Pathol Lab Med* 1997; 17: 369-89.
76. Jeon YK, Jung HW, Park SH. Infratentorial giant cell ependymoma: a rare variant of ependymoma. *Pathol Res Pract* 2004; 200: 717-25.
77. Abbott JJ, Amirkhan RH, Hoang MP. Malignant melanoma with a rhabdoid phenotype: histologic, immunohistochemical, and ultrastructural study of a case and review of the literature. *Arch Pathol Lab Med* 2004; 128: 686-8.
78. Wyatt-Ashmead J, Kleinschmidt-DeMasters BK, Hill DA, *et al.* Rhabdoid glioblastoma. *Clin Neuropathol* 2001; 20: 248-55.

Dysembryoplastic Neuroepithelial Tumors

Yeon-Lim Suh

Department of Pathology, Samsung Medical Center, Sungkyunkwan University School of Medicine, Seoul, Korea

Received: September 16, 2015

Accepted: October 5, 2015

Corresponding Author

Yeon-Lim Suh, MD, PhD
Department of Pathology, Samsung Medical Center, Sungkyunkwan University School of Medicine, 81 Irwon-ro, Gangnam-gu, Seoul 06351, Korea
Tel: +82-2-3410-2800
Fax: +82-2-3410-0025
E-mail: yisuh76@skku.edu

Dysembryoplastic neuroepithelial tumor (DNT) is a benign glioneuronal neoplasm that most commonly occurs in children and young adults and may present with medically intractable, chronic seizures. Radiologically, this tumor is characterized by a cortical topography and lack of mass effect or perilesional edema. Partial complex seizures are the most common presentation. Three histologic subtypes of DNTs have been described. Histologically, the recognition of a unique, specific glioneuronal element in brain tumor samples from patients with medically intractable, chronic epilepsy serves as a diagnostic feature for complex or simple DNT types. However, non-specific DNT has diagnostic difficulty because its histology is indistinguishable from conventional gliomas and because a specific glioneuronal element and/or multinodularity are absent. This review will focus on the clinical, radiographic, histopathological, and immunohistochemical features as well as the molecular genetics of all three variants of DNTs. The histological and cytological differential diagnoses for this lesion, especially the nonspecific variant, will be discussed.

Key Words: Dysembryoplastic neuroepithelial tumor; Epilepsy; CD34; Microtubule-associated protein 2; *BRAF*^{V600E} mutation

This tumor was originally recognized in patients who underwent surgery for treatment of medically intractable seizures; however, recent progress in neuro-imaging has allowed for increased detection of dysembryoplastic neuroepithelial tumors (DNTs) in patients with a single episode of epilepsy or in older patients.¹ The original report in 1988 by Daumas-Duport *et al.*² describes morphologically unique features, including intracortical multi-nodularity, a specific glioneuronal (GN) element, and association with focal cortical dysplasia (FCD). The term “dysembryoplastic neuroepithelial tumor” was introduced for this unique tumor because tumors have a number of clinicopathological features, strongly suggesting a dysembryoplastic origin such as early onset of seizure, presence of FCD in the adjacent cortex, and deformity of the overlying skull.² The generic term “neuroepithelial tumors” was used so that a large range of morphologic variants could be integrated into this entity.²

The complex type of DNTs was first categorized as neuronal and mixed neuronal-glial tumors in the 1993 World Health Organization (WHO) classification of central nervous system (CNS) tumors. Additionally, simple and nonspecific histologic variants of DNTs have been described. The simple types of DNTs consist of only specific GN elements and the complex types are characterized by specific GN elements associated with glial nodules and/or FCD. Nonspecific types of DNTs lack multinodular architecture and specific GN elements, but show similar histo-

logic findings to those seen in glial nodules of complex DNTs.^{3,4} Nonspecific DNTs have been controversial because their histology is indistinguishable from conventional gliomas and because of the lack of a specific GN element and/or multinodularity of typical DNTs. The 2007 WHO classification of CNS tumors includes the simple and complex subtypes of DNT.⁵ However, several studies demonstrated three histologic forms of DNTs under the different terms “multinodular, solitary nodular, and diffuse” or “simple, complex, and diffuse.”⁶⁻⁸ The frequent immunoreactivity of CD34, nestin, and microtubule-associated protein 2 (MAP2)⁹ and the identification of *BRAF*^{V600E} mutation in nonspecific DNTs¹⁰ suggest that DNTs exhibit a broad spectrum of histopathology from simple to nonspecific forms.

A large series of DNTs demonstrated intrinsic epileptogenicity of DNTs in three histologic subtypes by intralesional recordings and simple and complex types showed localization of the epileptogenicity to the tumor, but non-specific temporal DNTs showed more extensive areas with the epileptogenicity. In their series, FCD was found in approximately two-thirds of patients with DNTs and was more common in nonspecific (85%) than in complex types (47%).¹¹

CLINICAL FEATURES

DNTs are found in approximately 17.8%–20% of patients

who undergo surgical resection for chronic epilepsy.^{11,12} DNTs are the second most common tumors in surgically resected cases for intractable epileptic seizures.^{13,14} Gangliogliomas and DNTs account for 65% of 1,551 tumors collected at the European Epilepsy Brain Bank.¹³ DNTs comprised 87% of 31 cases with tumor-associated, temporal lobe epilepsy.¹⁵ In children (below 18 years of age), the frequency of DNTs was reported to be 0.6% among 340 primary CNS tumors.¹⁶ In another report, the estimated prevalence of DNTs was 0.8% in 233 children with hemato-oncologic problems.¹⁷

Partial complex seizures are the most common clinical manifestation, followed by generalized tonic-clonic, simple partial, and partial seizures with secondary generalization.¹⁸ Secondary generalized seizures are more common in simple DNT cases.⁶ An additional neurologic symptom is headache only. Over 90% of patients with DNTs have epilepsy before the age of 20 years.¹¹ In one of the largest series, the mean age at seizure onset and surgery was 14.6 years (range, 3 months to 54 years), and 30.5 years (range, 6 to 65 years), respectively, with no significant difference among the DNT types.⁶ In pediatric DNTs, the mean age at seizure onset and surgery was 8.1 years (2 months–14 years) and 12.4 years (3.25–18.5 years), respectively.¹⁹ Patients generally do not have neurological deficits or evidence of elevated intracranial pressure. Males are more frequently affected, and tumors have a predilection for the temporal lobe, followed by the frontal and parietal or occipital lobes. Multifocal DNTs affecting the different sites in the CNS have been reported²⁰ and unusual locations for DNTs include the septum pellucidum, caudate nucleus, thalamus, pons, cerebellum, brainstem, and ventricles.^{21–23} Familial occurrence of DNTs has been described.²⁴

Lesionectomy alone controls seizures and tumors in most cases.²⁵ Seizure recurrence is associated with the presence of residual tumors or FCD in the peritumoral cortex. Therefore, complete removal of tumors and FCD in the adjacent cortex achieves seizure-free outcomes.¹⁸ Chassoux *et al.*^{26,27} reported that favorable prognostic factors for seizure-free outcomes are complete removal of tumor and epileptogenic zones, shorter epilepsy duration, and absence of cortico-subcortical damage at the resection site. The surgical outcome is not different in the three histological types of DNTs. Rarely, tumor recurrence has been reported in cases with gross total or subtotal resection. The histology of recurrent tumors is found to be similar to those of primary tumors. Malignant transformation into high-grade astrocytoma is also reported and may be induced by radiation therapy.^{6,28} Aggressive histopathological findings such as increased mitosis, necrosis, microvascular proliferation or high Ki-67 labeling index, and incom-

plete removal of tumors have not correlated with poor outcomes.

NEUROIMAGING

Cortical topography and the lack of mass effect and perilesional edema are common characteristics of neuroimaging.²⁹ In a large series of DNT, cystic change (23.9%), expansion of the overlying calvarium (19.5%), focal enhancement (19.5%), and calcification (15.2%) are common radiologic features.⁶ On non-contrast computed tomography scans, tumors are hypodense with a cystic appearance in half of the cases and can appear as a calcific hyperdensity and frequently show focal contrast enhancement. Deformity can also be seen in the overlying calvarium that is indicative of chronic focal pressure. Magnetic resonance imaging (MRI) shows a well-delineated tumor with pseudocystic or multicystic appearance, and low signal intensity on T1-weighted images but high signal intensity on T2-weighted images. Focal ring enhancement can rarely be seen on contrast-enhanced T1-weighted images.

Recently, MRI features in histologic variants of DNTs are classified into three types as follows: type 1 (cystic/polycystic-like, well-delineated, strongly hypointense on T1), type 2 (nodular-like, heterogeneous signal), or type 3 (dysplastic-like, isosignal/hyposignal T1, poor delineation, gray-white matter blurring)²⁹ (Fig. 1A–F). Simple or complex DNTs are always seen as type 1 on MRI, whereas nonspecific DNTs are seen as either type 2 or type 3 on MRI. Epileptogenic zones are found to be significantly different among MRI subtypes. The epileptogenic zone co-localizes to the tumor in type 1 MRI and involves the peritumoral cortex in type 2 MRI, while there are more extensive areas involved in type 3 MRI.

HISTOPATHOLOGY

Lesions vary in size from 10 to 25 mm, although occasionally larger tumors of up to 70 mm have been reported.¹¹ Grossly, tumors appear as well-defined, solitary nodular masses or poorly demarcated lesions (Fig. 2A). On the cut section, most tumors are cortically located and may extend into the underlying subcortical white matter in larger tumors. Multi-nodular appearance or cystic changes are commonly found (Fig. 2B, C).

Among three histologic variants of DNTs (Fig. 3), both simple and complex subtypes are characterized by the presence of specific GN elements that consist of small, round monotonous cells, so-called oligodendroglia-like cells (OLCs) and floating neurons in an abundant mucinous matrix. The specific GN ele-

ments may form typical nodules (Fig. 3A), but they may also show a diffuse pattern. The OLCs are arranged in a columnar pattern perpendicular to the cortical surface and separated by a

mucinous matrix. Depending on the amount of mucinous matrix in the specific GN elements, OLCs may show their arrangement in various patterns including microcystic, alveolar, com-

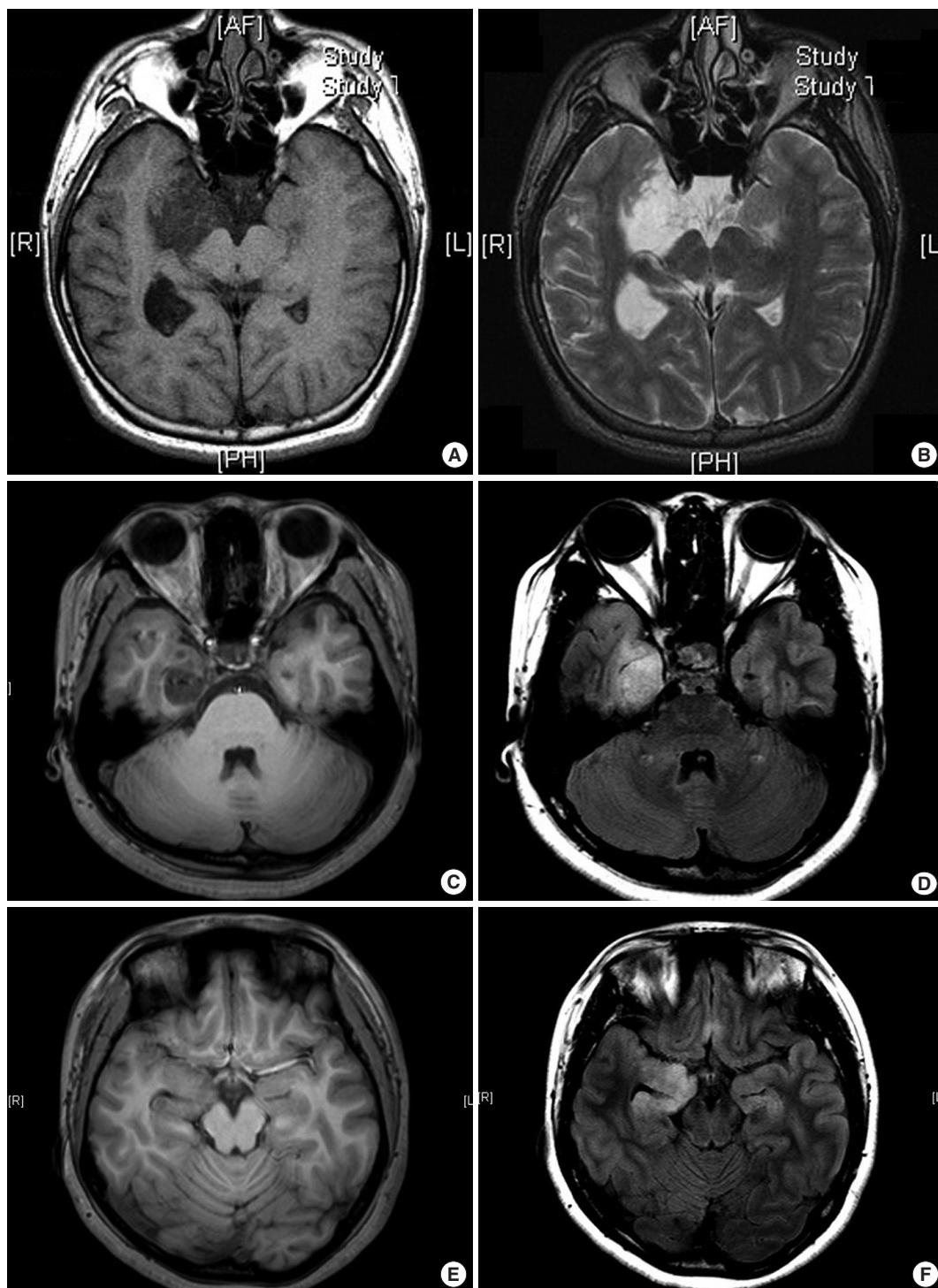


Fig. 1. Three different types of magnetic resonance imaging in dysembryoplastic neuroepithelial tumors. (A, B) Type 1 shows a well-delineated, polycystic-like tumor with strongly hypointense on T1- and hyperintense on T2-weighted images. (C, D) Type 2 shows a nodular-like, heterogeneous lesion. (E, F) Type 3 shows a poorly delineated, dysplastic-like, iso/hypointense T1 with gray-white matter blurring. Type 1 is mainly found in simple or complex forms, and type 2 and 3 are observed in nonspecific forms. (A, C, E) T1-weighted images. (B, D, F) T2 FLARE images.

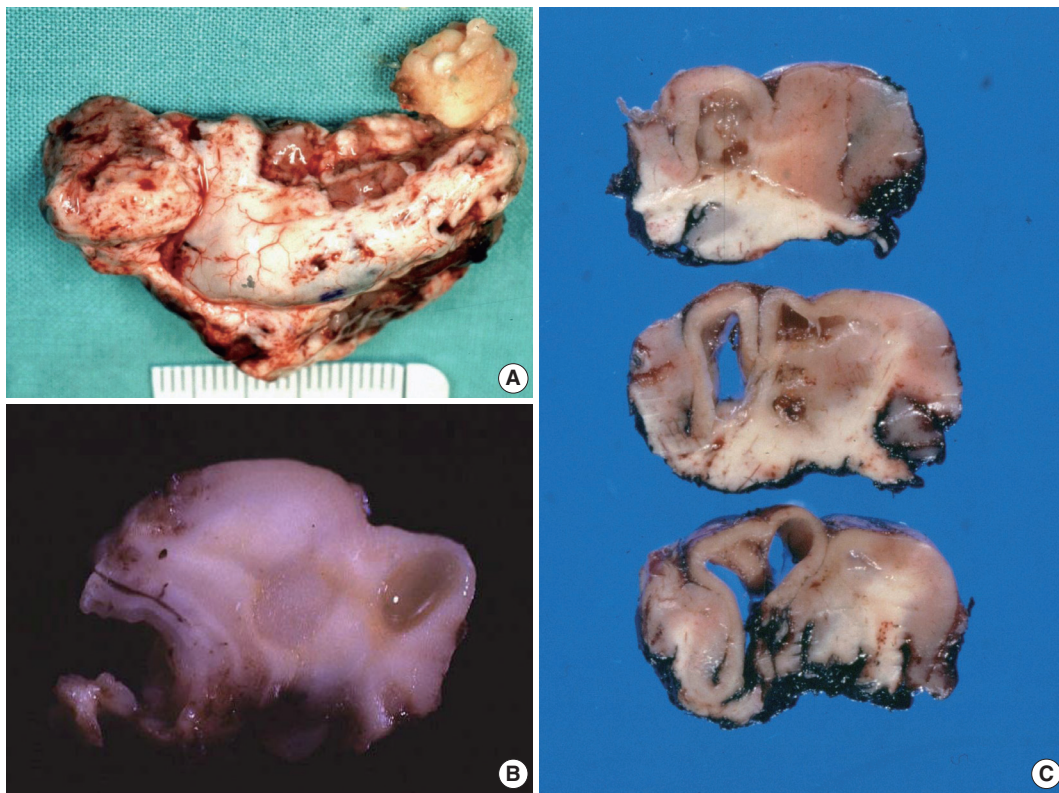


Fig. 2. Gross findings of dysembryoplastic neuroepithelial tumors (DNTs). (A) A hippocampectomy specimen shows a well circumscribed, gray white mass with two small satellite nodules. (B) On the cut section, a complex type of DNT shows multiple gray-white or gelatinous nodules affecting the cortex and white matter. (C) Nonspecific DNT shows a poorly demarcated, cortical thickening with underlying area of white matter rarefaction and cyst formation.

pact, or targetoid structure (Fig. 3B–D). Floating neurons that are observed within the mucin pool typically lack perineuronal satellitosis or nuclear atypia (Fig. 3E). The simple type of DNT consists only of the specific GN elements, and the complex type additionally has glial nodules and/or FCD of the adjacent cortex. The glial nodules show morphological similarity to low-grade gliomas, including oligodendroglioma, astrocytoma, mixed oligoastrocytoma, pleomorphic xanthoastrocytoma, and pilocytic astrocytoma (Fig. 3E, G). Frank nuclear atypia and multinucleated cells are commonly observed in glial components (Fig. 3H). The internodular areas are frequently abnormal, and may contain oligodendroglial and/or astrocytic components, although in some tumors, they are normal. Nonspecific DNT consists of poorly demarcated, diffuse cortical lesions with blurred normal anatomical landmarks (Fig. 3I). The various glial components seen in this type of DNT are similar to those seen in the glial nodules of the complex forms of DNTs or resemble diffuse components observed in the internodular areas of classical multi-nodular DNTs^{4,6,7} (Fig. 3J). Nuclear pleomorphism of glial cells is commonly found in all three types of tumors and

predominantly affects the astrocytic component. In one of the largest series studied, rarefaction of the underlying white matter (34%), leptomeningeal involvement (51%), and hemosiderin pigmentation (53%) are frequently found but are less common in simple DNTs. Calcification (25%) is not uncommon. Necrosis, mitosis, and microvascular proliferation are rarely observed.⁶ Foci of FCD in the adjacent neocortex are found in roughly two-thirds of DNT cases.¹¹

IMMUNOHISOCHEMISTRY

In specific GN elements, floating neurons have expressed neuronal markers including synaptophysin neurofilament, NeuN, neuron specific enolase, MAP2, and class-III beta-tubulin (Fig. 4A, B). The majority of OLCs are strongly positive for S-100 protein and Oligo-2 but generally negative for glial fibrillary acidic protein (GFAP) (Fig. 4C, D). Rarely, OLCs may show immunorexpression of NeuN. Glial nodules contain variable numbers of GFAP-positive astrocytes. In the nonspecific type of DNTs, synaptophysin granular staining is slightly decreased in

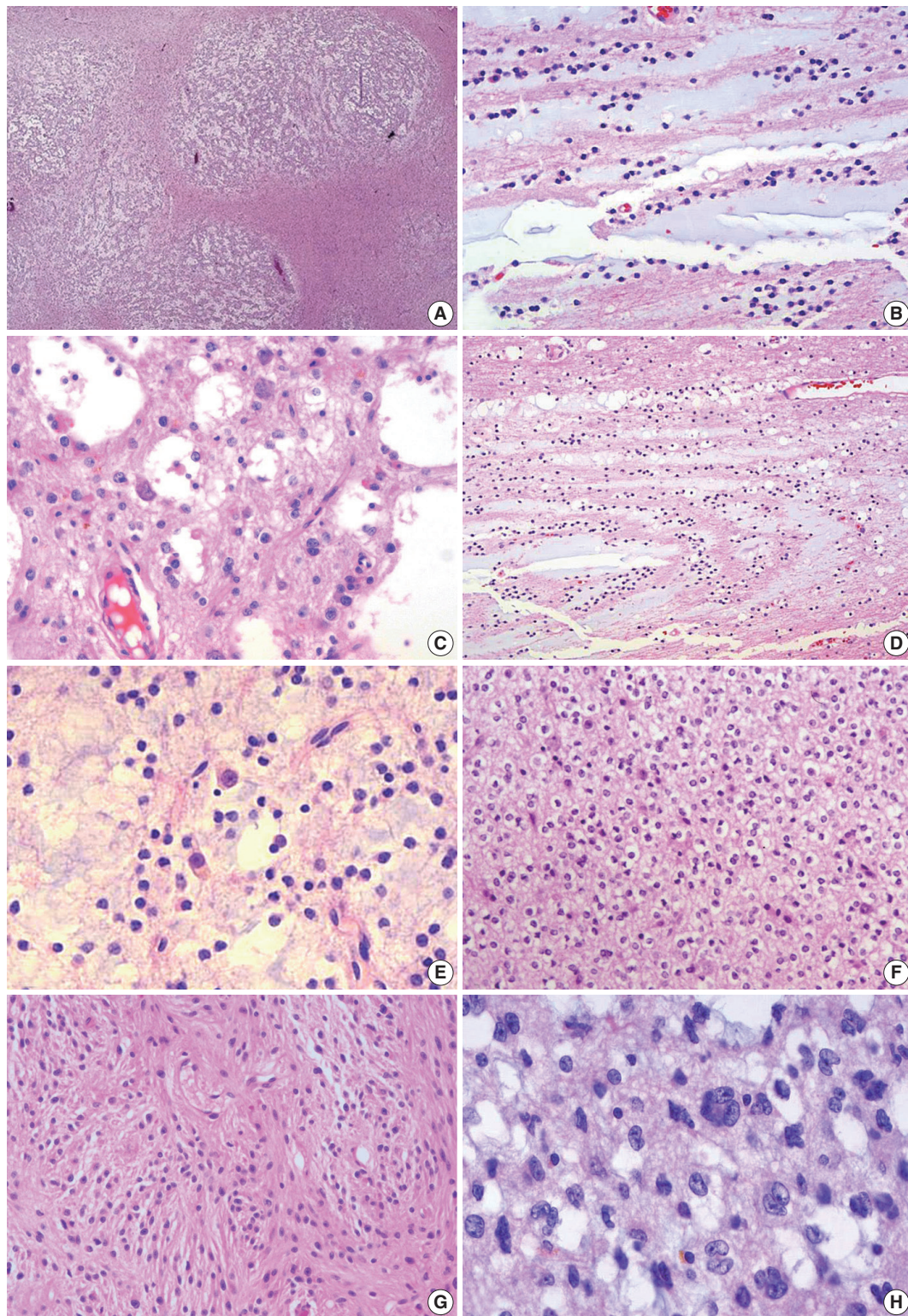


Fig. 3. Histopathological findings of dysembryoplastic neuroepithelial tumors (DNTs). (A) Multi-nodular appearance typical of complex DNTs. (B) Column arrangement of oligodendrogloma-like tumor cells (OLCs) in the specific glioneuronal element. (C) The characteristic appearance of DNTs with OLCs and mature neurons. (D) Targetoid structure of the specific glioneuronal element. (E) Floating neurons in the mucinous matrix. (F) The histology of glial nodules resembling oligodendrogloma. (G) This glial nodule with predominantly astrocytic differentiation. (H) Nuclear pleomorphism in glial component of DNTs. *(Continued to the next page)*

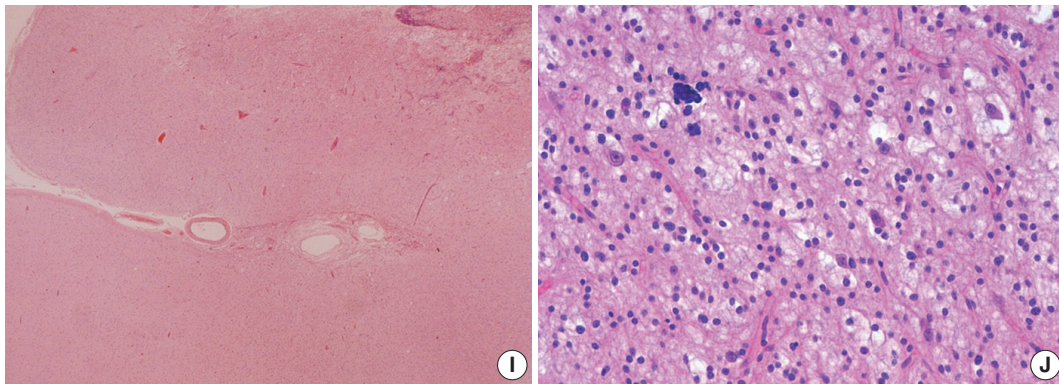


Fig. 3. (Continued from the previous page) Histopathological findings of dysembryoplastic neuroepithelial tumors (DNTs). (I) A poorly demarcated cortical lesion of nonspecific DNT. (J) The similar histology of nonspecific DNTs to that observed within the glial nodules of complex DNTs.

the lesion compared with that seen in the adjacent normal cortex (Fig. 4E). Other neuronal markers except MAP2 are negative in nonspecific DNTs, but MAP2 is frequently expressed.⁸ The expression of CD34 has been reported in 25% to 61% of cases.⁶⁻⁸ In our study, CD34 expression was more frequently observed in nonspecific types (83.3%) than in simple (10%) and complex types (30.8%). CD34 was positive in the neuronal cell membrane, pericellular stroma, and cytoplasm of OLCs and stellate cells with astroglial morphology (Fig. 4F). CD34 positive cells were focally identified in specific GN elements, whereas most nonspecific tumors and glial nodules of some complex DNTs showed a focal, multifocal, or diffuse pattern of CD34 immunoreactivity (Fig. 4G, H). CD34 was expressed in the peritumoral cortex (Fig. 5A–C), which is more frequent in nonspecific (94.4%) than in classic (26.1%) DNTs. Different expression patterns of nestin and MAP2 in three subtypes of DNTs have also been demonstrated.^{8,30} Combined analysis of CD34 and MAP2 is useful in differential diagnosis between nonspecific DNTs and diagnostically challenging mimickers, which will be discussed in the section on differential diagnosis. The Ki-67 labeling index is generally low, below 1% or 2%. The immunohistochemical detection of *BRAF*^{V600E} has been described in 30% of DNTs, including specific and nonspecific tumors.³¹ *BRAF*^{V600E} immunostaining is diffusely and strongly positive in glial nodules and usually negative in the floating neurons. However, dysplastic neurons show strong *BRAF*^{V600E} immunoreactivity in complex DNTs associated with FCD.

ULTRASTRUCTURAL FINDINGS

Ultrastructurally, OLCs exhibit round to oval invaginated nuclei with evenly dispersed chromatin, marginally condensed heterochromatin, and frequently a single small nucleolus (Fig.

6A). The cytoplasm of OLCs has scanty numbers of organelles, such as rough endoplasmic reticulum, mitochondria, microtubules, and clear vesicles. Unlike oligodendroglial cells, OLCs do not show abundant microtubules, although oligodendroglial differentiation such as pericellular lamination of cell processes has been demonstrated in one case.³² OLCs may show features of neuronal differentiation.³³ The neuronal features include scant dense core granules (45–60 μm), clear vesicles, synaptic junctions, or neuropil-like cellular processes (Fig. 6B, C). OLCs may show astrocytic features with small numbers of intermediate filaments. Ganglion cells are also observed but never exhibit the dysplastic features or abundant dense core granules of gangliogliomas. Ribosome-lamellae complexes can be found in a few OLCs (Fig. 6D). They are cylindrical and resemble “laboratory tubes with cone-like endings.”³³ The presence of these inclusions in OLCs suggests an astrocytic differentiation, because they have been demonstrated in tumors of astrocytic lineage, including glioblastomas.

SQUASH CYTOLOGICAL FEATURES

The cytological features of squash preparations of DNT during intraoperative consultation are fairly characteristic and reliable for correct intraoperative diagnosis, which helps to determine the appropriate neurosurgical procedure. The floating neurons and extracellular mucin that are typical of DNT are more easily demonstrated in cytological preparations than in frozen sections³⁴ (Fig. 7A, B). OLCs appear as aggregates or are dispersed around abundant arborizing capillaries or in the mucinous or focal fibrillary background. Round to oval naked nuclei of OLCs are larger than non-neoplastic and neoplastic oligodendrocytes. Cytologically, distinguishing features of OLCs from oligodendrogliomas include frequent indentation of the

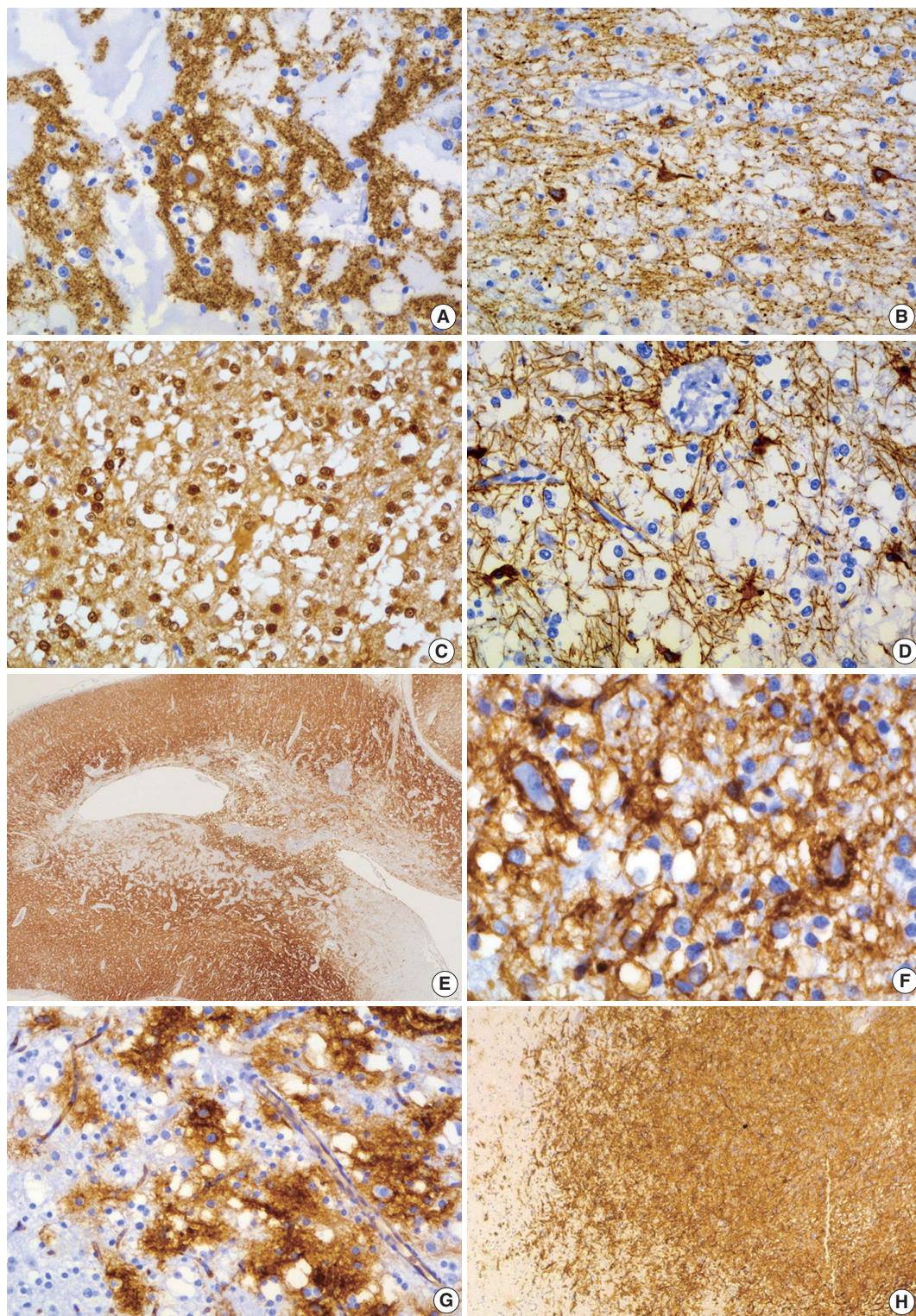


Fig. 4. Immunohistochemical findings of dysembryoplastic neuroepithelial tumors (DNTs). (A, B) Floating neurons are positive for synaptophysin (A) and phosphorylated neurofilament (B). (C, D) The oligodendrogloma-like cells (OLCs) are diffusely positive for S-100 (C) but negative for glial fibrillary acidic protein (D). (E) Nonspecific DNTs show slightly decreased synaptophysin granular staining compared with that seen in the adjacent normal cortex. (F) In the specific glioneuronal element, CD34 is expressed along the perikarya and in membrane of the floating neurons, pericellular stroma, and cytoplasm of OLCs. (G, H) The specific glioneuronal element shows cluster staining pattern of CD34 (G), while diffuse CD34 immunoreactivity in glial nodules of complex DNTs (H).

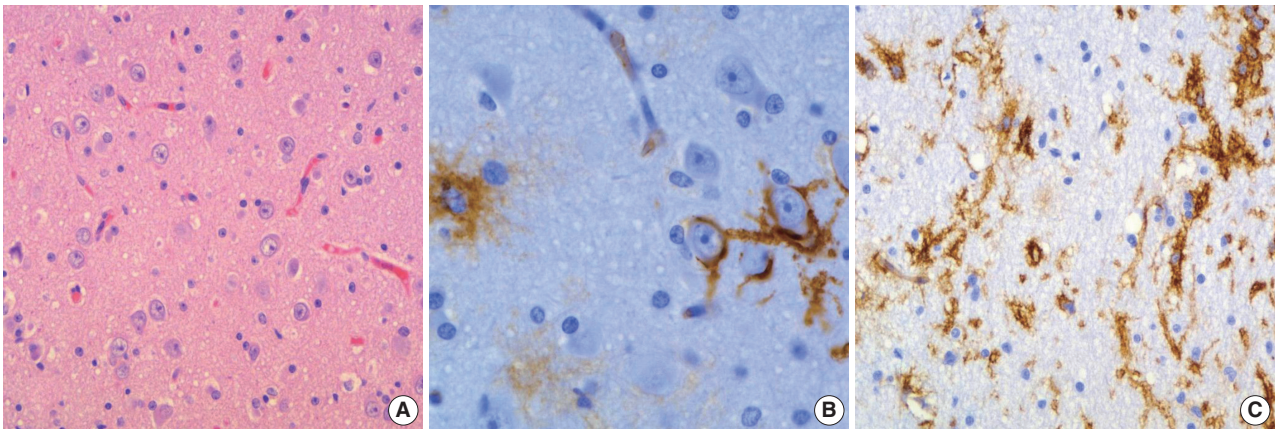


Fig. 5. The histology and CD34 immunoreactivity of focal cortical dysplasia (FCD) in the peritumoral cortex. (A) Dysplastic neurons and abnormalities in cortical lamination are observed. (B, C) CD34 immunoreactivity patterns of FCD are similar to that seen in dysembryoplastic neuroepithelial tumors.

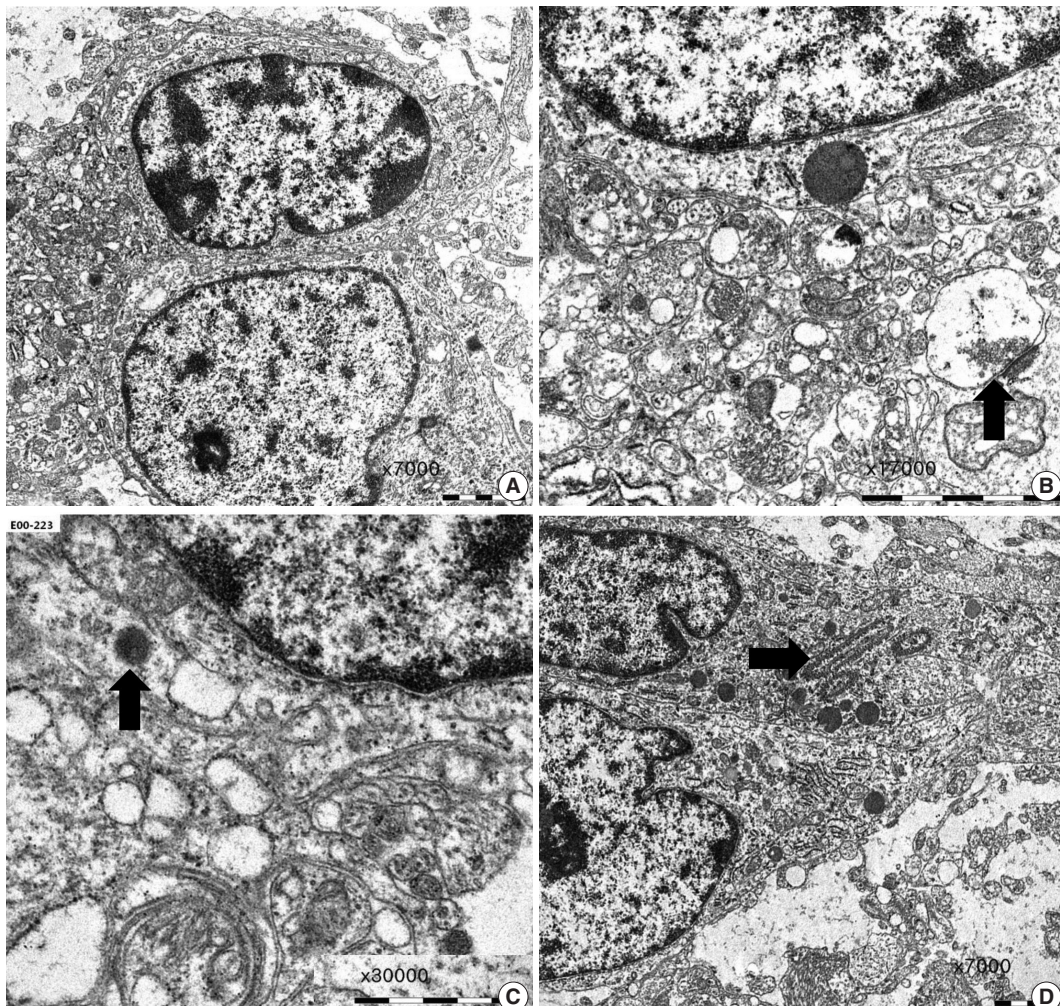


Fig. 6. Ultrastructural findings of dysembryoplastic neuroepithelial tumors. (A) Oligodendrogloma-like cells (OLCs) show oval nuclei with small indentation, marginal aggregates of heterochromatin, and their cytoplasm with scanty organelles ($\times 7,000$). (B, C) Neuropil-like network of cellular process with a synaptic contact (arrow) (B, $\times 17,000$) and scant dense core granules (arrow) (C, $\times 30,000$) indicates neuronal differentiation of OLCs. (D) A few OLCs contain ribosome-lamellae complex inclusions (arrow) ($\times 7,000$).

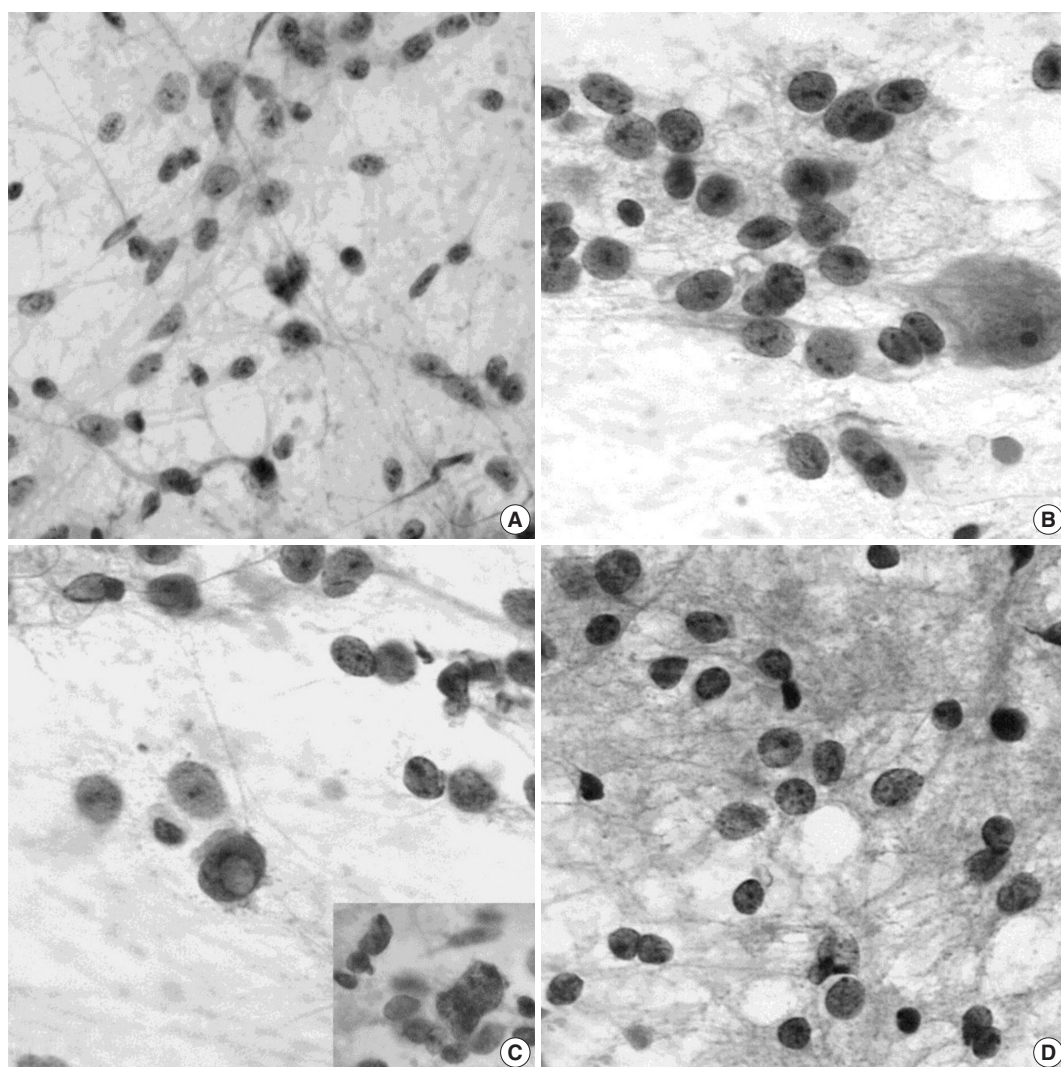


Fig. 7. Squash cytological findings of dysembryoplastic neuroepithelial tumors. (A) Squash preparation shows round, oval to elongated naked nuclei in the mucinous background. (B) The nuclei of oligodendrogloma-like cells (OLCs) are irregular with small indentations or deep grooves, and fine, granular chromatin and 1–4 small nucleoli. There is a large, normal-looking neuron in the mucinous background. (C) OLCs shows multinuclear giant cell formation (inset) and an intranuclear pseudoinclusion. (D) Squash preparation of oligodendrogloma shows smaller, dark nuclei without nucleoli and larger nuclei with granular chromatin and micronucleoli.

nuclear membrane and multiple, small nucleoli (Fig. 7C). The nuclei of oligodendrogliomas are round with a smooth outline and contain one or two occasional nucleoli (Fig. 7D). The presence of eosinophilic granular bodies in the background favors DNTs rather than oligodendrogliomas.

DIFFERENTIAL DIAGNOSIS

Histologically, the recognition of a unique, specific GN element in brain tumor samples from patients with medically intractable, chronic epilepsy serves as a diagnostic feature for complex or simple forms of DNT. The appreciation of unique

histological features may be difficult in fragmented specimens. The nonspecific forms, which lack specific GN elements and multi-nodular architecture, are often not distinguished from epilepsy-associated gliomas. Prominent perineuronal satellitosis and subpial aggregates of tumor cells favor gliomas, although a limited degree of secondary structure formation can be seen in DNTs. Distinguishing DNTs, particularly simple and nonspecific types, from gangliogliomas is often difficult because of overlap in their clinicopathological features, including an association with FCD. Gangliogliomas can be distinguished by the presence of neuronal atypia, perivascular lymphocytic infiltration, and reticulin networks surrounding glial cells. DNTs may rarely

show perivascular lymphocytic infiltration and mild neuronal atypia, but they do not show reticulin deposition within tumors.

It is important to differentiate DNTs from gliomas or gangliogliomas that may undergo malignant transformation. Combined immunostains for CD34 and MAP2 can facilitate the differential diagnosis between DNTs and epilepsy-associated tumors that mimic DNTs.⁸ Nonspecific DNTs and gangliogliomas share similar immunoreactivity patterns for CD34, but show different immunoreactivity for MAP2 in their glial components. MAP2 immunostaining is faintly positive or negative in the glial component of gangliogliomas, whereas it is frequently seen in DNTs. Most ordinary glial tumors, such as astrocytomas and oligodendrogliomas, are diffusely positive for MAP2 but negative for CD34. The “isomorphic subtype of long-term epilepsy-associated astrocytomas” described by Blumcke *et al.*³⁵ shows the absence of both MAP2 and CD34 immunoreactivity. Since *BRAF*^{V600E} mutations have not been detected in oligodendrogliomas, identification of *BRAF*^{V600E} mutation by immunohistochemistry or molecular study has diagnostic utility for distinguishing DNT from oligodendroglioma.⁹

GENETICS

In a study of 13 DNTs, none of the tumors showed 1p19q deletion, *IDH1*-2, or p53 mutation,³⁶ but a large series of DNTs found *IDH1* mutation in three cases, loss of heterozygosity (LOH) 1p/19q in 10 cases, isolated LOH 19q in two cases, LOH 10q (*PTEN* locus) in three cases, and combined LOH 1p/19q and 10q in one case.⁶ Other studies, however, including this one, did not show *IDH1* mutation.^{9,26} *IDH2* mutation or epidermal growth factor receptor amplification has not been identified. Recently, *BRAF*^{V600E} mutations were identified in 30%–51% of DNTs.^{9,31} In our study, the frequency of *BRAF*^{V600E} in DNTs was related to the location of tumors and was more frequent in extratemporal location (68.2% vs 37.9%). *BRAF*^{V600E} mutation was more common in classical DNTs (59.4%) than nonspecific DNTs (36.8%). Recently, copy number aberrations (CNAs) have been identified in DNTs, and the most frequent are gains at chromosomes 5 and 7, often concurrent, and at chromosome 6. CNAs in DNTs are not correlated with their histological subtypes, CD34 expression or clinical features.³⁷

HISTOGENESIS

DNTs were initially believed to be a hamartoma in nature,²⁻⁴

but recent identification of genetic alterations in DNTs, including classical and nonspecific types, indicate that this tumor is a neoplastic condition. The histogenesis of DNTs remains unknown. The developmental origin from the secondary germinal layer has been proposed based on the mixed cellularity of DNTs, their preponderance in the temporal lobe, and their association with FCD.² The origin of DNTs from pluripotent precursor cells is also suggested based on ultrastructural findings of OLCs showing neuronal and glial differentiation. This hypothesis is supported by the immunoexpression of both nestin and MAP2 in OLCs, which has been identified in neural and glial precursor cells during human development. Higher expression levels of nestin, MAP2 and CD34, stem cell markers, in nonspecific rather than simple or complex DNTs suggests an earlier developmental origin of the nonspecific DNTs.^{8,30}

Because DNTs share CD34 expression, *BRAF*^{V600E} mutations, and chromosomal copy number profiles with gangliogliomas, and occurrence of composite tumors with ganglioglioma and DNT, both tumors may represent different morphological variants of the same tumor entity.³⁸

Conflicts of Interest

No potential conflict of interest relevant to this article was reported.

Acknowledgments

The authors are very grateful to Professor Je G. Chi, who passed away last winter. He was a great mentor and friend to all of us. This work is dedicated to his memory.

REFERENCES

1. Burneo JG, Tellez-Zenteno J, Steven DA, *et al.* Adult-onset epilepsy associated with dysembryoplastic neuroepithelial tumors. *Seizure* 2008; 17: 498-504.
2. Dumas-Duport C, Scheithauer BW, Chodkiewicz JP, Laws ER Jr, Vedrenne C. Dysembryoplastic neuroepithelial tumor: a surgically curable tumor of young patients with intractable partial seizures. Report of thirty-nine cases. *Neurosurgery* 1988; 23: 545-56.
3. Dumas-Duport C. Dysembryoplastic neuroepithelial tumours. *Brain Pathol* 1993; 3: 283-95.
4. Dumas-Duport C, Varlet P, Bacha S, Beuvon F, Cervera-Pierot P, Chodkiewicz JP. Dysembryoplastic neuroepithelial tumors: nonspecific histological forms: a study of 40 cases. *J Neurooncol* 1999; 41: 267-80.
5. Louis DN, Ohgaki H, Wiestler OD, *et al.* The 2007 WHO classifica-

- tion of tumours of the central nervous system. *Acta Neuropathol* 2007; 114: 97-109.
6. Thom M, Toma A, An S, *et al.* One hundred and one dysembryoplastic neuroepithelial tumors: an adult epilepsy series with immunohistochemical, molecular genetic, and clinical correlations and a review of the literature. *J Neuropathol Exp Neurol* 2011; 70: 859-78.
 7. Honavar M, Janota I, Polkey CE. Histological heterogeneity of dysembryoplastic neuroepithelial tumour: identification and differential diagnosis in a series of 74 cases. *Histopathology* 1999; 34: 342-56.
 8. Bodi I, Selway R, Bannister P, *et al.* Diffuse form of dysembryoplastic neuroepithelial tumour: the histological and immunohistochemical features of a distinct entity showing transition to dysembryoplastic neuroepithelial tumour and ganglioglioma. *Neuropathol Appl Neurobiol* 2012; 38: 411-25.
 9. Sung CO, Suh YL, Hong SC. CD34 and microtubule-associated protein 2 expression in dysembryoplastic neuroepithelial tumours with an emphasis on dual expression in non-specific types. *Histopathology* 2011; 59: 308-17.
 10. Lee D, Cho YH, Kang SY, Yoon N, Sung CO, Suh YL. *BRAF* V600E mutations are frequent in dysembryoplastic neuroepithelial tumors and subependymal giant cell astrocytomas. *J Surg Oncol* 2015; 111: 359-64.
 11. Chassoux F, Landré E, Mellerio C, Laschet J, Devaux B, Daumas-Duport C. Dysembryoplastic neuroepithelial tumors: epileptogenicity related to histologic subtypes. *Clin Neurophysiol* 2013; 124: 1068-78.
 12. Devaux B, Chassoux F, Guenot M, *et al.* Epilepsy surgery in France. *Neurochirurgie* 2008; 54: 453-65.
 13. Blumcke I, Aronica E, Urbach H, Alexopoulos A, Gonzalez-Martinez JA. A neuropathology-based approach to epilepsy surgery in brain tumors and proposal for a new terminology use for long-term epilepsy-associated brain tumors. *Acta Neuropathol* 2014; 128: 39-54.
 14. Piao YS, Lu DH, Chen L, *et al.* Neuropathological findings in intractable epilepsy: 435 Chinese cases. *Brain Pathol* 2010; 20: 902-8.
 15. Kirkpatrick PJ, Honavar M, Janota I, Polkey CE. Control of temporal lobe epilepsy following en bloc resection of low-grade tumors. *J Neurosurg* 1993; 78: 19-25.
 16. Rickert CH, Paulus W. Epidemiology of central nervous system tumors in childhood and adolescence based on the new WHO classification. *Childs Nerv Syst* 2001; 17: 503-11.
 17. Spalice A, Ruggieri M, Grosso S, *et al.* Dysembryoplastic neuroepithelial tumors: a prospective clinicopathologic and outcome study of 13 children. *Pediatr Neurol* 2010; 43: 395-402.
 18. Chang EF, Christie C, Sullivan JE, *et al.* Seizure control outcomes after resection of dysembryoplastic neuroepithelial tumor in 50 patients. *J Neurosurg Pediatr* 2010; 5: 123-30.
 19. Lee J, Lee BL, Joo EY, *et al.* Dysembryoplastic neuroepithelial tumors in pediatric patients. *Brain Dev* 2009; 31: 671-81.
 20. Leung SY, Gwi E, Ng HK, Fung CF, Yam KY. Dysembryoplastic neuroepithelial tumor: a tumor with small neuronal cells resembling oligodendroglioma. *Am J Surg Pathol* 1994; 18: 604-14.
 21. Cervera-Pierot P, Varlet P, Chodkiewicz JP, Daumas-Duport C. Dysembryoplastic neuroepithelial tumors located in the caudate nucleus area: report of four cases. *Neurosurgery* 1997; 40: 1065-9.
 22. Fujimoto K, Ohnishi H, Tsujimoto M, Hoshida T, Nakazato Y. Dysembryoplastic neuroepithelial tumor of the cerebellum and brainstem: case report. *J Neurosurg* 2000; 93: 487-9.
 23. Ongürü O, Deveci S, Sirin S, Timurkaynak E, Günhan O. Dysembryoplastic neuroepithelial tumor in the left lateral ventricle. *Minimum Invasive Neurosurg* 2003; 46: 306-9.
 24. Hasselblatt M, Kurlemann G, Rickert CH, *et al.* Familial occurrence of dysembryoplastic neuroepithelial tumor. *Neurology* 2004; 62: 1020-1.
 25. Ranger A, Diosy D. Seizures in children with dysembryoplastic neuroepithelial tumors of the brain: a review of surgical outcomes across several studies. *Childs Nerv Syst* 2015; 31: 847-55.
 26. Chassoux F, Daumas-Duport C. Dysembryoplastic neuroepithelial tumors: where are we now? *Epilepsia* 2013; 54 Suppl 9: 129-34.
 27. Chassoux F, Rodrigo S, Mellerio C, *et al.* Dysembryoplastic neuroepithelial tumors: an MRI-based scheme for epilepsy surgery. *Neurology* 2012; 79: 1699-707.
 28. Moazzam AA, Wagle N, Shiroishi MS. Malignant transformation of DNETs: a case report and literature review. *Neuroreport* 2014; 25: 894-9.
 29. Stanesco Cosson R, Varlet P, Beuvon F, *et al.* Dysembryoplastic neuroepithelial tumors: CT, MR findings and imaging follow-up: a study of 53 cases. *J Neuroradiol* 2001; 28: 230-40.
 30. Sung CO, Suh YL. Different pattern of expression of nestin in the non-specific form of dysembryoplastic neuroepithelial tumors compared to the simple and complex forms. *J Neurooncol* 2009; 92: 7-13.
 31. Chappé C, Padovani L, Scavarda D, *et al.* Dysembryoplastic neuroepithelial tumors share with pleomorphic xanthoastrocytomas and gangliogliomas *BRAF*(V600E) mutation and expression. *Brain Pathol* 2013; 23: 574-83.
 32. Hirose T, Scheithauer BW, Lopes MB, VandenBerg SR. Dysembryoplastic neuroepithelial tumor (DNT): an immunohistochemical and ultrastructural study. *J Neuropathol Exp Neurol* 1994; 53: 184-95.
 33. Biernat W, Liberski PP, Kordek R, Zakrzewski K, Polis L, Budka H. Dysembryoplastic neuroectodermal tumor: an ultrastructural study of six cases. *Ultrastruct Pathol* 2001; 25: 455-67.

34. Park JY, Suh YL, Han J. Dysembryoplastic neuroepithelial tumor: features distinguishing it from oligodendroglioma on cytologic squash preparations. *Acta Cytol* 2003; 47: 624-9.
35. Blümcke I, Luyken C, Urbach H, Schramm J, Wiestler OD. An isomorphic subtype of long-term epilepsy-associated astrocytomas associated with benign prognosis. *Acta Neuropathol* 2004; 107: 381-8.
36. Padovani L, Colin C, Fernandez C, *et al.* Search for distinctive markers in DNT and cortical grade II glioma in children: same clinicopathological and molecular entities? *Curr Top Med Chem* 2012; 12: 1683-92.
37. Prabowo AS, van Thuijl HF, Scheinin I, *et al.* Landscape of chromosomal copy number aberrations in gangliogliomas and dysembryoplastic neuroepithelial tumours. *Neuropathol Appl Neurobiol* 2015; 41: 743-55.
38. Prayson RA, Napekoski KM. Composite ganglioglioma/dysembryoplastic neuroepithelial tumor: a clinicopathologic study of 8 cases. *Hum Pathol* 2012; 43: 1113-8.

Neuroendocrine Tumors of the Female Reproductive Tract: A Literature Review

Yi Kyeong Chun

Department of Pathology, Cheil General Hospital
and Women's Healthcare Center, Dankook
University College of Medicine, Seoul, Korea

Received: September 2, 2015
Revised: September 17, 2015
Accepted: September 19, 2015

Corresponding Author

Yi Kyeong Chun, MD
Department of Pathology, Cheil General Hospital
and Women's Healthcare Center, Dankook
University College of Medicine, 17 Seoae-ro 1-gil,
Jung-gu, Seoul 04619, Korea
Tel: +82-2-2000-7663
Fax: +82-2-2000-7779
E-mail: ykcmd@naver.com

Neuroendocrine tumors of the female reproductive tract are a heterogeneous group of neoplasms that display various histologic findings and biologic behaviors. In this review, the classification and clinicopathologic characteristics of neuroendocrine tumors of the female reproductive tract are described. Differential diagnoses are discussed, especially for non-neuroendocrine tumors showing high-grade nuclei with neuroendocrine differentiation. This review also discusses recent advances in our pathogenetic understanding of these disorders.

Key Words: Neuroendocrine tumors; Carcinoma, neuroendocrine; Gynecologic tract; Female reproductive tract

Neuroendocrine tumors (NETs) of the female reproductive tract are rare and account for about 2% of all gynecologic cancers. These tumors are a heterogeneous group of neoplasms that show various histologic findings and biologic behaviors. The four-category scheme proposed by Travis *et al.*¹ with respect to lung NETs in 1991 includes typical carcinoid tumor (TC), atypical carcinoid tumor (AC), large cell neuroendocrine carcinoma (LCNEC), and small cell neuroendocrine carcinoma (SCNEC), and is also applied to NETs of the female reproductive tract. Regardless of the organ of origin, the morphologic features of these four subtypes are similar to those of their pulmonary counterparts. Two clinically and histologically distinct types of small cell carcinoma of the ovary have been described: pulmonary and hypercalcemic. Although hypercalcemic-type small cell carcinoma is not a NET, it has been included here because the terminology 'small cell carcinoma' frequently results in its misclassification as a subtype of neuroendocrine carcinoma (NEC).

This review describes the classification and clinicopathologic characteristics of NETs of the female reproductive tract. Differential diagnoses are discussed, especially for non-NETs showing high-grade nuclei with neuroendocrine differentiation. This review also discusses recent advances in our pathogenetic under-

standing of these disorders.

NEUROENDOCRINE TUMORS OF THE UTERINE CERVIX

Classification of cervical NETs

Cervical NETs have been described using various terminologies without strict diagnostic criteria, such as carcinoid tumor, argyrophil cell carcinoma, apudoma, poorly differentiated small cell carcinoid, small cell tumor with neuroepithelial features, neuroendocrine carcinoid tumor, endocrine carcinoma intermediate cell type, small cell undifferentiated carcinoma, oat cell carcinoma, small cell carcinoma, SCNEC, NEC, neuroendocrine features in poorly differentiated and undifferentiated carcinoma, large cell carcinoma, and LCNEC.²⁻⁵ These varied terminologies have led to poor recognition of the incidence, clinicopathologic features, and biologic behavior of cervical NETs.

The present four-category classification of cervical NETs composed of TC, AC, LCNEC, and SCNEC was established in 1997 by the College of American Pathologists and the National Cancer Institute⁴ and has been used as the World Health Organization (WHO) classification scheme since 2003.⁶ SCNEC is by far

the most common NET of the cervix, followed by LCNEC. Cervical TCs are extremely rare.⁶ Briefly, TCs show trabecular, insular, or sheet-like architectural patterns. The small, round, and uniform tumor cells have a finely granular chromatin pattern and inconspicuous nucleoli. Mitotic activity is exceedingly low. ACs share patterns of growth with TC, but show hypercellularity, cytologic atypia, increased mitotic activity (five to 10 mitotic figures per 10 high power fields [HPFs]), and necrotic foci. LCNECs grow in sheets with organoid, trabecular, or cord-like patterns, often with peripheral palisading and necrosis. These large neoplastic cells have abundant eosinophilic cytoplasm with vesicular high-grade nuclei and prominent nucleoli. This tumor type has more than 10 mitotic figures per 10 HPFs. Immunohistochemical confirmation of neuroendocrine differentiation is required based on neuroendocrine markers, such as chromogranin, synaptophysin, and CD56. SCNECs show small, round or fusiform cells with scant cytoplasm and hyperchromatic nuclei, with finely granular chromatin, and absent or inconspicuous nucleoli. Nuclear molding, numerous mitotic figures, and apoptotic bodies are common. Architectural patterns include nesting, trabeculae, peripheral palisading, rosette formations, and sheet-like growth. Immunohistochemical staining for neuroendocrine markers is not required for diagnosis.⁴

The WHO classification of gastroentero-pancreatic NETs is a three-tiered grading system, primarily based on tumor mitotic activity and Ki-67 labeling index.⁷ Ki-67 labeling index is also incorporated in the recent WHO classification of pulmonary NETs.⁸ However, the Ki-67 index is not included in the 2014 WHO diagnostic criteria for cervical NETs.⁶ Further study is required to validate the correlation between Ki-67 index and clinical outcomes in cervical NETs.

Carcinoid tumors

Primary cervical carcinoids are extremely rare, and metastatic carcinoids should be excluded to ensure a diagnosis of primary cervical carcinoid tumor. In 1976, Albores-Saavedra *et al.*⁵ reported 12 cases of 'carcinoid' tumor, dividing them into well-differentiated and poorly differentiated types based on microscopic findings. Cancers resembling islet cell tumors or medullary thyroid carcinoma were diagnosed as well-differentiated 'carcinoid,' while those similar to oat cell carcinoma of the lung were diagnosed as poorly differentiated 'carcinoid.' These authors appear to have used 'carcinoid' as a comprehensive term for NET.

Generally, the prognosis of TC and AC is better than that of LCNEC and SCNEC. The prognosis of cervical TC is uncertain

due to confusing usage of diagnostic terminology and limited follow-up data.⁵ Cervical AC is regarded as an aggressive tumor, like SCNEC and LCNEC. AC and LCNEC can be differentiated based on mitotic activity, nuclear atypia, and extent of necrosis. Due to the overlapping histologic features of these tumors, differentiating between AC and LCNEC can be problematic.^{9,10}

Neuroendocrine carcinomas

LCNEC and SCNEC comprise about 2% of cervical carcinomas and are highly aggressive, even at early stages.⁴ Due to the aggressive clinical behaviors of both SCNEC and LCNEC, the clinical significance of subdividing cervical NECs is uncertain. NECs are regarded by some as a different morphologic expression of the same neoplasm.^{10,11} They tend to have early nodal involvement, distant metastasis, and advanced surgical stage at initial diagnosis. The overall prognosis of cervical NECs is worse than that of cervical squamous cell carcinoma or adenocarcinoma of comparable stage.^{12,13}

The majority (> 90%) of cervical NECs are associated with high-risk human papillomavirus (HPV), with type 18 being the most prevalent. Immunohistochemical staining for p16 is almost always positive in cervical NECs because of this HPV association.¹⁴

These tumors often coexist with carcinoma *in situ*, invasive squamous cell carcinoma, or adenocarcinoma. It is important that clinicians do not miss the NEC component, because the prognosis of pure NEC is not significantly different from that of NEC admixed with non-NEC. The trickiest differential diagnosis of SCNEC is a small cell variant of squamous cell carcinoma. The important morphologic features favoring SCNEC are nuclear molding, finely dispersed nuclear chromatin, necrosis, crush artifact, mitosis, and numerous apoptotic bodies.¹⁵ Differential diagnoses of NECs, especially LCNECs, include poorly differentiated squamous carcinoma and adenocarcinoma, basaloid squamous cell carcinoma, undifferentiated carcinoma, embryonal rhabdomyosarcoma, lymphoma, melanoma, and peripheral neuroectodermal tumor.^{13,15}

The origin of cervical NETs is not clear. Unlike diffuse idiopathic pulmonary neuroendocrine cell hyperplasia, which is a precursor to pulmonary NETs, there is no defined precursor lesion in the normal endocervix, though isolated neuroendocrine cells are seen in normal endocervical glands.¹⁶ An X-chromosome clonality assay showed monoclonality of both components in a case of mixed LCNEC and mucinous carcinoma. This suggests that LCNEC might have arisen from an invasive mucinous adenocarcinoma.¹⁷

Immunohistochemical staining

The diagnosis of SCNEC is based on histologic features. Neuroendocrine markers do not have to be demonstrated if morphologic findings are suitable for this aggressive tumor. The tumor displays 33% to 100% positivity for neuroendocrine markers.^{4,13,15,18,19} Unlike SCNEC of the cervix, a definitive diagnosis of LCNEC requires positive staining of at least one neuroendocrine marker.^{4,15} Chromogranin, synaptophysin, and CD56 are commonly used neuroendocrine markers. However, CD56 is considered a less specific marker of neuroendocrine differentiation compared to chromogranin and synaptophysin.^{11,20} This staining should be carefully interpreted, as CD56 can be present in non-NECs, such as squamous cell carcinomas and adenocarcinomas.²⁰

Neuroendocrine differentiation is common in cervical non-NECs such as adenocarcinoma, adenosquamous carcinoma, and squamous cell carcinoma. Positive staining for chromogranin and synaptophysin has been reported in 14 (20.9%) and 5 (9%) cervical non-NEC cases, respectively.^{21,22} Without morphologic features of neuroendocrine differentiation, these cases should not be diagnosed as LCNEC. Controversial results have been reported regarding the clinical significance of neuroendocrine differentiation in otherwise typical carcinomas. Savargaonkar *et al.*²¹ found that chromogranin expression does not influence the clinical behavior of cervical non-NECs. On the contrary, Chavez-Blanco *et al.*²² reported that synaptophysin expression seems to be correlated with a poor outcome in cervical non-NECs. Thyroid transcription factor-1 (TTF-1) is commonly positive (33%–84%) in cervical NECs and might be a useful marker of these tumors, though it cannot distinguish these tumors from primary pulmonary tumors.^{23,24} In conjunction with neuroendocrine markers, p63 is useful in distinguishing between squamous cell carcinoma and small or large cell NECs.²⁴ Focal or diffuse p63 positivity is seen in 43% of cervical NECs, illustrating that this marker is not specific for squamous differentiation.^{24,25} p53 protein is expressed in 43% of cervical NECs.²⁶

NEUROENDOCRINE TUMORS OF THE ENDOMETRIUM

NETs of the endometrium include TC, SCNEC, and LCNEC. Only three cases of primary endometrial TCs have been reported in the English literature.^{27–29} One International Federation of Gynecology and Obstetrics (FIGO) stage 1 case showed vaginal recurrence approximately six and a half years after the initial presentation.²⁹ To the best of our knowledge, endometrial AC

has not been described in the English literature.

Neuroendocrine carcinomas

SCNEC and LCNEC of the endometrium are very uncommon, representing only 0.8% of endometrial cancers.³⁰ These are highly aggressive tumors with a propensity for systemic spread and poor prognosis. The tumors usually form bulky, intraluminal masses with deep myometrial invasion.

SCNEC of the endometrium requires morphologically prototypic features of small cell carcinoma, unequivocal evidence of endometrial origin, and immunohistochemical staining of at least one neuroendocrine marker, according to the diagnostic criteria proposed by van Hoesen *et al.*³¹ However, as with other sites, a small number of SCNEC cases show distinctive histologic features of small cell carcinoma without any immunohistochemical evidence of neuroendocrine differentiation.¹⁵

Endometrial NECs are often combined with other epithelial neoplasms. Endometrioid carcinoma is the most common non-NEC component, and 50% to 80% of NEC cases are admixed with FIGO grade 1 or 2 endometrioid carcinoma. Mixed NEC and conventional endometrial carcinoma can be misinterpreted as FIGO grade 3 endometrioid carcinoma and dedifferentiated carcinoma.^{30,32,33} The frequent association of NEC with low-grade endometrioid carcinoma suggests that some endometrial NECs may arise from neuroendocrine cells in endometrioid carcinomas. Interestingly, scattered neuroendocrine cells are reported in the normal endometrial gland and in endometrial carcinoma.³⁴ These tumors can also form from pluripotent stem cells of the epithelium, which have a capacity for both neuroendocrine and endometrioid glandular differentiation. Lastly, a collision tumor could arise from separate epithelial and NETs.³⁵

NEC might be a part of the carcinoma component of carcinosarcoma.^{36,37} Uncommon endometrial tumors composed of papillary serous carcinoma and small cell carcinoma have been reported.^{35,38}

Differential diagnoses of NEC

NECs of the endometrium should be differentiated from various tumors showing high-grade nuclear features with a predominantly solid growth pattern. LCNEC is much more difficult to diagnose than SCNEC, as the tumor might not show the characteristic morphologic features of neuroendocrine differentiation, such as hyperchromatic nuclei, salt and pepper chromatin, and nuclear molding. To establish a diagnosis of endometrial LCNEC, neuroendocrine patterns (nesting, trabeculae, rosettes, and palisading) should be present in at least part of the

tumor, along with expression of one or more of the neuroendocrine markers (Fig. 1).

Undifferentiated endometrial carcinoma is defined as a malignant epithelial neoplasm with no evidence of differentiation. When undifferentiated carcinoma is associated with a well to moderately differentiated endometrioid carcinoma, it should be diagnosed as a dedifferentiated carcinoma. Dedifferentiated carcinoma does not appear to confer better clinical outcomes than undifferentiated carcinoma, despite the presence of a better differentiated non-NEC component. As NEC is often accompanied by low-grade endometrioid carcinoma, it can be misinterpreted as dedifferentiated carcinoma. In addition, dedifferentiated carcinoma is frequently misdiagnosed as NEC, FIGO grade 2 or 3 endometrioid carcinoma, carcinosarcoma, high-grade endometrial stromal sarcoma, lymphoma, granulosa cell tumor, or epithelioid sarcoma.³⁹

Morphologically undifferentiated carcinoma is composed of

small to intermediate-sized, discohesive cells growing in a patternless fashion without gland formation. Most cases have necrosis and more than 25 mitotic figures per 10 HPFs. Immunohistochemical staining for cytokeratin and epithelial membrane antigen (EMA) shows focal positivity, usually in less than 10% of tumor cells. Dedifferentiated carcinoma has different cytologic features in the undifferentiated carcinoma and endometrioid carcinoma components (Fig. 2). On the contrary, poorly differentiated endometrioid carcinoma shows similar tumor cells in the solid and glandular areas (Fig. 3). The solid area often resembles poorly differentiated non-keratinizing squamous cell carcinoma and tends to have a cohesive appearance and diffuse positivity for cytokeratin and EMA.⁴⁰ Poorly differentiated endometrioid carcinoma should be distinguished from NEC and undifferentiated/dedifferentiated carcinoma.⁴¹ This distinction has important clinical implications, as endometrioid carcinoma confers a much better prognosis than NEC and undifferentiat-

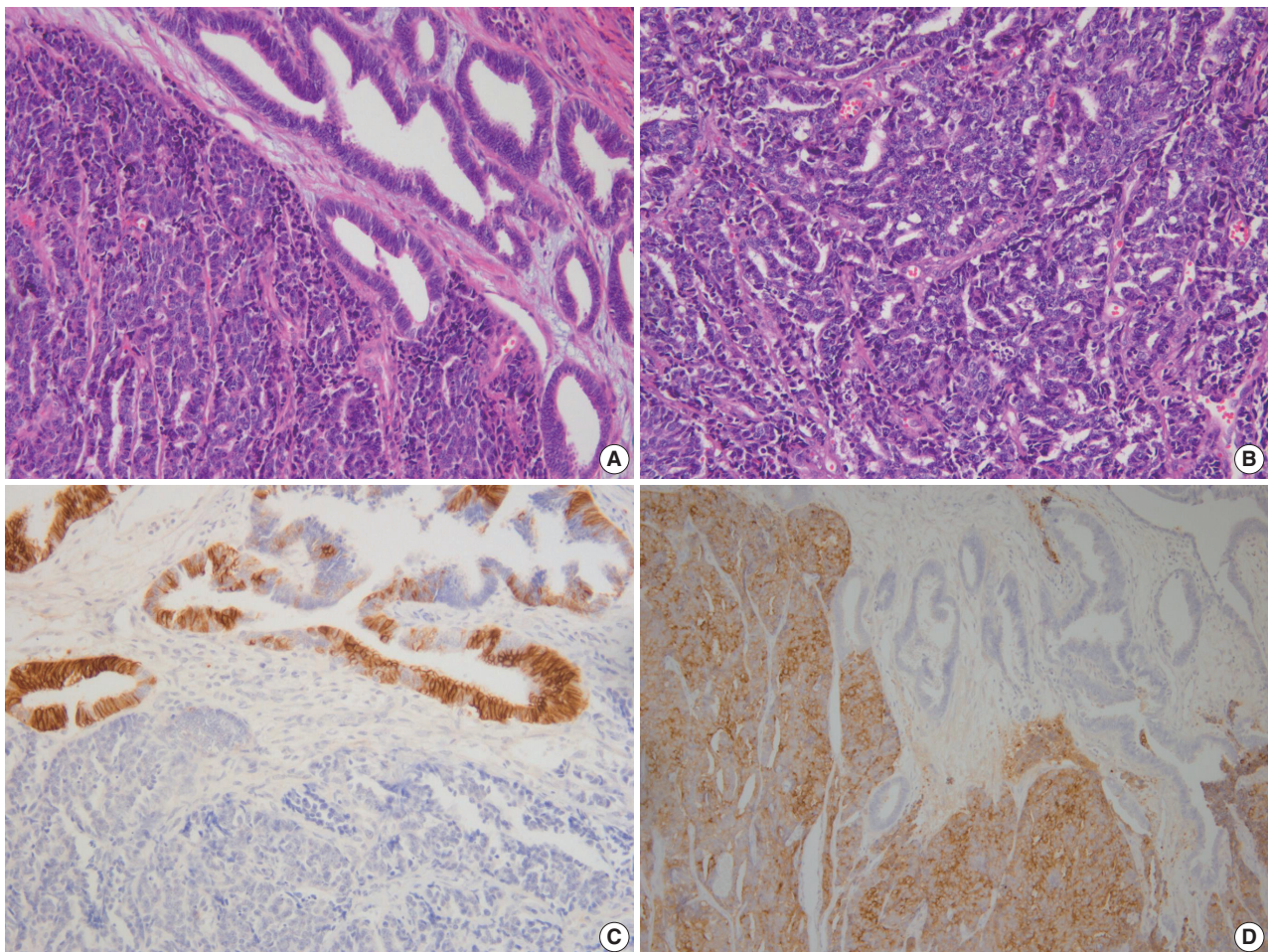


Fig. 1. (A) Endometrial large cell neuroendocrine carcinoma (LCNEC) admixed with grade 1 endometrioid carcinoma. (B) Large vesicular nuclei and prominent nucleoli in LCNEC. (C) CD56 immunostaining: positive in endometrioid carcinoma and negative in LCNEC. (D) Diffuse synaptophysin expression in LCNEC.

ed/ dedifferentiated carcinoma.⁴²

Serous carcinoma with a solid growth pattern and massive necrosis should be differentiated from LCNEC, dedifferentiated carcinoma, and poorly differentiated endometrioid carcinoma. The serous component is negative for neuroendocrine markers, but diffuse expressions of p16 and p53 have been reported in both serous carcinoma and NEC.⁴³ Along with neuroendocrine makers, it is important to find diagnostic foci of classical serous carcinoma even when the tumor is predominantly solid.³⁸

Neuroendocrine expression in non-NECs

Non-NECs of the endometrium can express neuroendocrine markers but lack typical neuroendocrine histomorphology. Expression of neuroendocrine markers is reported in 62.5% of FIGO grade 3 endometrioid carcinomas, which are more frequently associated with deep myometrial invasion, metastasis to distant organs, and decreased survival than tumors without neuroendocrine expression. A high-grade tumor with diffuse,

strong neuroendocrine positivity should be classified as a NEC rather than a poorly differentiated endometrioid carcinoma.⁴⁴

Expression of neuroendocrine markers is reported in 30% and 41% of undifferentiated carcinomas, and most cases exhibit focal neuroendocrine expression in less than 10% of the cells.^{39,45} There is no reported difference in overall survival with or without neuroendocrine differentiation in undifferentiated carcinomas. Undifferentiated carcinoma is a highly aggressive tumor, regardless of neuroendocrine expression.^{40,45}

NEUROENDOCRINE TUMORS OF THE OVARY

Carcinoid tumors

Ovarian carcinoid tumors are monodermal teratomas occurring in a pure form (15%) or combined with other teratomatous components (85%), such as a dermoid cyst or a struma ovarii. They can also be a component of mucinous and Brenner tumors. Carcinoid tumors of the ovary can be primary or metastatic;

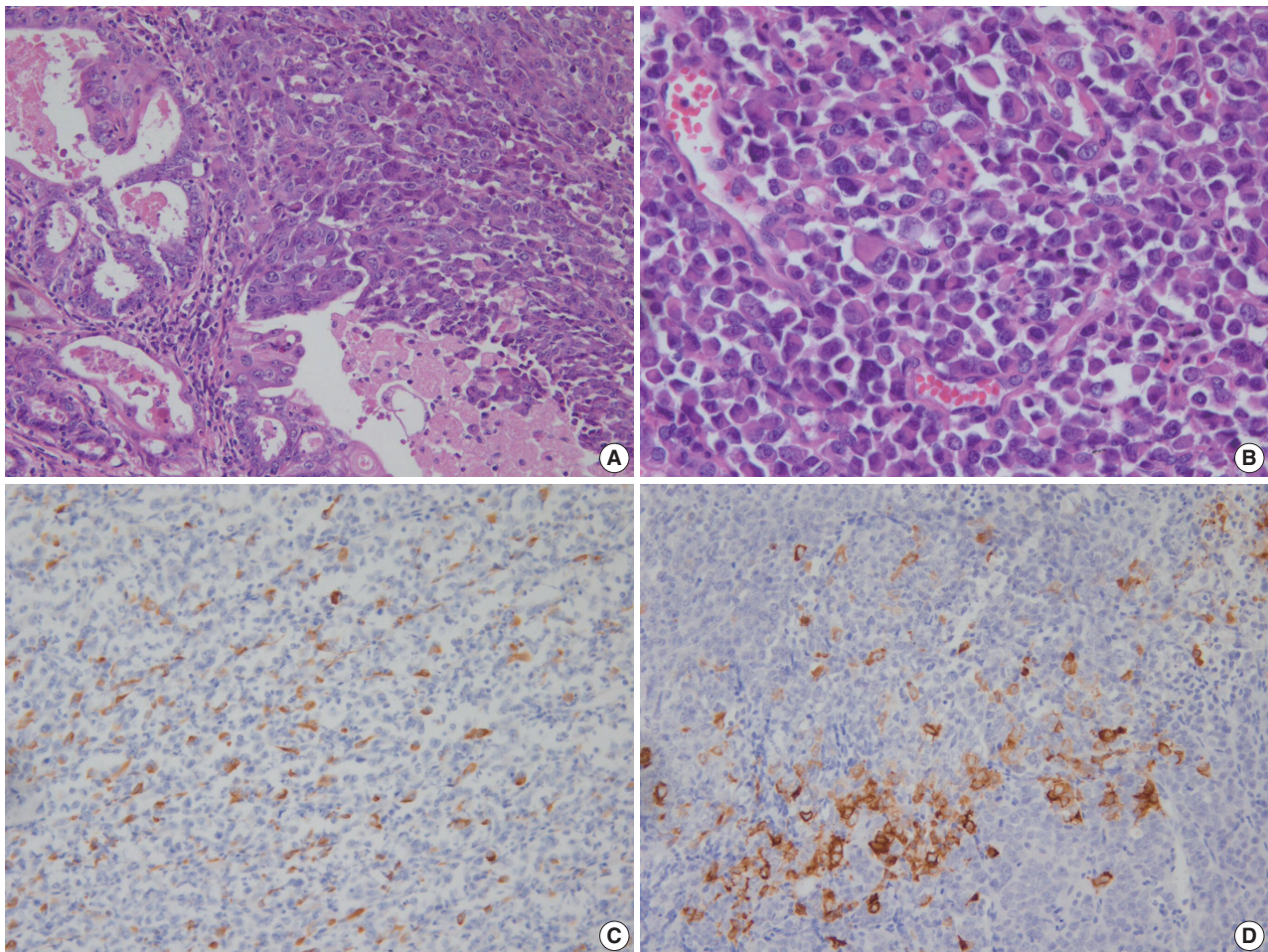


Fig. 2. (A) Dedifferentiated carcinoma composed of undifferentiated carcinoma and grade 1 endometrioid carcinoma. (B) Discohesive tumor cells growing in a patternless fashion without gland formation. Focal positivity of cytokeratin (C) and synaptophysin (D) immunostaining.

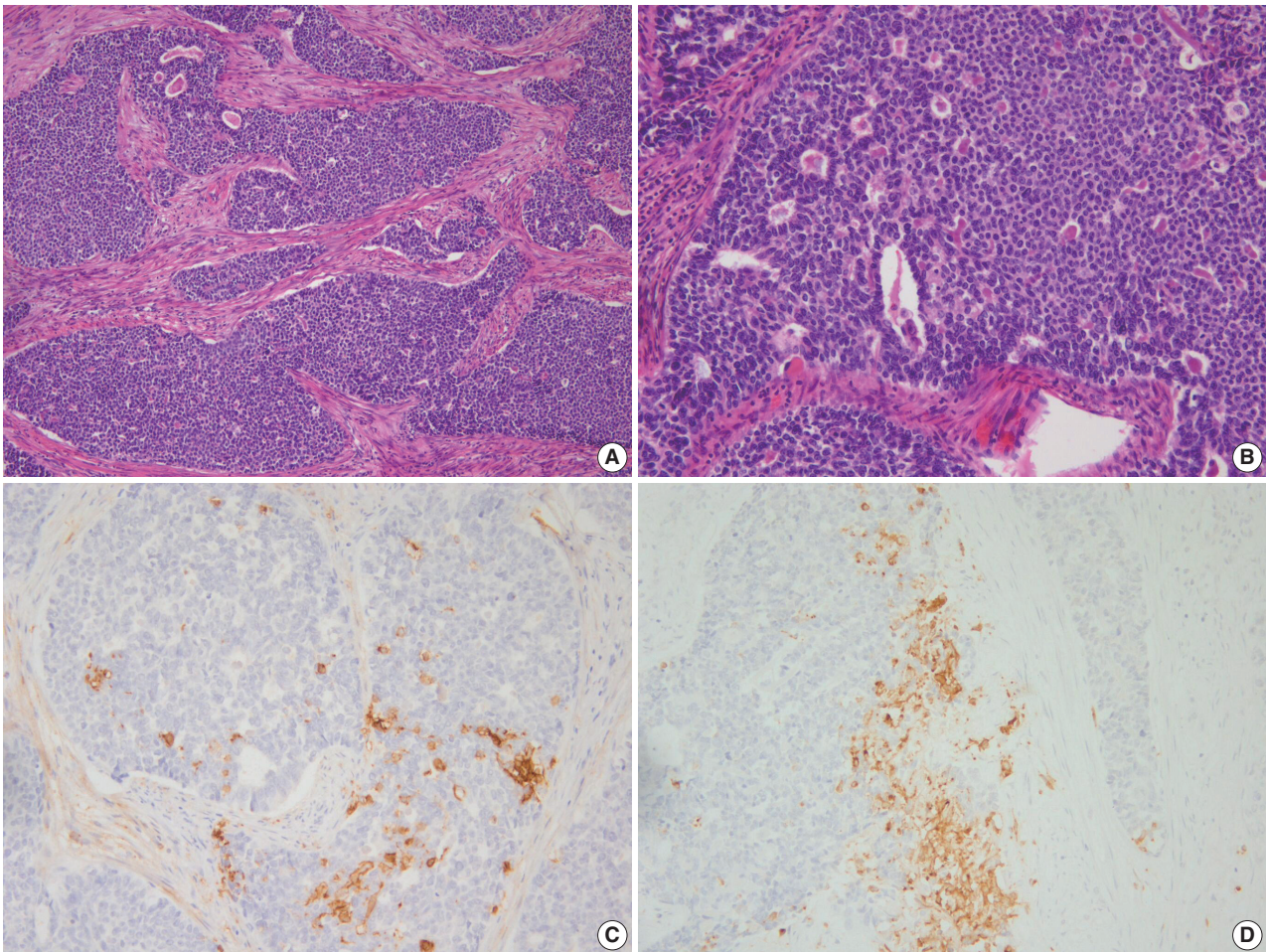


Fig. 3. (A) Grade 3 endometrioid carcinoma mimicking neuroendocrine carcinoma at low magnification. (B) At high magnification, grade 3 endometrioid carcinoma shows similar tumor cells in the solid and glandular areas. Focal positivity for neuroendocrine markers of CD56 (C) and synaptophysin (D).

these metastases are usually from gastrointestinal tumors. Primary ovarian carcinoids are mostly confined to a unilateral ovary and behave in an indolent fashion, whereas metastatic tumors tend to be aggressive and associated with poor outcome. Therefore, the distinction between ovarian primary and metastatic carcinoids is critical. In addition to a clinical history of carcinoid tumor in an extraovarian site, such as the gastrointestinal tract or lung, metastatic carcinoids more often show bilateral distribution, multinodular growth, extraovarian tumor nodules, lymphovascular invasion, and absence of teratomatous elements. Ovarian carcinoids can be confused with other primary ovarian tumors, particularly Brenner tumors, granulosa cell tumors, and Sertoli or Sertoli-Leydig cell tumors.^{15,46-51}

Primary carcinoid tumors of the ovary are divided into insular, trabecular, strumal, and mucinous carcinoids. Mixed forms include carcinoid tumors that contain two or more of the aforementioned categories and those that are mixed other types of pri-

mary ovarian tumors. Briefly, insular carcinoid, considered to be of midgut derivation, is the most common type of primary ovarian carcinoid tumor. It is composed of small acini and solid nests of round cells with uniform nuclei and abundant eosinophilic cytoplasm. Carcinoid syndrome occurs in about one-third of patients with insular carcinoid, despite the absence of metastasis.⁴⁸ Trabecular carcinoid, considered to be of hindgut or foregut derivation, shows wavy ribbons or a trabecular arrangement of cells in a dense fibrous stroma. The tumor cells are one or two layers thick, and the nuclei are perpendicular to the axis of the ribbon or the trabeculae. Strumal carcinoid is characterized by the coexistence of carcinoid and thyroid tissue. Mucinous carcinoid, the least common type of ovarian carcinoid, resembles a goblet cell carcinoid arising in the appendix. It must be distinguished from a Krukenberg tumor and has been subdivided into well differentiated mucinous carcinoid, atypical mucinous carcinoid, carcinoma arising in mucinous carcinoid, and mixed mucinous

carcinoid and other carcinoid types.^{15,46-51}

Primary ovarian carcinoid tumors confined to the ovary and treated with surgery alone are expected to have an excellent overall outcome.⁴⁷ Robboy *et al.*⁴⁸ reported two recurrences in 48 cases of primary insular carcinoid of the ovary and calculated a survival rate of 95% and 88% at 5 and 10 years, respectively. Mucinous carcinoids might have more aggressive behavior than other types of ovarian carcinoids, particularly if associated with atypical features.⁵⁰ Some ovarian AC cases have been misdiagnosed as 'carcinoid' or 'strumal carcinoid'.^{52,53} Kurabayashi *et al.*⁵³ reported a case of stage IA strumal 'carcinoid' tumor showing multiple bone and breast metastases 3.5 years postoperatively. Histologic features of the case were consistent with AC. The term 'AC' is not included in the past or current WHO classification of ovarian NETs.^{51,54} Division into four subcategories (insular, trabecular, strumal, and mucinous) instead of TC and AC has complicated the comparison between follow-up data from ovarian carcinoids and carcinoids from other organs. Further study is clearly necessary to better understand the clinical course of ovarian carcinoids.

Carcinoid tumors are immunoreactive to neuroendocrine markers, such as chromogranin, synaptophysin, and CD56. Chromogranin and synaptophysin are excellent discriminatory neuroendocrine markers for a carcinoid tumor. In a study of 42 carcinoid tumors, chromogranin, synaptophysin, and CD56 were expressed in 100%, 98%, and 57% of samples, respectively. CD56 was also positive in 48% of Sertoli cell tumors and in 25% of endometrioid carcinomas. CD56 is neither highly sensitive nor specific enough for neuroendocrine lineage and is of limited value in the identification of ovarian carcinoid tumors.⁵⁵ Various peptide hormones such as serotonin, gastrin, pancreatic polypeptide, glucagon, vasoactive intestinal peptide, prolactin, and somatostatin can be detected in about 25% of cases.⁵⁶ Estrogen receptors and progesterone receptors are usually negative in carcinoid tumors. CDX2, TTF-1, PAX8, and cytokeratins 7 and 20 are used for the discrimination of primary and metastatic carcinoids. As ovarian carcinoid can arise from various teratomatous elements, such as the midgut, hindgut, and respiratory epithelium, the interpretation of immunohistochemical staining should be conducted very prudently.^{57,58}

Small cell carcinoma, pulmonary type

Two types of clinically and histologically distinct small cell carcinoma of the ovary have been described: small cell carcinoma, hypercalcemic type (SCCOHT), and small cell carcinoma, pulmonary type (SCCOPT). Clinical features favoring SCCOPT

include older age and the absence of hypercalcemia. Histologically, SCCOPT shows characteristic features of SCNEC, such as finely dispersed chromatin, inconspicuous nucleoli, and nuclear molding, whereas SCCOHT has clumped chromatin, prominent nucleoli, and the presence of larger cells in about 50% of cases. Follicle-like spaces are frequently seen in the hypercalcemic type, but are lacking in the pulmonary type. Ovarian surface epithelial tumors are present in more than 50% of pulmonary type tumors, but are absent in the hypercalcemic type.⁵⁹

SCCOPT is a highly aggressive SCNEC and must be distinguished from metastatic small cell carcinoma from other locations, particularly the lung. Usually, bilateral ovarian involvement is a substantial clue for a metastatic tumor, but is also seen in 45% of SCCOPTs. As this tumor shows variable TTF-1 expression, expression of this marker cannot reliably distinguish SCCOPT from pulmonary small cell carcinoma.⁶⁰ These tumors are probably of surface epithelial-stromal origin because they are frequently associated with surface epithelial tumors. In a previous study, eight of 11 SCCOPT cases were associated with surface epithelial tumors.⁵⁹ Rare cases arising in an ovarian teratoma have been reported.^{61,62} A diagnosis of SCCOPT can be made in the absence of neuroendocrine marker positivity if the morphologic appearance is typical SCNEC. Perinuclear dot-like cytokeratin 20 staining has been reported in this tumor, as in Merkel cell carcinoma and salivary gland small cell carcinoma.⁶³

Large cell neuroendocrine carcinoma

LCNECs of the ovary have also been reported as non-small cell NEC, undifferentiated non-small cell carcinoma, and NEC, non-small cell type.⁶⁴⁻⁶⁷ Primary ovarian LCNEC is extremely rare and has a worse prognosis than usual ovarian carcinomas, even when the diagnosis is made at an early stage. In most cases, there are concomitant ovarian surface epithelial tumors, such as mucinous borderline tumor or mucinous carcinoma, endometrioid carcinoma, serous carcinoma, unclassified high-grade carcinoma, or teratoma.⁶⁴⁻⁶⁷ The NEC component varies from 10% to 90% when it is combined with an epithelial tumor or teratoma. The presence of an NEC component in an otherwise usual epithelial tumor should be reported because of the potential negative prognostic impact of NEC histology. Generally speaking, a neuroendocrine component might have a prognostic impact when it reaches a certain proportion of the overall tumor. The percentage of NEC component that is necessary to confer a prognosis worse than that of the accompanying epithelial tumor is not clear.⁶⁷ Primary pure LCNEC of the ovary is very rare.^{68,69}

LCNECs probably arise from the neuroendocrine cells present

in surface epithelial-stromal tumors or germ cell tumors.⁷⁰ In a case of mixed LCNEC and mucinous borderline ovarian tumor, clonality analysis using the human androgen receptor gene showed monoclonality in both components, suggesting that the LCNEC might have arisen from the mucinous epithelial tumor.⁷¹ The common coexistence of NEC and epithelial tumors, along with the monoclonality of the two components, implies a common cellular origin of the neuroendocrine and epithelial components.^{17,72} A case of LCNEC associated with serous carcinoma revealed a different pattern of microsatellite instability in both components. A dual origin with concomitant transformation of epithelial cells and neuroendocrine cells might be possible in that case.⁶⁵

In one previous study, ovarian LCNECs were misdiagnosed as dysgerminoma, sex cord tumor, or other types of carcinoma in eight of 11 cases.⁶⁴ Attention to the histologic features of neuroendocrine differentiation and the use of immunohistochemical stains are necessary to resolve this potential under-recognition.⁶⁴ CD56 is known to be a less specific neuroendocrine marker compared to chromogranin and synaptophysin.^{11,20,55} However, chromogranin and synaptophysin can be detected in ovarian Sertoli cell tumors, Sertoli-Leydig cell tumors, and endometrioid tumors, which could be a potential pitfall resulting in the misdiagnosis of NETs.^{55,73}

LCNEC associated with serous carcinoma has rarely been reported in the ovary, as in the endometrium.^{65,74} Immunohistochemical evidence of neuroendocrine differentiation in ovarian serous carcinoma is more frequent than morphological evidence. Taube *et al.*⁷⁵ reported synaptophysin and chromogranin expression in 6.7% and 20.7% of high-grade ovarian serous carcinomas, respectively, and found that patients with synaptophysin expression in more than 20% of tumor cells had a significantly shorter survival time than those with 0% to 20% positive cells.

Small cell carcinoma, hypercalcemic type

SCCOHT of the ovary is a highly aggressive neoplasm affecting young females and is associated with paraneoplastic hypercalcemia in two-thirds of cases. Microscopic findings show a sheet-like arrangement of cells punctuated by follicle-like spaces. The tumor cells are typically small and round with hyperchromatic nuclei and brisk mitotic activity. A large cell component with moderate to abundant eosinophilic cytoplasm is seen in about 50% of cases. Tumors composed exclusively of large cells are designated the 'large cell variant' of SCCOHT. The large cells can have a rhabdoid appearance. Differential diagnoses include juvenile and adult granulosa cell tumors, high-grade se-

rous carcinoma, desmoplastic small round cell tumor, dysgerminoma, Ewing sarcoma, primitive neuroectodermal tumor, neuroblastoma, round cell sarcoma, high-grade endometrial stromal sarcoma, undifferentiated carcinoma, lymphoma, melanoma, and SCNEC.⁷⁶

Ovarian SCCOHT is often misunderstood or confused with a subtype of NEC due to the usage of the term 'small cell carcinoma'. This tumor is included in a miscellaneous category in the 2014 WHO classification of female reproductive organs.⁷⁷ Recently, somatic and germline *SMARCA4* mutations accompanied by the loss of BRG1 protein expression in immunohistochemistry have been described in SCCOHTs.⁷⁸⁻⁸¹ To date, the diagnosis of SCCOHT has been made on the basis of microscopic findings without any specific immunohistochemical markers. The loss of BRG1 protein expression is confirmed to be a useful marker for diagnosing SCCOHT, although the interpretation should be conducted carefully due to the possible heterogeneity and variable intensity of this immunostaining.⁸² BRG1 and INI-1 are members of the SWI/SNF complex and are involved in chromatin remodeling. The alternative expression of INI-1 and BRG1 is regarded as a molecular hallmark of malignant rhabdoid tumor. The histological resemblance between SCCOHT and malignant rhabdoid tumor became a trigger to evaluate INI-1 and BRG1 immunostaining in SCCOHT. In addition to the lack of BRG1 immunoreactivity, SCCOHT cases also showed retained INI-1 expression.^{78,82,83} Currently, SCCOHT is considered to be an ovarian malignant rhabdoid tumor.^{78,82,83}

CONCLUSION

The four-category scheme including TC, AC, LCNEC, and SCNEC is still applied to NETs of the female reproductive tract. Ki-67 labeling index is not included in the diagnostic criteria of the 2014 WHO classification of cervical NETs.⁶

The prevalence and biologic behavior of NETs vary along the female reproductive tract. Carcinoid tumors are extremely rare in the cervix and the endometrium, and their clinical behavior is uncertain due to the scarcity of follow-up data. However, in the ovary, carcinoid tumors are the most common NET. Division into four subcategories (insular, trabecular, strumal, and mucinous) instead of TC and AC has obscured the comparison of follow up data from ovarian carcinoids with that of carcinoids in other organs.

Both small cell and large cell NECs show highly aggressive clinical behavior, regardless of the site of origin. The uterine cervix is the most common site for NECs, especially SCNECs in

the female reproductive tract. Since endometrial NEC is often accompanied by low-grade endometrioid carcinoma, it can be misdiagnosed as FIGO grade 3 endometrioid carcinoma or de-differentiated carcinoma.^{30,33} As NECs are rare and tumors with neuroendocrine differentiation are infrequently found in the endometrium or ovary, various tumors are included in the differential diagnoses. Attention to the histologic features of neuroendocrine differentiation and the immunohistochemical staining of neuroendocrine markers is necessary to reach a correct diagnosis. CD56 is known to be a less specific neuroendocrine marker compared to chromogranin and synaptophysin.^{11,20,55} The common coexistence of NEC and epithelial tumors along with the monoclonality of the two components implies a common cellular origin of the neuroendocrine and epithelial components.^{17,72}

Ovarian SCCOPT is a highly aggressive SCNEC and must be distinguished from metastatic small cell carcinoma from other locations. Currently, SCCOHT is considered to be an ovarian malignant rhabdoid tumor, as inactivation of *SMARCA4* accompanied by the loss of BRG1 protein and the retention of INI-1 in immunohistochemistry has been described in this aggressive tumor.^{78,82,83}

Conflicts of Interest

No potential conflict of interest relevant to this article was reported.

Acknowledgments

The author is very grateful to Professor Je G. Chi, who passed away last winter. He was a great mentor and friend of mine. This work is dedicated to his memory.

REFERENCES

1. Travis WD, Linnoila RI, Tsokos MG, *et al.* Neuroendocrine tumors of the lung with proposed criteria for large-cell neuroendocrine carcinoma: an ultrastructural, immunohistochemical, and flow cytometric study of 35 cases. *Am J Surg Pathol* 1991; 15: 529-53.
2. Matsuyama M, Inoue T, Ariyoshi Y, *et al.* Argyrophil cell carcinoma of the uterine cervix with ectopic production of ACTH, beta-MSH, serotonin, histamine, and amylase. *Cancer* 1979; 44: 1813-23.
3. Johannessen JV, Capella C, Solcia E, Davy M, Sobrinho-Simões M. Endocrine cell carcinoma of the uterine cervix. *Diagn Gynecol Obstet* 1980; 2: 127-34.
4. Albores-Saavedra J, Gersell D, Gilks CB, *et al.* Terminology of endocrine tumors of the uterine cervix: results of a workshop sponsored by the College of American Pathologists and the National Cancer Institute. *Arch Pathol Lab Med* 1997; 121: 34-9.
5. Albores-Saavedra J, Larraza O, Poucell S, Rodríguez Martínez HA. Carcinoid of the uterine cervix: additional observations on a new tumor entity. *Cancer* 1976; 38: 2328-42.
6. Colgan TJ, Kim I, Hirschowitz L, McCluggage WG. Neuroendocrine tumours. In: Kurman RJ, Carcangiu ML, Herrington CS, Young RH, eds. WHO classification of tumours of female reproductive organs. 4th ed. Lyon: IARC Press, 2014; 196-8.
7. Rindi G, Arnold R, Bosman FT, *et al.* Nomenclature and classification of neuroendocrine neoplasms of the digestive system. In: Bosman FT, Carneiro F, Hruban RH, Theise ND, eds. WHO classification tumours of the digestive system. 4th ed. Lyon: IARC Press, 2010; 13-4.
8. Brambilla E, Gazdar A, Powell CA, *et al.* Neuroendocrine tumours small cell carcinoma. In: Travis WD, Brambilla E, Burke AP, Marx A, Nicholson AG, eds. WHO classification tumours of the lung, pleura, thymus and heart. 4th ed. Lyon: IARC Press, 2015; 63-8.
9. Yasuoka T, Hashimoto H, Hamada K, Fujioka T, Nawa A. Atypical carcinoid of the uterine cervix with aggressive clinical behavior: a case report. *Gynecol Oncol Case Rep* 2014; 7: 4-6.
10. Witkiewicz AK, Wright TC, Ferenczy A, Ronnett BM, Kurman RJ. Carcinoma and other tumors of the cervix. In: Kurman RJ, Ellenson LH, Ronnett BM, eds. Blaustein's pathology of the female genital tract. 6th ed. New York: Springer, 2011; 253-304.
11. Albores-Saavedra J, Latif S, Carrick KS, Alvarado-Cabrero I, Fowler MR. CD56 reactivity in small cell carcinoma of the uterine cervix. *Int J Gynecol Pathol* 2005; 24: 113-7.
12. Atienza-Amores M, Guerini-Rocco E, Soslow RA, Park KJ, Weigelt B. Small cell carcinoma of the gynecologic tract: a multifaceted spectrum of lesions. *Gynecol Oncol* 2014; 134: 410-8.
13. Rekhi B, Patil B, Deodhar KK, *et al.* Spectrum of neuroendocrine carcinomas of the uterine cervix, including histopathologic features, terminology, immunohistochemical profile, and clinical outcomes in a series of 50 cases from a single institution in India. *Ann Diagn Pathol* 2013; 17: 1-9.
14. Masumoto N, Fujii T, Ishikawa M, *et al.* p16 overexpression and human papillomavirus infection in small cell carcinoma of the uterine cervix. *Hum Pathol* 2003; 34: 778-83.
15. Rouzbahman M, Clarke B. Neuroendocrine tumors of the gynecologic tract: select topics. *Semin Diagn Pathol* 2013; 30: 224-33.
16. Koo CW, Baliff JP, Torigian DA, Litzky LA, Gefter WB, Akers SR. Spectrum of pulmonary neuroendocrine cell proliferation: diffuse idiopathic pulmonary neuroendocrine cell hyperplasia, tumorlet, and carcinoids. *AJR Am J Roentgenol* 2010; 195: 661-8.
17. Yasuoka H, Tsujimoto M, Ueda M, *et al.* Monoclonality of composite large-cell neuroendocrine carcinoma and invasive intestinal-

- type mucinous adenocarcinoma of the cervix: a case study. *Int J Gynecol Pathol* 2013; 32: 416-20.
18. Kuji S, Hirashima Y, Nakayama H, *et al.* Diagnosis, clinicopathologic features, treatment, and prognosis of small cell carcinoma of the uterine cervix: Kansai Clinical Oncology Group/Intergroup study in Japan. *Gynecol Oncol* 2013; 129: 522-7.
 19. Tsunoda S, Jobo T, Arai M, *et al.* Small-cell carcinoma of the uterine cervix: a clinicopathologic study of 11 cases. *Int J Gynecol Cancer* 2005; 15: 295-300.
 20. Li JD, Zhuang Y, Li YF, *et al.* A clinicopathological aspect of primary small-cell carcinoma of the uterine cervix: a single-centre study of 25 cases. *J Clin Pathol* 2011; 64: 1102-7.
 21. Savargaonkar PR, Hale RJ, Mutton A, Manning V, Buckley CH. Neuroendocrine differentiation in cervical carcinoma. *J Clin Pathol* 1996; 49: 139-41.
 22. Chavez-Blanco A, Taja-Chayeb L, Cetina L, *et al.* Neuroendocrine marker expression in cervical carcinomas of non-small cell type. *Int J Gynecol Pathol* 2002; 21: 368-74.
 23. Ordóñez NG. Value of thyroid transcription factor-1 immunostaining in distinguishing small cell lung carcinomas from other small cell carcinomas. *Am J Surg Pathol* 2000; 24: 1217-23.
 24. Houghton O, McCluggage WG. The expression and diagnostic utility of p63 in the female genital tract. *Adv Anat Pathol* 2009; 16: 316-21.
 25. McCluggage WG, Kennedy K, Busam KJ. An immunohistochemical study of cervical neuroendocrine carcinomas: neoplasms that are commonly TTF1 positive and which may express CK20 and p63. *Am J Surg Pathol* 2010; 34: 525-32.
 26. Conner MG, Richter H, Moran CA, Hameed A, Albores-Saavedra J. Small cell carcinoma of the cervix: a clinicopathologic and immunohistochemical study of 23 cases. *Ann Diagn Pathol* 2002; 6: 345-8.
 27. Chetty R, Clark SP, Bhathal PS. Carcinoid tumour of the uterine corpus. *Virchows Arch A Pathol Anat Histopathol* 1993; 422: 93-5.
 28. González-Bosquet E, González-Bosquet J, García Jiménez A, Gil A, Xercavins J. Carcinoid tumor of the uterine corpus: a case report. *J Reprod Med* 1998; 43: 844-6.
 29. Hong SR, Kim HS, Shim JU. Primary carcinoid tumor of the uterine corpus: a case report. *Korean J Pathol* 2004; 38: 109-12.
 30. Huntsman DG, Clement PB, Gilks CB, Scully RE. Small-cell carcinoma of the endometrium: a clinicopathological study of sixteen cases. *Am J Surg Pathol* 1994; 18: 364-75.
 31. van Hoesen KH, Hudock JA, Woodruff JM, Suhland MJ. Small cell neuroendocrine carcinoma of the endometrium. *Int J Gynecol Pathol* 1995; 14: 21-9.
 32. Koo YJ, Kim DY, Kim KR, *et al.* Small cell neuroendocrine carcinoma of the endometrium: a clinicopathologic study of six cases. *Taiwan J Obstet Gynecol* 2014; 53: 355-9.
 33. Mulvany NJ, Allen DG. Combined large cell neuroendocrine and endometrioid carcinoma of the endometrium. *Int J Gynecol Pathol* 2008; 27: 49-57.
 34. Satake T, Matsuyama M. Argrophil cells in normal endometrial glands. *Virchows Arch A Pathol Anat Histopathol* 1987; 410: 449-54.
 35. Shaco-Levy R, Manor E, Piura B, Ariel I. An unusual composite endometrial tumor combining papillary serous carcinoma and small cell carcinoma. *Am J Surg Pathol* 2004; 28: 1103-6.
 36. Manivel C, Wick MR, Sibley RK. Neuroendocrine differentiation in mullerian neoplasms. An immunohistochemical study of a "pure" endometrial small-cell carcinoma and a mixed mullerian tumor containing small-cell carcinoma. *Am J Clin Pathol* 1986; 86: 438-43.
 37. Toptas T, Tasova-Yildirim G, Karaveli S, Simsek T. Malignant mixed Mullerian tumor with small cell neuroendocrine differentiation: a case report and review of the literature. *Eur J Gynaecol Oncol* 2014; 35: 180-4.
 38. Posligua L, Malpica A, Liu J, Brown J, Deavers MT. Combined large cell neuroendocrine carcinoma and papillary serous carcinoma of the endometrium with pagetoid spread. *Arch Pathol Lab Med* 2008; 132: 1821-4.
 39. Tafe LJ, Garg K, Chew I, Tornos C, Soslow RA. Endometrial and ovarian carcinomas with undifferentiated components: clinically aggressive and frequently underrecognized neoplasms. *Mod Pathol* 2010; 23: 781-9.
 40. Altrabulsi B, Malpica A, Deavers MT, Bodurka DC, Broaddus R, Silva EG. Undifferentiated carcinoma of the endometrium. *Am J Surg Pathol* 2005; 29: 1316-21.
 41. Bartosch C, Manuel Lopes J, Oliva E. Endometrial carcinomas: a review emphasizing overlapping and distinctive morphological and immunohistochemical features. *Adv Anat Pathol* 2011; 18: 415-37.
 42. Silva EG, Deavers MT, Bodurka DC, Malpica A. Association of low-grade endometrioid carcinoma of the uterus and ovary with undifferentiated carcinoma: a new type of dedifferentiated carcinoma? *Int J Gynecol Pathol* 2006; 25: 52-8.
 43. Albores-Saavedra J, Martinez-Benitez B, Luevano E. Small cell carcinomas and large cell neuroendocrine carcinomas of the endometrium and cervix: polypoid tumors and those arising in polyps may have a favorable prognosis. *Int J Gynecol Pathol* 2008; 27: 333-9.
 44. Tamura T, Jobo T, Watanabe J, Kanai T, Kuramoto H. Neuroendocrine features in poorly differentiated endometrioid adenocarcinomas of the endometrium. *Int J Gynecol Cancer* 2006; 16: 821-6.
 45. Taraif SH, Deavers MT, Malpica A, Silva EG. The significance of neuroendocrine expression in undifferentiated carcinoma of the endometrium. *Int J Gynecol Pathol* 2009; 28: 142-7.
 46. Reed NS, Gomez-Garcia E, Gallardo-Rincon D, *et al.* Gynecologic

- Cancer InterGroup (GFIG) consensus review for carcinoid tumors of the ovary. *Int J Gynecol Cancer* 2014; 24(9 Suppl 3): S35-41.
47. Davis KP, Hartmann LK, Keeney GL, Shapiro H. Primary ovarian carcinoid tumors. *Gynecol Oncol* 1996; 61: 259-65.
 48. Robboy SJ, Norris HJ, Scully RE. Insular carcinoid primary in the ovary: a clinicopathologic analysis of 48 cases. *Cancer* 1975; 36: 404-18.
 49. Robboy SJ, Scully RE. Strumal carcinoid of the ovary: an analysis of 50 cases of a distinctive tumor composed of thyroid tissue and carcinoid. *Cancer* 1980; 46: 2019-34.
 50. Baker PM, Oliva E, Young RH, Talerman A, Scully RE. Ovarian mucinous carcinoids including some with a carcinomatous component: a report of 17 cases. *Am J Surg Pathol* 2001; 25: 557-68.
 51. Prat JC, Cao D, Carinelli SG, Nogales FF, Vang R, Zaloudek CJ. Monodermal teratoma and somatic-type tumors arising from a dermoid cyst. In: Kurman RJ, Carcangiu ML, Herrington CS, Young RH, eds. WHO classification of tumours of female reproductive organs. 4th ed. Lyon: IARC Press, 2014; 63-5.
 52. Kim HS, Yoon G, Jang HI, Song SY, Kim BG. Primary ovarian carcinoid tumor showing unusual histology and nuclear accumulation of beta-catenin. *Int J Clin Exp Pathol* 2015; 8: 5749-52.
 53. Kurabayashi T, Minamikawa T, Nishijima S, *et al.* Primary strumal carcinoid tumor of the ovary with multiple bone and breast metastases. *J Obstet Gynaecol Res* 2010; 36: 567-71.
 54. Nogales F, Talerman A, Kubik-Huch RA, Tavassoli FA, Devouassoux-Shisheboran M. Germ cell tumours. In: Tavassoli FA, Devilee P, eds. Pathology and genetics of tumours of the breast and female genital organs. 3rd ed. Lyon: IARC Press, 2003; 163-75.
 55. Zhao C, Bratthauer GL, Barner R, Vang R. Comparative analysis of alternative and traditional immunohistochemical markers for the distinction of ovarian sertoli cell tumor from endometrioid tumors and carcinoid tumor: a study of 160 cases. *Am J Surg Pathol* 2007; 31: 255-66.
 56. Sporrang B, Falkmer S, Robboy SJ, *et al.* Neurohormonal peptides in ovarian carcinoids: an immunohistochemical study of 81 primary carcinoids and of intraovarian metastases from six mid-gut carcinoids. *Cancer* 1982; 49: 68-74.
 57. Rabban JT, Lerwill MF, McCluggage WG, Grenert JP, Zaloudek CJ. Primary ovarian carcinoid tumors may express CDX-2: a potential pitfall in distinction from metastatic intestinal carcinoid tumors involving the ovary. *Int J Gynecol Pathol* 2009; 28: 41-8.
 58. Desouki MM, Lioyd J, Xu H, Cao D, Barner R, Zhao C. CDX2 may be a useful marker to distinguish primary ovarian carcinoid from gastrointestinal metastatic carcinoids to the ovary. *Hum Pathol* 2013; 44: 2536-41.
 59. Eichhorn JH, Young RH, Scully RE. Primary ovarian small cell carcinoma of pulmonary type: a clinicopathologic, immunohistologic, and flow cytometric analysis of 11 cases. *Am J Surg Pathol* 1992; 16: 926-38.
 60. Grandjean M, Legrand L, Waterkeyn M, *et al.* Small cell carcinoma of pulmonary type inside a microinvasive mucinous cystadenocarcinoma of the ovary: a case report. *Int J Gynecol Pathol* 2007; 26: 426-31.
 61. Rubio A, Schuldt M, Chamorro C, Crespo-Lora V, Nogales FF. Ovarian small cell carcinoma of pulmonary type arising in mature cystic teratomas with metastases to the contralateral ovary. *Int J Surg Pathol* 2015; 23: 388-92.
 62. Ikota H, Kaneko K, Takahashi S, *et al.* Malignant transformation of ovarian mature cystic teratoma with a predominant pulmonary type small cell carcinoma component. *Pathol Int* 2012; 62: 276-80.
 63. Rund CR, Fischer EG. Perinuclear dot-like cytokeratin 20 staining in small cell neuroendocrine carcinoma of the ovary (pulmonary-type). *Appl Immunohistochem Mol Morphol* 2006; 14: 244-8.
 64. Veras E, Deavers MT, Silva EG, Malpica A. Ovarian non-small cell neuroendocrine carcinoma: a clinicopathologic and immunohistochemical study of 11 cases. *Am J Surg Pathol* 2007; 31: 774-82.
 65. Choi YD, Lee JS, Choi C, Park CS, Nam JH. Ovarian neuroendocrine carcinoma, non-small cell type, associated with serous carcinoma. *Gynecol Oncol* 2007; 104: 747-52.
 66. Behnam K, Kabus D, Behnam M. Primary ovarian undifferentiated non-small cell carcinoma, neuroendocrine type. *Gynecol Oncol* 2004; 92: 372-5.
 67. Eichhorn JH, Lawrence WD, Young RH, Scully RE. Ovarian neuroendocrine carcinomas of non-small-cell type associated with surface epithelial adenocarcinomas: a study of five cases and review of the literature. *Int J Gynecol Pathol* 1996; 15: 303-14.
 68. Dundr P, Fischerová D, Povýsil C, Cibula D. Primary pure large-cell neuroendocrine carcinoma of the ovary. *Pathol Res Pract* 2008; 204: 133-7.
 69. Shakuntala PN, Uma Devi K, Shobha K, Bafna UD, Geetashree M. Pure large cell neuroendocrine carcinoma of ovary: a rare clinical entity and review of literature. *Case Rep Oncol Med* 2012; 2012: 120727.
 70. Khurana KK, Tornos C, Silva EG. Ovarian neuroendocrine carcinoma associated with a mucinous neoplasm. *Arch Pathol Lab Med* 1994; 118: 1032-4.
 71. Yasuoka H, Tsujimoto M, Fujita S, *et al.* Monoclonality of composite large cell neuroendocrine carcinoma and mucinous epithelial tumor of the ovary: a case study. *Int J Gynecol Pathol* 2009; 28: 55-8.
 72. Voutsadakis IA. Large cell neuroendocrine carcinoma of the ovary: a pathologic entity in search of clinical identity. *World J Clin Oncol* 2014; 5: 36-8.

73. Ki EY, Park JS, Lee KH, Bae SN, Hur SY. Large cell neuroendocrine carcinoma of the ovary: a case report and a brief review of the literature. *World J Surg Oncol* 2014; 12: 314.
74. Draganova-Tacheva RA, Khurana JS, Huang Y, Hernandez E, Zhang X. Large cell neuroendocrine carcinoma of the ovary associated with serous carcinoma with mucin production: a case report and literature review. *Int J Clin Exp Pathol* 2009; 2: 304-9.
75. Taube ET, Denkert C, Pietzner K, Dietel M, Sehouli J, Darb-Esfahani S. Prognostic impact of neuroendocrine differentiation in high-grade serous ovarian carcinoma. *Virchows Arch* 2015; 466: 333-42.
76. Young RH, Oliva E, Scully RE. Small cell carcinoma of the ovary, hypercalcemic type: a clinicopathological analysis of 150 cases. *Am J Surg Pathol* 1994; 18: 1102-16.
77. McCluggage WG, Daya D, Ip P, Malpica A, Oliva E, Young RH. Miscellaneous tumours. In: Kurman RJ, Carcangiu ML, Herrington CS, Young RH, eds. *WHO classification of tumours of female reproductive organs*. 4th ed. Lyon: IARC Press, 2014; 69-73.
78. Kupryjańczyk J, Dansonka-Mieszkowska A, Moes-Sosnowska J, *et al*. Ovarian small cell carcinoma of hypercalcemic type: evidence of germline origin and *SMARCA4* gene inactivation. a pilot study. *Pol J Pathol* 2013; 64: 238-46.
79. Jelinic P, Mueller JJ, Olvera N, *et al*. Recurrent *SMARCA4* mutations in small cell carcinoma of the ovary. *Nat Genet* 2014; 46: 424-6.
80. Ramos P, Karnezis AN, Craig DW, *et al*. Small cell carcinoma of the ovary, hypercalcemic type, displays frequent inactivating germline and somatic mutations in *SMARCA4*. *Nat Genet* 2014; 46: 427-9.
81. Witkowski L, Carrot-Zhang J, Albrecht S, *et al*. Germline and somatic *SMARCA4* mutations characterize small cell carcinoma of the ovary, hypercalcemic type. *Nat Genet* 2014; 46: 438-43.
82. Karanian-Philippe M, Velasco V, Longy M, *et al*. *SMARCA4* (BRG1) loss of expression is a useful marker for the diagnosis of ovarian small cell carcinoma of the hypercalcemic type (ovarian rhabdoid tumor): a comprehensive analysis of 116 rare gynecologic tumors, 9 soft tissue tumors, and 9 melanomas. *Am J Surg Pathol* 2015; 39: 1197-205.
83. Foulkes WD, Clarke BA, Hasselblatt M, Majewski J, Albrecht S, McCluggage WG. No small surprise: small cell carcinoma of the ovary, hypercalcaemic type, is a malignant rhabdoid tumour. *J Pathol* 2014; 233: 209-14.

Acute Atherosclerosis of the Uterine Spiral Arteries: Clinicopathologic Implications

Joo-Yeon Kim¹ · Yeon Mee Kim^{1,2}

¹Department of Pathology, Haeundae Paik Hospital, Inje University College of Medicine, Busan; ²Department of Molecular Medicine, Kungpook National University School of Medicine, Daegu, Korea

Received: September 19, 2015

Revised: October 20, 2015

Accepted: October 23 2015

Corresponding Author

Yeon Mee Kim, MD

Department of Pathology, Haeundae Paik Hospital, Inje University College of Medicine, 875 Haeun-daero, Haeundae-gu, Busan 48108, Korea
Tel: +82-51-797-3100
Fax: +82-51-797-3101
E-mail: ykim.haeundae@gmail.com

Acute atherosclerosis is unique vascular changes of the placenta associated with poor placentation. It is characterized by subendothelial lipid-filled foam cells, fibrinoid necrosis of the arterial wall, perivascular lymphocytic infiltration, and it is histologically similar to early-stage atherosclerosis. Acute atherosclerosis is rare in normal pregnancies, but is frequently observed in non-transformed spiral arteries in abnormal pregnancies, such as preeclampsia, small for gestational age (SGA), fetal death, spontaneous preterm labor and preterm premature rupture of membranes. In preeclampsia, spiral arteries fail to develop physiologic transformation and retain thick walls and a narrow lumen. Failure of physiologic transformation of spiral arteries is believed to be the main cause of uteroplacental ischemia, which can lead to the production of anti-angiogenic factors and induce endothelial dysfunction and eventually predispose the pregnancy to preeclampsia. Acute atherosclerosis is more frequently observed in the spiral arteries of the decidua of the placenta (parietalis or basalis) than in the decidual or myometrial segments of the placental bed. The presence and deeper location of acute atherosclerosis is associated with poorer pregnancy outcomes, more severe disease, earlier onset of preeclampsia, and a greater frequency of SGA neonates in patients with preeclampsia. Moreover, the idea that the presence of acute atherosclerosis in the placenta may increase the risk of future cardiovascular disease in women with a history of preeclampsia is of growing concern. Therefore, placental examination is crucial for retrospective investigation of pregnancy complications and outcomes, and accurate placental pathology based on universal diagnostic criteria in patients with abnormal pregnancies is essential for clinicopathologic correlation.

Key Words: Acute atherosclerosis; Spiral artery; Physiologic transformation; Preeclampsia; Atherosclerosis; Lipid; Cholesterol

Acute atherosclerosis was first described in 1945 by Hertig¹ and was named by Zeek and Assali.² Acute atherosclerosis is unique vascular changes observed in non-transformed spiral arteries of the placenta. The histologic findings of acute atherosclerosis, including fibrinoid necrosis, inflammatory cell infiltration of the vessel walls and collection of subendothelial lipid-laden macrophages,¹⁻⁴⁹ are similar to those of early-stage atherosclerosis of the coronary and other larger arteries, as well as allograft rejection.^{27,50} Acute atherosclerosis is rare in normal pregnancy,^{2,5,22,31,42} but is frequently observed in abnormal pregnancies, such as preeclampsia, small for gestational age (SGA), fetal death, spontaneous preterm labor and preterm premature rupture of membranes (PROM).^{2,4,5,7-13,16-19,21,23,24,26-31,40-42,44-48,51} The etiology and pathogenesis of preeclampsia is complicated and remains unclear, despite its role as one of the leading causes of maternal and neonatal morbidity and mortality in pregnancy. Failure of physiologic remodeling of the spiral arteries is a main cause of preeclampsia, and these

arteries are prone to develop acute atherosclerosis.⁵² Moreover, accumulating evidence suggests that women with a history of preeclampsia exhibit a high prevalence of major cardiovascular risk factors.⁵³⁻⁵⁷ This gives rise to the question of whether acute atherosclerosis in the placenta is related to possible future cardiovascular disease in the mother.

This review describes (1) spiral artery changes in normal and abnormal placentation during pregnancy, (2) histologic findings of acute atherosclerosis, (3) acute atherosclerosis frequency in normal and abnormal pregnancies, (4) placental lesions associated with acute atherosclerosis, (5) possible pathogenic mechanisms of acute atherosclerosis, and (6) clinical implications of acute atherosclerosis.

POOR PLACENTATION AND ACUTE ATHEROSIS

Normal physiologic transformation of the uterine spiral arter-

ies during early pregnancy is considered a foundation of successful pregnancy.⁵⁸ The spiral arteries are normally transformed into large dilated vessels, with dramatic structural changes to the vessel wall. The key findings of normal transformation of the spiral arteries are (1) dilation of the lumen, (2) trophoblast invasion into the vessel wall, and (3) replacement of the muscular and elastic tissue of the arterial wall by a thick fibrinoid material (Fig. 1A).^{58,59} These changes maximize the delivery of maternal blood to the intervillous space of the placenta, so that a sufficient blood supply through transformed spiral arteries enables the transfer of enough nutrition and oxygen from the mother to the fetus. Maternal blood from dilated spiral arteries meets fetal blood in the intervillous space, while the intervillous space drains blood back to the utero-placental veins.⁶⁰ For successful placentation, trophoblast invasion from the maternal-fetal interface to the myometrium through the decidua during the first 3 months of pregnancy is critical.

Poor placentation is defined as the failure of physiologic transformation of spiral arteries and appears to arise from an inadequate or shallow trophoblast invasion.^{8,58,61} Poor placentation is also a leading cause of preeclampsia and other abnormal pregnancies, such as spontaneous abortion, SGA, preterm labor and preterm PROM.^{7,9,62-65} In preeclampsia, spiral arteries of the myometrial segment of the uterus fail to achieve physiologic transformation and retain thick walls and a narrow lumen; this is believed to be the main cause of uteroplacental ischemia (Fig. 1B).^{7,9} Uteroplacental ischemia can lead to the production of anti-angiogenic factors,⁶⁶⁻⁶⁸ such as soluble fms-like tyrosine kinase 1,^{64,69} and endoglin,^{70,71} which can induce endothelial dysfunction and eventually predispose the pregnancy to preeclampsia.

Spiral arteries that fail to achieve physiologic transformation are prone to develop acute atherosclerosis.⁷²⁻⁷⁹

HISTOLOGIC CHARACTERISTICS AND TOPOGRAPHIC DISTRIBUTION OF ACUTE ATHEROSIS

Histologic findings of acute atherosclerosis consist of the presence of fibrinoid necrosis of the artery wall, a subendothelial collection of lipid-laden macrophages, and vascular or perivascular lymphocytic infiltration in non-transformed uterine spiral arteries (Fig. 2A).^{1,11} Lipids in the spiral arteries with acute atherosclerosis are stained red with oil-red O (Fig. 2B).

Acute atherosclerosis was more frequently observed in the spiral arteries of the decidua (parietalis or basalis) of the placenta than in the decidual or myometrial segments of the placental bed. The depth of acute atherosclerosis is associated with the severity of preeclampsia. Briefly, the presence of atherosclerosis in the myometrial segment is associated with a severe form and an earlier onset of preeclampsia than those without this lesion in the myometrial segment.^{51,80}

FREQUENCY OF ACUTE ATHEROSIS

Acute atherosclerosis used to be considered a characteristic finding of spiral arteries of patients with preeclampsia and has been reported to occur in 5% to 40% of patients with preeclampsia.^{5,7,8,10-13,16-19,23,24,26-31,40,42,45,46} The variable frequency of acute atherosclerosis may be explained by the following reasons: (1) variation in the number of tissue sections taken (size of sample), (2)

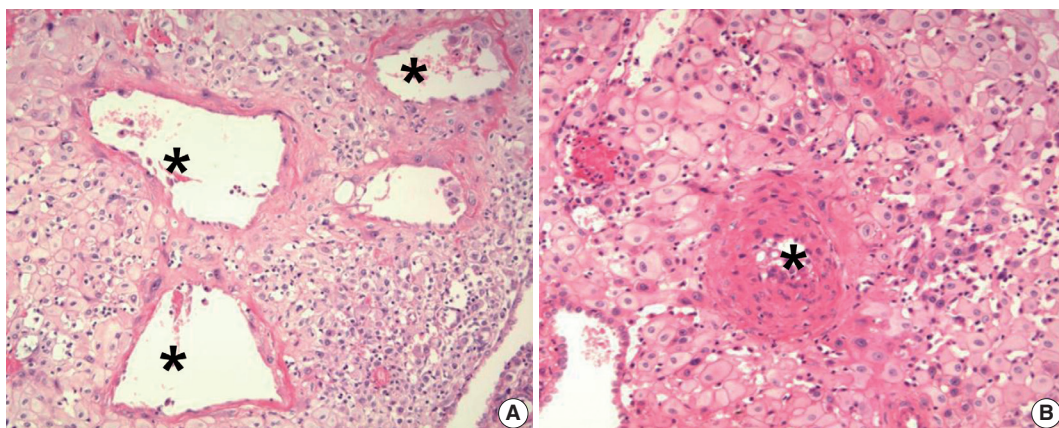


Fig. 1. Spiral artery changes during pregnancy. (A) Normal physiologic transformation of spiral arteries in a normal pregnancy. The lumen of the spiral artery (asterisks) is dilated. Trophoblastic cells are infiltrating the wall of the spiral artery. (B) Failure of physiologic transformation of spiral arteries in a patient with preeclampsia. The lumen of the arteries (asterisk) is not dilated. The medial layers of the spiral arteries are intact. Although many interstitial trophoblasts surround the spiral artery, trophoblasts have not invaded the vessel wall.

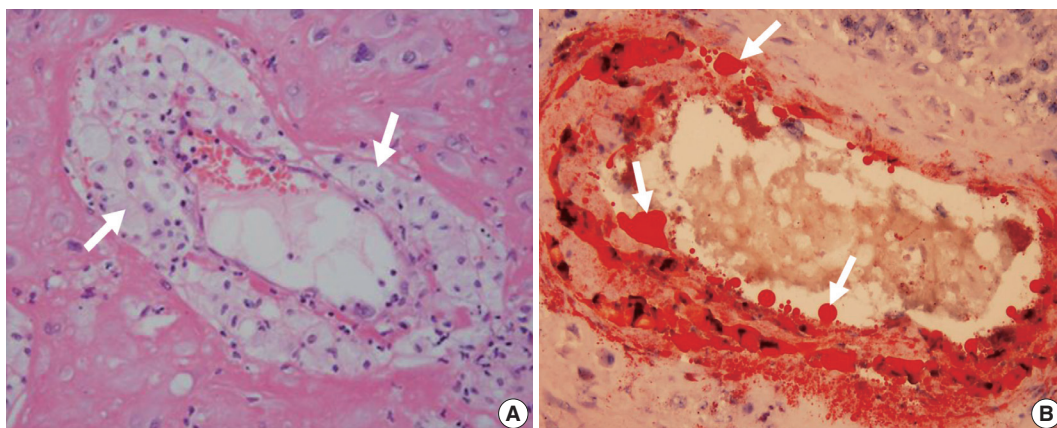


Fig. 2. Acute atherosclerosis in decidual spiral arteries. (A) Many lipid-laden macrophages (arrows) are seen in the spiral arteries. (B) Acute atherosclerosis on oil-red O staining. Fat droplets (arrows) in the non-transformed spiral artery are stained red.

location of tissue sections, (3) variation in tissue staining methods (hematoxylin and eosin [H&E] staining only or additional immunohistochemical staining) for the diagnosis of acute atherosclerosis, and (4) differences in the pathologist's diagnostic skill. In a previous study with over 14,000 placenta samples using only H&E staining for the diagnosis of acute atherosclerosis and taking an average of two sections from each placenta based on routine histology laboratory tasks,⁵¹ the prevalence of acute atherosclerosis in uncomplicated pregnancies was 0.4% and the frequency of acute atherosclerosis varied based on the specific obstetrical syndrome: preeclampsia, 10%; fetal death, 9%; mid-trimester spontaneous abortion, 2.5%; SGA neonates without preeclampsia, 1.7%; and spontaneous preterm labor, 1.2%. Acute atherosclerosis is associated with more severe disease, earlier onset of preeclampsia, and a greater frequency of SGA neonates in patients with preeclampsia.^{51,80}

PLACENTAL LESIONS ASSOCIATED WITH ACUTE ATHEROSIS

A previous study found that acute atherosclerosis is associated with an increased risk of placental lesions consistent with maternal underperfusion, fetal vascular thrombo-occlusive disease and chronic chorioamnionitis, but not with other chronic inflammatory lesions.⁸¹

The correlation between acute atherosclerosis and chronic chorioamnionitis indicates the presence of circulating maternal T cells and adaptive immune response may also play a role in the genesis of acute atherosclerosis.^{73,77,78,82-91}

In chronic chorioamnionitis, maternal T cells infiltrating the chorion laeve cause trophoblast apoptosis, which resembles allograft rejection.⁹² Chronic chorioamnionitis is also associated with anti-fetal HLA maternal sensitization⁹³ and complement

deposition in the umbilical vein endothelium,⁹⁴ which has been associated with a novel form of fetal systemic inflammatory response characterized by the over-expression of T-cell chemokines such as CXCL10.⁹⁵

Higher concentrations of CXCL9, CXCL10, and CXCL11 have been found in mothers with chronic placental inflammation compared to those without.⁹² Similarly, T lymphocytes have been detected in the early stages of atheroma formation.⁹⁶ Moreover, differential expression of three interferon (IFN) gamma-inducible CXC chemokines, IFN-inducible protein 10 (CXCL10 or IP-10), monokine induced by IFN- γ (CXCL9 or Mig) and IFN-inducible T-cell α chemoattractant (CXCL11 or I-TAC) were found in atherosclerosis.⁹⁶

PATHOGENESIS OF ACUTE ATHEROSIS

Multiple factors including excessive decidual inflammation,^{42,47,48,97} immune dysregulation at the maternal-fetal interface²⁷ and immunological mismatch between the mother and fetus²⁷ have been proposed as causes or initiators of acute atherosclerosis.

Recently, Staff *et al.*⁴⁸ suggested four serial mechanisms for the development of acute atherosclerosis, with excessive decidual inflammation as the final common pathway: (1) shear flow stress caused by abnormal blood flow in inadequately remodeled spiral arteries, (2) decidual inflammation, including maternal alloreactivity to feto-paternal HLA-C or minor histocompatibility antigens, (3) background (systemic) maternal inflammatory stress secondary to the changes induced by pregnancy and preeclampsia, and (4) maternal genetic predisposition (for example, polymorphism in regulator of G protein signaling 2).

Elevation of signs of intravascular inflammation have been reported in both normal⁹⁸⁻¹⁰¹ and abnormal pregnancies, such as

spontaneous preterm labor with intact membranes,¹⁰²⁻¹⁰⁸ preterm PROM,¹⁰⁹⁻¹¹⁴ preeclampsia,¹¹⁵⁻¹⁴⁴ SGA,^{119,134,136,138,145-154} and pyelonephritis.^{99,155-157} Since chronic vascular inflammation is one of the main causes of atherosclerosis and acute atherosclerosis, the possibility of activation of cholesterol crystal-induced inflammation in macrophages¹⁵⁸ should be investigated as an important link between cholesterol metabolism and acute atherosclerosis.

THE CLINICAL IMPLICATIONS OF ACUTE ATHEROSCLEROSIS

Maternal serum lipid level of patients with acute atherosclerosis in the placenta

In atherosclerosis, medium-sized and large arteries fueled by lipids, as well as the deposition of excess cholesterol in the blood stream, initiate atherosclerosis.¹⁵⁹ Similarly, acute atherosclerosis in non-transformed uterine spiral arteries also show variable amounts of lipid deposition in the wall of spiral arteries, and it is stained red with oil-red O staining (Fig. 2B). Moreover, serum triglycerides are about 50% higher in preeclamptic women than in normal pregnant women. However, there are no differences in other lipid profiles, including total cholesterol and high-density lipoprotein.^{51,160-162} Whether there are differences in low-density lipoprotein remains controversial.^{143-145,163}

Acute atherosclerosis and future cardiovascular risk

Accumulating evidence suggests that women with a history of preeclampsia show a high prevalence of major cardiovascular risk factors.⁵³⁻⁵⁷ Similarities between preeclampsia and atherosclerosis, as well as between acute atherosclerosis of the spiral arteries and coronary atherosclerosis, have been observed. Intravascular inflammation,^{98,118,120,164,165} changes in lipid metabolism,^{162,166-168} and macrophage infiltration of the intima and media are seen in both acute atherosclerosis and atherosclerosis.^{27,169,170} Therefore, hyperlipidemia and abnormal lipid metabolism combined with intravascular inflammation can defect endothelial cell function and may lead to atherosclerosis in non-pregnant women who have a past history of preeclampsia.⁷²⁻⁷⁹ We recommend that women who have a past history of preeclampsia be considered at high risk for cardiovascular disease and recommend implementation of regular screenings and prevention programs.

CONCLUSION

The presence and deeper location of acute atherosclerosis is associated with worse pregnancy outcomes, more severe disease, earlier

onset, and a greater frequency of SGA neonates in patients with preeclampsia. Moreover, the idea that acute atherosclerosis in the placenta may increase the risk of future cardiovascular disease in women with a history of preeclampsia is of growing concern. Therefore, placental examination is crucial for investigation of pregnancy complications and outcomes, and accurate placental pathology based on universal diagnostic criteria in patients with abnormal pregnancies is essential for clinicopathologic correlation.

Conflicts of Interest

No potential conflict of interest relevant to this article was reported.

Acknowledgments

The authors are very grateful to Professor Je G. Chi, who passed away during the winter of 2014. He was a great mentor and friend to all of us. This work is dedicated to his memory.

REFERENCES

- Hertig AT. Vascular pathology in the hypertensive albuminuric toxemias of pregnancy. *Clinics* 1945; 4: 602-14.
- Zeek PM, Assali NS. Vascular changes in the decidua associated with eclamptogenic toxemia of pregnancy. *Am J Clin Pathol* 1950; 20: 1099-109.
- Hanssens M, Pijnenborg R, Keirse MJ, Vercruyse L, Verbist L, Van Assche FA. Renin-like immunoreactivity in uterus and placenta from normotensive and hypertensive pregnancies. *Eur J Obstet Gynecol Reprod Biol* 1998; 81: 177-84.
- Sexton LI, Hertig AT, Reid DE, Kellogg FS, Patterson WA. Premature separation of the normally implanted placenta; a clinicopathological study of 476 cases. *Am J Obstet Gynecol* 1950; 59: 13-24.
- Maqueo M, Chavezazuela J, Dosaldelavega M. Placental pathology in eclampsia and preeclampsia. *Obstet Gynecol* 1964; 24: 350-6.
- Driscoll SG. The pathology of pregnancy complicated by diabetes mellitus. *Med Clin N Am* 1965; 49: 1053-67.
- Robertson WB, Brosens I, Dixon HG. The pathological response of the vessels of the placental bed to hypertensive pregnancy. *J Pathol Bacteriol* 1967; 93: 581-92.
- Brosens IA, Robertson WB, Dixon HG. The role of the spiral arteries in the pathogenesis of preeclampsia. *Obstet Gynecol Annu* 1972; 1: 177-91.
- Brosens I, Renaer M. On the pathogenesis of placental infarcts in pre-eclampsia. *J Obstet Gynaecol Br Commonw* 1972; 79: 794-9.
- Emmrich P, Birke R, Gödel E. Morphology of myometrial and de-

- cidial arteries in normal pregnancy, in toxemia of pregnancy, and in maternal diabetes (author's transl). *Pathol Microbiol (Basel)* 1975; 43: 38-61.
11. De Wolf F, Robertson WB, Brosens I. The ultrastructure of acute atherosclerosis in hypertensive pregnancy. *Am J Obstet Gynecol* 1975; 123: 164-74.
 12. Robertson WB, Brosens I, Dixon G. Uteroplacental vascular pathology. *Eur J Obstet Gynecol Reprod Biol* 1975; 5: 47-65.
 13. Robertson WB, Brosens I, Dixon G. Maternal uterine vascular lesions in the hypertensive complications of pregnancy. *Perspect Nephrol Hypertens* 1976; 5: 115-27.
 14. De Wolf F, Brosens I, Renaer M. Fetal growth retardation and the maternal arterial supply of the human placenta in the absence of sustained hypertension. *Br J Obstet Gynaecol* 1980; 87: 678-85.
 15. Abramowsky CR, Vegas ME, Swinehart G, Gyves MT. Decidual vasculopathy of the placenta in lupus erythematosus. *N Engl J Med* 1980; 303: 668-72.
 16. Kitzmiller JL, Watt N, Driscoll SG. Decidual arteriopathy in hypertension and diabetes in pregnancy: immunofluorescent studies. *Am J Obstet Gynecol* 1981; 141: 773-9.
 17. Sheppard BL, Bonnar J. An ultrastructural study of utero-placental spiral arteries in hypertensive and normotensive pregnancy and fetal growth retardation. *Br J Obstet Gynaecol* 1981; 88: 695-705.
 18. De Wolf F, Carreras LO, Moerman P, Vermeylen J, Van Assche A, Renaer M. Decidual vasculopathy and extensive placental infarction in a patient with repeated thromboembolic accidents, recurrent fetal loss, and a lupus anticoagulant. *Am J Obstet Gynecol* 1982; 142: 829-34.
 19. Hustin J, Foidart JM, Lambotte R. Maternal vascular lesions in pre-eclampsia and intrauterine growth retardation: light microscopy and immunofluorescence. *Placenta* 1983; 4 Spec No: 489-98.
 20. Althabe O, Labarrere C, Telenta M. Maternal vascular lesions in placentae of small-for-gestational-age infants. *Placenta* 1985; 6: 265-76.
 21. Labarrere C, Alonso J, Manni J, Domenichini E, Althabe O. Immunohistochemical findings in acute atherosclerosis associated with intrauterine growth retardation. *Am J Reprod Immunol Microbiol* 1985; 7: 149-55.
 22. Labarrere C, Althabe O. Chronic villitis of unknown etiology and maternal arterial lesions in preeclamptic pregnancies. *Eur J Obstet Gynecol Reprod Biol* 1985; 20: 1-11.
 23. Khong TY, De Wolf F, Robertson WB, Brosens I. Inadequate maternal vascular response to placentation in pregnancies complicated by pre-eclampsia and by small-for-gestational age infants. *Br J Obstet Gynaecol* 1986; 93: 1049-59.
 24. McFadyen IR, Price AB, Geirsson RT. The relation of birthweight to histological appearances in vessels of the placental bed. *Br J Obstet Gynaecol* 1986; 93: 476-81.
 25. Labarrere CA, Catoggio LJ, Mullen EG, Althabe OH. Placental lesions in maternal autoimmune diseases. *Am J Reprod Immunol Microbiol* 1986; 12: 78-86.
 26. Khong TY, Pearce JM, Robertson WB. Acute atherosclerosis in pre-eclampsia: maternal determinants and fetal outcome in the presence of the lesion. *Am J Obstet Gynecol* 1987; 157: 360-3.
 27. Labarrere CA. Acute atherosclerosis: a histopathological hallmark of immune aggression? *Placenta* 1988; 9: 95-108.
 28. Frusca T, Morassi L, Pecorelli S, Grigolato P, Gastaldi A. Histological features of uteroplacental vessels in normal and hypertensive patients in relation to birthweight. *Br J Obstet Gynaecol* 1989; 96: 835-9.
 29. Khong TY. Acute atherosclerosis in pregnancies complicated by hypertension, small-for-gestational-age infants, and diabetes mellitus. *Arch Pathol Lab Med* 1991; 115: 722-5.
 30. Meekins JW, Pijnenborg R, Hanssens M, McFadyen IR, van Assche A. A study of placental bed spiral arteries and trophoblast invasion in normal and severe pre-eclamptic pregnancies. *Br J Obstet Gynaecol* 1994; 101: 669-74.
 31. Meekins JW, Pijnenborg R, Hanssens M, van Assche A, McFadyen IR. Immunohistochemical detection of lipoprotein(a) in the wall of placental bed spiral arteries in normal and severe preeclamptic pregnancies. *Placenta* 1994; 15: 511-24.
 32. Salafia CM, Parke AL. Placental pathology in systemic lupus erythematosus and phospholipid antibody syndrome. *Rheum Dis Clin North Am* 1997; 23: 85-97.
 33. Brosens I, Dixon HG, Robertson WB. Fetal growth retardation and the arteries of the placental bed. *Br J Obstet Gynaecol* 1977; 84: 656-63.
 34. Gerretsen G, Huisjes HJ, Elema JD. Morphological changes of the spiral arteries in the placental bed in relation to pre-eclampsia and fetal growth retardation. *Br J Obstet Gynaecol* 1981; 88: 876-81.
 35. Nayar R, Lage JM. Placental changes in a first trimester missed abortion in maternal systemic lupus erythematosus with antiphospholipid syndrome; a case report and review of the literature. *Hum Pathol* 1996; 27: 201-6.
 36. Hayati AR, Azizah A, Wahidah A. Incidence of acute atherosclerosis in complete molar pregnancy. *Malays J Pathol* 1998; 20: 113-4.
 37. Khong TY, Hague WM. The placenta in maternal hyperhomocysteinaemia. *Br J Obstet Gynaecol* 1999; 106: 273-8.
 38. Ogishima D, Matsumoto T, Nakamura Y, Yoshida K, Kuwabara Y. Placental pathology in systemic lupus erythematosus with antiphospholipid antibodies. *Pathol Int* 2000; 50: 224-9.
 39. Sebire NJ, Rees H, Paradinas F, et al. Extravillous endovascular im-

- plantation site trophoblast invasion is abnormal in complete versus partial molar pregnancies. *Placenta* 2001; 22: 725-8.
40. Moldenhauer JS, Stanek J, Warshak C, Khoury J, Sibai B. The frequency and severity of placental findings in women with preeclampsia are gestational age dependent. *Am J Obstet Gynecol* 2003; 189: 1173-7.
 41. Faye-Petersen O, Heller DS, Joshi VV. *Handbook of placental pathology*. 2nd ed. London: Taylor & Francis, 2006; 53-78.
 42. Harsem NK, Roald B, Braekke K, Staff AC. Acute atherosclerosis in decidua: not associated with systemic oxidative stress in preeclampsia. *Placenta* 2007; 28: 958-64.
 43. Fox H, Sebire NJ. *Pathology of the placenta*. 3rd ed. Philadelphia: Saunders-Elsevier, 2007; 147-86.
 44. Brosens I, Khong TY. Defective spiral artery remodeling. In: Pijnenborg R, Brosens I, Romero R, eds. *Placental bed disorders*. Cambridge: Cambridge University Press, 2010; 11.
 45. Staff AC, Dechend R, Pijnenborg R. Learning from the placenta: acute atherosclerosis and vascular remodeling in preeclampsia—novel aspects for atherosclerosis and future cardiovascular health. *Hypertension* 2010; 56: 1026-34.
 46. Stevens DU, Al-Nasiry S, Bulten J, Spaanderman ME. Decidual vasculopathy in preeclampsia: lesion characteristics relate to disease severity and perinatal outcome. *Placenta* 2013; 34: 805-9.
 47. Staff AC, Dechend R, Redman CW. Review: preeclampsia, acute atherosclerosis of the spiral arteries and future cardiovascular disease: two new hypotheses. *Placenta* 2013; 34 Suppl: S73-8.
 48. Staff AC, Johnsen GM, Dechend R, Redman CW. Preeclampsia and uteroplacental acute atherosclerosis: immune and inflammatory factors. *J Reprod Immunol* 2014; 101-102: 120-6.
 49. Staff AC, Redman CW. IFPA Award in Placentology Lecture: preeclampsia, the decidua battleground and future maternal cardiovascular disease. *Placenta* 2014; 35 Suppl: S26-31.
 50. Mitchell RN. Graft vascular disease: immune response meets the vessel wall. *Annu Rev Pathol* 2009; 4: 19-47.
 51. Kim YM, Chaemsaitong P, Romero R, *et al*. The frequency of acute atherosclerosis in normal pregnancy and preterm labor, preeclampsia, small-for-gestational age, fetal death and midtrimester spontaneous abortion. *J Matern Fetal Neonatal Med* 2015; 28: 2001-9.
 52. Pijnenborg R, Vercruyse L, Hanssens M. The uterine spiral arteries in human pregnancy: facts and controversies. *Placenta* 2006; 27: 939-58.
 53. van Rijn BB, Nijdam ME, Bruinse HW, *et al*. Cardiovascular disease risk factors in women with a history of early-onset preeclampsia. *Obstet Gynecol* 2013; 121: 1040-8.
 54. Veerbeek JH, Hermes W, Breimer AY, *et al*. Cardiovascular disease risk factors after early-onset preeclampsia, late-onset preeclampsia, and pregnancy-induced hypertension. *Hypertension* 2015; 65: 600-6.
 55. Sattar N, Ramsay J, Crawford L, Cheyne H, Greer IA. Classic and novel risk factor parameters in women with a history of preeclampsia. *Hypertension* 2003; 42: 39-42.
 56. Berends AL, de Groot CJ, Sijbrands EJ, *et al*. Shared constitutional risks for maternal vascular-related pregnancy complications and future cardiovascular disease. *Hypertension* 2008; 51: 1034-41.
 57. van Rijn BB, Veerbeek JH, Scholtens LC, *et al*. C-reactive protein and fibrinogen levels as determinants of recurrent preeclampsia: a prospective cohort study. *J Hypertens* 2014; 32: 408-14.
 58. Brosens I, Robertson WB, Dixon HG. The physiological response of the vessels of the placental bed to normal pregnancy. *J Pathol Bacteriol* 1967; 93: 569-79.
 59. Espinoza J, Romero R, Kim YM, *et al*. Normal and abnormal transformation of the spiral arteries during pregnancy. *J Perinat Med* 2006; 34: 447-58.
 60. Freese UE. The uteroplacental vascular relationship in the human. *Am J Obstet Gynecol* 1968; 101: 8-16.
 61. Brosens IA. Morphological changes in the utero-placental bed in pregnancy hypertension. *Clin Obstet Gynaecol* 1977; 4: 573-93.
 62. Kim YM, Chaiworapongsa T, Gomez R, *et al*. Failure of physiologic transformation of the spiral arteries in the placental bed in preterm premature rupture of membranes. *Am J Obstet Gynecol* 2002; 187: 1137-42.
 63. Kim YM, Bujold E, Chaiworapongsa T, *et al*. Failure of physiologic transformation of the spiral arteries in patients with preterm labor and intact membranes. *Am J Obstet Gynecol* 2003; 189: 1063-9.
 64. Redman CW, Sargent IL. Latest advances in understanding preeclampsia. *Science* 2005; 308: 1592-4.
 65. Steegers EA, von Dadelszen P, Duvekot JJ, Pijnenborg R. Preeclampsia. *Lancet* 2010; 376: 631-44.
 66. Makris A, Thornton C, Thompson J, *et al*. Uteroplacental ischemia results in proteinuric hypertension and elevated sFLT-1. *Kidney Int* 2007; 71: 977-84.
 67. Bujold E, Romero R, Chaiworapongsa T, *et al*. Evidence supporting that the excess of the sVEGFR-1 concentration in maternal plasma in preeclampsia has a uterine origin. *J Matern Fetal Neonatal Med* 2005; 18: 9-16.
 68. Kusanovic JP, Romero R, Chaiworapongsa T, *et al*. A prospective cohort study of the value of maternal plasma concentrations of angiogenic and anti-angiogenic factors in early pregnancy and midtrimester in the identification of patients destined to develop preeclampsia. *J Matern Fetal Neonatal Med* 2009; 22: 1021-38.
 69. Maynard SE, Min JY, Merchan J, *et al*. Excess placental soluble fms-like tyrosine kinase 1 (sFlt1) may contribute to endothelial dysfunction

- tion, hypertension, and proteinuria in preeclampsia. *J Clin Invest* 2003; 111: 649-58.
70. Lain KY, Roberts JM. Contemporary concepts of the pathogenesis and management of preeclampsia. *JAMA* 2002; 287: 3183-6.
 71. Venkatesha S, Toporsian M, Lam C, *et al.* Soluble endoglin contributes to the pathogenesis of preeclampsia. *Nat Med* 2006; 12: 642-9.
 72. Libby P, Ridker PM, Maseri A. Inflammation and atherosclerosis. *Circulation* 2002; 105: 1135-43.
 73. Libby P. Inflammation in atherosclerosis. *Nature* 2002; 420: 868-74.
 74. Young JL, Libby P, Schönbeck U. Cytokines in the pathogenesis of atherosclerosis. *Thromb Haemost* 2002; 88: 554-67.
 75. Hansson GK, Libby P. The immune response in atherosclerosis: a double-edged sword. *Nat Rev Immunol* 2006; 6: 508-19.
 76. Libby P. Inflammatory mechanisms: the molecular basis of inflammation and disease. *Nutr Rev* 2007; 65(12 Pt 2): S140-6.
 77. Rocha VZ, Libby P. Obesity, inflammation, and atherosclerosis. *Nat Rev Cardiol* 2009; 6: 399-409.
 78. Galkina E, Ley K. Immune and inflammatory mechanisms of atherosclerosis (*). *Annu Rev Immunol* 2009; 27: 165-97.
 79. Libby P, Okamoto Y, Rocha VZ, Folco E. Inflammation in atherosclerosis: transition from theory to practice. *Circ J* 2010; 74: 213-20.
 80. Brosens I, Pijnenborg R, Vercruyse L, Romero R. The "Great Obstetrical Syndromes" are associated with disorders of deep placentation. *Am J Obstet Gynecol* 2011; 204: 193-201.
 81. Kim YM, Chaemsaitong P, Romero R, *et al.* Placental lesions associated with acute atherosclerosis. *J Matern Fetal Neonatal Med* 2015; 28: 1554-62.
 82. Libby P. Atherosclerosis: disease biology affecting the coronary vasculature. *Am J Cardiol* 2006; 98: 3Q-9Q.
 83. Libby P, Ridker PM, Hansson GK; Leducq Transatlantic Network on Atherothrombosis. Inflammation in atherosclerosis: from pathophysiology to practice. *J Am Coll Cardiol* 2009; 54: 2129-38.
 84. Packard RR, Lichtman AH, Libby P. Innate and adaptive immunity in atherosclerosis. *Semin Immunopathol* 2009; 31: 5-22.
 85. Andersson J, Libby P, Hansson GK. Adaptive immunity and atherosclerosis. *Clin Immunol* 2010; 134: 33-46.
 86. Libby P, Ridker PM, Hansson GK. Progress and challenges in translating the biology of atherosclerosis. *Nature* 2011; 473: 317-25.
 87. Legein B, Temmerman L, Biessen EA, Lutgens E. Inflammation and immune system interactions in atherosclerosis. *Cell Mol Life Sci* 2013; 70: 3847-69.
 88. Libby P, Lichtman AH, Hansson GK. Immune effector mechanisms implicated in atherosclerosis: from mice to humans. *Immunity* 2013; 38: 1092-104.
 89. Rosenfeld ME. Inflammation and atherosclerosis: direct versus indirect mechanisms. *Curr Opin Pharmacol* 2013; 13: 154-60.
 90. Woollard KJ. Immunological aspects of atherosclerosis. *Clin Sci (Lond)* 2013; 125: 221-35.
 91. Ait-Oufella H, Sage AP, Mallat Z, Tedgui A. Adaptive (T and B cells) immunity and control by dendritic cells in atherosclerosis. *Circ Res* 2014; 114: 1640-60.
 92. Kim CJ, Romero R, Kusanovic JP, *et al.* The frequency, clinical significance, and pathological features of chronic chorioamnionitis: a lesion associated with spontaneous preterm birth. *Mod Pathol* 2010; 23: 1000-11.
 93. Lee J, Romero R, Xu Y, *et al.* Maternal HLA panel-reactive antibodies in early gestation positively correlate with chronic chorioamnionitis: evidence in support of the chronic nature of maternal anti-fetal rejection. *Am J Reprod Immunol* 2011; 66: 510-26.
 94. Lee J, Romero R, Xu Y, *et al.* A signature of maternal anti-fetal rejection in spontaneous preterm birth: chronic chorioamnionitis, anti-human leukocyte antigen antibodies, and C4d. *PLoS One* 2011; 6: e16806.
 95. Lee J, Kim JS, Park JW, *et al.* Chronic chorioamnionitis is the most common placental lesion in late preterm birth. *Placenta* 2013; 34: 681-9.
 96. Mach F, Sauty A, Iarossi AS, *et al.* Differential expression of three T lymphocyte-activating CXC chemokines by human atheroma-associated cells. *J Clin Invest* 1999; 104: 1041-50.
 97. Pijnenborg R, McLaughlin PJ, Vercruyse L, *et al.* Immunolocalization of tumour necrosis factor-alpha (TNF-alpha) in the placental bed of normotensive and hypertensive human pregnancies. *Placenta* 1998; 19: 231-9.
 98. Sacks GP, Studena K, Sargent K, Redman CW. Normal pregnancy and preeclampsia both produce inflammatory changes in peripheral blood leukocytes akin to those of sepsis. *Am J Obstet Gynecol* 1998; 179: 80-6.
 99. Naccasha N, Gervasi MT, Chaiworapongsa T, *et al.* Phenotypic and metabolic characteristics of monocytes and granulocytes in normal pregnancy and maternal infection. *Am J Obstet Gynecol* 2001; 185: 1118-23.
 100. Brenner B. Haemostatic changes in pregnancy. *Thromb Res* 2004; 114: 409-14.
 101. Watts DH, Krohn MA, Wener MH, Eschenbach DA. C-reactive protein in normal pregnancy. *Obstet Gynecol* 1991; 77: 176-80.
 102. Gervasi MT, Chaiworapongsa T, Naccasha N, *et al.* Phenotypic and metabolic characteristics of maternal monocytes and granulocytes in preterm labor with intact membranes. *Am J Obstet Gynecol* 2001; 185: 1124-9.
 103. Pitiphat W, Gillman MW, Joshipura KJ, Williams PL, Douglass CW, Rich-Edwards JW. Plasma C-reactive protein in early pregnancy and preterm delivery. *Am J Epidemiol* 2005; 162: 1108-13.

104. Gotsch F, Romero R, Kusanovic JP, *et al.* The anti-inflammatory limb of the immune response in preterm labor, intra-amniotic infection/inflammation, and spontaneous parturition at term: a role for interleukin-10. *J Matern Fetal Neonatal Med* 2008; 21: 529-47.
105. Kim MA, Lee BS, Park YW, Seo K. Serum markers for prediction of spontaneous preterm delivery in preterm labour. *Eur J Clin Invest* 2011; 41: 773-80.
106. Laudanski P, Raba G, Kuc P, Lemancewicz A, Kisielewski R, Laudanski T. Assessment of the selected biochemical markers in predicting preterm labour. *J Matern Fetal Neonatal Med* 2012; 25: 2696-9.
107. Cruciani L, Romero R, Vaisbuch E, *et al.* Pentraxin 3 in maternal circulation: an association with preterm labor and preterm PROM, but not with intra-amniotic infection/inflammation. *J Matern Fetal Neonatal Med* 2010; 23: 1097-105.
108. Stampalija T, Chaiworapongsa T, Romero R, *et al.* Soluble ST2, a modulator of the inflammatory response, in preterm and term labor. *J Matern Fetal Neonatal Med* 2014; 27: 111-21.
109. Ismail MA, Zinaman MJ, Lowensohn RI, Moawad AH. The significance of C-reactive protein levels in women with premature rupture of membranes. *Am J Obstet Gynecol* 1985; 151: 541-4.
110. Yoon BH, Jun JK, Park KH, Syn HC, Gomez R, Romero R. Serum C-reactive protein, white blood cell count, and amniotic fluid white blood cell count in women with preterm premature rupture of membranes. *Obstet Gynecol* 1996; 88: 1034-40.
111. Gervasi MT, Chaiworapongsa T, Naccasha N, *et al.* Maternal intravascular inflammation in preterm premature rupture of membranes. *J Matern Fetal Neonatal Med* 2002; 11: 171-5.
112. Loukovaara MJ, Alftan HV, Kurki MT, Hiilesmaa VK, Andersson SH. Serum highly sensitive C-reactive protein in preterm premature rupture of membranes. *Eur J Obstet Gynecol Reprod Biol* 2003; 110: 26-8.
113. Moghaddam Banaem L, Mohamadi B, Asghari Jaafarabadi M, Aliyan Moghadam N. Maternal serum C-reactive protein in early pregnancy and occurrence of preterm premature rupture of membranes and preterm birth. *J Obstet Gynaecol Res* 2012; 38: 780-6.
114. Gulati S, Agrawal S, Raghunandan C, *et al.* Maternal serum interleukin-6 and its association with clinicopathological infectious morbidity in preterm premature rupture of membranes: a prospective cohort study. *J Matern Fetal Neonatal Med* 2012; 25: 1428-32.
115. Vince GS, Starkey PM, Austgulen R, Kwiatkowski D, Redman CW. Interleukin-6, tumour necrosis factor and soluble tumour necrosis factor receptors in women with pre-eclampsia. *Br J Obstet Gynaecol* 1995; 102: 20-5.
116. Hamai Y, Fujii T, Yamashita T, *et al.* Evidence for an elevation in serum interleukin-2 and tumor necrosis factor-alpha levels before the clinical manifestations of preeclampsia. *Am J Reprod Immunol* 1997; 38: 89-93.
117. Conrad KP, Miles TM, Benyo DF. Circulating levels of immunoreactive cytokines in women with preeclampsia. *Am J Reprod Immunol* 1998; 40: 102-11.
118. Redman CW, Sacks GP, Sargent IL. Preeclampsia: an excessive maternal inflammatory response to pregnancy. *Am J Obstet Gynecol* 1999; 180(2 Pt 1): 499-506.
119. Sabatier F, Bretelle F, D'Ercole C, Boubli L, Sampol J, Dignat-George F. Neutrophil activation in preeclampsia and isolated intrauterine growth restriction. *Am J Obstet Gynecol* 2000; 183: 1558-63.
120. Gervasi MT, Chaiworapongsa T, Pacora P, *et al.* Phenotypic and metabolic characteristics of monocytes and granulocytes in preeclampsia. *Am J Obstet Gynecol* 2001; 185: 792-7.
121. Teran E, Escudero C, Moya W, Flores M, Vallance P, Lopez-Jaramillo P. Elevated C-reactive protein and pro-inflammatory cytokines in Andean women with pre-eclampsia. *Int J Gynaecol Obstet* 2001; 75: 243-9.
122. Chaiworapongsa T, Romero R, Yoshimatsu J, *et al.* Soluble adhesion molecule profile in normal pregnancy and pre-eclampsia. *J Matern Fetal Neonatal Med* 2002; 12: 19-27.
123. Chaiworapongsa T, Gervasi MT, Refuerzo J, *et al.* Maternal lymphocyte subpopulations (CD45RA+ and CD45RO+) in preeclampsia. *Am J Obstet Gynecol* 2002; 187: 889-93.
124. Velzing-Aarts FV, Muskiet FA, van der Dijs FP, Duits AJ. High serum interleukin-8 levels in afro-caribbean women with pre-eclampsia: relations with tumor necrosis factor-alpha, duffy negative phenotype and von Willebrand factor. *Am J Reprod Immunol* 2002; 48: 319-22.
125. Serin IS, Ozcelik B, Basbug M, Kilic H, Okur D, Erez R. Predictive value of tumor necrosis factor alpha (TNF-alpha) in preeclampsia. *Eur J Obstet Gynecol Reprod Biol* 2002; 100: 143-5.
126. Belo L, Santos-Silva A, Caslake M, *et al.* Neutrophil activation and C-reactive protein concentration in preeclampsia. *Hypertens Pregnancy* 2003; 22: 129-41.
127. Levine RJ, Qian C, Leshane ES, *et al.* Two-stage elevation of cell-free fetal DNA in maternal sera before onset of preeclampsia. *Am J Obstet Gynecol* 2004; 190: 707-13.
128. Kocyigit Y, Atamer Y, Atamer A, Tuzcu A, Akkus Z. Changes in serum levels of leptin, cytokines and lipoprotein in pre-eclamptic and normotensive pregnant women. *Gynecol Endocrinol* 2004; 19: 267-73.
129. Freeman DJ, McManus F, Brown EA, *et al.* Short- and long-term changes in plasma inflammatory markers associated with preeclampsia. *Hypertension* 2004; 44: 708-14.
130. Kim YM, Romero R, Oh SY, *et al.* Toll-like receptor 4: a potential link

- between “danger signals,” the innate immune system, and preeclampsia? *Am J Obstet Gynecol* 2005; 193(3 Pt 2): 921-7.
131. Braekke K, Holthe MR, Harsem NK, Fagerhol MK, Staff AC. Calprotectin, a marker of inflammation, is elevated in the maternal but not in the fetal circulation in preeclampsia. *Am J Obstet Gynecol* 2005; 193: 227-33.
 132. Enquobahrie DA, Williams MA, Qiu C, Woelk GB, Mahomed K. Maternal plasma transforming growth factor-beta1 concentrations in preeclamptic and normotensive pregnant Zimbabwean women. *J Matern Fetal Neonatal Med* 2005; 17: 343-8.
 133. Jonsson Y, Rubèr M, Matthesen L, et al. Cytokine mapping of sera from women with preeclampsia and normal pregnancies. *J Reprod Immunol* 2006; 70: 83-91.
 134. Kusanovic JP, Romero R, Hassan SS, et al. Maternal serum soluble CD30 is increased in normal pregnancy, but decreased in preeclampsia and small for gestational age pregnancies. *J Matern Fetal Neonatal Med* 2007; 20: 867-78.
 135. Sharma A, Satyam A, Sharma JB. Leptin, IL-10 and inflammatory markers (TNF-alpha, IL-6 and IL-8) in pre-eclamptic, normotensive pregnant and healthy non-pregnant women. *Am J Reprod Immunol* 2007; 58: 21-30.
 136. Laskowska M, Laskowska K, Leszczyńska-Gorzela B, Oleszczuk J. Comparative analysis of the maternal and umbilical interleukin-8 levels in normal pregnancies and in pregnancies complicated by preeclampsia with intrauterine normal growth and intrauterine growth retardation. *J Matern Fetal Neonatal Med* 2007; 20: 527-32.
 137. Sibai B, Romero R, Klebanoff MA, et al. Maternal plasma concentrations of the soluble tumor necrosis factor receptor 2 are increased prior to the diagnosis of preeclampsia. *Am J Obstet Gynecol* 2009; 200: 630.e1-8.
 138. Ogge G, Romero R, Chaiworapongsa T, et al. Leukocytes of pregnant women with small-for-gestational age neonates have a different phenotypic and metabolic activity from those of women with preeclampsia. *J Matern Fetal Neonatal Med* 2010; 23: 476-87.
 139. Soto E, Romero R, Richani K, et al. Preeclampsia and pregnancies with small-for-gestational age neonates have different profiles of complement split products. *J Matern Fetal Neonatal Med* 2010; 23: 646-57.
 140. Szarka A, Rigó J Jr, Lázár L, Beko G, Molvarec A. Circulating cytokines, chemokines and adhesion molecules in normal pregnancy and preeclampsia determined by multiplex suspension array. *BMC Immunol* 2010; 11: 59.
 141. Xie C, Yao MZ, Liu JB, Xiong LK. A meta-analysis of tumor necrosis factor-alpha, interleukin-6, and interleukin-10 in preeclampsia. *Cytokine* 2011; 56: 550-9.
 142. Twina G, Sheiner E, Shahaf G, et al. Lower circulation levels and activity of alpha-1 antitrypsin in pregnant women with severe preeclampsia. *J Matern Fetal Neonatal Med* 2012; 25: 2667-70.
 143. Stampalija T, Chaiworapongsa T, Romero R, et al. Maternal plasma concentrations of sT2 and angiogenic/anti-angiogenic factors in preeclampsia. *J Matern Fetal Neonatal Med* 2013; 26: 1359-70.
 144. Sahin S, Ozakpinar OB, Eroglu M, et al. The impact of platelet functions and inflammatory status on the severity of preeclampsia. *J Matern Fetal Neonatal Med* 2015; 28: 643-8.
 145. Labarrere C, Manni J, Salas P, Althabe O. Intrauterine growth retardation of unknown etiology. I. Serum complement and circulating immune complexes in mothers and infants. *Am J Reprod Immunol Microbiol* 1985; 8: 87-93.
 146. Labarrere CA, Althabe OH. Intrauterine growth retardation of unknown etiology: II. Serum complement and circulating immune complexes in maternal sera and their relationship with parity and chronic villitis. *Am J Reprod Immunol Microbiol* 1986; 12: 4-6.
 147. Johnston TA, Greer IA, Dawes J, Calder AA. Neutrophil activation in small for gestational age pregnancies. *Br J Obstet Gynaecol* 1991; 98: 105-6.
 148. Johnson MR, Anim-Nyame N, Johnson P, Sooranna SR, Steer PJ. Does endothelial cell activation occur with intrauterine growth restriction? *BJOG* 2002; 109: 836-9.
 149. Coata G, Pennacchi L, Bini V, Liotta L, Di Renzo GC. Soluble adhesion molecules: marker of pre-eclampsia and intrauterine growth restriction. *J Matern Fetal Neonatal Med* 2002; 12: 28-34.
 150. Tjoa ML, van Vugt JM, Go AT, Blankenstein MA, Oudejans CB, van Wijk IJ. Elevated C-reactive protein levels during first trimester of pregnancy are indicative of preeclampsia and intrauterine growth restriction. *J Reprod Immunol* 2003; 59: 29-37.
 151. Cetin I, Cozzi V, Pasqualini F, et al. Elevated maternal levels of the long pentraxin 3 (PTX3) in preeclampsia and intrauterine growth restriction. *Am J Obstet Gynecol* 2006; 194: 1347-53.
 152. Girardi G, Yarin D, Thurman JM, Holers VM, Salmon JE. Complement activation induces dysregulation of angiogenic factors and causes fetal rejection and growth restriction. *J Exp Med* 2006; 203: 2165-75.
 153. Laskowska M, Laskowska K, Leszczyńska-Gorzela B, Oleszczuk J. Maternal and umbilical sTNF-R1 in preeclamptic pregnancies with intrauterine normal and growth retarded fetus. *Hypertens Pregnancy* 2007; 26: 13-21.
 154. Erez O, Romero R, Hoppensteadt D, et al. Tissue factor and its natural inhibitor in pre-eclampsia and SGA. *J Matern Fetal Neonatal Med* 2008; 21: 855-69.
 155. Duff P. Pyelonephritis in pregnancy. *Clin Obstet Gynecol* 1984; 27: 17-31.
 156. Gilstrap LC 3rd, Lucas MJ. Urinary tract infections in women. *Curr*

- Opin Obstet Gynecol 1990; 2: 643-8.
157. Soto E, Richani K, Romero R, *et al*. Increased concentration of the complement split product C5a in acute pyelonephritis during pregnancy. *J Matern Fetal Neonatal Med* 2005; 17: 247-52.
 158. Rajamäki K, Lappalainen J, Oörni K, *et al*. Cholesterol crystals activate the NLRP3 inflammasome in human macrophages: a novel link between cholesterol metabolism and inflammation. *PLoS One* 2010; 5: e11765.
 159. Small DM, Shipley GG. Physical-chemical basis of lipid deposition in atherosclerosis. *Science* 1974; 185: 222-9.
 160. Sattar N, Bendoric A, Berry C, Shepherd J, Greer IA, Packard CJ. Lipoprotein subfraction concentrations in preeclampsia: pathogenic parallels to atherosclerosis. *Obstet Gynecol* 1997; 89: 403-8.
 161. Lorentzen B, Endresen MJ, Hovig T, Haug E, Henriksen T. Sera from preeclamptic women increase the content of triglycerides and reduce the release of prostacyclin in cultured endothelial cells. *Thromb Res* 1991; 63: 363-72.
 162. Hubel CA, McLaughlin MK, Evans RW, Hauth BA, Sims CJ, Roberts JM. Fasting serum triglycerides, free fatty acids, and malondialdehyde are increased in preeclampsia, are positively correlated, and decrease within 48 hours post partum. *Am J Obstet Gynecol* 1996; 174: 975-82.
 163. Belo L, Santos-Silva A, Quintanilha A, Rebelo I. Similarities between pre-eclampsia and atherosclerosis: a protective effect of physical exercise? *Curr Med Chem* 2008; 15: 2223-9.
 164. Lau SY, Guild SJ, Barrett CJ, *et al*. Tumor necrosis factor-alpha, interleukin-6, and interleukin-10 levels are altered in preeclampsia: a systematic review and meta-analysis. *Am J Reprod Immunol* 2013; 70: 412-27.
 165. Chaiworapongsa T, Chaemsaihong P, Yeo L, Romero R. Pre-eclampsia part 1: current understanding of its pathophysiology. *Nat Rev Nephrol* 2014; 10: 466-80.
 166. Boyd EM. The lipemia of pregnancy. *J Clin Invest* 1934; 13: 347-63.
 167. Potter JM, Nestel PJ. The hyperlipidemia of pregnancy in normal and complicated pregnancies. *Am J Obstet Gynecol* 1979; 133: 165-70.
 168. Baker AM, Klein RL, Moss KL, Haeri S, Boggess K. Maternal serum dyslipidemia occurs early in pregnancy in women with mild but not severe preeclampsia. *Am J Obstet Gynecol* 2009; 201: 293.e1-4.
 169. Labarrere CA, Faulk WP. Antigenic identification of cells in spiral artery trophoblastic invasion: validation of histologic studies by triple-antibody immunocytochemistry. *Am J Obstet Gynecol* 1994; 171: 165-71.
 170. Roberts JM, Redman CW. Pre-eclampsia: more than pregnancy-induced hypertension. *Lancet* 1993; 341: 1447-51.

Therapeutic Effects of Umbilical Cord Blood Derived Mesenchymal Stem Cell-Conditioned Medium on Pulmonary Arterial Hypertension in Rats

Jae Chul Lee^{1,2,3} · Choong Ik Cha³
Dong-Sik Kim² · Soo Young Choe¹

¹Department of Biology, School of Life Sciences, Chungbuk National University, Cheongju, ²Department of Surgery, Brain Korea 21 PLUS Project for Medical Sciences and HBP Surgery and Liver Transplantation, Korea University College of Medicine, Seoul; ³Department of Anatomy, Seoul National University College of Medicine, Seoul, Korea

Received: September 4, 2015

Accepted: September 9, 2015

Corresponding Authors

Soo Young Choe, PhD
Department of Biology, School of Life Sciences, Chungbuk National University, 1 Chungdae-ro, Seowon-gu, Cheongju 28644, Korea
Tel: +82-43-261-2297
Fax: +82-43-275-2291
E-mail: leejc@chungbuk.ac.kr

Dong-Sik Kim, MD, PhD
Department of Surgery, Brain Korea 21 PLUS Project for Medical Sciences and HBP Surgery and Liver Transplantation, Korea University College of Medicine, 145 Anam-ro, Seongbuk-gu, Seoul 02841, Korea
Tel: +82-2-2286-1431
Fax: +82-2-2286-1428
E-mail: beas100@korea.ac.kr

Background: Human umbilical cord blood-derived mesenchymal stem cells (hUCB-MSCs) may have multiple therapeutic applications for cell based therapy including the treatment of pulmonary artery hypertension (PAH). As low survival rates and potential tumorigenicity of implanted cells could undermine the mesenchymal stem cell (MSC) cell-based therapy, we chose to investigate the use of conditioned medium (CM) from a culture of MSC cells as a feasible alternative. **Methods:** CM was prepared by culturing hUCB-MSCs in three-dimensional spheroids. In a rat model of PAH induced by monocrotaline, we infused CM or the control unconditioned culture media via the tail-vein of 6-week-old Sprague-Dawley rats. **Results:** Compared with the control unconditioned media, CM infusion reduced the ventricular pressure, the right ventricle/(left ventricle+interventricular septum) ratio, and maintained respiratory function in the treated animals. Also, the number of interleukin 1 α (IL-1 α), chemokine (C-C motif) ligand 5 (CCL5), and tissue inhibitor of metalloproteinase 1 (TIMP-1)-positive cells increased in lung samples and the number of terminal deoxynucleotidyl transferase-mediated deoxyuridine triphosphate nick-end labeling technique (TUNEL)-positive cells decreased significantly in the CM treated animals. **Conclusions:** From our *in vivo* data in the rat model, the observed decreases in the TUNEL staining suggest a potential therapeutic benefit of the CM in ameliorating PAH-mediated lung tissue damage. Increased IL-1 α , CCL5, and TIMP-1 levels may play important roles in this regard.

Key Words: Apoptosis; Culture media, conditioned; Gene expression; Mesenchymal stromal cells; Pulmonary artery hypertension

Pulmonary artery hypertension (PAH) is a progressive chronic disease with a high mortality rate.¹ PAH has a complex disease mechanism, but its cardinal signs are an elevation of pulmonary artery pressure, right ventricular (RV) hypertrophy, and arteriolar wall remodeling.² Increased pulmonary vascular resistance and over-proliferation of pulmonary artery endothelial cells leads to remodeling of the pulmonary vasculature.³⁻⁵ There is also damage to the pulmonary microvasculature impacting the blood flow from the heart to the lungs.^{6,7} Although current treatments may prolong and improve quality of life for the patients, the long-term prognosis for PAH is poor with a 2- to 3-year survival at the time of diagnosis.¹

Autologous implantation of bone marrow mononuclear cells, known to be enriched in mesenchymal stem cells (MSCs), has demonstrated safety and effectiveness in therapeutic angiogenesis.⁸ A number of studies have also indicated a therapeutic benefit from bone marrow derived MSCs in increasing respiratory function in animal models of PAH.^{9,10} In separate studies, human umbilical cord blood-derived MSCs (hUCB-MSCs) have also improved lung function in animal models of PAH and in a number of human PAH patients.¹¹⁻¹³

In previous studies, we demonstrated the neuroprotective potential of various conditioned media (CM), namely human adipose tissue-derived stem cell (hADSC)-conditioned media and

human neural stem cell (hNSC)-conditioned media to treat rats with stroke and Huntington's disease.^{14,15} We also investigated gene expression changes by microarray analysis after injection of hUCB-MSCs into rats in an experimental model of PAH.¹⁶ Based on our findings from that study, we undertook an investigation to assess the feasibility and safety of conditioned medium from hUCB-MSCs (hUCB-MSC-CM) in the same rat PAH model. We also tested the hypothesis that the conditioned media from these cells may lead to improved lung function in the affected rats. Here, we elaborate on our results and demonstrate that the conditioned media provides a therapeutic benefit in the rat model of PAH. As there are certain advantages in using conditioned media in lieu of autologous whole bone marrow or umbilical cord cells as sources for MSCs, our data may provide a means of increasing the accessibility of MSCs to treat various diseases including PAH.

MATERIALS AND METHODS

Animals

Six-week-old male Sprague-Dawley rats were used. All rats were housed in climate-controlled conditions with a 12-hour light/12-hour dark cycle, and had free access to food and water. All animal experiments were approved by the appropriate Institutional Review Boards of the Seoul National University College of Medicine (Seoul, Korea; SNU-101122-2) and conducted in accordance with National Institutes of Health Guide for the Care Use of Laboratory Animals (NIH publication No. 86-23, revised in 1996).

Pulmonary arterial hypertension rat model

PAH was induced by subcutaneous injection of 50 mg/kg monocrotaline (MCT; Sigma-Aldrich, St. Louis, MO, USA) dissolved in 0.5 N HCl. The rats were grouped into a control group (C group) (n = 20), injection of α -minimal essential medium (α MEM) followed by MCT group (M group) (n = 20), and injection of MCT followed by hUCB-MSC-CM transfusion group (CM group) (n = 20). α MEM and hUCB-MSC-CM (0.5 μ L/hr) were transfused by tail-vein 7 days after MCT injection. The animals were sacrificed at 7, 14, 21, and 28 days after hUCB-MSC-CM transfusion. Tissues were removed and immediately frozen at -70°C for enzyme analysis.

Cell preparation and culture of hUCB-MSCs

hUCB-MSCs were obtained from the Biomedical Research Institute (Seoul, Korea). Isolated human MSCs were expanded

in culture as previously described.⁶ hUCB-MSCs were maintained in α MEM (Gibco, Grand Island, NY, USA) supplemented with 10% fetal bovine serum (Gibco), 100 U/mL penicillin (Gibco), and 100 g/mL streptomycin (Gibco). Passages up to 5 were used for experiments.

Preparation of hUCB-MSC-CM

To generate hUCB-MSC-CM spheroids,^{16,17} 30 μ L of cell suspension (1×10^6 cells/mL) were applied to the lid of a Petri dish containing phosphate buffered saline (PBS). After 24 hours of incubation, spheroids formed in the drops were retrieved. For the three-dimensional bioreactor culture, hUCB-MSC spheroids (4.2×10^7 cells) were cultured in a siliconized spinner flask (Bellco, Vineland, NJ, USA) containing 70 mL α MEM with stirring at 70 rpm. To obtain CM, the medium was changed to α MEM without serum, and the cells were cultured for 2 days. CM was collected by centrifugation.¹⁴

Determination of the organ weights and right hypertrophy index

The rats were weighed and observed for general appearance during the study period. The animals were sacrificed at the scheduled time. The wet weights of the excised right ventricle (RV), left ventricle (LV), and interventricular septum (IVS) were measured. The weights of the LV and IVS were added (LV + IVS) to determine the RV to LV + IVS ratio [RV/(LV + IVS)], which was used to determine the right hypertrophy index.

Pulmonary hemodynamics

Rats were anaesthetized by intraperitoneal injection of urethane and secured on a surgical stage. An 8-mm-long right internal jugular vein was isolated and ligated at the distal end. The vessel was cut at the proximal end of ligation. A catheter filled with heparinized saline was rapidly inserted along the incision and slowly advanced for about 5 cm to enter the pulmonary artery. The standard of pulmonary hypertension was defined as a systolic pulmonary pressure (SPAP) larger than 50 mm Hg.¹⁸ Hemodynamic parameters were recorded at baseline and at 7, 14, 21, and 28 days.

Immunohistochemistry

Excised lung tissues were incubated overnight in 10% buffered formalin. Four-micrometer-thick sections were cut from paraffin embedded tissue blocks, deparaffinized in xylene, and rehydrated in graded alcohol solutions (70%–100%). Heat antigen retrieval was achieved by boiling the tissue sections in an

tigen retrieval solution in pH 6.0 or pH 9.0 (Dako, Carpinteria, CA, USA) for 10 minutes in a microwave prior to incubation at 4°C overnight with primary antibodies against interleukin 1 α (IL-1 α), chemokine (C-C motif) ligand 5 (CCL5), and tissue inhibitor of metalloproteinase 1 (TIMP-1; Abcam, Cambridge, MA, USA). After incubation with the appropriate biotinylated secondary antibodies for 30 minutes at 4°C and subsequently with streptavidin (Dako, Kyoto, Japan), color development was done using diaminobenzidine (DAB) as a chromogen and counterstained with hematoxylin.

Western blot analysis

The tissue was homogenized in 10 mM Tris HCl buffer, pH 7.4 containing 0.5 mM ethylenediaminetetraacetic acid, pH 8.0, 0.25 M sucrose, 1 mM phenylmethylsulfonyl fluoride, 1 mM Na₄VO₃, and a protease inhibitor cocktail (Roche-Boehringer-Mannheim, Mannheim, Germany). After centrifugation, the supernatant was subjected to sodium dodecyl sulfate polyacrylamide gel electrophoresis (SDS-PAGE). Samples equivalent to 25 μ g of protein content were loaded and size-separated by 8%–12% SDS-PAGE. The proteins on the acrylamide gel were transferred to a polyvinylidene difluoride membrane (Millipore, Bedford, MA, USA) at 400 mA in a transfer buffer containing 25 mM Tris and 192 mM glycine, pH 8.4. The nitrocellulose membrane was blocked in tris-buffered saline with 5% non-fat dry milk at room temperature for 1 hour in 0.1% Tween 20 and incubated with the appropriated primary antibodies, including anti-IL-1 α (Santa Cruz Biotechnology, Santa Cruz, CA, USA), anti-CCL5 (Fitzgerald Industries International, Concord, MA, USA), anti-TIMP-1 (Abcam), and anti-caspase-3, anti-Bcl-2, anti-actin (Santa Cruz Biotechnology) at 4°C for overnight. The membranes were then incubated with horseradish peroxidase-conjugated secondary antibody (Cell Signaling Technology, Danvers, MA, USA) for 1 hour at room temperature. After washing, the membranes were visualized by a chemiluminescent ECL-detection kit from GE-Healthcare (Piscataway, NJ, USA).

Cytokine array and gene expression in lung tissues

The lung samples were collected at termination (4 days after hUCB-MSC-CM injection) and quickly frozen in liquid nitrogen. A rat cytokine array (ARY008, R&D Systems, Minneapolis, MN, USA) was used to screen the lung homogenates according to the manufacturer's instructions. The samples were pooled per treatment group and equal amounts of protein were loaded on the blots.

In situ terminal deoxynucleotidyl transferase-mediated deoxyuridine triphosphate nick-end labeling technique assay for lung cell apoptosis

Apoptotic cells in the tissue sections were detected by the terminal deoxynucleotidyl transferase-mediated deoxyuridine triphosphate nick-end labeling technique (TUNEL) using a commercial apoptosis kit (TACS TM TdT Kit, R&D Systems), according to the supplier's instructions. In brief, the lung tissue sections were de-paraffinized with xylene and ethanol and rinsed with PBS. The sections were then treated with proteinase K in PBS followed by quenching of endogenous peroxidase. A biotinylated dNTP mix was added to the 3'-OH ends of DNA by terminal deoxynucleotidyl transferase (TdT). After incubating with streptavidin-horseradish peroxidase, the sections were stained with DAB and counterstained with methyl green. Finally, the sections were dehydrated in ethanol, cleared with xylene, and mounted with coverslips in a permanent medium. According to the supplier's instructions, experimental controls included for the assay were TACS-nuclease-treated thyroid tissue sections as the positive control and the omission of the TdT reaction step as the negative control.

Statistical analyses

Results were expressed as the mean \pm standard deviation. An unpaired two-tailed t test and Mann-Whitney test were used, and a p-value less than .05 was considered statistically significant. SPSS ver. 14.0 for Windows (SPSS Inc., Chicago, IL, USA) was used for all statistical analyses.

RESULTS

Changes in body and organ weights and systolic pulmonary artery pressure after injection with hUCB-MSC-CM in PAH rats

hUCB-MSC-CM has the potential to increase cell differentiation and induce immune modulation in various disease models.^{19,20} However, the role of hUCB-MSC-CM in PAH has not been well elucidated. To address this, in our rat model of PAH, following MCT treatment, we treated rats with hUCB-MSC-CM and sham treated for the control group. There was a significant decrease in body weight at 14, 21, and 28 days in the MCT group (M group) compared to the control group (C group). However, body weight increased at 21 and 28 days in the conditioned media treated group (CM group) compared to the M group. The M group also showed increased weights of the RV at 21 and 28 days. The sum weight of LV + IVS was not signifi-

Table 1. Changes of body and organ weights after hUCB-MSCs-CM injection in PAH rats

Day	Group	Body weight (g)	RV (g)	LV + IVS (g)	RV / (LV + IVS) (%)
7	Control	318.63 ± 14.78	0.132 ± 0.02	0.611 ± 0.02	0.21 ± 0.01
	M	278.50 ± 32.71	0.155 ± 0.03	0.543 ± 0.03	0.28 ± 0.02
	CM	280.46 ± 29.82	0.164 ± 0.02	0.561 ± 0.03	0.29 ± 0.02
14	Control	343.65 ± 24.52	0.156 ± 0.02	0.731 ± 0.03	0.21 ± 0.02
	M	256.71 ± 45.57 ^a	0.234 ± 0.03	0.671 ± 0.02	0.34 ± 0.03 ^a
	CM	271.21 ± 38.82	0.224 ± 0.04	0.699 ± 0.03	0.32 ± 0.02
21	Control	393.81 ± 24.62	0.166 ± 0.03	0.782 ± 0.03	0.21 ± 0.02
	M	249.67 ± 47.29 ^a	0.314 ± 0.06 ^a	0.677 ± 0.05	0.46 ± 0.05 ^a
	CM	271.00 ± 51.55 ^b	0.284 ± 0.05	0.631 ± 0.03	0.45 ± 0.03
28	Control	394.00 ± 41.61	0.171 ± 0.02	0.801 ± 0.03	0.21 ± 0.02
	M	229.71 ± 44.82 ^a	0.394 ± 0.08 ^a	0.751 ± 0.06	0.52 ± 0.07 ^a
	CM	319.29 ± 36.62 ^b	0.261 ± 0.06 ^b	0.732 ± 0.04	0.35 ± 0.04 ^b

Values are presented as mean ± standard deviation.

hUCB-MSCs-CM, conditioned medium from human umbilical-cord blood derived mesenchymal cells; PAH, pulmonary artery hypertension; RV, right ventricle; LV, left ventricle; IVS, interventricular septum; M, monocrotaline; CM, hUCB-MSCs-CM.

^ap < .05 compared with the C group; ^bp < .05 compared with the M group.

cantly different between the C, M, and CM groups at the time point tested. The ratio of RV to LV + IVS, namely RV/LV + IVS, was significantly higher at 14, 21, and 28 days in the M group compared with the C group. However, the RV/LV + IVS ratio was significantly decreased at 28 days in the CM group compared with the M group. Also, LV + IVS was significantly lower in both M and CM groups compared to the C group at 14, 21, and 28 days. The lung weight was significantly increased in the M group compared with the C group at 21 and 28 days. However, the lung weight was significantly decreased in the CM group compared to the M group at 28 days (Table 1). The mean SPAP was also significantly increased in the M group compared to the C and CM groups at 14, 21, and 28 days (Table 2).

Cytokine profile in the lung tissues after hUCB-MSC-CM treatment

A profile of the cytokines in the lung homogenates was made to investigate potential changes from hUCB-MSC-CM treatment (Fig. 1). Ten pro-inflammatory cytokines that included cytokine-induced neutrophil chemoattractant-1 (CINC-1), cytokine-induced neutrophil chemoattractant-2a/b (CINC-2a/b), chemokine (C-X-C motif) ligand 1 (CX3CL1), lipopolysaccharide-induced CXC chemokine (LIX), leukocyte endothelial cell adhesion molecule 1 (LECAM-1), chemokine (C-X-C motif) ligand 7, TIMP-1, vascular endothelial growth factor (VEGF), IL-1 α , and CCL5 were examined in the C, M, and CM groups. CINC-1, CINC-2a/b, CX3CL1, LIX, LECAM-1, TIMP-1, and VEGF were lower in the M and CM groups, whereas TIMP-1, IL-1 α , and CCL5 were higher in the CM group compared to the C and M groups. CCL7 was higher in the M group, whereas CCL7

Table 2. Change of systolic pulmonary artery pressure after hUCB-MSCs-CM injection in PAH rats

Day	C group	M group	CM group
7	22.7 ± 0.6	24.5 ± 2.1	23.2 ± 3.4
14	22.0 ± 1.1	37.8 ± 3.2 ^a	30.9 ± 4.6
21	23.3 ± 0.9	50.2 ± 4.7 ^a	39.2 ± 5.2 ^b
28	22.9 ± 2.1	58.0 ± 6.4 ^a	37.8 ± 4.1 ^b

Values are presented as mean ± standard deviation.

hUCB-MSCs-CM, conditioned medium from human umbilical-cord blood derived mesenchymal cells; PAH, pulmonary artery hypertension; C, control; M, monocrotaline; CM, hUCB-MSCs-CM.

^ap < .05 compared with the C group; ^bp < .05 compared with the M group.

was lower in the CM group compared to the M group (Fig. 1).

Immunohistochemistry analysis of lung samples

Immunohistochemistry (IHC) staining of the lung tissue revealed that TIMP-1-, IL-1 α -, and CCL5-positive cells were more prevalent in the CM group, and then followed by the M group in comparison with the C group at 28 days (Fig. 2A–R). These results confirmed that hUCB-MSC-CM increased the expression of certain immunomodulating cytokines (at the protein level) in the lungs of treated animals. Three weeks after hUCB-MSC-CM transfusion, TIMP-1-, IL-1 α -, and CCL5-positive cells were still observed at the transplanted lung area in the CM group. The increased levels of TIMP-1, IL-1 α , and CCL5 immunoreactivity observed in the M group were statistically significant (p < .05). The increased levels of CCL5 immunoreactivity were also significant in the CM group compared with the M group (Fig. 2S).

Western blot analysis

The protein expressions of CCL5 at 28 days were significant-

ly increased in the M group compared to the C group. The protein expressions of TIMP-1, IL-1 α , and CCL5 at 28 days were significantly increased in the CM group compared to the M group (Fig. 3). The protein expressions of caspase-3 and Bcl-2 were significantly increased in the M group compared to the C group at 28 days. The protein expressions of caspase-3 and Bcl-

2 were significantly decreased in the CM group compared to the M group at 28 days (Fig. 4).

TUNEL apoptosis assay

The TUNEL staining was performed to detect apoptotic DNA in the lung tissue. The assayed C group did not have any positive

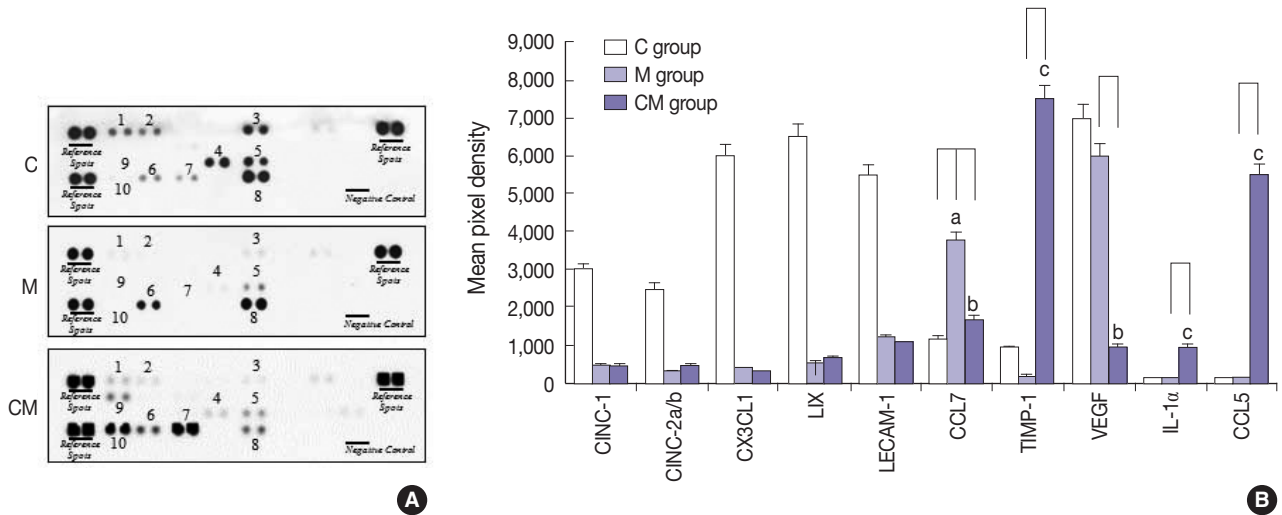


Fig. 1. Inflammatory cytokine expressions in the three groups. (A) To screen whether hUCB-MSCs-CM affect local production of inflammatory cytokines by lung cells in the three groups, a cytokine array is performed on lung homogenates. (B) TIMP-1, IL-1 α , and CCL5 are higher in the CM group compared to the C and M groups, whereas CCL7 and VEGF are lower in the CM group compared to the M group. CINC-1, CINC-2a/b, CX3CL1, LIX, and LECAM-1 are higher in the C group compared to the M and CM groups. C group, control group (n = 7); M group, monocrotaline group (n = 7); CM group, hUCB-MSCs-CM group (n = 7). hUCB-MSCs-CM, conditioned medium from human umbilical-cord blood derived mesenchymal cells; CINC-1, cytokine-induced neutrophil chemoattractant-1; CINC-2a/b, cytokine-induced neutrophil chemoattractant-2a/b; CX3CL1, chemokine (C-X-C motif) ligand 1; LIX, lipopolysaccharide-induced CXC chemokine; LECAM-1, leukocyte endothelial cell adhesion molecule 1; CCL7, chemokine (C-C motif) ligand 7; TIMP-1, tissue inhibitor of metalloproteinase 1; VEGF, vascular endothelial growth factor; IL-1 α , interleukin 1 α . ^ap < .05 compared with the C group; ^bp < .05 compared with the M group.

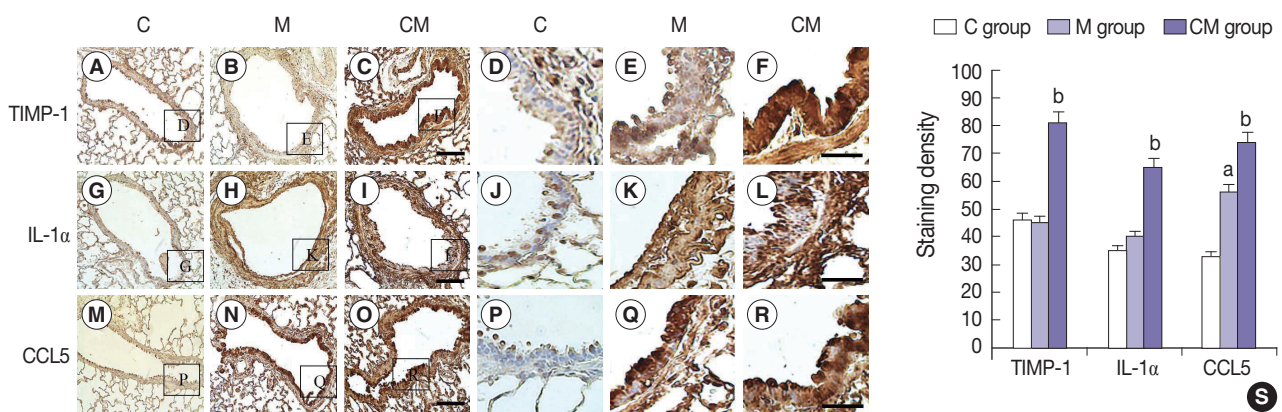


Fig. 2. Localization of IL-1 α , CCL5, and TIMP-1-immunoreactive cells in the lung tissues at 28 days. (A–R) Immunohistochemical expression reveals that the positive cells of IL-1 α , CCL5, and TIMP-1 are significantly higher in the CM group than that in the C and M groups, and they are higher in the M group than that in the C group. (S) The increased levels of IL-1 α , CCL5, and TIMP-1 immunoreactivity observed in the CM group are statistically significant. The levels of IL-1 α , CCL5, and TIMP-1 immunoreactivity are significantly decreased in the CM group compared with the C and M groups. Panels A–C, G–I, and M–O are high power views of panels D–F, J–L, and P–R, respectively. C, control; M, monocrotaline; CM, hUCB-MSCs-CM; hUCB-MSCs-CM, conditioned medium from human umbilical-cord blood derived mesenchymal cells; TIMP-1, tissue inhibitor of metalloproteinase 1; IL-1 α , interleukin 1 α ; CCL5, chemokine (C-C motif) ligand 5. ^ap < .05 compared with the C group; ^bp < .05 compared with the M group.

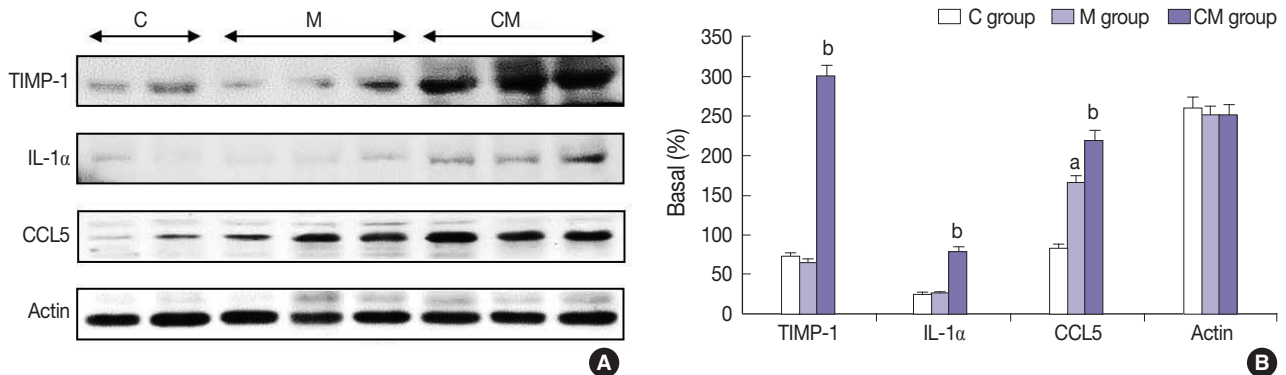


Fig. 3. Changes of IL-1 α , CCL5, and TIMP-1 protein expression levels after hUCB-MSCs-CM injection in PAH rats. (A) These are pictures of protein expression levels of IL-1 α , CCL5, and TIMP-1 in the lung tissues. (B) The protein expressions levels of IL-1 α , CCL5, and TIMP-1 at 28 days are significantly increased in the CM group compared to the C and M groups. The protein expressions of CCL are increased in the M group compared to the C group. C, control; M, monocrotaline; CM, hUCB-MSCs-CM; hUCB-MSCs-CM, conditioned medium from human umbilical-cord blood derived mesenchymal cells; TIMP-1, tissue inhibitor of metalloproteinase 1; IL-1 α , interleukin 1 α ; CCL5, chemokine (C-C motif) ligand 5. ^a $p < .05$ compared with the C group; ^b $p < .05$ compared with the M group.

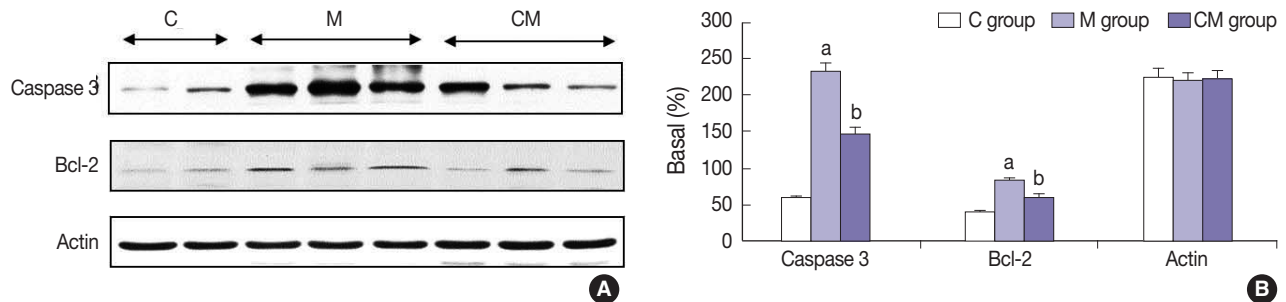


Fig. 4. Changes of caspase-3 and Bcl-2 protein expression levels after hUCB-MSCs-CM injection in PAH rats. (A) These are pictures of protein expression levels of caspase-3 and Bcl-2 in the lung tissues. (B) The protein expressions levels of caspase-3 and Bcl-2 at 28 days are significantly increased in the M group compared to the C groups. However, the protein expressions levels of caspase-3 and Bcl-2 are decreased in the CM group compared to the M group. C, control; M, monocrotaline; CM, hUCB-MSCs-CM; hUCB-MSCs-CM, conditioned medium from human umbilical-cord blood derived mesenchymal cells. ^a $p < .05$ compared with the C group; ^b $p < .05$ compared with the M group.

staining (Fig. 5A, D). However, the M group had lung tissues with a positive TUNEL staining as seen by the presence of dark brown nuclei (Fig. 5B, E). CM group also contained cells with brown nuclei, indicating apoptotic DNA (Fig. 5C, F). Apoptotic cells were significantly more prevalent in the M group than in the C group, but they were less prevalent in the CM group than in the M group (Fig. 5G). The results indicated that hUCB-MSC-CM could attenuate apoptosis in the lung tissues of treated PAH rats.

DISCUSSION

In this study, we tested the effects of CM infusion on PAH affected lung tissue in a rat model. It was previously demonstrated that CM of hUCB-MSCs contain active levels of a number of disease modifying growth factors and cytokines.^{21,22} CM of

hUCB-MSCs contain sizable levels of angiopoietin, hepatocyte growth factor, interleukin-4, insulin-like growth factor, placental growth factor, vascular endothelial cell growth factor, angiogenin, stem cell factor, and tyrosine hydroxylase.^{5,23-25} Our previous studies demonstrated the neuroprotective effects of conditioned media from hADSC and hNSC in rat models of stroke and Huntington's disease.^{14,15} Therefore, we chose to test the CM prepared from hUCB-MSCs in a PAH rat model for therapeutic signals.

MSCs are multipotent stromal cells that have self-renewal capacity, and can differentiate into a variety of cell types such as osteoblasts, chondrocytes, myocytes, and adipocytes.^{26,27} MSCs have been isolated from several different sources such as embryonic tissue, bone marrow, adipose tissue, and the placenta.²⁸ MSCs are the source of many immune-dampening cytokines and in this regard, have demonstrated potency in a number of disease mod-

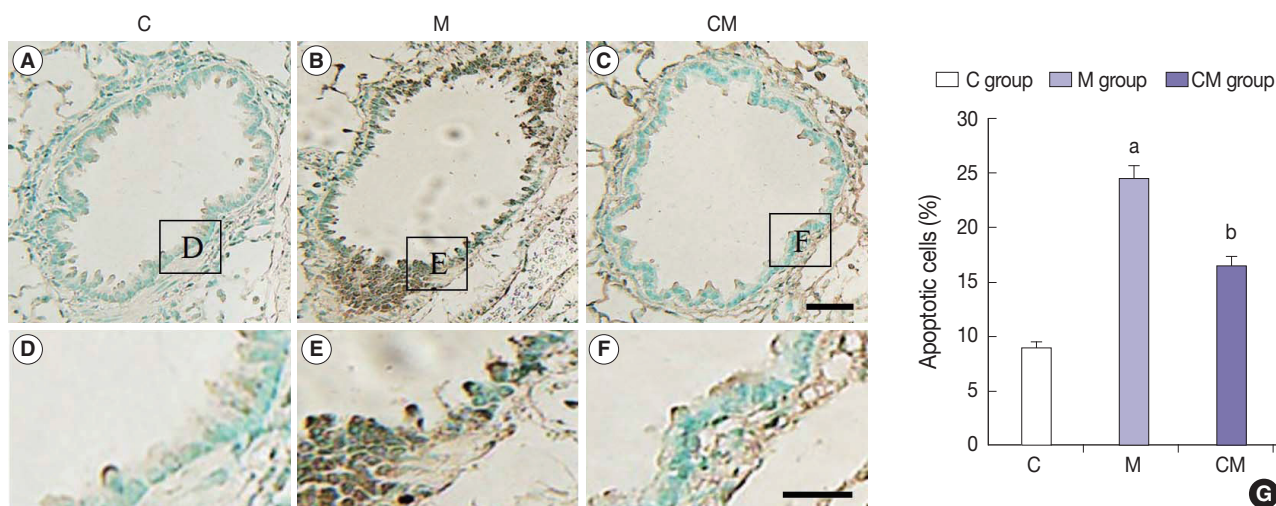


Fig. 5. TUNEL assay of lung tissues at 28 days after hUCB-MSCs-CM transfusion. (A–F) Immunohistochemical expression reveals that the positive cells of apoptosis are significantly higher in the M group than that in the C group; however, they are lower in the CM group than that in the M group. (G) The increased levels of TUNEL immunoreactivity observed in the M group are statistically significant. The levels of TUNEL immunoreactivity are significantly decreased in the CM group compared with the M group. This result indicates that hUCB-MSCs-CM could attenuate the vascular remodeling. Panels A–C are high power views of panels D–F, respectively. C, control; M, monocrotaline; CM, hUCB-MSCs-CM; hUCB-MSCs-CM, conditioned medium from human umbilical-cord blood derived mesenchymal cells. ^a $p < .05$ compared with the C group; ^b $p < .05$ compared with the M group.

els.^{29,30} In addition the secreted factors from MSCs display anti-apoptotic, proliferative activity and the cells may be involved in the removal of harmful factors from their vicinity.^{23,31}

From our study, we detected relatively high concentrations of CCL5, TIMP-1, and IL-1 α in hUCB-MSC-CM treated lung tissues compared with MCT alone (M) and control (C) groups as confirmed by a rat cytokine array panel (Fig. 1). Cytokines play important roles in a number of biological processes including innate immunity, apoptosis, angiogenesis, cell growth, and differentiation.³² These processes play important roles in disease protection and recovery.

Lipopolysaccharide-induced CXC chemokine (also termed CXCL5) is a member of the CXC chemokine family, and is a potent neutrophil chemoattractant.³³ A TIMP-1 is a naturally occurring inhibitor of metalloproteinases,^{34–36} and TIMPs inhibit tumorigenesis, cellular invasion, metastasis, and angiogenesis. TIMPs may also promote tumor growth and inhibit apoptosis. These opposite roles of TIMPs in tumor regression and progression have been attributed to modulation by the tissue microenvironment.³⁷ Many cytokines induce endothelial cells to express adhesion molecules and lead to secretion of chemokines that attract white blood cells to a site of injury.^{38,39} In our study, for the hUCB-MSC-CM treated PAH induced animals, the lung tissues showed significant increases in the number of IL-1 α -positive pulmonary arterioles compared with the control group.

IL-1 α (and also tumor necrosis factor α) are known to stimu-

late proliferation of endothelial cells and fibroblasts that increase the blood supply at the site of injury and repair damage.⁴⁰ The IL-1 family includes the structurally related proteins IL-1 α , IL-1 β , and IL-1 receptor antagonist that bind to the same receptor. The IL-1 family plays an important role in interstitial lung diseases. Previous research has demonstrated that IL-1 α expression levels in the lung correlated with the development of pulmonary fibrosis in rodents exposed to bleomycin or radiation.^{41,42} Furthermore, studies have demonstrated up-regulation of IL-1 α expression in fibro-proliferative areas within the lungs of idiopathic pulmonary fibrosis patients.⁴³ IHC for IL-1 α , CCL5, and TIMP-1 confirmed the lung cell increases for these three cytokines previously seen in the lung homogenates for the three cytokines (Fig. 2). How the characteristics of the above cytokines may either ameliorate or exacerbate the effects of PAH remain to be explored.

The numbers of TUNEL-positive cells in the lung areas were also significantly reduced by the infusion of hUCB-MSC-CM (Fig. 5). The hUCB-MSC-CM treatment was initiated 28 days after induction of PAH. Therefore, the reduction of apoptosis could be due to protective mechanisms of the hUCB-MSC-CM. These therapeutic effects could provide a clinically relevant benefit to patients. For our study, although no cells were implanted, our data demonstrated that an infusion of hUCB-MSC-CM can significantly reduce lung cell apoptosis due to PAH in our rat model. This novel therapeutic modality could be a viable

treatment for PAH and bypass several technical limitations of a direct MSC cell transplantation. The present study also revealed certain changes in chemokine, cytokine, and growth factor levels after hUCB-MSC-CM transfusion in a PAH rat model. Through a complex interaction of these mediators involved in immunomodulation and inflammation, we may expect a positive effect on reducing the impact of PAH on lung cells. Exactly how these cytokines and factors interact to impact the survival of the lung tissue cells remains to be explored. As there are several treatment options available for PAH in people, an effective therapy in prolonging survival remains elusive. Our data with factors present in hUCB-MSC-CM may present an exciting opportunity for more effective therapies.

The limitations of our study included the small sample size and a short follow-up of the treated animals. Future studies with larger sample sizes and a longer duration of treatment will be required, along with standardizing the quality and amount of hUCB-MSC-CM, frequency, and the duration required for the treatment.

Conflicts of Interest

No potential conflict of interest relevant to this article was reported.

Acknowledgments

This work was supported by a Korea University grant.

REFERENCES

- Farber HW, Loscalzo J. Pulmonary arterial hypertension. *N Engl J Med* 2004; 351: 1655-65.
- Liang OD, Mitsialis SA, Chang MS, *et al.* Mesenchymal stromal cells expressing heme oxygenase-1 reverse pulmonary hypertension. *Stem Cells* 2011; 29: 99-107.
- Can MM, Tanboga IH, Demircan HC, *et al.* Enhanced hemostatic indices in patients with pulmonary arterial hypertension: an observational study. *Thromb Res* 2010; 126: 280-2.
- Fukumoto Y, Shimokawa H. Recent progress in the management of pulmonary hypertension. *Circ J* 2011; 75: 1801-10.
- Liu Q, Luo Z, He S, *et al.* Conditioned serum-free medium from umbilical cord mesenchymal stem cells has anti-photoaging properties. *Biotechnol Lett* 2013; 35: 1707-14.
- Lee JC, Kim KC, Yang YS, *et al.* Microarray analysis after umbilical cord blood derived mesenchymal stem cells injection in monocrotaline-induced pulmonary artery hypertension rats. *Anat Cell Biol* 2014; 47: 217-26.
- Zhao YD, Courtman DW, Ng DS, *et al.* Microvascular regeneration in established pulmonary hypertension by angiogenic gene transfer. *Am J Respir Cell Mol Biol* 2006; 35: 182-9.
- Saigawa T, Kato K, Ozawa T, *et al.* Clinical application of bone marrow implantation in patients with arteriosclerosis obliterans, and the association between efficacy and the number of implanted bone marrow cells. *Circ J* 2004; 68: 1189-93.
- Kang H, Kim KH, Lim J, *et al.* The therapeutic effects of human mesenchymal stem cells primed with sphingosine-1 phosphate on pulmonary artery hypertension. *Stem Cells Dev* 2015; 24: 1658-71.
- Umar S, de Visser YP, Steendijk P, *et al.* Allogenic stem cell therapy improves right ventricular function by improving lung pathology in rats with pulmonary hypertension. *Am J Physiol Heart Circ Physiol* 2009; 297: H1606-16.
- Kim AK, Kim MH, Kim S, *et al.* Stem-cell therapy for peripheral arterial occlusive disease. *Eur J Vasc Endovasc Surg* 2011; 42: 667-75.
- Lee KB, Kang ES, Kim AK, *et al.* Stem cell therapy in patients with thromboangiitis obliterans: assessment of the long-term clinical outcome and analysis of the prognostic factors. *Int J Stem Cells* 2011; 4: 88-98.
- Yang SS, Kim NR, Park KB, *et al.* A phase I study of human cord blood-derived mesenchymal stem cell therapy in patients with peripheral arterial occlusive disease. *Int J Stem Cells* 2013; 6: 37-44.
- Cho YJ, Song HS, Bhang S, *et al.* Therapeutic effects of human adipose stem cell-conditioned medium on stroke. *J Neurosci Res* 2012; 90: 1794-802.
- Lim HC, Lee ST, Chu K, *et al.* Neuroprotective effect of neural stem cell-conditioned media in in vitro model of Huntington's disease. *Neurosci Lett* 2008; 435: 175-80.
- Lee EJ, Park SJ, Kang SK, *et al.* Spherical bullet formation via E-cadherin promotes therapeutic potency of mesenchymal stem cells derived from human umbilical cord blood for myocardial infarction. *Mol Ther* 2012; 20: 1424-33.
- Pereira T, Ivanova G, Caseiro AR, *et al.* MSCs conditioned media and umbilical cord blood plasma metabolomics and composition. *PLoS One* 2014; 9: e113769.
- Lipke DW, Arcot SS, Gillespie MN, Olson JW. Temporal alterations in specific basement membrane components in lungs from monocrotaline-treated rats. *Am J Respir Cell Mol Biol* 1993; 9: 418-28.
- Bieback K, Kern S, Kluter H, Eichler H. Critical parameters for the isolation of mesenchymal stem cells from umbilical cord blood. *Stem Cells* 2004; 22: 625-34.
- Wang M, Yang Y, Yang D, *et al.* The immunomodulatory activity of human umbilical cord blood-derived mesenchymal stem cells in vitro. *Immunology* 2009; 126: 220-32.
- Jeong SY, Kim DH, Ha J, *et al.* Thrombospondin-2 secreted by hu-

- man umbilical cord blood-derived mesenchymal stem cells promotes chondrogenic differentiation. *Stem Cells* 2013; 31: 2136-48.
22. Kim JY, Kim DH, Kim JH, *et al.* Soluble intracellular adhesion molecule-1 secreted by human umbilical cord blood-derived mesenchymal stem cell reduces amyloid-beta plaques. *Cell Death Differ* 2012; 19: 680-91.
 23. Jin H, Sanberg PR, Henning RJ. Human umbilical cord blood mononuclear cell-conditioned media inhibits hypoxic-induced apoptosis in human coronary artery endothelial cells and cardiac myocytes by activation of the survival protein Akt. *Cell Transplant* 2013; 22: 1637-50.
 24. Yang S, Sun HM, Yan JH, *et al.* Conditioned medium from human amniotic epithelial cells may induce the differentiation of human umbilical cord blood mesenchymal stem cells into dopaminergic neuron-like cells. *J Neurosci Res* 2013; 91: 978-86.
 25. Yang C, Lei D, Ouyang W, *et al.* Conditioned media from human adipose tissue-derived mesenchymal stem cells and umbilical cord-derived mesenchymal stem cells efficiently induced the apoptosis and differentiation in human glioma cell lines *in vitro*. *Biomed Res Int* 2014; 2014: 109389.
 26. Jiang Y, Jahagirdar BN, Reinhardt RL, *et al.* Pluripotency of mesenchymal stem cells derived from adult marrow. *Nature* 2002; 418: 41-9.
 27. Mareschi K, Ferrero I, Rustichelli D, *et al.* Expansion of mesenchymal stem cells isolated from pediatric and adult donor bone marrow. *J Cell Biochem* 2006; 97: 744-54.
 28. Secco M, Zucconi E, Vieira NM, *et al.* Multipotent stem cells from umbilical cord: cord is richer than blood! *Stem Cells* 2008; 26: 146-50.
 29. Kim ES, Jeon HB, Lim H, *et al.* Conditioned media from human umbilical cord blood-derived mesenchymal stem cells inhibits melanogenesis by promoting proteasomal degradation of MITF. *PLoS One* 2015; 10: e0128078.
 30. Kim JY, Kim DH, Kim DS, *et al.* Galectin-3 secreted by human umbilical cord blood-derived mesenchymal stem cells reduces amyloid-beta42 neurotoxicity *in vitro*. *FEBS Lett* 2010; 584: 3601-8.
 31. Flynn A, Barry F, O'Brien T. UC blood-derived mesenchymal stromal cells: an overview. *Cytotherapy* 2007; 9: 717-26.
 32. Dranoff G. Cytokines in cancer pathogenesis and cancer therapy. *Nat Rev Cancer* 2004; 4: 11-22.
 33. Chandrasekar B, Melby PC, Sarau HM, *et al.* Chemokine-cytokine cross-talk. The ELR+ CXC chemokine LIX (CXCL5) amplifies a pro-inflammatory cytokine response via a phosphatidylinositol 3-kinase-NF-kappa B pathway. *J Biol Chem* 2003; 278: 4675-86.
 34. Brew K, Dinakarandian D, Nagase H. Tissue inhibitors of metalloproteinases: evolution, structure and function. *Biochim Biophys Acta* 2000; 1477: 267-83.
 35. Bourbouliou D, Stetler-Stevenson WG. Matrix metalloproteinases (MMPs) and tissue inhibitors of metalloproteinases (TIMPs): Positive and negative regulators in tumor cell adhesion. *Semin Cancer Biol* 2010; 20: 161-8.
 36. Jiang Y, Goldberg ID, Shi YE. Complex roles of tissue inhibitors of metalloproteinases in cancer. *Oncogene* 2002; 21: 2245-52.
 37. Stetler-Stevenson WG. Tissue inhibitors of metalloproteinases in cell signaling: metalloproteinase-independent biological activities. *Sci Signal* 2008; 1: re6.
 38. Furie MB, Randolph GJ. Chemokines and tissue injury. *Am J Pathol* 1995; 146: 1287-301.
 39. Kaneider NC, Leger AJ, Kuliopulos A. Therapeutic targeting of molecules involved in leukocyte-endothelial cell interactions. *FEBS J* 2006; 273: 4416-24.
 40. Kolb M, Margetts PJ, Anthony DC, Pitossi F, Gauldie J. Transient expression of IL-1beta induces acute lung injury and chronic repair leading to pulmonary fibrosis. *J Clin Invest* 2001; 107: 1529-36.
 41. Johnston CJ, Piedboeuf B, Rubin P, Williams JP, Baggs R, Finkelstein JN. Early and persistent alterations in the expression of interleukin-1 alpha, interleukin-1 beta and tumor necrosis factor alpha mRNA levels in fibrosis-resistant and sensitive mice after thoracic irradiation. *Radiat Res* 1996; 145: 762-7.
 42. Phan SH, Kunkel SL. Lung cytokine production in bleomycin-induced pulmonary fibrosis. *Exp Lung Res* 1992; 18: 29-43.
 43. Pan LH, Ohtani H, Yamauchi K, Nagura H. Co-expression of TNF alpha and IL-1 beta in human acute pulmonary fibrotic diseases: an immunohistochemical analysis. *Pathol Int* 1996; 46: 91-9.

Analysis of Mutations in Epidermal Growth Factor Receptor Gene in Korean Patients with Non-small Cell Lung Cancer: Summary of a Nationwide Survey

Sang Hwa Lee · Wan Seop Kim
Yoo Duk Choi¹ · Jeong Wook Seo²
Joung Ho Han³ · Mi Jin Kim⁴
Lucia Kim⁵ · Geon Kook Lee⁶
Chang Hun Lee⁷ · Mee Hye Oh⁸
Gou Young Kim⁹ · Sun Hee Sung¹⁰
Kyo Young Lee¹¹ · Sun Hee Chang¹²
Mee Sook Rho¹³ · Han Kyeom Kim¹⁴
Soon Hee Jung¹⁵ · Se Jin Jang¹⁶
The Cardiopulmonary Pathology
Study Group of Korean Society of
Pathologists

Department of Pathology, Konkuk University School of Medicine, Seoul; ¹Chonnam National University Medical School, Gwangju; ²Seoul National University College of Medicine, Seoul; ³Samsung Medical Center, Sungkyunkwan University School of Medicine, Seoul; ⁴Yeungnam University College of Medicine, Daegu; ⁵Inha University College of Medicine, Incheon; ⁶National Cancer Center, Goyang; ⁷Busan National University School of Medicine, Busan; ⁸Soonchunhyang University Cheonan Hospital, Soonchunhyang University College of Medicine, Cheonan; ⁹Kyung Hee University School of Medicine, Seoul; ¹⁰Ewha Womans University School of Medicine, Seoul; ¹¹Seoul St. Mary's Hospital, Catholic University of Korea, Seoul; ¹²Inje University Ilsan Paik Hospital, Goyang; ¹³Dong-A University College of Medicine, Busan; ¹⁴Korea University College of Medicine, Seoul; ¹⁵Yonsei University Wonju College of Medicine, Wonju; ¹⁶Asan Medical Center, University of Ulsan College of Medicine, Seoul, Korea

Received: April 24, 2015

Revised: September 13, 2015

Accepted: September 14, 2015

Corresponding Author

Wan Seop Kim, MD, PhD
Department of Pathology, Konkuk University
Medical Center, Konkuk University School of
Medicine, 120-1 Neungdong-ro, Gwangjin-gu,
Seoul 05030, Korea
Tel: +82-2-2030-5642
Fax: +82-2-2030-5629
E-mail: wskim@kuh.ac.kr

Background: Analysis of mutations in the epidermal growth factor receptor gene (*EGFR*) is important for predicting response to *EGFR* tyrosine kinase inhibitors. The overall rate of *EGFR* mutations in Korean patients is variable. To obtain comprehensive data on the status of *EGFR* mutations in Korean patients with lung cancer, the Cardiopulmonary Pathology Study Group of the Korean Society of Pathologists initiated a nationwide survey. **Methods:** We obtained 1,753 reports on *EGFR* mutations in patients with lung cancer from 15 hospitals between January and December 2009. We compared *EGFR* mutations with patient age, sex, history of smoking, histologic diagnosis, specimen type, procurement site, tumor cell dissection, and laboratory status. **Results:** The overall *EGFR* mutation rate was 34.3% in patients with non-small cell lung cancer (NSCLC) and 43.3% in patients with adenocarcinoma. *EGFR* mutation rate was significantly higher in women, never smokers, patients with adenocarcinoma, and patients who had undergone excisional biopsy. *EGFR* mutation rates did not differ with respect to patient age or procurement site among patients with NSCLC. **Conclusions:** *EGFR* mutation rates and statuses were similar to those in published data from other East Asian countries.

Key Words: Lung neoplasms; Receptor, epidermal growth factor; Mutation survey

Lung cancer is the leading cause of cancer-related death in Korea, accounting for approximately 20% of all cancer deaths.¹ Non-small cell lung cancer (NSCLC) accounts for more than 85% of all lung cancers, and the majority of patients with NSCLC present at an advanced cancer stage (stage III or IV).² In the last decade, several studies have been performed on the molecular stratification of NSCLC in order to provide targeted treatment based on activating or driver mutations in these tumors. Activating mutations in the epidermal growth factor receptor gene (*EGFR*) can be used as therapeutic targets for treatment of NSCLC. In the Iressa Pan-Asia Study, tumors with *EGFR* mutations showed a 71.2% clinical response to first-line treatment with gefitinib, while tumors with wild-type *EGFR* showed only a 1.1% response.³ Since then, several randomized control studies have shown an association between activating *EGFR* mutation and response to EGFR tyrosine kinase inhibitors (TKIs).⁴⁻⁹ Patient selection is important for using EGFR TKIs as the first-line treatment. At present, analysis of *EGFR* mutations is the accepted method for identifying patient response to EGFR TKIs. Direct DNA sequencing is a standard method for identifying mutations and is commonly used in the Asia-Pacific region.¹⁰ Any routinely available pathological specimen can be used for analyzing *EGFR* mutations, including formalin-fixed, paraffin-embedded tissues from surgical resections; small tissue biopsies; or cell block preparations.

Several publications have reported the prevalence of *EGFR* mutations in patients with NSCLC.¹⁰⁻¹⁴ The rates of *EGFR* mutations are higher in Asian countries than in Western countries. Further, rates of *EGFR* mutations in Korean patients range from 17.4% to 51.3%.^{10,15-22} Therefore, we performed a nationwide study of *EGFR* mutations in Korean patients with NSCLC in order to provide reliable information on the incidence and characteristics of *EGFR* mutations. This study was led by the Korean Cardiopulmonary Pathology Study Group.

MATERIALS AND METHODS

In all, 1,826 reports of *EGFR* mutation in patients with lung cancer were collected from 15 hospitals between January and December 2009 (Fig. 1). Of these, 24 reports of patients with small cell carcinoma and 49 reports of patients with malignancies from other than lung primary tumors were excluded from the study. Finally, 1,544 reports of primary tumor and 209 reports of metastatic tumor were included in the study. *EGFR* mutation status was compared with patient age, sex, history of smoking, histologic diagnosis, specimen type, procurement site,

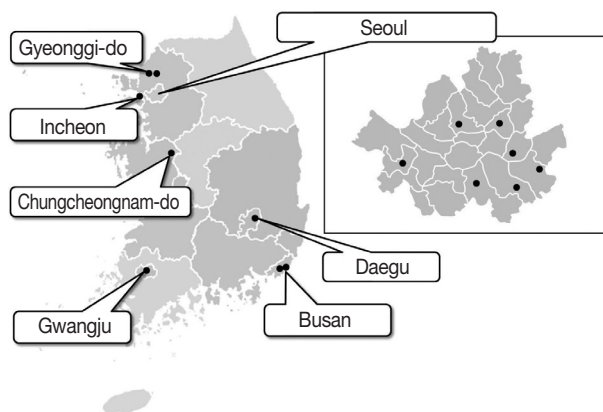


Fig. 1. Geographical distribution of the 15 hospitals in Korea.

tumor cell dissection, and laboratory status. Smoker status was defined as having a greater than 10 pack-year history and currently smoking cigarettes every day or most days. An ex-smoker was someone who had smoked more than 100 cigarettes in their lifetime and who does not currently smoke. A light smoker was defined as a current smoker with a less than 10 pack-year history. A never-smoker was an adult who had never smoked a cigarette or who smoked fewer than 100 cigarettes in their lifetime.

Tumor specimens were divided into three types, namely, biopsy, cytology, and excision specimens. Biopsy specimens included small biopsy specimens obtained by performing bronchoscopic biopsy, transbronchial lung biopsy, percutaneous needle biopsy, pleural biopsy, or needle biopsy of metastatic sites. Cytology included cytologic specimens such as sputum, bronchial washing/brushing, pleural fluids, and aspiration biopsy cytology of primary or metastatic sites. Excision specimens included specimens obtained by performing excisional surgical biopsy such as segmentectomy, lobectomy, pneumonectomy, and metastasectomy. Procurement sites were divided into two types, namely, metastasis and primary sites. Tumor dissection indicated whether or not to perform microdissection of tumor cells. Laboratory status was classified into two types: in-house mutation testing, indicating that *EGFR* mutation analysis was performed in the hospital's laboratory facility, and out-sourced mutation testing, indicating that *EGFR* mutation analysis was not performed in the hospital's laboratory facility. All participants in the study were active members of the Korean Cardiopulmonary Pathology Study Group. This study was approved by the Institutional Review Board of Konkuk University Medical Center (No. KUH 1210011).

Statistical analysis

All statistical analyses were performed using SPSS ver. 18.0 (SPSS Inc., Chicago, IL, USA). Chi-square test and Fisher exact test were used to determine the correlations between *EGFR* mutation status and clinicopathological parameters. A p-value of < .05 was considered statistically significant.

RESULTS

Patient characteristics

The average age of 1,753 patients with NSCLC was 62.74 ± 11.31 years (range, 16 to 89 years); of these, 875 patients (49.9%) were aged ≥ 65 years. Of the 1,753 patients, 1,000 (57%) were men and 753 (43%) were women. Of the 1,753 patients, 555 (31.7%) were smokers, 39 (2.2%) were light smokers, 170 (9.7%) were ex-smokers, 849 (48.4%) were never-smokers, and 140 (8.0%) patients had an unknown smoking history. Of the specimens used for *EGFR* mutation testing, 114 (6.5%) were cytology specimens, 1,066 (60.8%) were biopsy specimens, and 573 (32.7%) were excision specimens (Fig. 2). With respect to procurement sites, specimens from 1,544 patients (88.1%) were procured from primary tumor sites, while those from 209 patients (11.9%) were procured from metastatic sites. In all, 1,012 patients (57.7%) underwent tumor microdissection, while the remaining 741 patients (42.3%) did not. The histological types of the tumor specimens were as follows: adenocarcinoma in 1,292 (73.7%), squamous cell carcinoma in 347 (19.8%), NSCLC type undetermined in 69 (3.9%), pleomorphic carcinoma in 13 (0.7%), large cell neuroendocrine cell carcinoma in 12 (0.7%), large cell carcinoma in nine (0.5%), sarcomatoid carcinoma in five (0.3%), carcinoid tumor in two (0.1%), mucoepidermoid carcinoma in two (0.1%), carcinosarcoma in one (0.05%), and lymphoepithelioma-like carcinoma in one (0.05%). Among the 1,753 *EGFR* tests, 1,299 (7 institutions, 74.1%) were performed within the same pathology laboratory, and 454 (8 insti-

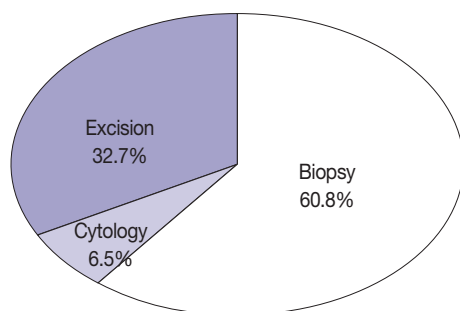


Fig. 2. Specimen types used for *EGFR* mutation testing. *EGFR*, epidermal growth factor receptor.

tutions, 25.9%) were performed in outside laboratories. *EGFR* mutations in specimens obtained from 14 hospitals were identified by direct sequencing, while those in specimens obtained from the remaining hospital were identified by pyrosequencing. Characteristics of patients included in the study are summarized in Table 1.

Frequency of *EGFR* mutations

In all, 601 cases of *EGFR* mutation (34.3%) were detected in NSCLC. Of these 601 patients, 560 (43.3%) had adenocarcinoma, 30 (8.6%) had squamous cell carcinoma, eight (11.6%) had NSCLC type undetermined, two (15.4%) had pleomorphic carcinoma, and one (8.3%) had large cell neuroendocrine carcinoma.

Table 1. Characteristics of patients

Characteristic	No. (%)
Age, mean (range, yr)	62.7 (16–89)
< 65	878 (50.1)
≥ 65	875 (49.9)
Sex	
Female	753 (43)
Male	1,000 (57)
Smoking history	
Smoker	555 (31.7)
Light smoker	39 (2.2)
Ex-smoker	170 (9.7)
Never smoker	849 (48.4)
Unknown	140 (8.0)
Specimen type	
Cytology	114 (6.5)
Biopsy	1,066 (60.8)
Excision	573 (32.7)
Procurement site	
Primary	1,544 (88.1)
Metastasis	209 (11.9)
Tumor dissection	
No	741 (42.3)
Yes	1,012 (57.7)
Histologic type	
Adenocarcinoma	1,292 (73.7)
Squamous cell carcinoma	347 (19.8)
Non-small cell carcinoma	69 (3.9)
Pleomorphic carcinoma	13 (0.7)
Large cell neuroendocrine carcinoma	12 (0.7)
Large cell carcinoma	9 (0.5)
Sarcomatoid carcinoma	5 (0.3)
Carcinoid tumor	2 (0.1)
Mucoepidermoid carcinoma	2 (0.1)
Carcinosarcoma	1 (0.05)
Lymphoepithelioma-like carcinoma	1 (0.05)
Laboratory status	
Out-sourcing	454 (25.9)
In-house	1,299 (74.1)

ma. In all, 389 never-smokers with adenocarcinoma (52.4%) had *EGFR* mutations. Of the 601 patients with NSCLC who had *EGFR* mutations, 30 (5%), 313 (52.1%), 31 (5.2%), and 205 (34.1%) had mutations in exons 18, 19, 20, and 21, respectively; in addition, 22 patients (3.7%) had double mutations (Fig. 3). Further, 13 patients (2.2%) had T790M mutation; of these, four patients had only the T790M mutation.

Interestingly, specimens obtained from two in-house laboratories showed low *EGFR* mutation rates of 16.7% (2/12 specimens) and 9.3% (4/43 specimens) in patients with NSCLC, respectively, and 28.6% (2/7 specimens) and 11.5% (3/26 specimens) in patients with adenocarcinoma and never-smokers (Fig. 4). In brief, one laboratory that detected a 16.7% mutation rate in patients with NSCLC analyzed tumor specimens from 12 patients. Of these 12 patients, 10 had adenocarcinoma, one had large cell carcinoma, and one had NSCLC. Of the 10 patients with adenocarcinoma, seven, two, and one were never-smokers,

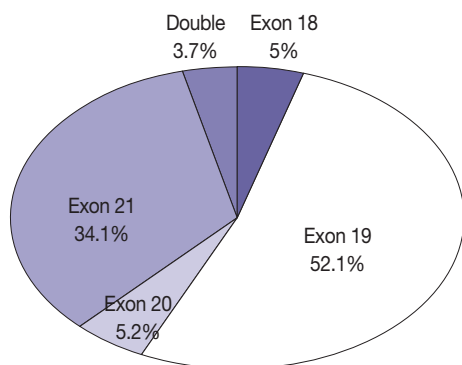


Fig. 3. Frequency of mutations according to exons: 601 mutations in 1,753 specimens from patients with non-small cell lung cancer.

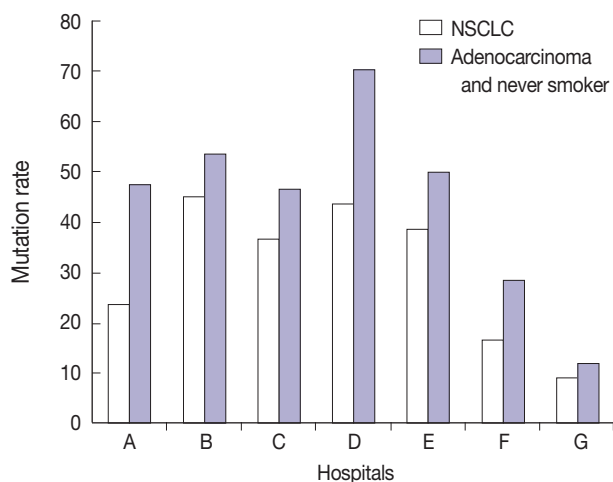


Fig. 4. *EGFR* mutation rates in in-house laboratories. *EGFR*, epidermal growth factor receptor.

ex-smokers, and smoker, respectively. All the specimens were obtained by surgical excision and were analyzed by tumor microdissection. The laboratory that detected a 9.3% mutation rate in patients with NSCLC analyzed tumor specimens from 43 patients. Of these 43 patients, 41 had adenocarcinoma, one had NSCLC, and one had squamous cell carcinoma. Of the 41 patients with adenocarcinoma, 25, 6, and 10 were never-smokers, ex-smokers, and smokers, respectively. Of the 43 specimens analyzed in this laboratory, six were surgical excision specimens, 29 were biopsy specimens, and eight were cytology specimens. All 43 specimens were analyzed without tumor microdissection. A total of four *EGFR* mutations were found, and all of them were adenocarcinoma. They included three never-smokers and one ex-smoker. Moreover, of the four mutations, two were detected in excision specimens and two were detected in biopsy specimens.

A total of 125 *EGFR* mutations were detected in a total of 430 male patients with adenocarcinoma who had a smoking history.

Differences in *EGFR* mutation status

Differences in *EGFR* mutation status according to clinicopathological variables are summarized in Table 2. Among patients with NSCLC, female ($p < .001$), age < 65 years ($p = .007$), light or no smoking ($p < .001$), excision specimen ($p = .002$), and in-house *EGFR* mutation testing ($p < .001$) were correlated with significantly higher *EGFR* mutation rate. Among patients with adenocarcinoma, female ($p < .001$), light or no smoking ($p < .001$), excision specimen ($p < .001$), tumor microdissection ($p = .001$), and in-house *EGFR* mutation testing ($p = .046$) were correlated with significantly higher *EGFR* mutation rate. According to specimen status, the *EGFR* mutation rate was 48.1%, 47.2%, and 63.4% in cytology, biopsy, and excision specimen, respectively, from a total of 742 patients with adenocarcinoma and never-smoker status. According to laboratory status, the *EGFR* mutation rate in patients with NSCLC (38.2% vs 23.1%, $p < .001$) and adenocarcinoma (44.7% vs 37.6%, $p = .046$) was significantly higher in in-house tested specimens. Among patients with squamous cell carcinoma, female ($p = .001$) and light to no smoking ($p = .017$) were correlated with significantly higher *EGFR* mutation rate.

DISCUSSION

The present study identified the frequencies of *EGFR* mutations in Korean patients with NSCLC. The *EGFR* mutation rate was 34.3% and 43.3% among patients with NSCLC and adeno-

Table 2. EGFR mutation status according to the clinicopathological variables

Variable	NSCLC			Adenocarcinoma			SqCC		
	Negative	Positive	p-value	Negative	Positive	p-value	Negative	Positive	p-value
Sex			<.001			<.001			.001
Female	374 (49.7)	379 (50.3)		314 (46.5)	361 (53.5)		31 (75.6)	10 (24.4)	
Male	778 (77.8)	222 (22.2)		418 (67.7)	199 (32.3)		286 (93.5)	20 (6.5)	
Age (yr)			.007			.911			.565
< 65	551 (62.7)	328 (37.3)		399 (56.5)	307 (43.5)		100 (90.1)	11 (9.9)	
> 65	601 (68.8)	273 (31.2)		333 (56.8)	253 (43.2)		217 (91.9)	19 (8.1)	
Smoking			<.001			<.001			.017
Ex-smoker	143 (84.1)	27 (15.9)		88 (77.2)	26 (22.8)		48 (98)	1 (2)	
Light smoker	22 (56.4)	17 (43.6)		17 (53.1)	15 (46.9)		2 (66.7)	1 (33.3)	
Never smoker	442 (52.1)	407 (47.9)		353 (47.6)	389 (52.4)		58 (82.9)	12 (17.1)	
Smoker	446 (80.4)	109 (19.6)		227 (70.7)	94 (29.3)		168 (92.8)	13 (7.2)	
Unknown	99 (70.7)	41 (29.3)		47 (56.6)	36 (43.4)		41 (93.2)	3 (6.8)	
Specimen type			.002			<.001			.535
Biopsy	728 (68.3)	338 (31.7)		453 (59.8)	305 (40.2)		215 (90.7)	22 (9.3)	
Cytology	80 (70.2)	34 (29.8)		70 (67.3)	34 (32.6)				
Excision	344 (60)	229 (40)		209 (48.6)	221 (51.4)		102 (92.7)	8 (7.3)	
Procurement site			.797			.586			.38
Metastasis	139 (66.5)	70 (33.5)		95 (58.6)	67 (41.4)		17 (100)	0 (0)	
Primary	1,013 (65.6)	531 (34.4)		637 (56.4)	493 (43.6)		300 (90.9)	30 (9.1)	
Tumor dissection			.362			.001			.105
No	478 (64.5)	263 (35.5)		401 (61.3)	253 (38.7)		45 (84.9)	8 (15.1)	
Yes	674 (66.6)	338 (33.4)		331 (51.9)	307 (48.1)		272 (92.5)	22 (7.5)	
Laboratory status			<.001			.046			.238
In-house	803 (61.8)	496 (38.2)		581 (55.3)	469 (44.7)		144 (89.4)	17 (10.6)	
Out-sourcing	349 (76.9)	105 (23.1)		151 (62.4)	91 (37.6)		173 (93)	13 (7)	

Values are presented as number (%).

EGFR, epidermal growth factor receptor; NSCLC, non-small cell lung cancer; SqCC, squamous cell carcinoma.

carcinoma, respectively, and 52.4% among never-smokers with adenocarcinoma. The frequencies were in the range of those previously reported in Korean studies, with 17.4%–40.8% in NSCLC, 21.5%–54.4% in adenocarcinoma, and 47%–64.9% in adenocarcinoma with never-smokers.^{10,15–21} The results of the present study were also in the range of those from other Asian countries (30%–61.1% in NSCLC and 44.1%–67.4% in adenocarcinoma) and showed a high mutation rate compared with those reported in Western countries (4.5%–13.3% in NSCLC and 16% in adenocarcinoma).^{3,11,12,23} Recently, a large retrospective database study was performed on EGFR mutation testing practices in the Asia-Pacific region.¹⁰ EGFR mutation rates among patients with NSCLC reported in the present study were very similar to those reported by Yatabe *et al.*¹⁰ (39.6% and 35.8% EGFR mutation rate among newly diagnosed patients with NSCLC) in the Asia-Pacific region and Korea, respectively, in 2011. The overall distribution pattern of EGFR mutations (i.e., high mutation rates in female patients, never-smokers, and patients with adenocarcinoma) was similar to that reported in previous studies.

The most frequent mutation was an exon 19 deletion, and the most frequent drug resistance-associated mutation was T790M. Chan *et al.*²⁴ identified EGFR mutation hot spots in exons 19 (48%) and 21 (41%) in 3,023 specimens. The highest incidence of mutations in EGFR was observed for L858R, del(E746-A750), and del(E749-T751), in that order. Shi *et al.*²⁵ reported 43% and 42.6% mutation rates in exons 19 and 21, respectively, among 1,450 specimens, with the most common drug resistance-associated mutation being S768I. The present study reported 52.1% and 34.1% mutation rates in exons 19 and 21, respectively. However, the sum of mutation rates in exons 19 and 21 was 86.2%, which was similar to that reported in studies performed in other countries.

Two laboratories in the present study detected low EGFR mutation rates. Commonalities between these two institutions included a period less than 1 year after starting the EGFR mutation analysis and use of the direct sequencing method. Well-equipped laboratories and technicians skilled at performing EGFR mutation analysis, active engagement of pathologists in molecular testing, and quality assurance were important for ob-

taining accurate results.

A high incidence of *EGFR* mutations (29.7%) has been reported in Korean male smokers with adenocarcinoma.²⁰ In the present study, *EGFR* mutation rate was 29.1% in male patients with adenocarcinoma who had a smoking history (125 out of 430 patients). This result supports the recommendation of a previous study that *EGFR* mutation tests should be performed in all patients with adenocarcinoma regardless of sex or smoking history.²⁰

Because minimally invasive diagnostic procedures are often used in the diagnostic workup of lung cancer, small tissue specimens and, more importantly, cytology specimens might be the only specimens available for *EGFR* mutation analysis. In the present study, a total of 73.3% of specimens were cytology or biopsy samples. However, these specimens showed a significantly low mutation rate compared to excision specimens in patients with NSCLC even in patients with adenocarcinoma and never-smokers. Although our results showed significantly higher mutation rates in surgically resected specimens, many studies have reported that small biopsy and cytology specimens are more suitable for performing mutation testing.²⁶⁻²⁹

A quick and accurate test for detecting *EGFR* mutations is very important for proper selection of patients for EGFR TKI therapy. This highlights the need for standard guidelines specific to medical conditions in Korea for *EGFR* mutation testing. Many methods are available for detecting *EGFR* mutations, and these methods have different advantages and disadvantages. However, there is no consensus on the best method for detecting *EGFR* mutations.³⁰ In Korea, most pathology laboratories use direct DNA sequencing, pyrosequencing, or the peptide nucleic acid (PNA) clamp method for detecting *EGFR* mutations in formalin-fixed, paraffin-embedded tissue specimens. In the present study, specimens obtained from 14 hospitals were analyzed using direct DNA sequencing, a classic method for detecting mutations. However, this technique is associated with low sensitivity and requires > 25% mutant DNA for analysis.³¹ Pyrosequencing is a more sensitive method that needs more than 1% to 20% mutant DNA for analysis.^{32,33} PNA clamping is a simple, rapid, and sensitive method that can detect mutations in as few as 1% mutant alleles in a mixture of mutant and wild-type DNA.³⁴ These three methods show a good concordance of 82%–87.5%.^{35,36} We recommend that the use of the available methods for *EGFR* mutation analysis in each institution and laboratory should be under strict quality control. The quality and quantity of DNA are important for avoiding false-negative results.²⁹ In the present study, tumor microdissection specimens from patients with adenocarcinoma showed higher

mutation rates than non-dissection specimens. We recommend that pathologists verify the adequacy of specimens and reanalyze *EGFR* mutations to prevent false-negative results.

According to laboratory status, the *EGFR* mutation rate in patients with NSCLC (38.2% vs 23.1%, $p < .001$) and adenocarcinoma (44.7% vs 37.6%, $p = .046$) was significantly higher in the in-house test in the present study. However, the proportion of never-smoker patients with adenocarcinoma was 48.3% (628 out of 1,299 patients) in the in-house test and 25.1% (114 out of 454 patients) in the out-sourced test. Moreover, *EGFR* mutation rate in never-smokers with adenocarcinoma was 52.7% based on in-house mutation testing and 50.9% based on out-sourced mutation testing. These results indicate significant differences between in-house and out-sourced mutation testing, which might be because of a bias in patient selection.

In the future, we will aim to develop recommendations for more standardized application and interpretation of results of *EGFR* mutation tests in patients with NSCLC. These recommendations will discuss patients, turnaround time, specimen type, minimum specimen size, specimen collection and storage, tumor cell content, methodology such as DNA extraction, and reporting form. In addition, we aim to design a QA program for use during *EGFR* mutation analysis.

The present study had limitations. Pathological diagnosis of patients included in the study was not confirmed. In addition, immunohistochemical staining to classify the histologic type of NSCLC was not performed for all patient samples. Further, our data were collected from hospitals where diagnosis was performed by pulmonary pathologists. Therefore, our results might represent the current status of NSCLC subtypes in Korea.

In conclusion, *EGFR* mutation rate showed significant differences with respect to sex, smoking history, histologic diagnosis, specimen type, tumor cell dissection, and institution. However, it did not show differences with respect to age, procurement site, or laboratory status. The relative frequency of *EGFR* mutations in Korea was not similar to those reported in other Asian countries.

Conflicts of Interest

No potential conflict of interest relevant to this article was reported.

Acknowledgments

We would like to sincerely thank Seo-Young Oh, MS; Noh-Young Lee, MS; and Yoo-Min Hong, MRA for their devoted efforts toward data set mining and cleaning.

REFERENCES

1. Jung KW, Won YJ, Kong HJ, *et al.* Cancer statistics in Korea: incidence, mortality, survival, and prevalence in 2012. *Cancer Res Treat* 2015; 47: 127-41.
2. Owonikoko TK, Ragin CC, Belani CP, *et al.* Lung cancer in elderly patients: an analysis of the surveillance, epidemiology, and end results database. *J Clin Oncol* 2007; 25: 5570-7.
3. Mok TS, Wu YL, Thongprasert S, *et al.* Gefitinib or carboplatin-paclitaxel in pulmonary adenocarcinoma. *N Engl J Med* 2009; 361: 947-57.
4. Rosell R, Carcereny E, Gervais R, *et al.* Erlotinib versus standard chemotherapy as first-line treatment for European patients with advanced *EGFR* mutation-positive non-small-cell lung cancer (EURTAC): a multicentre, open-label, randomised phase 3 trial. *Lancet Oncol* 2012; 13: 239-46.
5. Zhou C, Wu YL, Chen G, *et al.* Erlotinib versus chemotherapy as first-line treatment for patients with advanced *EGFR* mutation-positive non-small-cell lung cancer (OPTIMAL, CTONG-0802): a multicentre, open-label, randomised, phase 3 study. *Lancet Oncol* 2011; 12: 735-42.
6. Maemondo M, Inoue A, Kobayashi K, *et al.* Gefitinib or chemotherapy for non-small-cell lung cancer with mutated *EGFR*. *N Engl J Med* 2010; 362: 2380-8.
7. Mitsudomi T, Morita S, Yatabe Y, *et al.* Gefitinib versus cisplatin plus docetaxel in patients with non-small-cell lung cancer harbouring mutations of the epidermal growth factor receptor (WJ-TOG3405): an open label, randomised phase 3 trial. *Lancet Oncol* 2010; 11: 121-8.
8. Fukuoka M, Wu YL, Thongprasert S, *et al.* Biomarker analyses and final overall survival results from a phase III, randomized, open-label, first-line study of gefitinib versus carboplatin/paclitaxel in clinically selected patients with advanced non-small-cell lung cancer in Asia (IPASS). *J Clin Oncol* 2011; 29: 2866-74.
9. Yang JC, Wu YL, Schuler M, *et al.* Afatinib versus cisplatin-based chemotherapy for *EGFR* mutation-positive lung adenocarcinoma (LUX-Lung 3 and LUX-Lung 6): analysis of overall survival data from two randomised, phase 3 trials. *Lancet Oncol* 2015; 16: 141-51.
10. Yatabe Y, Kerr KM, Utomo A, *et al.* *EGFR* mutation testing practices within the Asia Pacific region: results of a multicenter diagnostic survey. *J Thorac Oncol* 2015; 10: 438-45.
11. Yang CH. *EGFR* tyrosine kinase inhibitors for the treatment of NSCLC in East Asia: present and future. *Lung Cancer* 2008; 60 Suppl 2: S23-30.
12. Shigematsu H, Lin L, Takahashi T, *et al.* Clinical and biological features associated with epidermal growth factor receptor gene mutations in lung cancers. *J Natl Cancer Inst* 2005; 97: 339-46.
13. Skov BG, Høgdall E, Clementsen P, *et al.* The prevalence of *EGFR* mutations in non-small cell lung cancer in an unselected Caucasian population. *APMIS* 2015; 123: 108-15.
14. Gahr S, Stoehr R, Geissinger E, *et al.* *EGFR* mutational status in a large series of Caucasian European NSCLC patients: data from daily practice. *Br J Cancer* 2013; 109: 1821-8.
15. Soung YH, Lee JW, Kim SY, *et al.* Mutational analysis of *EGFR* and *K-RAS* genes in lung adenocarcinomas. *Virchows Arch* 2005; 446: 483-8.
16. Bae NC, Chae MH, Lee MH, *et al.* *EGFR*, *ERBB2*, and *KRAS* mutations in Korean non-small cell lung cancer patients. *Cancer Genet Cytogenet* 2007; 173: 107-13.
17. Park S, Holmes-Tisch AJ, Cho EY, *et al.* Discordance of molecular biomarkers associated with epidermal growth factor receptor pathway between primary tumors and lymph node metastasis in non-small cell lung cancer. *J Thorac Oncol* 2009; 4: 809-15.
18. Lee YJ, Park IK, Park MS, *et al.* Activating mutations within the *EGFR* kinase domain: a molecular predictor of disease-free survival in resected pulmonary adenocarcinoma. *J Cancer Res Clin Oncol* 2009; 135: 1647-54.
19. Ahn MJ, Park BB, Ahn JS, *et al.* Are there any ethnic differences in molecular predictors of erlotinib efficacy in advanced non-small cell lung cancer? *Clin Cancer Res* 2008; 14: 3860-6.
20. Sun PL, Seol H, Lee HJ, *et al.* High incidence of *EGFR* mutations in Korean men smokers with no intratumoral heterogeneity of lung adenocarcinomas: correlation with histologic subtypes, *EGFR*/*TTF-1* expressions, and clinical features. *J Thorac Oncol* 2012; 7: 323-30.
21. Kim YT, Seong YW, Jung YJ, *et al.* The presence of mutations in epidermal growth factor receptor gene is not a prognostic factor for long-term outcome after surgical resection of non-small-cell lung cancer. *J Thorac Oncol* 2013; 8: 171-8.
22. Choi YL, Sun JM, Cho J, *et al.* *EGFR* mutation testing in patients with advanced non-small cell lung cancer: a comprehensive evaluation of real-world practice in an East Asian tertiary hospital. *PLoS One* 2013; 8: e56011.
23. Ma BB, Hui EP, Mok TS. Population-based differences in treatment outcome following anticancer drug therapies. *Lancet Oncol* 2010; 11: 75-84.
24. Chan SK, Gullick WJ, Hill ME. Mutations of the epidermal growth factor receptor in non-small cell lung cancer: search and destroy. *Eur J Cancer* 2006; 42: 17-23.
25. Shi Y, Au JS, Thongprasert S, *et al.* A prospective, molecular epidemiology study of *EGFR* mutations in Asian patients with advanced non-small-cell lung cancer of adenocarcinoma histology (PIO-

- NEER). *J Thorac Oncol* 2014; 9: 154-62.
26. Liu J, Zhao R, Zhang J, Zhang J. ARMS for *EGFR* mutation analysis of cytologic and corresponding lung adenocarcinoma histologic specimens. *J Cancer Res Clin Oncol* 2015; 141: 221-7.
 27. Heymann JJ, Bulman WA, Maxfield RA, *et al.* Molecular testing guidelines for lung adenocarcinoma: utility of cell blocks and concordance between fine-needle aspiration cytology and histology samples. *Cytojournal* 2014; 11: 12.
 28. Khode R, Larsen DA, Culbreath BC, *et al.* Comparative study of epidermal growth factor receptor mutation analysis on cytology smears and surgical pathology specimens from primary and metastatic lung carcinomas. *Cancer Cytopathol* 2013; 121: 361-9.
 29. Sun PL, Jin Y, Kim H, Lee CT, Jheon S, Chung JH. High concordance of *EGFR* mutation status between histologic and corresponding cytologic specimens of lung adenocarcinomas. *Cancer Cytopathol* 2013; 121: 311-9.
 30. Pirker R, Herth FJ, Kerr KM, *et al.* Consensus for *EGFR* mutation testing in non-small cell lung cancer: results from a European workshop. *J Thorac Oncol* 2010; 5: 1706-13.
 31. Pao W, Ladanyi M. Epidermal growth factor receptor mutation testing in lung cancer: searching for the ideal method. *Clin Cancer Res* 2007; 13: 4954-5.
 32. Kim SK, Kim DL, Han HS, *et al.* Pyrosequencing analysis for detection of a *BRAFV600E* mutation in an FNAB specimen of thyroid nodules. *Diagn Mol Pathol* 2008; 17: 118-25.
 33. Dufort S, Richard MJ, Lantuejoul S, de Fraipont F. Pyrosequencing, a method approved to detect the two major *EGFR* mutations for anti *EGFR* therapy in NSCLC. *J Exp Clin Cancer Res* 2011; 30: 57.
 34. Choi JJ, Cho M, Oh M, Kim H, Kil MS, Park H. PNA-mediated real-time PCR clamping for detection of *EGFR* mutations. *Bull Korean Chem Soc* 2010; 31: 3525-9.
 35. Lee HJ, Xu X, Kim H, *et al.* Comparison of direct sequencing, PNA clamping-real time polymerase chain reaction, and pyrosequencing methods for the detection of *EGFR* mutations in non-small cell lung carcinoma and the correlation with clinical responses to *EGFR* tyrosine kinase inhibitor treatment. *Korean J Pathol* 2013; 47: 52-60.
 36. Kim HJ, Lee KY, Kim YC, *et al.* Detection and comparison of peptide nucleic acid-mediated real-time polymerase chain reaction clamping and direct gene sequencing for epidermal growth factor receptor mutations in patients with non-small cell lung cancer. *Lung Cancer* 2012; 75: 321-5.

Chronic Placental Inflammation in Twin Pregnancies

Heejin Bang¹ · Go Eun Bae¹
Ha Young Park¹ · Yeon Mee Kim²
Suk-Joo Choi³ · Soo-young Oh³
Cheong-Rae Roh³ · Jung-Sun Kim^{1,4}

¹Department of Pathology and Translational Genomics, Samsung Medical Center, Sungkyunkwan University School of Medicine, Seoul; ²Department of Pathology, Inje University Haeundae Paik Hospital, Inje University College of Medicine, Busan; ³Department of Obstetrics and Gynecology, Samsung Medical Center, Sungkyunkwan University School of Medicine, Seoul; ⁴Department of Health Sciences and Technology, Sungkyunkwan University, SAHST, Seoul, Korea

Received: August 31, 2015
Accepted: September 9, 2015

Corresponding Author

Jung-Sun Kim, MD, PhD
Department of Pathology and Translational Genomics, Samsung Medical Center, Sungkyunkwan University School of Medicine, 81 Irwon-ro, Gangnam-gu, Seoul 06351, Korea
Tel: +82-2-3410-2767
Fax: +82-2-3410-0025
E-mail: jsunkim@skku.edu

Background: Chronic placental inflammation, such as villitis of unknown etiology (VUE) and chronic chorioamnionitis (CCA), is considered a placental manifestation of maternal anti-fetal rejection. The aim of this study is to investigate its frequency in twin pregnancies compared to singleton pregnancies. **Methods:** Three hundred twin placentas and 1,270 singleton placentas were consecutively collected at a tertiary medical center in Seoul, Republic of Korea from 2009 to 2012. Hematoxylin and eosin sections of tissue samples (full-thickness placental disc and chorioamniotic membranes) were reviewed. **Results:** Non-basal VUE was more frequent in twin placentas than in singleton placentas (6.0% vs 3.2%, $p < .05$). In preterm birth, CCA was found less frequently in twin placentas than in singleton placentas (9.6% vs 14.8%, $p < .05$), reaching its peak at an earlier gestational age in twin placentas (29–32 weeks) than in singleton placentas (33–36 weeks). CCA was more frequent in twin pregnancies with babies of a different sex than with those with the same sex (13.8% vs 6.9%, $p = .052$). Separate dichorionic diamniotic twin placentas were affected by chronic deciduitis more frequently than singleton placentas (16.9% vs 9.7%, $p < .05$). **Conclusions:** The higher frequency of non-basal VUE in twin placentas and of CCA in twin placentas with different fetal sex supports the hypothesis that the underlying pathophysiological mechanism is maternal anti-fetal rejection related to increased fetal antigens in twin pregnancies. The peak of CCA at an earlier gestational age in twin placentas than in singleton placentas suggests that CCA is influenced by placental maturation.

Key Words: Placenta; Inflammation; Twins; Preterm birth

Chronic inflammation of the placenta can be present in the chorionic villous tree, extraplacental chorioamniotic membranes, and the basal plate of the placenta, which are called chronic villitis, chronic chorioamnionitis (CCA), and chronic deciduitis (CD), respectively. Infection may cause some of the chronic placental inflammation; however, infectious microorganisms are not identified in a majority of cases. Chronic villitis in such cases is called villitis of unknown etiology (VUE). It is defined by the infiltration of maternal lymphocytes into the fetal chorionic villi, and we have shown that fetal placental macrophages also participate in VUE.¹ Its prevalence is reported to range from 2% to 33.8%,² and it is more frequent in placentas at term than at preterm. VUE at term is usually subclinical, while high-grade or diffuse VUE is associated with fetal growth restriction, intrauterine fetal death, or fetal central nervous system injury.^{3,4} CCA is characterized by maternal lymphocytic

infiltration into the chorioamniotic membranes and chorionic plate.^{5,6} A series of recent studies have demonstrated that CCA is another major pathology of preterm birth, especially of late preterm births.^{7,8} CCA is also frequently found in intrauterine fetal death cases.⁹ CD is defined by the accumulation of lymphocytes and plasma cells in the decidua of the basal plate¹⁰ and often accompanies basal VUE that involves anchoring villi. It is associated with fetal growth restriction and preterm labor.¹¹⁻¹⁴

The fetus and placenta are semi-allografts to the mother. Immune tolerance is required for successful pregnancy.^{15,16} Accumulating evidence from recent studies suggests that maternal anti-fetal rejection may explain the pathogenesis of VUE and CCA.^{17,17-19} An immune origin of CD has also been suggested, as this condition has been reported more frequently in pregnancies resulting from donor egg *in vitro* fertilization pregnancies.^{20,21}

The rate of multiple pregnancies has increased over the past three decades to reach 33.7 per 1,000 total births in the United States in 2013, which results from the expanded use of fertility enhancing therapies and an older maternal age at childbearing.²² Infants born in multiple gestation pregnancies are at a higher risk of adverse birth outcomes than singletons mainly because of the increased frequency of preterm birth in addition to twin-specific complications, such as twin-to-twin transfusion syndrome and discordant growth restriction.²² A thorough investigation of chronic placental inflammation in twin placentas has not been performed, though some reports have focused on the relationship between VUE and intrauterine growth restriction (IUGR) in twin placentas.²³⁻²⁵

In this study, we compared the frequencies of chronic placental inflammation, VUE, CCA, and CD between twin and singleton placentas collected consecutively at a tertiary medical center in order to investigate whether chronic inflammation is more frequent in twin placentas because of the increased burden of fetal semi-allograft antigens.

MATERIALS AND METHODS

Three hundred twin placentas (77 separate dichorionic diamniotic [DiDiS], 147 fused dichorionic diamniotic [DiDiF], 66 monochorionic diamniotic [MoDi], 8 monochorionic monoamniotic [MoMo], and 2 unknown type) and 1,270 singleton placentas were consecutively collected at Samsung Medical Center, Seoul, Republic of Korea, from 2009 to 2012. The study was approved by the institutional review board of the hospital (2011-07-063).

Preterm birth was defined as delivery before 37 weeks of gestation and was categorized as (1) spontaneous preterm births resulting from preterm labor and intact membranes, and preterm premature rupture of membranes; and (2) indicated preterm births due to maternal and/or fetal conditions necessitating preterm births. IUGR was defined as birth weight below the 10th percentile, and discordant growth in twins was defined as more than 15% difference in birth weight.

Tissue samples of the full-thickness placental disc ($n = 2$) and chorioamniotic membranes roll ($n = 1$) for each placenta, and also of the dividing membranes if present, were obtained for microscopic examination and were formalin-fixed for 24 hours. The hematoxylin and eosin stained sections were reviewed for the presence of chronic inflammation. VUE, CCA, and CD were diagnosed according to the previously described criteria in the literature.^{7,10,17} Briefly, VUE was defined as lymphohisto-

cytic infiltration affecting varying proportions of the villous tree of the placenta without any signs or symptoms of infection in either the mother or the infant.^{17,26} It is sub-classified as basal type, which involves villi anchoring to the basal plate, and non-basal (distal and proximal) type, which involves distal villi (terminal and mature intermediate villi) and/or stem villi. The diagnosis of CCA was made when there was lymphocytic infiltration into the chorionic trophoblast layer and/or chorioamniotic connective tissue.⁷ CD was diagnosed when lymphocytic infiltration was diffuse and/or any plasma cells were detected in the decidua.¹⁰ The cases were examined by a single pathologist (J.-S.K.) who was blind to clinical information.

The chi-square test and Fisher exact test were performed to compare proportions, and the Mann-Whitney U test was performed to determine the differences in the median values between the study groups. The SPSS ver. 21 (IBM Co., Armonk, NY, USA) was employed for all statistical analyses. A p -value of less than .05 was considered statistically significant.

RESULTS

Clinical characteristics of twin pregnancies in this study

The demographics and clinical characteristics of the study population are summarized in Table 1. There were significant differences in the gestational age at delivery, gravity, labor at delivery, preterm birth, and IUGR between singleton and twin pregnancies ($p < .05$). Maternal age, previous abortion, the ratio of spontaneous/indicated preterm birth, and hypertensive disorders were not significantly different.

Frequency of chronic inflammation in twin placentas

The frequencies of the three types of chronic placental inflammation (VUE, CCA, and CD) were not statistically different between twin and singleton placentas. Twin placentas had a tendency of high frequency of VUE (11.3% [34/300] vs 7.9% [100/1,270], $p = .054$) and CD (13.0% [36/300] vs 9.7% [123/1,270], $p = .09$) compared with singleton placentas, whereas they showed a tendency of low frequency of CCA (9.3% [28/300] vs 13.3% [169/1,270], $p = .062$) (Fig. 1A, C, D). The frequency of the non-basal type of VUE was higher in twin placentas than in singleton placentas (6.0% [18/300] vs 3.2% [41/1,270], $p < .05$). There was no difference in the frequency of basal VUE between twin and singleton placentas (5.3% [16/300] vs 4.6% [59/1,270], $p > .05$) (Fig. 1B).

There were no significant differences in the frequencies of VUE (10.2% [23/225] vs 15.1% [11/73]), CCA (9.3% [21/225]

vs 9.6% [7/73]), or CD (13.8% [31/225] vs 11.0% [8/73]) between dichorionic (DiDiS and DiDiF) and monozygotic (MoDi and MoMo) placentas ($p > .05$). CD was significantly more frequent in DiDiS twin placentas compared with singleton placentas (16.9% [13/77] vs. 9.7% [123/1,270], $p < .05$), but the frequencies of VUE and CCA were not significantly different among the twin types.

Chronic inflammation in twin placentas according to the gestational age

The frequency of VUE increased with increasing gestational age at birth in both singleton and twin placentas; however, there was no significant difference in the frequency of VUE between singleton and twin placentas when the cases were matched by gestational age (Fig. 2A). When the study population was divided into preterm and term births, term twin pla-

Table 1. Clinical characteristics of the study groups

Characteristic	Singleton (n=1,270)	Twin (n=300)	p-value
Age (yr)	33 (18–52)	34 (22–42)	.226
Gestational age at delivery (wk)	35 (20–42)	34 (21–40)	.001
Primigravida	514 (41)	143 (48)	.024
Abortion history	398 (31)	86 (29)	.367
Labor at delivery	833 (67)	160 (54)	.000
Preterm birth	886 (70)	230 (77)	.018
Spontaneous/indicated	651 (73)/235 (27)	175 (76)/55 (24)	.421
Maternal hypertensive disorders	149 (12)	35 (12)	.99
Intrauterine growth restriction	278 (22)	122 (41.1)	.000
Intrauterine fetal death	47 (4)	18 (6)	.072
Discordant growth of twin	-	95 (32)	-

Values are presented as median (range) or number (%).

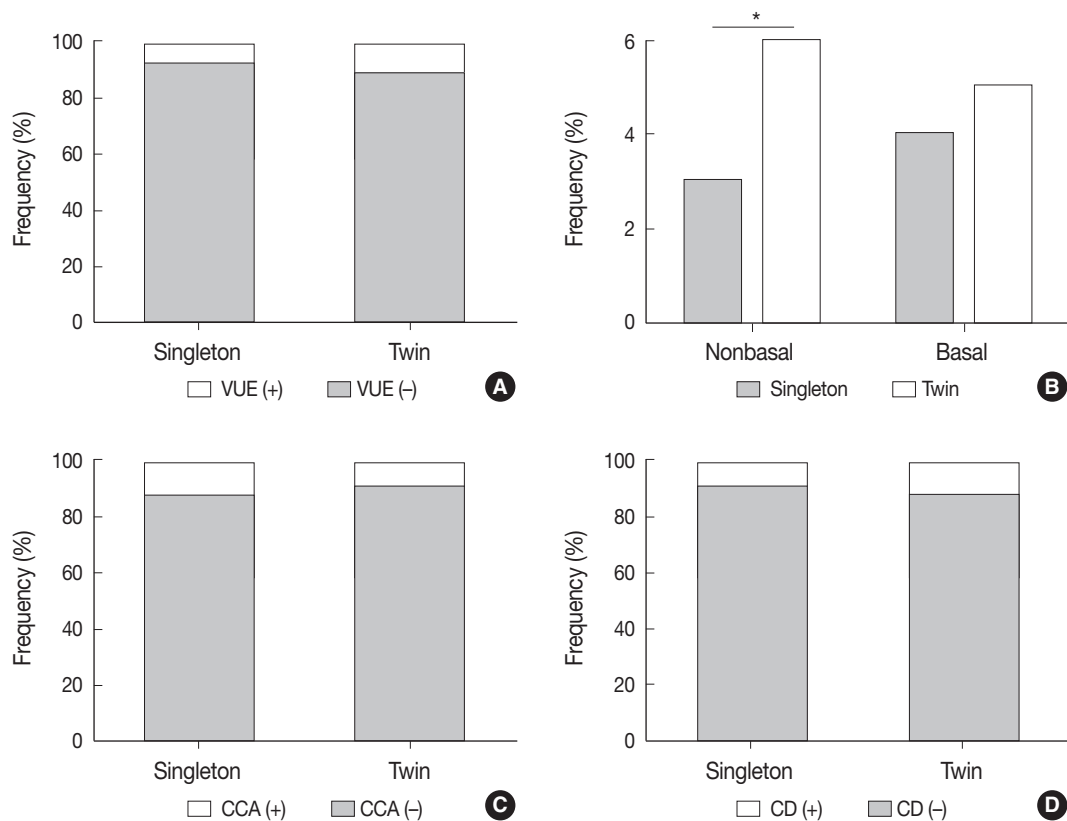


Fig. 1. The frequency of chronic placental inflammation in twin placentas. (A) The frequency of villitis of unknown etiology (VUE) is not statistically different between twin and singleton placentas. (B) Non-basal type of VUE is more frequent in twin placentas than in singleton placentas ($*p < .05$), but basal type of VUE is not. (C, D) The frequencies of chronic chorioamnionitis (CCA) (C) and chronic deciduitis (CD) (D) are not statistically different between twin and singleton placentas.

centas were affected by non-basal VUE more frequently than term singleton placentas (12.9% [9/70] vs 3.6% [14/384], $p < .01$), but the difference was not detected in preterm placentas (Fig. 2B). The frequencies of basal VUE were not significantly different between singleton and twin placentas either at preterm or at term (Fig. 2C).

CCA was found less frequently in twin placentas than singleton placentas of preterm birth (9.6% [22/230] vs 14.8% [131/886], $p < .05$) (Fig. 3A). Among preterm births, the decrease of CCA in twin placentas compared with singleton placentas was significant at 33–36 weeks of gestation (late preterm birth) (10.0% [12/120] vs 17.9% [90/503], $p < .05$). CCA in singleton placentas was most commonly observed at late preterm stage (33–36 weeks of gestation) during gestation as previously reported;⁸ however, CCA in twin placentas was most frequent at 29–32 weeks unexpectedly (14.0% [6/43]) (Fig. 3B).

CD was detected at similar frequencies between preterm and term placentas (Fig. 4A). The high frequency of CD in DiDiS

twin placentas compared with singleton placentas was more prominent at term (31.6% [6/19] vs 8.3% [32/384], $p < .01$) (Fig. 4B).

Correlation of chronic inflammation with clinical characteristics in twin placentas

VUE in singleton placentas was found more frequently in IUGR cases than in non-IUGR cases (12.9% [36/278] vs 6.5% [64/985], $p < .001$). Of these cases, non-basal VUE was more frequent in IUGR cases than in non-IUGR cases (7.6% [21/278] vs 2.0% [20/985]), $p < .001$). Non-basal VUE in twin placentas was more frequent in IUGR cases than in non-IUGR cases (9.8% [12/122] vs 3.4% [6/175], $p < .05$), though VUE showed no significant correlation with IUGR in twin placentas (13.1% [16/122] vs 10.3% [18/175]) (Fig. 5A, B). Neither CCA nor CD correlated with IUGR in this study (Fig. 5C, D).

VUE was more frequent in indicated preterm birth than in spontaneous birth of singleton placentas (10.2% [24/235] vs 6.3% [41/651], $p < .05$) (Fig. 6A). Non-basal VUE was more

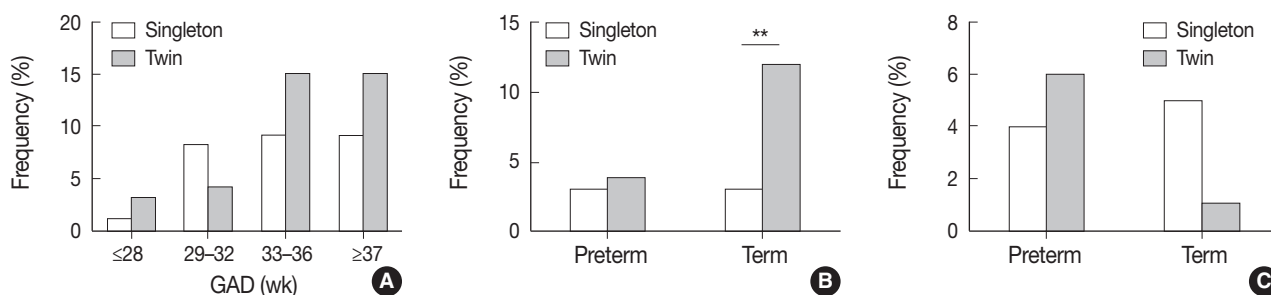


Fig. 2. The frequency of villitis of unknown etiology (VUE) in twin placentas according to the gestational age. (A) VUE in singleton and twin placentas is found more frequently as gestational age at birth increases. (B) Non-basal VUE is more frequent in twin placentas than in singleton placentas at term (** $p < .01$). (C) There is no significant difference in the frequency of basal VUE between singleton and twin placentas. GAD, gestational age at delivery.

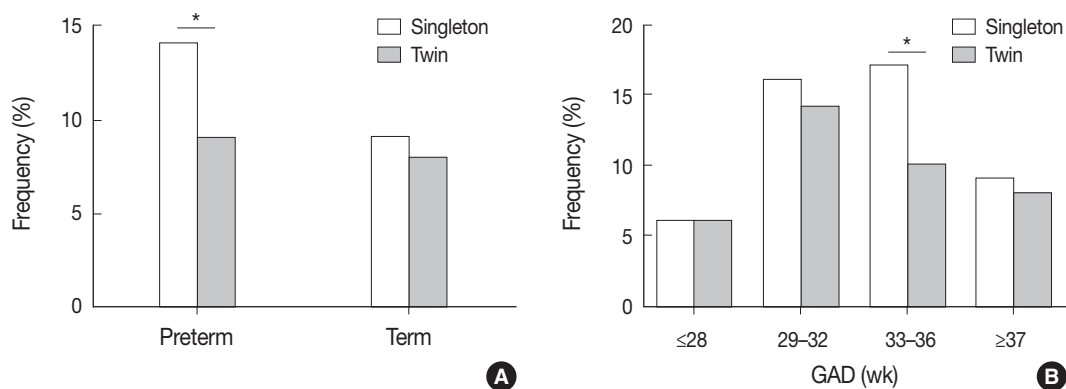


Fig. 3. The frequency of chronic chorioamnionitis (CCA) in twin placentas according to the gestational age. (A) CCA is less frequent in twin placentas than singleton placentas at preterm birth (* $p < .05$). (B) CCA in twin placentas is decreased significantly compared with singleton placentas at 33–36 weeks of gestation (* $p < .05$). Twin placentas are affected by CCA most frequently at 29–32 weeks, in contrast to singleton placentas at 33–36 weeks. GAD, gestational age at delivery.

frequent in indicated preterm birth than in spontaneous birth of both singleton and twin placentas (singleton, 5.5% [13/235] vs 2.2% [4/175]; twin, 9.1% [5/55] vs 2.3% [4/175], $p < .05$) (Fig. 6B). When the frequencies of chronic placental inflammation were compared after preterm cases were divided into spontaneous and indicated preterm birth groups, none of the chronic inflammation conditions showed any statistically significant differences between singleton and twin placentas (Fig. 6A–D).

CCA showed a tendency toward higher frequency in twin

pregnancies with babies of a different sex than with those of the same sex (13.8% [15/109] vs 6.9% [13/189], $p = .052$), whereas the frequencies of VUE and CD were not significantly different between twin pregnancies of a different sex and those of the same sex. The frequencies of chronic inflammation in twin placentas had no significant correlation with primigravida, previous abortion, intrauterine fetal death, or discordant growth ($p > .05$).

Chronic placental inflammation was detected in either one or

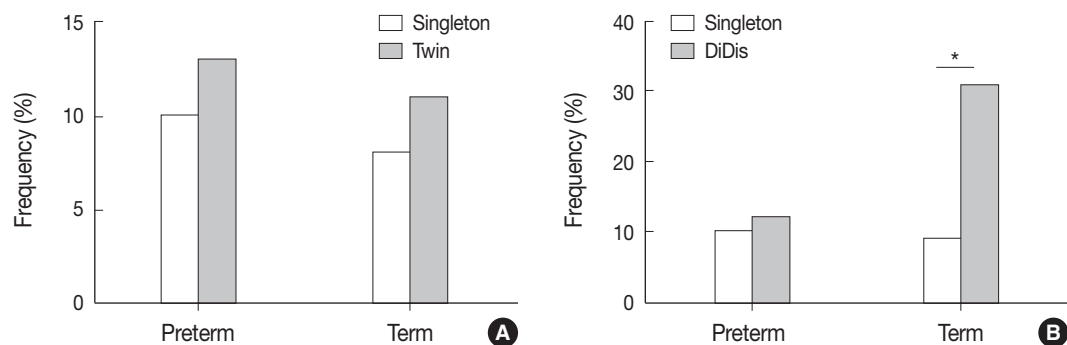


Fig. 4. The frequency of chronic deciduitis (CD) in twin placentas at preterm and term birth. (A) CD is detected at similar frequencies between preterm and term placentas. (B) Separate dichorionic diamniotic (DiDis) twin placentas are affected by CD more frequently than singleton placentas, especially at term (** $p < .01$).

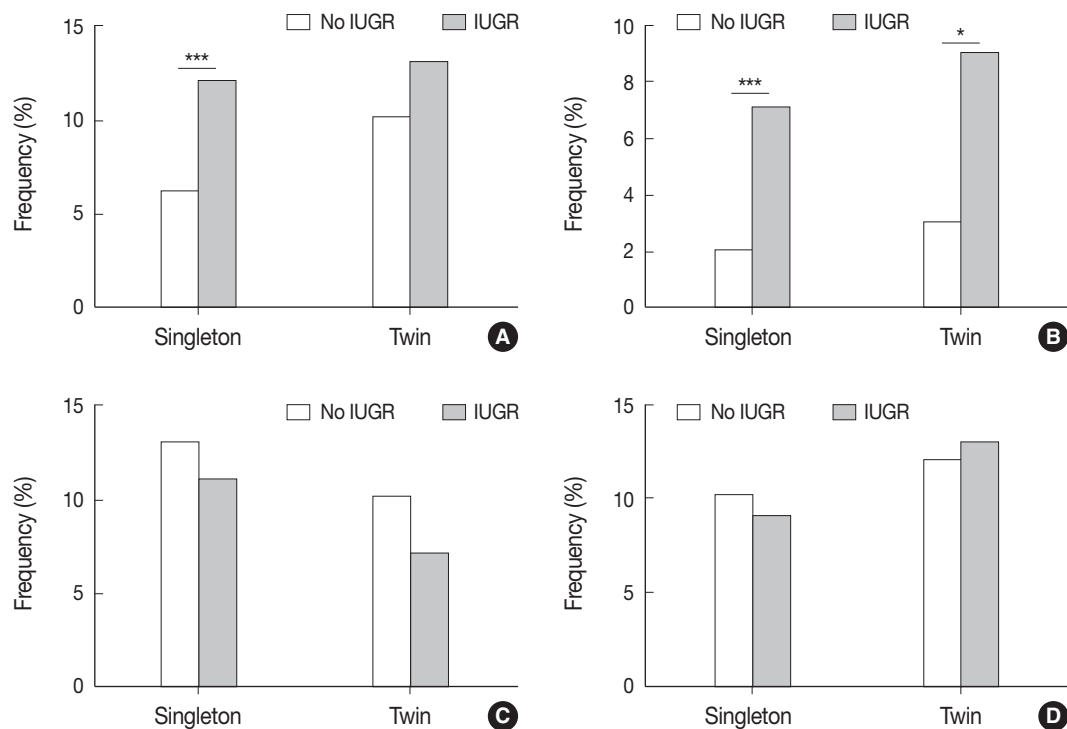


Fig. 5. Association of villitis of unknown etiology (VUE) with intrauterine growth restriction (IUGR). (A) VUE is found more frequently in singleton placentas of IUGR cases than in those of non-IUGR cases (*** $p < .001$). (B) Non-basal VUE in singleton and twin placentas is more frequent in IUGR cases than in non-IUGR cases (singleton, *** $p < .001$; twin, * $p < .05$). (C, D) The frequencies of chronic chorioamnionitis (C) and chronic deciduitis (D) are not associated with IUGR.

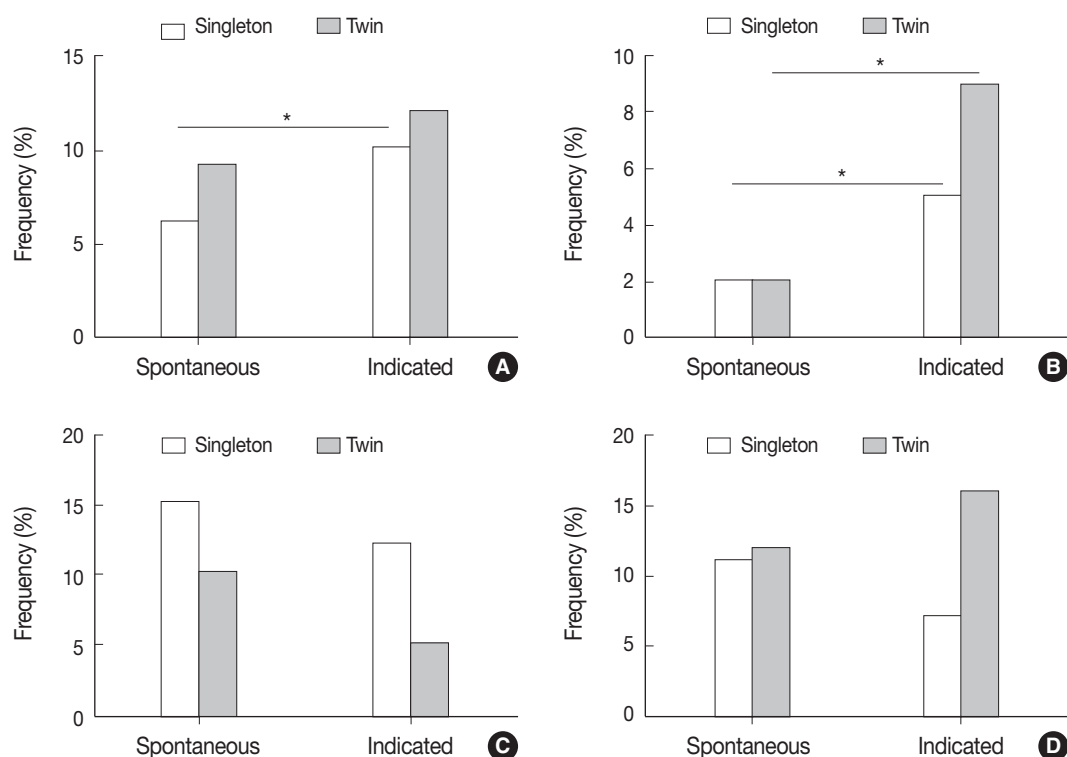


Fig. 6. The frequency of chronic placental inflammation in spontaneous preterm birth and indicated preterm birth. (A) Villitis of unknown etiology (VUE) is more frequent in indicated preterm birth than in spontaneous birth of singleton placentas ($*p < .05$). (B) Non-basal VUE is detected more frequently in indicated preterm birth than in spontaneous birth of singleton placentas as well as twin placentas ($*p < .05$). (C, D) The frequencies of chronic chorioamnionitis (C) and chronic deciduitis (D) are not different between spontaneous and indicated preterm birth.

both twin placentas (VUE, 7.3% [22/300] vs 4.0% [12/300]; CCA, 5.4% [16/300] vs 4.0% [12/300]; CD, 7.7% [23/300] vs 6.0% [18/300]). The presence of chronic inflammation in one or both twin placentas was not correlated with other clinical and placental characteristics, including baby sex, chorionicity, and discordant growth. There were 11 cases of IUGR in only one fetus of twin pregnancies with VUE, of which eight cases had VUE in only one placenta and the other three cases had VUE in both placentas, suggesting a tendency of correlation between IUGR and VUE that was not statistically significant.

DISCUSSION

In this study, the frequency of VUE, non-basal type, was higher in twin placentas than in singleton placentas. Non-basal VUE had a correlation with IUGR in twin placentas as in singleton placentas. Unexpectedly, CCA was found less frequently in twin placentas than in singleton placentas of preterm birth. The frequency peak of CCA in twin placentas was present at 29–32 weeks in contrast to that of singleton placentas at 33–36 weeks. CCA was more frequent in twin pregnancies of a differ-

ent sex than in those of the same sex. The frequency of CD was higher in DiDiS twin placentas than in singleton placentas.

Chronic placental inflammation is present as chronic villitis, CCA, and CD, depending on the affected compartment of the placenta. Some of the chronic placental inflammation may be caused by infectious agents, such as viruses, bacteria, and parasites.^{2,27,28} However, evidence of infectious etiology is not identified in most cases of chronic placental inflammation. Maternal anti-fetal rejection is suggested to play a role in the pathogenesis of these conditions. Destruction of chorionic villi (VUE) and chorionic trophoblast layer (CCA) of fetal origin by infiltration of maternal CD8⁺ T cells, along with activation of fetal macrophages, is the histopathological hallmark of these lesions.^{1,6,29} The pathogenetic mechanism of a rejection process is also supported by the elevation of local and systemic T-cell chemokines and the presence of fetal HLA-specific antibodies in the maternal serum.^{7,17,18}

VUE of non-basal type was more frequent in twin placentas than singleton placentas, and the difference was more prominent at term when VUE was detected more often in singleton placentas. The increased fetal antigen burden in twin placentas

could be related to its high frequency. In contrast, basal VUE was detected at a similar frequency between singleton and twin placentas. Basal VUE may be influenced partly by a different immunologic mechanism compared with non-basal VUE, which is supported by the presence of plasma cells in basal villitis as well as its association with CD. CD did not show a frequency difference between twin and singleton placentas in this study; however, the frequency of CD was increased in DiDiS twin placentas. DiDiS twin placentas are the type with the highest chance of dizygosity, which has more fetal antigens than the other types of twin placentas. This result suggests that it is also an anti-fetal rejection phenomenon, at least in part, which is relevant to the increase of CD in egg donor pregnancies.^{20,21} The frequency of CCA was increased in twin placentas of a different sex, which also indicated the increased fetal antigen burden. Twin pregnancies with different fetal sex are definitely dizygotic, therefore these placentas could have higher allograft antigenicity compared with those with the same fetal sex. Further studies are required to elucidate why there was no significant difference in VUE and CD between twin placentas with different fetal sex and those with the same sex.

Unexpectedly, CCA was decreased in twin placentas compared with singleton placentas at preterm. As previously reported, CCA was most frequent at 33–36 weeks gestation in singleton placentas in this study,⁸ while the highest frequency of CCA in twin placentas was detected at 29–32 weeks of gestation, which is earlier than in singleton placentas. In general, maturation of twin placentas is accelerated compared to singleton placentas at the same gestational age. The period of vulnerability to CCA may be shifted earlier due to accelerated maturation of twin placentas. These results suggest that CCA is also a manifestation of host anti-graft rejection, but a maturation-related factor may play a role in CCA.

The association of VUE with IUGR is well known by previous studies.^{28,30–32} In this study, it was confirmed in singleton placentas, and the non-basal type of VUE was associated with IUGR in twin placentas. This result also explains the high frequency of VUE in indicated preterm birth, which included most of the IUGR cases. Several previous reports showed that villitis was more severe in the placenta of the twin that weighed less, though the correlation was not confirmed statistically.^{23–25} In this study, the degree of VUE was not included for analysis. The absence of a significant association of IUGR with the total VUE in twin placentas might be influenced by various twin-specific factors resulting in IUGR, such as limitation of the uterine space, insufficient uteroplacental function, twin-to-twin

transfusion syndrome, and so on.³³

This study has some limitations. First, the enrollment of the study population was not prospective or fully consecutive, because some placentas from normal term pregnancies were not included. The institution where the placentas were collected was a tertiary medical center that takes care of more complicated cases; therefore, the cases likely do not represent the pregnancies of the general population. Second, the twin placentas were subdivided according to chorionicity but not zygosity, which would more reliably represent an increased antigen burden. These limitations might make the results less significant. However, it was clearly demonstrated that non-basal VUE was increased in twin placentas, and that CCA was decreased in preterm twin placentas. It is suggested that VUE and CCA are the region-specific manifestations of maternal anti-fetal rejection in the placenta, but their pathophysiology are partly different. Further studies are required to investigate the difference.

Conflicts of Interest

No potential conflict of interest relevant to this article was reported.

Acknowledgments

The authors are very grateful to Professor Je G. Chi, who passed away last winter (November 26, 2014). He was a great mentor and friend to all of us. This work is dedicated to his memory.

This study was supported by the Basic Science Research Program through the National Research Foundation of Korea (NRF) funded by the Ministry of Science, ICT and Future Planning (NRF-2012R1A1A3012668), and by the Korean Health Technology R&D Project, Ministry of Health & Welfare (HI1200024 (A120035)), Republic of Korea.

REFERENCES

1. Kim JS, Romero R, Kim MR, *et al.* Involvement of Hofbauer cells and maternal T cells in villitis of unknown aetiology. *Histopathology* 2008; 52: 457-64.
2. Boog G. Chronic villitis of unknown etiology. *Eur J Obstet Gynecol Reprod Biol* 2008; 136: 9-15.
3. Derricott H, Jones RL, Heazell AE. Investigating the association of villitis of unknown etiology with stillbirth and fetal growth restriction: a systematic review. *Placenta* 2013; 34: 856-62.
4. Redline RW, Ariel I, Baergen RN, *et al.* Fetal vascular obstructive lesions: nosology and reproducibility of placental reaction patterns.

- Pediatr Dev Pathol 2004; 7: 443-52.
5. Gersell DJ, Phillips NJ, Beckerman K. Chronic chorioamnionitis: a clinicopathologic study of 17 cases. *Int J Gynecol Pathol* 1991; 10: 217-29.
 6. Jacques SM, Qureshi F. Chronic chorioamnionitis: a clinicopathologic and immunohistochemical study. *Hum Pathol* 1998; 29: 1457-61.
 7. Kim CJ, Romero R, Kusanovic JP, *et al.* The frequency, clinical significance, and pathological features of chronic chorioamnionitis: a lesion associated with spontaneous preterm birth. *Mod Pathol* 2010; 23: 1000-11.
 8. Lee J, Kim JS, Park JW, *et al.* Chronic chorioamnionitis is the most common placental lesion in late preterm birth. *Placenta* 2013; 34: 681-9.
 9. Lee J, Romero R, Dong Z, *et al.* Unexplained fetal death has a biological signature of maternal anti-fetal rejection: chronic chorioamnionitis and alloimmune anti-human leucocyte antigen antibodies. *Histopathology* 2011; 59: 928-38.
 10. Khong TY, Bendon RW, Qureshi F, *et al.* Chronic deciduitis in the placental basal plate: definition and interobserver reliability. *Hum Pathol* 2000; 31: 292-5.
 11. Bendon RW, Miller M. Routine pathological examination of placentae from abnormal pregnancies. *Placenta* 1990; 11: 369-70.
 12. Edmondson N, Bocking A, Machin G, Rizek R, Watson C, Keating S. The prevalence of chronic deciduitis in cases of preterm labor without clinical chorioamnionitis. *Pediatr Dev Pathol* 2009; 12: 16-21.
 13. Yoo C, Jang DG, Jo YS, Yoo JL, Lee G. Pathologic differences between placentas from intrauterine growth restriction pregnancies with and without absent or reversed end diastolic velocity of umbilical arteries. *Korean J Pathol* 2011; 45: 36-44.
 14. Park SY, Kim MY, Kim YJ, *et al.* Placental pathology in intrauterine growth retardation. *Korean J Pathol* 2002; 36: 30-7.
 15. Trowsdale J, Betz AG. Mother's little helpers: mechanisms of maternal-fetal tolerance. *Nat Immunol* 2006; 7: 241-6.
 16. Erlebacher A. Mechanisms of T cell tolerance towards the allogeneic fetus. *Nat Rev Immunol* 2013; 13: 23-33.
 17. Kim MJ, Romero R, Kim CJ, *et al.* Villitis of unknown etiology is associated with a distinct pattern of chemokine up-regulation in the feto-maternal and placental compartments: implications for conjoint maternal allograft rejection and maternal anti-fetal graft-versus-host disease. *J Immunol* 2009; 182: 3919-27.
 18. Lee J, Romero R, Xu Y, *et al.* Maternal HLA panel-reactive antibodies in early gestation positively correlate with chronic chorioamnionitis: evidence in support of the chronic nature of maternal anti-fetal rejection. *Am J Reprod Immunol* 2011; 66: 510-26.
 19. Lee J, Romero R, Xu Y, *et al.* A signature of maternal anti-fetal rejection in spontaneous preterm birth: chronic chorioamnionitis, anti-human leucocyte antigen antibodies, and C4d. *PLoS One* 2011; 6: e16806.
 20. Perni SC, Predanic M, Cho JE, Baergen RN. Placental pathology and pregnancy outcomes in donor and non-donor oocyte in vitro fertilization pregnancies. *J Perinat Med* 2005; 33: 27-32.
 21. Gundogan F, Bianchi DW, Scherjon SA, Roberts DJ. Placental pathology in egg donor pregnancies. *Fertil Steril* 2010; 93: 397-404.
 22. Martin JA, Hamilton BE, Osterman MJ, Curtin SC, Matthews TJ. Births: final data for 2013. *Natl Vital Stat Rep* 2015; 64: 1-65.
 23. Eberle AM, Levesque D, Vintzileos AM, Egan JE, Tsapanos V, Salafia CM. Placental pathology in discordant twins. *Am J Obstet Gynecol* 1993; 169: 931-5.
 24. Jacques SM, Qureshi F. Chronic villitis of unknown etiology in twin gestations. *Pediatr Pathol* 1994; 14: 575-84.
 25. Yusuf K, Kliman HJ. The fetus, not the mother, elicits maternal immunologic rejection: lessons from discordant dizygotic twin placentas. *J Perinat Med* 2008; 36: 291-6.
 26. Redline RW. Villitis of unknown etiology: noninfectious chronic villitis in the placenta. *Hum Pathol* 2007; 38: 1439-46.
 27. Altshuler G, Russell P. The human placental villitides: a review of chronic intrauterine infection. *Curr Top Pathol* 1975; 60: 64-112.
 28. Becroft DM, Thompson JM, Mitchell EA. Placental villitis of unknown origin: epidemiologic associations. *Am J Obstet Gynecol* 2005; 192: 264-71.
 29. Redline RW, Patterson P. Villitis of unknown etiology is associated with major infiltration of fetal tissue by maternal inflammatory cells. *Am J Pathol* 1993; 143: 473-9.
 30. Knox WF, Fox H. Villitis of unknown aetiology: its incidence and significance in placentae from a British population. *Placenta* 1984; 5: 395-402.
 31. Redline RW, Patterson P. Patterns of placental injury. Correlations with gestational age, placental weight, and clinical diagnoses. *Arch Pathol Lab Med* 1994; 118: 698-701.
 32. Russell P. Inflammatory lesions of the human placenta. III. The histopathology of villitis of unknown aetiology. *Placenta* 1980; 1: 227-44.
 33. Breathnach FM, Malone FD. Fetal growth disorders in twin gestations. *Semin Perinatol* 2012; 36: 175-81.

Tongue Growth during Prenatal Development in Korean Fetuses and Embryos

Soo Jeong Hong · Bong Geun Cha¹
Yeon Sook Kim² · Suk Keun Lee
Je Geun Chi³

Departments of Oral Pathology and
¹Orthodontics, College of Dentistry,
Gangneung-Wonju National University,
Gangneung; ²Department of Dental Hygiene,
College of Health Sciences, Cheongju University,
Cheongju; ³Department of Pathology, Seoul
National University College of Medicine, Seoul,
Korea

Received: September 13, 2015
Accepted: September 17, 2015

Corresponding Author

Suk Keun Lee, DDS
Department of Oral Pathology, College of Dentistry,
Gangneung-Wonju National University,
7, Jukheon-gil, Gangneung 25457, Korea
Tel: +82-33-640-2228
Fax: +82-33-642-6410
E-mail: sukkeunlee@hanmail.net

Background: Prenatal tongue development may affect oral-craniofacial structures, but this muscular organ has rarely been investigated. **Methods:** In order to document the physiology of prenatal tongue growth, we histologically examined the facial and cranial base structures of 56 embryos and 106 fetuses. **Results:** In Streeter's stages 13–14 (fertilization age [FA], 28 to 32 days), the tongue protruded into the stomodeal cavity from the retrohyoid space to the cartilaginous mesenchyme of the primitive cranial base, and in Streeter's stage 15 (FA, 33 to 36 days), the tongue rapidly swelled and compressed the cranial base to initiate speno-occipital synchondrosis and continued to swell laterally to occupy most of the stomodeal cavity in Streeter's stage 16–17 (FA, 37 to 43 days). In Streeter's stage 18–20 (FA, 44 to 51 days), the tongue was vertically positioned and filled the posterior nasopharyngeal space. As the growth of the mandible and maxilla advanced, the tongue was pulled down and protruded anteriorly to form the linguomandibular complex. Angulation between the anterior cranial base (ACB) and the posterior cranial base (PCB) was formed by the emerging tongue at FA 4 weeks and became constant at approximately 124°–126° from FA 6 weeks until birth, which was consistent with angulations measured on adult cephalograms. **Conclusions:** The early clockwise growth of the ACB to the maxillary plane became harmonious with the counter-clockwise growth of the PCB to the tongue axis during the early prenatal period. These observations suggest that human embryonic tongue growth affects ACB and PCB angulation, stimulates maxillary growth, and induces mandibular movement to achieve the essential functions of oral and maxillofacial structures.

Key Words: Tongue; Development; Human embryos and fetuses

Embryonically, tongue development is described as a relatively prompt process: the tongue primordium emerges between fertilization age (FA) 4 and 5 weeks. Unlike maxillary and mandibular structures, the tongue primordium differentiates from the occipital myotome, and the primitive cell cluster of tongue primordium then migrates into the stomodeal cavity.¹⁻⁸ It has been well documented that tongue development has a notable effect on oral cavity development,^{2,9-13} and thus, tongue development should be monitored from the early embryonic stage, during which orofacial structures are not fully developed. However, the overall processes of tongue development cannot be monitored using conventional methods, because the tongue is not a uniform organ with a skeletal framework and its development is closely associated with the formation of branchial arches during the early embryonic stage.^{11,14-17} Nevertheless, a recent trial demonstrated the gene profile of developing tongues in mouse embryos.¹⁸

The book *Contribution to Embryology* published by the Carnegie Institute has played a pivotal role in the advancement of human

embryology.^{7,19-21} However, somewhat surprisingly, the determination of exact gestational age during early embryogenesis remains a controversial issue. Based on cumulated experience, Streeter^{19,20} introduced the concept of “developmental horizons” to describe the embryonic stage at different gestational ages. Later, O’Rahilly²¹ proposed that Streeter’s “developmental horizons” be modified for convenience, and that “horizon” and the use of Roman numerals be replaced by “stage” and Arabic numerals, respectively. In the present study, we use Streeter’s original classification method as modified by O’Rahilly.

The tongue is innervated by various nerves that subserve muscles, oral mucosa, taste buds, and minor salivary glands. These nerves include the lingual branch of the trigeminal nerve (V), the glossopharyngeal nerve (IX), the chorda tympani branch of the facial nerve (VII), and the hypoglossal nerve (XII), which are distributed to motor components of innervated muscles.^{17,22,23} In a previous study, we described the sequential prenatal development of the human maxilla, cranial base, and mandible.²⁴⁻²⁶ In addition, we published a book titled *Atlas of Human Embryo and*

Fetus: Embryonic, Anatomic, Histologic and Ultrasonographic Observation that describes human embryonic and fetal growth from the early embryonic period to full term based on studies performed on more than 2,500 Korean subjects.²⁷

Given the background described above, this study was undertaken to determine whether tongue development is closely related to the development of maxillofacial structures. To achieve this, we performed histological analyses on tongues and adjacent tissues from the early to the late embryonic stage. The preliminary study of human tongue development and growth was reported in 1990,²⁸ and this study reevaluated previous data for anatomical and dimensional changes of oral and craniofacial structures. Prenatal tongue growth was investigated by measuring the anterior cranial base (ACB) to posterior cranial base (PCB) angle (the so-called saddle angle), the ACB to maxillary plane angle, the tongue axis to PCB angle, and the tongue axis to maxillary plane angle. In addition, these angular measurements were compared with adult values obtained from cephalometric X-ray views.²⁹

MATERIALS AND METHODS

For the embryo study, serial sections were prepared from 56 embryos between FA 4 and 8 weeks filed in the Embryonal Serial Section Registry (ESR). For the fetus study, 106 normal Korean fetuses filed in the Registry of Congenital Malformation (RCM) and Children's Hospital for Autopsy (CHA) registry of Seoul National University Hospital (SNUH) were used. These fetuses were confirmed to be normal by complete autopsy, and their ages ranged between gestational age 10 and 41 weeks (Tables 1, 2). Human embryos and fetuses were used after obtaining consent from the Human Organ and Material Committee of SNUH.²⁷

Specimens were fixed in 10% neutral formalin and then paraffin-embedded. Sagittal serial sections of a thickness 4 to 6 μ m were prepared. When making these sections, head-and-neck size was considered; in smaller cases, the head and neck were serially sectioned, including the tongue, but in larger cases, the tongue was totally extracted from the oral cavity with surrounding structures and sectioned longitudinally at 4 to 6 μ m. For light microscopy, specimens were stained with hematoxylin and eosin.

For the analysis of normal adult cephalograms, we selected 30 representative cephalograms of normal subjects that visited Han Bit Clinic in Daejeon city for orthodontic counseling or treatment. All subjects had a normal craniofacial profile and showed no anterior-posterior craniofacial skeletal disharmony. In order to elucidate the developmental role of the tongue, we

Table 1. Human embryos used in this study

Embryonal age (day)	Streeter's stage	No. of ESR or RCM
28–30	13	5 (E49, E77, E83, E95, E176)
31–32	14	4 (E9, E27, E89, E94)
33–36	15	8 (E5, E45, E48, E82, E93, E113, E142, E180)
37–40	16	4 (E59, E61, E68, E183)
41–43	17	9 (E1, E8, E26, E30, E35, E37, E63, E72, E108)
44–46	18	3 (E12, E24, E168)
47–48	19	2 (E13, E48)
49–51	20	6 (E4, E18, E28, E31, E43, E92)
52–53	21	3 (E17, E67, E70)
54–55	22	4 (E25, E85, E96, R448)
≥56	23	8 (E2, E6, E55, E80, E84, E87, E96, E140)
Total		56

E (ESR), Embryo Serial Section Registry of Seoul National University Hospital (SNUH); R (RCM), Registry of Congenital Malformation at the SNUH.

Table 2. Human fetuses used in this study

Gestational age (wk)	No. of ESR, RCM, or CHA
10	4 (E11, E41, E81, E156)
11	3 (E111, R1057, R1532)
12	1 (E123)
13–14	3 (E50, E98, R1529)
15–16	3 (R308, R1526, R1533)
17–18	1 (R1524)
19–20	7 (R291, R293, R379, R398, R414, R567, A89-2)
21–22	6 (R299, R326, R422, R738, R1419, A89-54)
23–24	12 (R247, R248, R263, R285, R301, R318, R352, R353, R437, R727, R733, R736)
25–26	8 (R281, R284, R287, R300, R399, R403, R737, R1483)
27–28	11 (R249, R250, R253, R267, R270, R375, R406, R438, R506, R739, R1535)
29–30	9 (R259, R309, R316, R349, R388, R390, R409, R429, R507)
31–32	9 (R252, R297, R303, R311, R358, R362, R382, R424, R451)
33–34	6 (R266, R289, R366, R407, R416, A80-34)
35–36	4 (R355, R402, R1480, A80-20)
37–38	9 (R298, R347, R354, R361, R364, R365, R389, R451, A88-76)
39–40	6 (R294, R295, R319, R356, R370, R408)
≥41	4 (R423, A87-87, A88-72, A87-94)
Total	106

E (ESR), Embryonal Serial Section Registry of Seoul National University Hospital (SNUH); R (RCM), Registry of Congenital Malformation at the SNUH; A (CHA), Children's Hospital for Autopsy at the SNUH.

analyzed tongue positions relative to the facial and cranial base structures. In sagittal sections of microscopic specimens, four developmental planes were traced (1) the ACB plane (from the center of the hypophyseal fossa to the embryonic soft tissue nasion), (2) the PCB plane (the slope of the PCB starting from the center of the hypophyseal fossa), (3) the primary maxillary plane (from the center of the hypophyseal fossa to the most inferior

and anterior point of the premaxilla), and (4) the tongue axis (from the foramen cecum of the tongue to the tongue apex). On adult cephalometric X-ray films, these respectively constitute the ACB plane (nasion-sella turcica), the PCB plane (sella turcica-articulare), the maxillary plane (sella turcica to point A), and the tongue axis (foramen cecum of the tongue to the tongue apex). In order to analyze the role played by the tongue in embryogenesis, we measured the angles made by these planes in sagittal sections of histologic specimens and on cephalometric X-ray films.

During embryogenesis, tongue growth and development were prominent between FA 28 and 56 days (Streeter's stages, 13 and 23), and thus, we used a grading system for morphogenesis of the tongue described in the literature,^{6,7,30-33} which classifies tongue development (TD) into eight stages (Table 3).

In TD stage 1 (score 1), tongue primordium aggregates on the medial mandible and bulges on the posterior side of the stomodeum while compressing Rathke's pouch. During this stage, tongue primordium is visualized as a mesial swelling, which forms the tuberculum impar. However, at this stage it is not well demarcated from the first branchial arch.

In TD stage 2 (score 2), the hypoglossal nerve (XII) is distributed into the tongue primordium. As a result, the hypoglossal nerve fibers are observed as thick bundles. The tongue apex is proliferative and bulges to the lateral side to form the central lingual septum. Subsequently, the tongue primordium produces a pair of lateral swellings. The tongue gradually compresses the nasopharynx and grows both superiorly and anteriorly to fill the superior and posterior stomodeal spaces underneath the PCB. Simultaneously, the posterior 1/3 of the tongue and the copula bulge eventually influence formation of the posterior

curvature of the PCB. As a result, the apex of the tongue is located at the anterior region of the PCB, i.e., around Rathke's pouch.

In TD stage 3 (score 3), the tongue grows continuously and its apex is located vertical to the posterior region of the nasal cavity. At this time, the dorsal surface of the tongue fills the nasopharynx. While the olfactory placode continues to grow actively and communicates with the posterior nasal cavity, the apex of the tongue is located within the posterior nasal cavity and subsequently attaches to the orifice of the olfactory placode. Meanwhile, extrinsic tongue muscle is rapidly rearranged by myoblast differentiation to create the hyoglossus, genioglossus, and styloglossus muscle groups. In addition, proliferation of the hypoglossal nerve advanced to the distribution of the lingual nerve to the lateral sides of the tongue.

In TD stage 4 (score 4), the tongue changes from a vertical to a horizontal position. Arranged in an orderly concentric manner, the genioglossus muscle is attached to Meckel's cartilage of the mandibular arch and then closely connects with the tongue. Extrinsic tongue muscle fibers of the genioglossus and hyoglossus muscles become thickened but show no cross-striation. The apex remains located at the posterior side of the nasal cavity, and the palatal shelf rapidly proliferates and progresses to the lateral side of the tongue.

In TD stage 5 (score 5), the tongue is positioned horizontally within the oral cavity. The mandibular arch grows in the anterior and inferior directions, and the genioglossus muscle attached to Meckel's cartilage pulls the tongue both anteriorly and inferiorly in order to position the tongue horizontally in the oral cavity. At this time, most palatal shelves proliferate rapidly with mesenchymal swelling to cover the dorsal surface of the tongue, which results in closure of the secondary palate. The extrinsic

Table 3. Score points according to the TD developmental stages

TD stage	Characteristic findings
Score 1 (TD stage 1)	Mesial swelling of tongue primordium: tuberculum impar formation, concentration of mesenchymal cells.
Score 2 (TD stage 2)	Lateral swelling of tongue primordium and vertically occupation of the entire stomodeal space. It was elongated into the nasopharyngeal area, which was innervated by the hypoglossal nerve. The copula was formed from a second mesial swelling at the posterior tongue.
Score 3 (TD stage 3)	Vertical positioning of tongue: involving occupation of the posterior nasopharyngeal space, development of the hypoglossal nerve and tongue muscle, and rapid growth of the olfactory placode to form the naso-pharyngeal passage.
Score 4 (TD stage 4)	Transitional stage of the tongue from a vertical to a horizontal position. During this stage, genioglossus muscle was attached tightly in a radiating fashion on Meckel's cartilage.
Score 5 (TD stage 5)	Horizontal positioning of the tongue: as the mandible grew inferior-anteriorly the tongue was pulled by thick genioglossus muscle inferior-anteriorly. The vertical surface of the tongue was parallel to the palatal shelf.
Score 6 (TD stage 6)	Protrusion of the tongue on the horizontal plane: indentation by both alveolar ridges at the anterior tongue; cross-striation began to appear in extrinsic tongue muscle.
Score 7 (TD stage 7)	Differentiation of tongue muscle: intrinsic tongue muscle developed well and extrinsic tongue muscles were in the state of equilibrium with each other. However, many myoblasts were observed between mature striated muscles.
Score 8 (TD stage 8)	Maturation of tongue muscle: muscle bundles were thickened with prominent cross-striation; few immature myoblasts were observed.

TD, tongue development.

tongue muscles become prominent; that is, the genioglossus muscle develops extensively in the anterior and posterior regions in a concentric manner, and the hyoglossus and styloglossus muscles thicken.

In TD stage 6 (score 6), the tongue protrudes to the anterior region of the oral cavity and attaches to the palatal side of the premaxilla while vertical to the palatal plane within the oral cavity. During forward and backward movement of the tongue, the anterior tongue is indented by intimate attachment to the upper and lower lips. In addition, primitive maxillary and mandibular swellings become dominant in the space between the tongue and the upper and lower lips.

In TD stage 7 (score 7), the cells forming tongue muscles are actively differentiated into intrinsic and extrinsic muscles. In particular, the alignments of extrinsic tongue muscles such as the hyoglossus, genioglossus, and geniohyoid muscles become distinct. The pulling of these muscles anteriorly and posteriorly proportionally positions the tongue within the oral cavity. Furthermore, tongue muscles begin to show cross-striation.

In TD stage 8 (score 8), tongue muscles undergo maturation. Muscle fibers become enlarged with conspicuous cross-striation, and the muscles are closely arranged. Due to forward tongue movement, the anterior tongue shows an indentation formed by the upper and lower lips and maxillary and mandibular arches.

RESULTS

Evaluation of prenatal human TD stages

TD was observed with serial sections of human embryos and in representative sections of fetal tongues and estimated by the 8 TD stages (8 scores) described above and in Tables 3 and 4.

TD stage 1: Mesial swelling of tongue primordium in the stomodeal cavity

From Streeter's stage 13 (FA, 28 to 30 days), primitive branchial arches were observed around the cervix and became prominent through Streeter's stage 14–15 (FA, 31 to 36 days). These branchial arches were covered with a thin layer of epithelial cells with a mesenchymal cell core (Fig. 1A, B). In Streeter's stage 15 (FA, 33 to 36 days) the first branchial arch swelled dominantly and became the largest and was demarcated from surrounding tissues. The first branchial arch formed the lower face and gradually bulged. Blood vessels actively proliferated within the first branchial arch, and subsequently, the second, third, fourth, and fifth branchial arches gradually and sequentially bulged. In addition, blood vessel proliferation was observed within these

Table 4. Developmental scores of human tongue during prenatal period

Prenatal period	No. of cases	Score average ^a
Streeter's stage		
13	5	1.0
14	4	1.0
15	8	1.0
16	4	1.8
17	9	2.0
18	3	2.7
19	2	3.0
20	6	3.0
21	3	3.7
22	4	4.0
23	8	4.8
Subtotal	56	
Weeks (GA)		
10	4	5.3
11	3	6.3
Months (GA)		
3	3	6.7
4	5	7.0
5	13	7.2
6	20	7.7
7	20	7.9
8	15	8.0
9	13	8.0
10	10	8.0
Total	106	

GA, gestational age.

^aThe developmental score of human tongue is based on the tongue development stages.

arches. Finally, the cervix was partly outlined.

The tongue primordium was observed on the medial side of the first and second branchial arches, which were arch-shaped from Streeter's stage 13, and primitive mesenchymal cells of the primordium migrated from the inferior to the superior. At this time, the first mesial swelling of the tongue, the tuberculum impar, was seen in the oral cavity. Posteriorly to the mesial swelling, infiltration and proliferation of the thyroid primordium were also noted (Fig. 2A). In Streeter's stage 14 (FA, 31 to 32 days), the second and third mesial tongue swellings were clearly seen posterior to the first mesial swelling; these were destined to differentiate into copula (or hypobranchial eminence) and epiglottal swelling, respectively (Fig. 1C).

From Streeter's stage 15 (FA, 33 to 36 days) mesenchymal cells of branchial arches actively migrated distally to differentiate in a uniform direction. Migrating from the occipital myotome to the oral cavity, most of the distally extended mesenchyme of the tongue primordium differentiated into extrinsic tongue muscles. At this time, the mandibular primordium was

located more posteriorly than the cranial region. Accordingly, mesial swelling of the tongue protruded superiorly from the posterior oral cavity and compressed the inferior portion of Rathke's pouch. The tongue continuously proliferated towards

the spheno-occipital synchondrosis, which corresponded to prechordal mesenchyme in the superior to posterior portions of the oral stomodeum (Figs. 1A–D, 2A, 2B). TD stage 1 corresponds to Streeter's stages 13–15 (FA, 28 to 36 days).

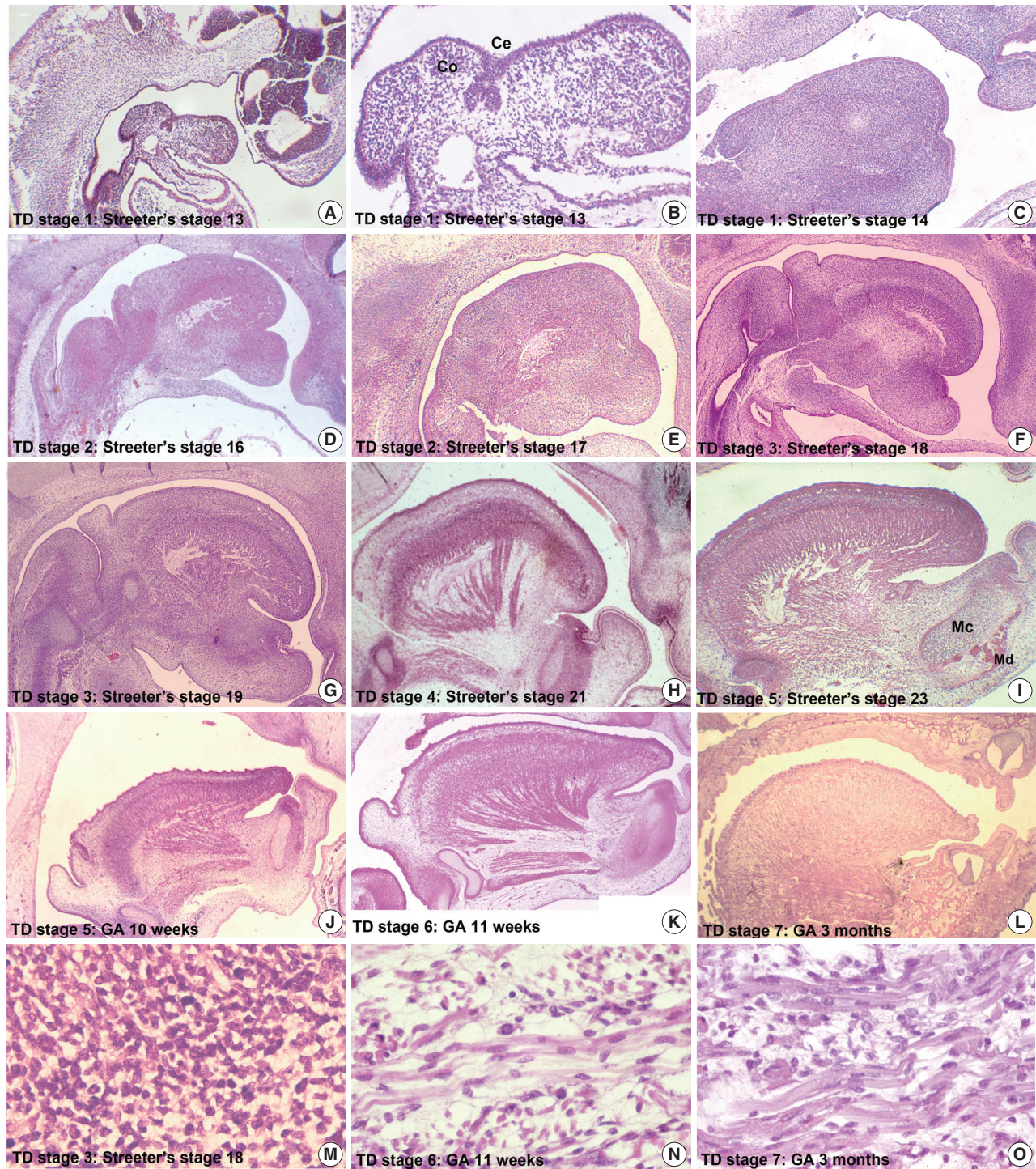


Fig. 1. Organogenesis of a fetal tongue. Photographs of mid-sagittal sections of an embryonic human tongue. (A, B) Tongue development (TD) stage 1. Co, copula; Ce, foramen cecum. (C) TD stage 1. (D, E) TD stage 2. (F, G) TD stage 3. (H) TD stage 4. (I, J) TD stage 5. MC, Meckel's cartilage; Md, mandible. (K) TD stage 6. (L) TD stage 7. Microscopic features of tongue muscle at TD stage 3 (M), TD stage 6 (N), and TD stage 7 (O).

TD stage 2: Lateral swelling of tongue primordium and its vertical occupation of the whole stomodeal cavity

At Streeter's stage 16 (FA, 37 to 40 days), the mandibular primordium of the first branchial arch differentiated into Meck-

el's cartilage, and Reichert's cartilage was formed within the second branchial arch. A mesial swelling was differentiated into a pair of lateral swellings both anteriorly and superiorly on bi-lateral sides (Fig. 2B). Continuously protruding both anteriorly



Fig. 2. Sequential tongue development (TD) stages during the early embryonic period aligned with anterior cranial base (ACB) and posterior cranial base (PCB) lines. (A) TD stage 1. (B) TD stage 2. (C–E) TD stage 3. (F) TD stage 4. (G, H) TD stage 5. (I) TD stage 6.

and superiorly and then indistinguishably from mesial swelling, the lateral swelling was separated bilaterally by the lingual septum (Fig. 1D). In Streeter's stage 17 (FA, 41 to 43 days), copula swelling (hypobranchial eminence) became distinct. This lateral swelling filled the posterior curvature of the pharynx and then proliferated both anteriorly and superiorly (Fig. 1E). Subsequently, the primitive stomodeal cavity was wholly occupied by the proliferating and protruding tongue (Figs. 1E, 1F, 2C, 2D). The TD stage 2 corresponds with Streeter's stages 16–17 (FA, 37 to 43 days).

TD stage 3: Vertical position of the tongue and its occupation of nasopharyngeal space

From Streeter's stage 18 (FA, 44 to 46 days), the tongue mesenchyme proliferated and was filled with undifferentiated myoblasts (Fig. 1M). The hyoglossus muscle was arranged between the tongue and hyoid cartilage, the genioglossus muscle was arranged between the tongue center and Meckel's cartilage, and the styloglossus muscle was between the tongue center and the temporal portion of the cranial base. At this time, the mandible was located more posteriorly and was smaller than the maxilla. Accordingly, the tongue protruded vertically and expanded the posterior stomodeal space for nasopharyngeal development (Figs. 1F, 2C). In Streeter's stage 19 (FA, 47 to 48 days), as the mandible grew anteriorly and inferiorly, the tongue was pulled slightly downward and forward by the anterior portion of the genioglossus muscle (Fig. 2D). The nasal plate actively proliferated and then communicated with the posterior nasal cavity. The apex of the tongue moved to communicate between the nasal plate and the posterior nasal cavity and began to curve anteriorly, although the tongue body was still located at the proximal site (Fig. 1G). However, in Streeter's stage 20 (FA, 49 to 51 days), the tongue was widely distended superiorly, anteriorly, and inferiorly (Fig. 2E). TD stage 3 corresponds to Streeter's stages 18–20 (FA, 44 to 51 days).

TD stage 4: Transitional stage from a vertical to horizontal tongue position

In Streeter's stage 21 (FA, 52 to 53 days) the tongue protruded and elongated within the oral cavity (Fig. 2F). The mandible was still located more posteriorly than the maxilla. While Meckel's cartilage enlarged, mandible growth was initiated on the lateral side of Meckel's cartilage and then progressed anteriorly and inferiorly. Fibers of the genioglossus muscle became distinct and tracked the tongue to attach to the perichondral mesenchymal tissue of Meckel's cartilage. This process lowered

the tongue both anteriorly and inferiorly as illustrated in Fig. 3. A huge empty space appeared for the nasopharyngeal structure in the posterior stomodeal cavity (Fig. 1H). In Streeter's stage 22 (FA, 54 to 55 days), the extrinsic tongue muscles appeared much more mature, and the genioglossus muscle fibers previously attached to Meckel's cartilage migrated anteriorly to the posterior side of the mandible (Fig. 1N). Accordingly, the arrangement of the genioglossus muscle fibers attached to the tongue center became concentric and distinct. Moreover, the arrangement of hyoglossus muscle cells became distinct and hyoglossus muscle fibers actively proliferated. At this time, the genioglossus muscle pulls the tongue both anteriorly and inferiorly. As a result, the tongue was rapidly lowered in the same direction and located in transition between the vertical and horizontal positions (Figs. 1I, 2G). TD stage 4 corresponds to Streeter's stages 21–22 (FA, 52 to 55 days).

TD stage 5: Horizontal positioning of the tongue in the oral cavity

In Streeter's stage 23 (FA, 56 days), the tongue was lowered both anteriorly and inferiorly and located on the horizontal

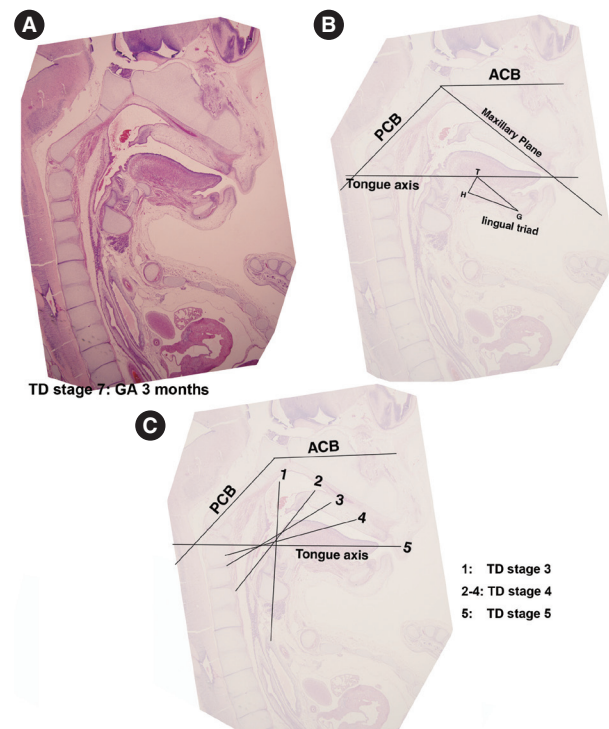


Fig. 3. Measurements of the dispositions of tongue developmental planes, tongue development (TD) stage 7. (A, B) Planes of the anterior cranial base (ACB), the posterior cranial base (PCB), the maxillary plane, and tongue axis. (C) The tongue axis gradually rotated in a clock-wise manner, vertical to the horizontal (1 → 5) during the prenatal period. GA, gestational age.

plane. However, the mandible was still shifted slightly posterior to the maxilla. Accordingly, the tongue apex was attached to incisive papilla of the premaxilla. In addition, the lower lip was seen within the oral cavity. The palatal shelf rapidly proliferated and gradually closed as the nasal septum grew downward to result in nasal cavity formation (Fig. 2G). Tongue muscle cells were arranged in a relatively harmonious manner; the genioglossus, hyoglossus, styloglossus, and geniohyoid muscles were clearly distinguishable. Nevertheless, no cross-striation was observed in these muscles at this stage. In particular, genioglossus muscle growth became prominent both anteriorly and posteriorly, and the arrangement of the posterior genioglossus muscle fibers, which track the tongue both anteriorly and inferiorly, became notable in the center of the tongue (Fig. 1I). Subsequently, a large space for the nasopharynx was generated (Fig. 2G). At the same time, the sphenoccipital synchondrosis became active and enlarged, producing an anteroposterior cranial base angle, which eventually formed the roof of the nasopharynx.

At gestational age (GA) 10 weeks, growth of the nasal capsule gradually progressed. Accordingly, the nasal septum was inferiorly enlarged. The anterior part of the nasal septum fused with the premaxilla to form the primary palate. Meanwhile, the posterior part of the nasal septum grew progressively. The lowered palatal shelf migrated from the posterior part to the dorsal side of tongue and was positioned horizontally (Figs. 1J, 2H). Subsequently, the palatal shelf rapidly enlarged and formed the secondary palate by fusing with the nasal septum, which was inferiorly growing from the prechordal mesoderm. TD stage 5 corresponds to Streeter's stage 23 (FA, 56 days; GA, 10 weeks).

TD stage 6: Protrusion of the tongue in the horizontal plane

At approximately GA 11 weeks, mandibular growth was more advanced than maxillary growth, resulting in the two being at almost the same level. As the tongue was located in the horizontal plane, its forward movement gradually progressed (Fig. 2I). The tongue apex was attached to incisive papilla of the premaxilla. Growth of the mandible became prominent and the mandible body was enlarged on the lateral side of Meckel's cartilage, from which it gradually separated. The growth of mandibular bony trabeculae progressed laterally (Fig. 1K). Insertions of digastric and mylohyoid muscles were completely changed from Meckel's cartilage to the mandible. The lower lip was located posterior to the upper lip and closely associated with the tongue apex, causing an indentation in the anterior tongue. On the other hand, the nasal septum continued to proliferate inferiorly. Meanwhile, the nasal septum was involved in

the formation of the vomer, a plate-like structure posterior to its anterior part, and subsequently associated with the formation of the hard palate by fusing with the palatal shelf. Moreover, the posterior extended tissue of the palatal shelf formed the soft palate as it fused with the nasal septum without any communications. Finally, the soft palate covered the anteriorly located tongue root. TD stage 6 corresponds to GA 11 weeks.

TD stage 7: Differentiation of tongue muscle cells

At around GA 3 months, when facial muscles are not well-developed, the genioglossus and hyoglossus muscles were found to exhibit bundle-like arrangements of muscle fibers with conspicuous cross-striation (Fig. 1O). In the tongue, the hyoglossus, genioglossus, styloglossus, and glossopalatinus muscles are classified as extrinsic muscles; at the hyoid bone, mandible, and cranial base, they are classified as the geniohyoid, mylohyoid, and stylohyoid muscles, respectively (Fig. 1L). At approximately GA 4 months, the tongue muscles were well developed and subsequently enlarged. Intrinsic tongue muscles were not well developed until approximately GA 5 months. TD stage 7 corresponds to GA 3–5 months.

TD stage 8: Maturation of tongue muscle

After GA 6 months, tongue muscle growth became prominent, muscle fibers were enlarged, and cross-striation was clearly observed. The fascicles of the extrinsic tongue muscles were tightly connected, and the development of intrinsic muscles became prominent. Thus, they were distinguishable from extrinsic muscles. At approximately GA 8 months, tongue muscle maturation was almost complete. At this time, cross-striation was clearly observed and muscular fascicles became thicker with few undifferentiated myoblasts (Fig. 1O). TD stage 8 corresponds to the period from GA 6 months.

Formation of the lingual frenum

In Streeter's stage 19, the tongue was superiorly directed to the nasal cavity, and in Streeter's stage 23, it was anteriorly tracked by mandible growth and the genioglossus muscle. At this time, mucosa located anterior to the genioglossus muscle was much extended, and a thin membranous structure was formed on the ventral surface (termed the lingual frenum) (Fig. 4A, B). Until GA 10 weeks, the lingual frenum was covered with thin oral mucosal epithelium, and it contained only a small amount of connective tissue and subsequently fused to the lingual septum (Fig. 4C). The tongue apex migrated both anteriorly and inferiorly after GA 11 weeks. At approximately GA 12 weeks, mus-

cle fibers of the external tongue muscles were more matured, and at this stage, the tongue performed forward and backward movements in the horizontal plane. The membranous lingual frenum became the anterior margin that supported forward and backward movements of the tongue (Fig. 4).

Relations between the cranial base and facial structures

ACB plane to PCB plane angle (Saddle angle)

The angle between the ACB and PCB planes constitutes a basic craniofacial structure and was almost flat (180°) in Street-



Fig. 4. Formation of the lingual frenum in human embryos. (A) Mid-sagittal section of the human tongue at tongue development (TD) stage 4, the vertical line indicates the frontal section planes for panel B. (B) Frontal section of human embryo at TD stage 4, indicating the membranous covering of the lingual frenum (arrows). (C) Frontal section of a human embryo at TD stage 5, showing the close connection between the lingual frenum and lingual septum (LS). GA, gestational age.

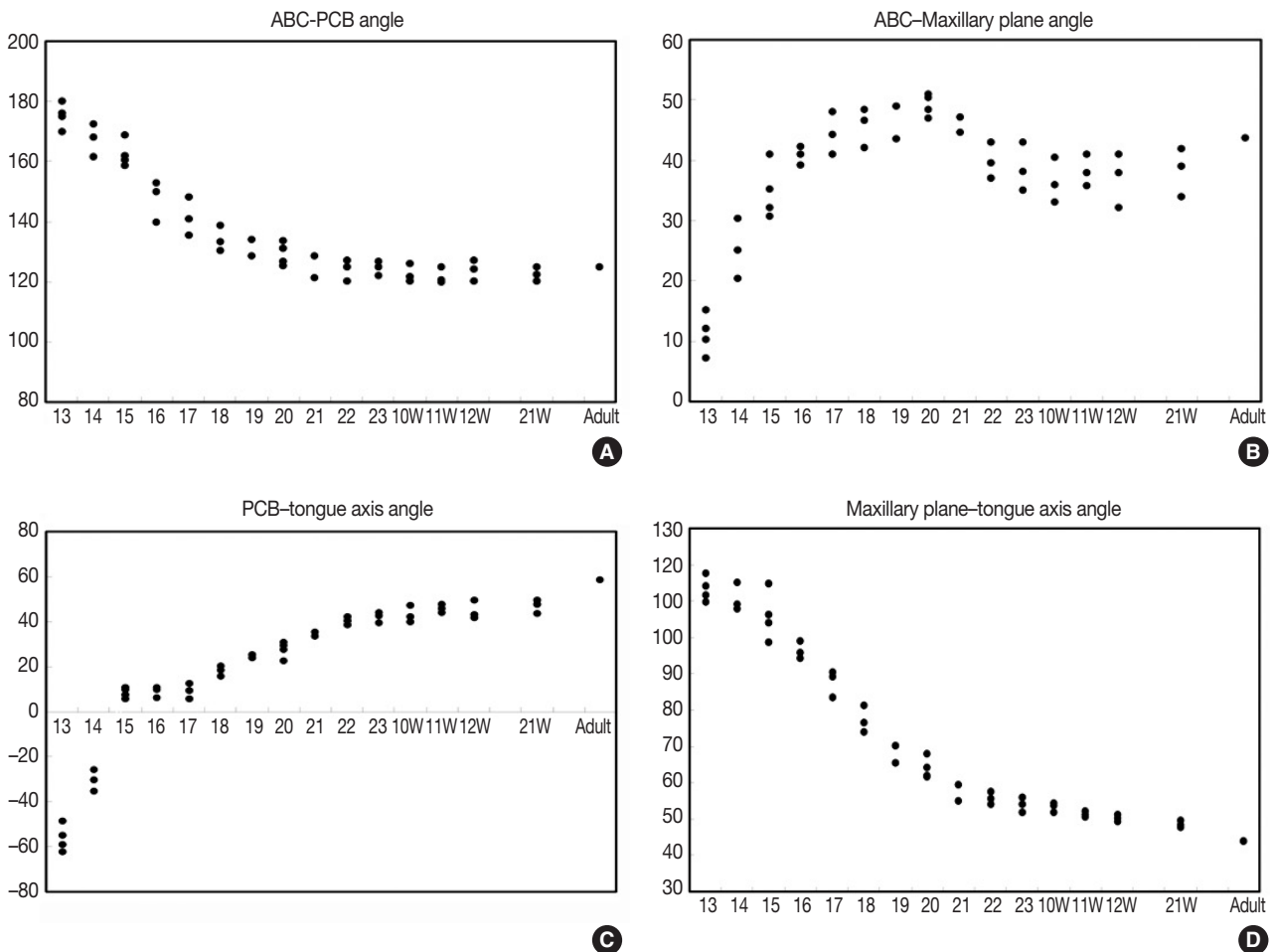


Fig. 5. (A–D) Incremental change graphs of the four developmental angles (Table 5); anterior cranial base (ACB) to posterior cranial base (PCB) angle, ACB–maxillary plane angle, PCB–tongue axis angle, and maxillary plane–tongue axis angle.

er's stage 13 before the tongue pressed the cranial base (Fig. 2A). The tongue migrated from the occipital myotome to the stomodeal cavity and pressed the hypophyseal fossa area to form this angle, which reduced in accordance with FA. In Streeter's stage 17, this angle was about 160°, and in Streeter's stage 19 it reduced from 120° to 130° to reach 124° to 126° in Streeter's stage 23. We observed that this value was maintained at FA 21 weeks in histological sections and was similar in adult cephalograms. The mean saddle angle obtained by the cephalogram tracing of 30 normal adults was 116° to 131° with a mean of 124.8°, which is comparable to other reports that the saddle angle of normal adult men and women are 124° ± 5° and 126° ± 5°, respectively. Therefore, we presume that this saddle angle almost matures during the early prenatal period (at FA 8 weeks) due to compression by the emerging tongue (Fig. 5A).

ACB plane to maxillary plane angle

The ACB to maxillary plane angle represents facial clockwise growth. It was almost rudimentary at FA 4–5 weeks, but as the premaxilla grew downward from late during the fifth FA week, the ACB to maxillary plane angle increased to 32° to 52°. This angulation was conspicuously observed in the mid-sagittal sections of embryos and early fetuses until GA 12 weeks. However, in the cephalograms of 30 normal adults, the ACB plane to maxillary plane angle averaged 40.5° to 51.5° (Fig. 5B).

Tongue axis to PCB angle

The tongue axis to PCB angle is an important factor of facial

counter-clockwise growth; it was almost negative when the tongue emerged at FA 4–5 weeks, but thereafter as the tongue protruded forward, this angle gradually became positive and increased to 47° at FA 8 weeks. The tongue axis and PCB angle were relatively stable at 43° at GA 12 weeks and remained almost constant until GA 21 weeks. In the cephalograms of 30 normal adults, the tongue axis to PCB plane angle ranged from 42° to 72.5° with an average value of 58.3° (Fig. 5C).

Tongue axis to maxillary plane angle

Angulation between the tongue axis and the maxillary plane was observed from FA 5 weeks at 110°. As the tongue grew forward and downward and the tip of the tongue gradually fixed to the premaxilla, the tongue axis to maxillary plane angle became approximately 48° from the FA 8 weeks and then remained constant until GA 21 weeks. In the cephalograms of 30 normal adults, the tongue axis to maxillary plane angle ranged from 32.5° to 53.5° with an average value of 43.7° (Fig. 5D). Relations between the tongue and craniofacial structures are summarized in Table 5.

DISCUSSION

According to Moore (1982),¹⁴ the tongue primordium bulges late during the fourth FA week, and one mesial swelling and two lateral swellings proliferate while the tongue protrudes into the oral cavity. In the present study, we investigated the locations of TD with respect to overall maxillofacial structures, and

Table 5. Angulation changes during tongue development

Age	ACB-PCB angle	ACB-maxillary plane angle	PCB-tongue axis angle	Maxillary plane-tongue axis angle
Streeter's stage				
13	113.4±3.51	-56.2±5.85	175.3±4.11	11.2±3.35
14	110.7±3.84	-30.4±4.70	167.4±5.34	25.3±4.95
15	105.9±6.68	8.5±2.20	162.6±4.55	34.8±4.59
16	96.3±2.51	8.8±2.31	147.6±6.69	40.8±1.46
17	87.7±3.61	9.2±3.41	141.5±6.37	44.4±3.50
18	77.2±3.62	18.1±2.31	134.2±4.23	45.7±3.29
19	67.8±3.94	24.5±0.85	131.3±3.96	46.3±3.82
20	64.1±2.90	27.6±3.59	129.3±3.92	49.3±1.85
21	57.2±2.97	34.4±0.99	125.1±5.09	45.9±1.77
22	55.7±1.70	40.4±1.80	124.2±3.58	39.9±3.01
23	53.9±2.06	42.1±2.35	124.6±2.36	38.7±4.03
Gestational age (wk)				
10	53.4±1.33	43.0±3.79	122.8±3.04	36.5±3.78
11	51.3±0.72	45.9±1.80	121.8±2.87	38.2±2.66
12	50.2±0.90	44.7±-4.08	123.9±3.46	37.0±4.53
21	48.5±0.89	47.0±2.98	122.6±2.50	38.3±4.10
Adult	43.8±5.00	58.4±6.98	124.8±6.98	43.8±5.00

ACB, anterior cranial base; PCB, posterior cranial base.

we noted that the tongue and mandibular primordium were severely retruded as compared with the maxillary primordium.^{16,34,35} In particular, the origin of TD was located in the pharyngeal region and proliferation was rapid and resulted in compression of the inferior part of the PCB. This expanded the pharyngeal region and then affected the complete osteogenesis of the cranial base^{25,28} and secondary palate,^{34,36-38} in time for the formation of the sphenoccipital synchondrosis. Trenouth^{39,40} examined the fetal growth and development of the maxilla and mandible and found mandibular protrusion is obvious between GA 8 and 10 weeks, and that thereafter, the maxillary protrusion appears while the naso-maxillary segment enlarges. At the same time, the mandible grows anteriorly and inferiorly in harmony with maxillary growth. Diwert³⁴ stressed that chondrocranium and Meckel's cartilage determine the locations of cranial base angulation and maxilla during the late fetal stage when early skeletal structures are formed. Our results showed cranial base angulation is closely associated with lingual swelling and vertical positioning of the tongue.

At approximately FA 8 weeks, mandibular growth, centered by Meckel's cartilage, pulls the tongue downward and forward, while growth of Meckel's cartilage is greatly increased. Our results showed that the tongue is transposed from the vertical to the horizontal axis from FA 7 weeks to the early eighth week (Streeter's stages, 20–23). At this time, the muscle cells forming the tongue muscles are premature. Between GA 10 and 12 weeks, protrusion of the tongue was noted while extrinsic tongue muscles were arranged in a harmonious manner. Furthermore, cells forming extrinsic muscles were progressively differentiated and cross-striation was observed, which suggests that forward and backward movement of tongue was initiated.

Humphrey^{35,41,42} proposed that opening and closing movements are caused by masseter and temporal muscle reflexes at approximately GA 12 weeks and suggested that prompt mandibular growth in the early embryonic stage is due to the intraoral appearance of the tongue and to the opening and closing movement. Our results show that TD progressed much faster than maxillofacial structural growth. To determine whether the developing tongue is associated with its adjacent branchial arches, we performed a histologic analysis to examine nerve distributions in serial sections. This analysis revealed that tongue muscles were closely related to masticatory and facial muscles and indicated that the earlier maturations of tongue muscles rather than facial musculature substantially affected the growth and development of maxillofacial structures. The present study demonstrates that the embryonic tongue originates from the

occipital myotome, actively migrates into the stomodeal cavity through the retrohyoid space, and gradually swells beneath the primordial mesenchyme of the cranial base to form the angulation between the ACB and PCB. Furthermore, this angulation occurred rapidly, and the swollen tongue was directed perpendicularly to the angulation point. Subsequently, Rathke's pouch invaginated into the center of the sphenoid body, and thus, we propose that the swelling of embryonic tongue is related to angulation of ACB and PCB and to the formation of Rathke's pouch. In addition, we confirmed that the ACB-PCB angle matured at FA 8 weeks and then remained almost constant until full term and during postnatal life.

It has been reported that the developing tongue adjusts to functional changes during the postnatal stage.⁴³ In patients with acromegaly, mandibular prognathism is rarely accompanied by a change in tongue size, but tongue size is greatly reduced in Beckwith-Wiedemann syndrome.⁴⁴⁻⁴⁶ However, in Down syndrome, muscular dystrophy is accompanied by tongue enlargement,⁴⁷ which could compress the pharynx and lead to mandibular prognathism.⁴⁸ Furthermore, it is well known that tongue enlargement occurs rapidly in Down syndrome patients who have a reduced number of teeth.⁴⁷ Our results showed that TD affects the development of maxillofacial structures such as the maxilla, mandible, nasal cavity, pharynx, and larynx, either directly or indirectly. Because TD is one of the earliest events that progresses through the fetal stage, it can be inferred that the developmental rate of maxillofacial structures should be evaluated with reference to TD. As noted above, in the early embryonic stage, the tongue grows while it fills the pharynx, protrudes upward, and compresses the cranial base.

TD cannot be easily explained by its associations with other maxillofacial structures because its development involves its migration from the occipital myotome, which is unlike that of prechordal mesoderm or branchial arches of the cervix that form maxillofacial structures.^{6,7} In addition, the tongue is innervated by major cranial nerves. The lingual branch of the trigeminal nerve (V) is distributed in mucosa at the tongue anterior, the chorda tympani branch of the facial nerve (VII) is distributed among taste buds in the anterior region, the glossopharyngeal nerve (IX) distributes to mucosa in the posterior region, branches of the vagus nerve (X) are distributed in laryngeal constrictor muscle, and the hypoglossal nerve (XII) is distributed as a motor component in the skeletal muscles constituting tongue tissues.^{6,7,49-53} From early embryogenesis, the tongue is imbued with a wide variety of innervated cells, and thus, TD is influenced by the regulation of interactive functional reflexes,

and this eventually affects the growth and development of maxillofacial structures.

In the present study, we examined lingual frenum formation during the embryonic period and defined the lingual frenum as a structure that supports anterior to posterior movement of the tongue. At the beginning of TD, the lingual frenum is a thin membranous covering of stomodeal mucosa that is gradually connected with the lingual septum centered by intrinsic tongue musculature. Previously, we supposed fibrous thickening of the lingual frenum in postnatal life limits tongue movement and results in ankyloglossia and designed a lingual myoplasty that differed from ordinary frenectomy to reduce the range of tongue movement.^{28,54,55} However, the present study demonstrates that the lingual frenum is produced as a result of positional changes of the embryonic tongue and that it functions as a reserved space for anterior extension of tongue movement.

In the present study, TD has been described as an 8-stage event involving mesial swelling of the tongue primordium, lateral swelling of the tongue within the oral fossa, vertical protrusion of the tongue, tongue transposition, horizontal location, anterior location, muscle differentiation, and tongue muscle maturation. Importantly, TD precedes that of other maxillofacial structures, and thus, changes in tongue position could be regarded as primary events of maxillofacial growth and development. In addition, because tongue muscles, masticatory muscles, and facial muscles move continually during fetal development, it is likely that the effects of the tongue on other maxillofacial structures continue even after birth. This suggests the tongue is an important organ that plays critical roles in the development of adjacent maxillofacial structures, such as the oral and nasal cavities, pharynx, and maxilla, and that abnormal TD might be related to congenital maxillofacial anomalies.

In summary, TD as observed during the present study indicates that the human tongue develops at an early embryonic age, that is, at approximately Streeter's stage 13 (FA, 28 to 30 days) as an anterior extension of the occipital myotome, which is earlier than that of any other orofacial structure, and that the tongue continues to develop and affects the formation of the cranial base, jaws, and nasopharyngeal structures. In our opinion, the morphogenetic impact of the tongue on craniofacial structures is substantial enough to affect the anatomy and essential functions of oro-facial structures. However, the extents of these changes and the mechanisms involved remain to be elucidated.

Conflicts of Interest

No potential conflict of interest relevant to this article was reported.

Acknowledgments

We express our sincere appreciation to the donors of human materials that made it possible to perform this study, which was initiated after obtaining legal approval from the Embryonal Serial Section Registry (ESR), the Registry of Congenital Malformation (RCM), and the Children's Hospital for Autopsy (CHA), Seoul National University Hospital (Seoul). We also express our gratitude to the late Professor Je G. Chi, who founded the ESR, RCM, and CHA. Professor Chi was a mentor and friend to all of the authors. We dedicate this study to his memory.

REFERENCES

1. Achtel LW, Cole LJ, Bailey JS. X-irradiation of defined areas of the heads of weanling rats: effect on body growth and incisor development. *Radiat Res* 1967; 31: 430-40.
2. Siebert JR. Prenatal growth of the median face. *Am J Med Genet* 1986; 25: 369-79.
3. Yamane A, Bringas P Jr, Mayo ML, *et al.* Transforming growth factor alpha up-regulates desmin expression during embryonic mouse tongue myogenesis. *Dev Dyn* 1998; 213: 71-81.
4. Uchiyama K, Ishikawa A, Hanaoka K. Expression of Ibx1 involved in the hypaxial musculature formation of the mouse embryo. *J Exp Zool* 2000; 286: 270-9.
5. Nagata J, Yamane A. Progress of cell proliferation in striated muscle tissues during development of the mouse tongue. *J Dent Res* 2004; 83: 926-9.
6. Wozniak W. The peripheral part of the hypoglossal nerve in human embryos at stage 14 (32 days). *Folia Morphol (Warsz)* 1995; 54: 227-30.
7. O'Rahilly R, Muller F. The early development of the hypoglossal nerve and occipital somites in staged human embryos. *Am J Anat* 1984; 169: 237-57.
8. Vasyutina E, Stebler J, Brand-Saberi B, Schulz S, Raz E, Birchmeier C. CXCR4 and Gab1 cooperate to control the development of migrating muscle progenitor cells. *Genes Dev* 2005; 19: 2187-98.
9. Abu-Elteen KH, Abu-Elteen RM. The prevalence of *Candida albicans* populations in the mouths of complete denture wearers. *New Microbiol* 1998; 21: 41-8.
10. Aduss H, Pruzansky S. Postnatal craniofacial development in chil-

- dren with the oral-facial-digital syndrome. *Arch Oral Biol* 1964; 9: 193-203.
11. Achiron R, Ben Arie A, Gabbay U, Mashiach S, Rotstein Z, Lipitz S. Development of the fetal tongue between 14 and 26 weeks of gestation: *in utero* ultrasonographic measurements. *Ultrasound Obstet Gynecol* 1997; 9: 39-41.
 12. Slavkin HC. Regulatory issues during early craniofacial development: a summary. *Cleft Palate J* 1990; 27: 101-9.
 13. Dalrymple KR, Prigozy TI, Shuler CF. Embryonic, fetal, and neonatal tongue myoblasts exhibit molecular heterogeneity *in vitro*. *Differentiation* 2000; 66: 218-26.
 14. Moore KL. *The developing human: clinically oriented embryology*. Philadelphia: W. B. Saunders, 1982.
 15. Egerbacher M, Bock P. Lingual papillae. *Am J Surg Pathol* 1997; 21: 360.
 16. Kim CH, Park HW, Kim K, Yoon JH. Early development of the nose in human embryos: a stereomicroscopic and histologic analysis. *Laryngoscope* 2004; 114: 1791-800.
 17. Yamane A. Embryonic and postnatal development of masticatory and tongue muscles. *Cell Tissue Res* 2005; 322: 183-9.
 18. Nie X. Apoptosis, proliferation and gene expression patterns in mouse developing tongue. *Anat Embryol (Berl)* 2005; 210: 125-32.
 19. Streeter GL. Developmental horizons in human embryos: description of age groups XV, XVI, XVII, and XVIII, being the third issue of a survey of the Carnegie Collection. Carnegie Institution of Washington Publication 575. *Contrib Embryol* 1948; 32: 133-203.
 20. Streeter GL, Heuser CH, Corner GW. Developmental horizons in human embryos: description of age groups XIX, XX, XXI, XXII, and XXIII, being the fifth issue of a survey of the Carnegie collection. Carnegie Institution of Washington Publication 592. *Contrib Embryol* 1951; 34: 165-96.
 21. O'Rahilly R. Guide to the staging of human embryos. *Anat Anz* 1972; 130: 556-9.
 22. Barlow LA, Northcutt RG. The role of innervation in the development of taste buds: insights from studies of amphibian embryos. *Ann N Y Acad Sci* 1998; 855: 58-69.
 23. Swanson JJ, Kuehl-Kovarik MC, Elmquist JK, Sakaguchi DS, Jacobson CD. Development of the facial and hypoglossal motor nuclei in the neonatal Brazilian opossum brain. *Brain Res Dev Brain Res* 1999; 112: 159-72.
 24. Lee SK, Kim YS, Lim CY, Chi JG. Prenatal growth pattern of the human maxilla. *Acta Anat (Basel)* 1992; 145: 1-10.
 25. Lee SK, Kim YS, Jo YA, Seo JW, Chi JG. Prenatal development of cranial base in normal Korean fetuses. *Anat Rec* 1996; 246: 524-34.
 26. Lee SK, Kim YS, Oh HS, Yang KH, Kim EC, Chi JG. Prenatal development of the human mandible. *Anat Rec* 2001; 263: 314-25.
 27. Chi JG, Suh YL, Lee SK, *et al.* *Atlas of human embryo and fetus: embryonic, anatomic, histologic and ultrasonographic observations*. Seoul: Academy, 2001.
 28. Lee SK, Lim CY, Chi JG. Development and growth of tongue in Korean fetuses. *Korean J Pathol* 1990; 24: 358-74.
 29. Hong SJ. Study on the prenatal growth and development of tongue in Korean fetuses. Gangneung: Department of Oral Pathology, College of Dentistry Graduate School, Gangneung-Wonju National University, 2006.
 30. Tamatsu Y, Gasser RF. Development of the sensory nerves to the dorsum of the tongue in staged human embryos. *Clin Anat* 2004; 17: 99-106.
 31. Shuler CF, Dalrymple KR. Molecular regulation of tongue and craniofacial muscle differentiation. *Crit Rev Oral Biol Med* 2001; 12: 3-17.
 32. Sato M, Sato T. Fine structure of developed human tongue muscle. *Okajimas Folia Anat Jpn* 1992; 69: 115-30.
 33. Langdon H, Klueber K, Barnwell Y. The anatomy of M. genioglossus in the 15-week human fetus. *Anat Embryol (Berl)* 1978; 155: 107-13.
 34. Diewert VM. A morphometric analysis of craniofacial growth and changes in spatial relations during secondary palatal development in human embryos and fetuses. *Am J Anat* 1983; 167: 495-522.
 35. Humphrey T. Development of oral and facial motor mechanisms in human fetuses and their relation to craniofacial growth. *J Dent Res* 1971; 50: 1428-41.
 36. Diewert VM. Differential changes in cartilage cell proliferation and cell density in the rat craniofacial complex during secondary palate development. *Anat Rec* 1980; 198: 219-28.
 37. Diewert VM, Pratt RM. Selective inhibition of mandibular growth and induction of cleft palate by diazo-oxo-norleucine (DON) in the rat. *Teratology* 1979; 20: 37-51.
 38. Greene RM, Pratt RM. Developmental aspects of secondary palate formation. *J Embryol Exp Morphol* 1976; 36: 225-45.
 39. Trenouth MJ. Angular changes in cephalometric and centroid planes during foetal growth. *Br J Orthod* 1981; 8: 77-81.
 40. Trenouth MJ. Changes in the jaw relationships during human foetal cranio-facial growth. *Br J Orthod* 1985; 12: 33-9.
 41. Humphrey T. The relation between human fetal mouth opening reflexes and closure of the palate. *Am J Anat* 1969; 125: 317-44.
 42. Humphrey T. Palatopharyngeal fusion in a human fetus and its relation to cleft palate formation. *Ala J Med Sci* 1970; 7: 398-426.
 43. Niikuni N, Nakajima I, Akasaka M. The relationship between tongue-base position and craniofacial morphology in preschool children. *J Clin Pediatr Dent* 2004; 28: 131-4.
 44. Friede H, Figueroa AA. The Beckwith-Wiedemann syndrome: a

- longitudinal study of the macroglossia and dentofacial complex. *J Craniofac Genet Dev Biol Suppl* 1985; 1: 179-87.
45. Laroche C, Testelin S, Devauchelle B. Cleft palate and Beckwith-Wiedemann syndrome. *Cleft Palate Craniofac J* 2005; 42: 212-7.
46. Wang J, Goodger NM, Pogrel MA. The role of tongue reduction. *Oral Surg Oral Med Oral Pathol Oral Radiol Endod* 2003; 95: 269-73.
47. Ardran GM, Harker P, Kemp FH. Tongue size in Down's syndrome. *J Ment Defic Res* 1972; 16: 160-6.
48. Skrinjaric T, Glavina D, Jukic J. Palatal and dental arch morphology in Down syndrome. *Coll Antropol* 2004; 28: 841-7.
49. Bradley RM, Mistretta CM, Nagai T. Demonstration of sensory innervation of rat tongue with anterogradely transported horseradish peroxidase. *Brain Res* 1986; 367: 364-7.
50. Matsushima TA, Satou M, Ueda K. Glossopharyngeal and tectal influences on tongue-muscle motoneurons in the Japanese toad. *Brain Res* 1986; 365: 198-203.
51. Mbiene JP, Mistretta CM. Initial innervation of embryonic rat tongue and developing taste papillae: nerves follow distinctive and spatially restricted pathways. *Acta Anat (Basel)* 1997; 160: 139-58.
52. Berger AJ, Bayliss DA, Viana F. Development of hypoglossal motoneurons. *J Appl Physiol (1985)* 1996; 81: 1039-48.
53. Vij S, Kanagasuntheram R. Development of the nerve supply to the human tongue. *Acta Anat (Basel)* 1972; 81: 466-77.
54. Lee SK, Kim YS, Lim CY. A pathological consideration of ankyloglossia and lingual myoplasty. *J Korean Dent Assoc* 1989; 27: 287-308.
55. Yoon JY, Lee I, Lee SS, *et al.* Cephalometric changes after lingual myoplasty for ankyloglossia associated malocclusions. *Port Ortod* 2005; 10: 1-17.

Comprehensive Cytomorphologic Analysis of Pulmonary Adenoid Cystic Carcinoma: Comparison to Small Cell Carcinoma and Non-pulmonary Adenoid Cystic Carcinoma

Seokhwi Kim · Jinah Chu ·
Hojoong Kim¹ · Jounggho Han

Department of Pathology, ¹Division of Pulmonary and Critical Care Medicine, Department of Medicine, Samsung Medical Center, Sungkyunkwan University School of Medicine, Seoul, Korea

Received: August 3, 2015
Revised: September 4, 2015
Accepted: September 7, 2015

Corresponding Author

Jounggho Han, MD, PhD
Department of Pathology, Samsung Medical Center, Sungkyunkwan University School of Medicine, 81 Irwon-ro, Gangnam-gu, Seoul 06351, Korea
Tel: +82-2-3410-2765
Fax: +82-2-3410-0025
E-mail: hanjho@skku.edu

Background: Cytologic diagnosis of pulmonary adenoid cystic carcinoma (AdCC) is frequently challenging and differential diagnosis with small cell carcinoma is often difficult. **Methods:** Eleven cytologically diagnosed cases of pulmonary AdCC were collected and reviewed according to fifteen cytomorphologic characteristics: small cell size, cellular uniformity, coarse chromatin, hyperchromasia, distinct nucleolus, frequent nuclear molding, granular cytoplasm, organoid cluster, sheet formation, irregular border of cluster, hyaline globule, hyaline basement membrane material, individual cell necrosis or apoptotic body, and necrotic background. Twenty cases of small cell carcinoma and fifteen cases of non-pulmonary AdCC were also reviewed for the comparison. **Results:** Statistically significant differences were identified between pulmonary AdCC and small cell carcinoma in fourteen of the fifteen cytomorphologic criteria (differences in sheet formation were not statistically significant). Cellular uniformity, distinct nucleolus, granular cytoplasm, distinct cell border, organoid cluster, hyaline globule, and hyaline basement membrane material were characteristic features of AdCC. Frequent nuclear molding, individual cell necrosis, and necrotic background were almost exclusively identified in small cell carcinoma. Although coarse chromatin and irregular cluster border were observed in both, they favored the diagnosis of small cell carcinoma. Hyaline globules were more frequently seen in non-pulmonary AdCC cases. **Conclusions:** Using the fifteen cytomorphologic criteria described by this study, pulmonary AdCC could be successfully distinguished from small cell carcinoma. Such a comprehensive approach to an individual case is recommended for the cytologic diagnosis of pulmonary AdCC.

Key Words: Carcinoma, adenoid cystic; Lung; Carcinoma, small cell; Cytology

Adenoid cystic carcinoma (AdCC) is rare in the lower respiratory tract (less than 0.2% incidence was reported among the all primary pulmonary tumors).¹⁻³ Using aspiration and exfoliative cytology for diagnosis, less than twenty cases have been reported in the English literature.⁴⁻⁶ Due to its rare incidence, cytopathologic features of pulmonary AdCC have not been collectively described yet.⁷⁻¹¹

In salivary glands where AdCC is commonly found, cytologic characteristics of AdCC have been frequently studied and are relatively well-established. Round or ovoid nuclei and indistinct nucleoli are reported as cellular features of the AdCC. The organoid structure formed by tumor cells and hyaline globules are also helpful diagnostic features.¹² A Japanese group suggested 17 cellular and architectural features of AdCC for the cytologic diagnosis. According to the report, the AdCC could be distinguished from other salivary gland-type tumors by using the 17

items.¹³ However, the subtyping of salivary gland-type tumors by fine needle aspiration (FNA) cytology is not simple, and the accuracy has been low compared to the core needle biopsy.¹⁴

Additionally, in clinical practice, a sufficient amount of a sample is not always obtained, especially in the lower respiratory tract where the specimen acquisition by bronchoscope is usually difficult. When examining a pulmonary lesion, it is important to distinguish AdCC from other non-salivary gland-type tumors such as small cell carcinoma. Although both can share the similar cytomorphologies, the therapeutic regimens are far different.^{15,16} There had been a few case reports that pulmonary AdCC was misinterpreted as small cell carcinoma.^{6,11}

In this study, we analyzed cytomorphologic features of 11 primary and metastatic pulmonary AdCC cases. Cytology of twenty small cell carcinomas and fifteen non-pulmonary AdCCs were also investigated for the points of differential diagnosis.

MATERIALS AND METHODS

Patients and specimen preparation

Among 93 patients who were diagnosed to have pulmonary AdCC in the Samsung Medical Center between September 1995 and June 2015, aspiration or bronchial washing cytology was performed in 36 cases. Tumor cells were identified in 11 cases and the remaining 25 cases were reported to be negative for malignant cells. The 11 cases of primary and metastatic pulmonary AdCC were all histologically confirmed as AdCC by biopsy or resection. Among the 11 AdCC cytology cases, samples for seven cases (64%) were obtained from bronchial washing specimens, and samples for four cases (36%) were acquired by endobronchial ultrasound-guided transbronchial needle aspiration (EBUS-TBNA). Nine of the cases (82%) were obtained from trachea or bronchus samples and the remaining two cases (18%) were obtained from mediastinal lymph nodes by EBUS-TBNA. The computerized record system of Samsung Medical Center identified a total of 466 cases of small cell carcinoma which were diagnosed from cytologic specimens of mediastinal lymph nodes. Twenty cases of small cell carcinoma were randomly selected from 109 recent cases (from July 2013 to June 2015) for the cytologic comparison to pulmonary AdCC. In addition, among 426 primary AdCC cases of non-primary origin in the Samsung Medical Center between September 1995 and June 2015, both cytologic and histologic specimens were available for the review in fifteen patient cases and thus they were chosen for our study. All non-pulmonary AdCC specimens were obtained from the salivary gland or other head and neck region tumors.

Clinicopathologic information—sex, age, smoking history, site of tumor, stage, and progress was investigated by using electronic medical records. Patients were categorized into the smoker or non-smoker group according to their smoking history.¹⁷

EBUS-TBNA and bronchial washing of the respiratory tract were performed by pulmonologists using a rigid or flexible bronchoscope. A 22-gauge needle was used in TBNA. The aspirate was smeared onto glass slides, air dried, immediately fixed with 95% alcohol and subsequently stained with hematoxylin and eosin (H&E) and a Papanicolaou solution. Bronchial washing was conducted by injecting saline solution into the bronchial tree and subsequent suctioning. The acquired washing specimen was centrifuged, fixed in a 95% alcohol and stained using H&E and a Papanicolaou solution. FNAs of the salivary gland and head and neck tumors were performed either by radiologists or pathologists using a 22- or 23-gauge needle attached to a 10-mL syringe. Ultrasonographic guidance was used in the cases

performed by radiologists.

In cases that subsequent biopsies or surgical resection of the tumor were performed, histologic slides were also collected for the review.

This study was approved by the Institutional Review Board of the Samsung Medical Center (IRB No. 2015-07-154).

Cytopathologic and histopathologic analysis

The cytologic slides were reviewed by three pathologists (J.H., S.K., and J.C.), including a pathologist (J.H.) who has more than 20-year experience of pulmonary pathology and cytopathology. The cases were evaluated according to fifteen cytomorphological features: (1) small cell size, (2) cellular uniformity, (3) coarse chromatin, (4) hyperchromasia, (5) distinct nucleolus, (6) frequent molding, (7) granular cytoplasm, (8) distinct individual cell border, (9) organoid cluster, (10) sheet formation, (11) irregular border of cluster, (12) hyaline globule, (13) hyaline basement membrane material, (14) individual cell necrosis or apoptotic body, and (15) necrotic background. The small cell was defined by the cell size of less than three times the diameter of the background lymphocyte. When the nuclear molding was shown in more than 50% of the entire tumor cell population, it was regarded as the frequent molding. The organoid cluster represented a cylindrical, spherical, fingerform or other distinctive architectural arrangements of tumor cells. The organoid cluster and sheet formation were indicated when more than 10% of the tumor area showed the morphologies. The above 15 features were selected by a comprehensive summary of the literature regarding AdCC and small cell carcinoma.^{8,12,13,18}

The histologic slides of the all pulmonary and non-pulmonary AdCC cases were also blindly reviewed.

Immunohistochemistry

Immunohistochemical staining of c-kit was performed to confirm the diagnosis of AdCC. Formalin-fixed, paraffin-embedded tissue samples of biopsied or resected tumors were prepared in 4- μ m thickness slices and stained with a rabbit polyclonal antibody (1:50, Dako, Carpinteria, CA, USA).

Statistical analysis

Student's t tests and Mann-Whitney tests were performed to compare the age and the duration of follow up between the pulmonary AdCC group and the small cell carcinoma group, and between the pulmonary AdCC group and the non-pulmonary AdCC group. Whether to use Student's t test or Mann-Whitney test was decided after testing the normal distribution of data, by

performing a Kolmogorov-Smirnov test and a Shapiro-Wilk test. The chi-square test, Fisher exact test, and linear-by-linear association were performed to analyze the differences in sex distribution, smoking history, stage and progression status in clinicopathologic data and the cytomorphic items. Each test was applied in the appropriate setting. A one-tailed test was used in the case that showed unidirectional tendency. Values were considered statistically significant when the p-value was less than .05. Statistical analyses were performed by using the SPSS ver. 20 (SPSS Inc., Chicago, IL, USA).

RESULTS

Clinicopathologic characteristics of pulmonary AdCC

The clinical and pathological characteristics of the 11 pulmonary AdCC cases are summarized in Table 1. Patients included in the pulmonary AdCC group were six males and five females and the median age was 57 years old. Among the nine patients whose smoking histories were available, five patients were smokers (median, 12.5 pack-years; range, 10 to 30 pack-years). Most of the pulmonary AdCC cases were observed as obstructive masses or narrowing of trachea/bronchus in bronchoscopy. Except for the one case that lacked staging information, stage I, II, III, and IV constituted 20%, 10%, 60%, and 10% of the cases, respectively. In three cases (27%), the tumors had recurred on their original sites. Metastasis was identified in two patients during follow-up (18%).

Only one case (9%) was confirmatively diagnosed as AdCC in the cytologic specimen (case 3). Eight cases (73%) were diagnosed as malignancy or suspicious for malignancy but specific types were not mentioned. The remaining two cases (18%) were diagnosed as the presence of atypical cells.

All cases were confirmed as AdCC by subsequent biopsies and surgical resections. Nine cases (82%) showed a cribriform pattern of growth, whereas the remaining two cases (18%) showed a solid pattern.

Clinical characteristics of small cell carcinoma and non-pulmonary AdCC

Clinical features of the selected small cell carcinoma cases and the non-pulmonary AdCC cases are summarized in Table 2. Among the small cell carcinoma cases, 15 cases (75%) were obtained from N1 mediastinal lymph nodes. Three cases (15%) were acquired from N2 lymph nodes. Eleven patients (55%) were in the limited stage of disease whereas the remaining nine patients (45%) were in the extensive stage. Tumor recurrence was

Table 1. Clinicopathologic characteristics of 11 pulmonary adenoid cystic carcinoma cases

Case No.	Sex	Age (yr)	Specimen	Site	Cytologic diagnosis	Histologic pattern	Bronchoscopic finding	Stage	TNM	Progression	Follow-up period (mo)
1	M	42	FNA	LN, 1R	Metastatic carcinoma from trachea	Solid	Bronchial narrowing	IIIA	T1bN2M0	NED	3
2	F	47	BW	Lt main bronchus	PFMC	Solid	Endobronchial tumor infiltration	IB	T2aN0M0	NED	8
3	M	52	FNA	LN, 7	Metastatic AdCC from lung	Cribriform	Bronchial obstruction	IIIA	T1bN2M0	Metastasis to LN	54
4	F	61	FNA	Trachea	AdCC cannot be excluded	Cribriform	NA	IIIA	T4N0M0	Metastasis to lung	34
5	M	57	BW	Rt lower bronchus	A nest of atypical cells	Cribriform	Bronchial obstructing mass	IIIA	T2aN2M0	NED	108
6	M	65	BW	Carina	Atypical cells	Cribriform	Tracheal obstruction	IV	T2aN0M1	NED	52
7	F	75	BW	Lt main bronchus	Suspicious malignancy	Cribriform	Bronchial narrowing	NA	NA	Local recurrence	48
8	M	60	BW	Rt upper bronchus	Suspicious malignancy	Cribriform	Bronchial obstruction	IIIB	T3N0M0	Local recurrence	177
9	M	53	BW	Trachea	AdCC cannot be excluded	Cribriform	Tracheal mass	IA	T1bN0M0	Local recurrence	123
10	F	58	BW	Rt main bronchus	PFMC	Cribriform	Bronchial obstructing mass	IIIA	T4N0M0	NED	6
11	F	55	FNA	Trachea	AdCC versus epithelial myoepithelial carcinoma	Cribriform	NA	IIIA	T4N0M0	NED	17

M, male; FNA, fine-needle aspiration; LN, lymph node; NED, no evidence of disease; F, female; BW, bronchial washing; Lt, left; PFMC, positive for malignant cells; AdCC, adenoid cystic carcinoma; NA, not available; Rt, right.

Table 2. Clinical characteristics of pulmonary adenoid cystic carcinoma, metastatic small cell carcinoma, and non-pulmonary adenoid cystic carcinoma cases

Characteristic	Pulmonary AdCC (n=11)	SC (n=20)	Non-pulmonary AdCC (n=15)	p-value
Sex				
Male	6 (55)	18 (90)	6 (40)	.067 ^{a,b}
Female	5 (45)	2 (10)	9 (60)	.462 ^{c,d}
Median age (range, yr)	57 (42–75)	68 (57–77)	53 (32–76)	<.001 ^{a,e} .168 ^{c,e}
Smoking history				
Smoker ^f	5 (56) ^g	19 (95)	2 (14) ^g	.022 ^{a,b}
Never smoker ^h	4 (44) ^g	1 (5)	12 (86) ^g	.066 ^{c,b}
Site				
Trachea: 4 (36)		N1 LN: 15 (75)	Salivary gland: 12 (80)	-
Bronchus: 5 (46)		N2 LN: 3 (15)	EAC: 2 (13)	
Mediastinal LN: 2 (18)		Unspecified: 2 (10)	Mouth floor: 1 (7)	
Stage				
I: 2 (20) ⁱ		Limited: 11 (55)	I: 3 (20)	.667 ^{c,j}
II: 1 (10) ⁱ		Extensive: 9 (45)	II: 4 (27)	
III: 6 (60) ⁱ			III: 1 (7)	
IV: 1 (10) ⁱ			IV: 7 (46)	
Recurrence or metastasis				
Present	5 (45)	2 (10)	5 (33)	.067 ^{a,d}
Absent	6 (55)	18 (90)	10 (67)	.689 ^{c,d}
Median follow up (range, mo)	48 (3–177)	7.5 (1–19)	41 (4–70)	.003 ^{a,k} .264 ^{c,e}

Values are presented as number (%) unless otherwise indicated.

AdCC, adenoid cystic carcinoma; SC, small cell carcinoma; LN, lymph node; EAC, external auditory canal.

^ap-value between pulmonary AdCC and small cell carcinoma; ^bFisher's exact test; ^cp-value between pulmonary AdCC and non-pulmonary AdCC; ^dChi-square test; ^eStudent's t-test; ^fSmoker group includes ex-smoker (stopped smoking for more than 365 days), habitual smoker (more than 1 tobacco product/day) and occasional smoker (less than 1 tobacco product/day); ^gSmoking history was not able to obtain in two pulmonary AdCC cases and one non-pulmonary AdCC case; ^hNever smokers had smoked less than 20 g of tobacco (equivalent to 100 or fewer cigarettes) in lifetime; ⁱStaging information was not available in one pulmonary AdCC case; ^jLinear by linear association; ^kMann-Whitney test.

identified in two patients (10%). The patients' age at diagnosis was older and the follow-up period was shorter in the patients with small cell carcinoma compared to the patients with pulmonary AdCC. All except one of the small cell carcinoma patients had a smoking history (median, 45 pack-years; range, 30 to 112.5 pack-years).

Non-pulmonary AdCC cases were all obtained by FNA. Twelve cases (80%) were taken from either parotid or submandibular glands. Two cases (13%) were the tumors of external auditory canal. One case (7%) was obtained by FNA of the floor of the mouth. Sex ratio, median age, smoking history (median, 33.75 pack-years; range, 22.5 to 45 pack-years in smoker group), stage, presence of recurrence or metastasis and follow-up period were not statistically different from those of the pulmonary AdCC group.

Comprehensive cytomorphologic comparison among pulmonary AdCC, small cell carcinoma, and non-pulmonary AdCC

The fifteen cytomorphologic criteria described above were evaluated in the pulmonary and the non-pulmonary AdCC and the

small cell carcinoma cases (Table 3). Except for sheet formation, all other cytomorphologic criteria showed statistically significant differences between pulmonary AdCC and small cell carcinoma. Although 45% of the pulmonary AdCC cases manifested small cell size, the tumor cells were cytologically uniform and they frequently had distinct nucleoli which were not noted in small cell carcinoma. While six cases (55%) of pulmonary AdCC revealed a coarse chromatin pattern, it was identified in all but one case of small cell carcinoma. Nucleoli were distinct in six cases (55%) of pulmonary AdCC, but all of the small cell carcinoma cases showed indistinct nucleoli. Nuclear molding was occasionally identified in seven out of 10 available pulmonary AdCC cases (70%). However, none exceeded 50% of the entire tumor cell population. In contrast, the extensive nuclear molding was noted in 95% of the small cell carcinoma cases. Many pulmonary AdCC cases had tumor cells with scant cytoplasm and/or naked nuclei similar to small cell carcinoma. However, rigorous microscopic examination revealed granular cytoplasm in the majority of the cases (73%). The cellular border was distinct in the three pulmonary cases (27%), while none of the small cell carcinoma cases showed distinguishable cellular

Table 3. Cytomorphologic features of pulmonary AdCC, SC, and non-pulmonary AdCC

Feature	Pulmonary AdCC (n=11)	SC (n=20)	Non-pulmonary AdCC (n=15)	p-value (pulmonary AdCC/SC)	p-value (pulmonary AdCC/non-pulmonary AdCC)
Histologic pattern					
AdCC, tubular pattern	0/11	-	2/14	-	.167 ^a
AdCC, cribriform pattern	9/11	-	11/14		
AdCC, solid pattern	2/11	-	1/14		
Cytologic findings					
Specimen cellularity				.031 ^a	.138 ^a
3	3/11	13/20	9/15		
2	4/11	5/20	4/15		
1	4/11	2/20	2/15		
Small cell	5/11	20/20	13/15	.001 ^b	.038 ^b
Cellular uniformity	9/10	2/20	12/15	<.001 ^b	.626 ^b
Coarse chromatin	6/11	19/20	7/15	.013 ^b	.691 ^c
Hyperchromasia	5/11	20/20	12/15	.001 ^b	.103 ^b
Distinct nucleolus	6/11	0/20	10/15	.001 ^b	.689 ^b
Frequent molding	0/11	19/20	1/15	<.001 ^b	.577 ^b
Granular cytoplasm	8/11	0/20	12/15	<.001 ^b	.509 ^b
Distinct cell border	3/11	0/20	4/15	.037 ^b	.655 ^b
Organoid cluster	8/8	2/20	12/15	<.001 ^b	.526 ^b
Sheet formation	4/9	13/20	14/15	.422 ^b	.015 ^b
Irregular cluster border	4/9	20/20	7/15	.001 ^b	.625 ^b
Hyaline globule	4/11	0/20	12/15	.010 ^b	.043 ^b
Hyaline BM material	3/11	0/20	5/15	.037 ^b	.543 ^b
Cell necrosis/apoptotic body	0/11	18/20	2/15	<.001 ^b	.492 ^b
Necrotic background	2/11	16/20	2/15	.002 ^b	.574 ^b

AdCC, adenoid cystic carcinoma; SC, small cell carcinoma; p-value (pulmonary AdCC/SC), p-value between pulmonary AdCC and small cell carcinoma; p-value (pulmonary AdCC/non-pulmonary AdCC), p-value between pulmonary AdCC and non-pulmonary AdCC; BM, basement membrane.

^aLinear by linear association; ^bFisher exact test; ^cChi-square test.

borders. Regarding the architectural patterns, organoid cluster formation was observed in all of the pulmonary AdCC cases, but two small cell carcinoma cases also revealed vaguely organoid clusters. Whereas the border of cell clusters was irregular in all of the small cell carcinoma cases, regular borders were identified in 56% of the pulmonary AdCC cases. Hyaline globules and hyaline basement membrane materials were exclusively identified in the pulmonary AdCC cases; however, the frequency is lower than expected (36% and 27%, respectively). The single cell necrosis or apoptotic body was not observed in any pulmonary AdCC case. Although the two pulmonary AdCC cases (18%) revealed necrotic background, it was identified in 80% of small cell carcinoma cases (Figs. 1, 2). In summary, cellular uniformity, distinct nucleolus, granular cytoplasm, distinct cell border, organoid cluster, hyaline globule and hyaline basement membrane were revealed as cytologic features of pulmonary AdCC compared to small cell carcinoma. Coarse chromatin, frequent nuclear molding, irregular border of cluster, individual cell necrosis or apoptotic body, and necrotic background could be considered as characteristic cytologic findings of small cell carcinoma.

When comparing pulmonary AdCC to non-pulmonary AdCC cases according to the fifteen cytomorphologic features, small cell size and sheet formation were less frequently observed in the pulmonary AdCC cases. Whereas 80% of the non-pulmonary AdCC cases had hyaline globules, they were only seen in 36% of the pulmonary AdCC cases.

Histopathologic correlation and immunohistochemical confirmation of pulmonary AdCC

The review of biopsy or surgical resection slides of the 11 pulmonary AdCC cases revealed that nine cases had a cribriform growth pattern while two cases showed a solid pattern of growth. Tumors with a solid pattern of growth were confirmed by immunohistochemical staining with c-kit (data not shown). In the non-pulmonary AdCC cases, 11 cases (79%) showed cribriform predominant histology, while the tubular and solid growth patterns were noted in the rest cases (14% and 7%, respectively).

DISCUSSION

Pulmonary AdCC is often difficult to diagnose based on cyto-

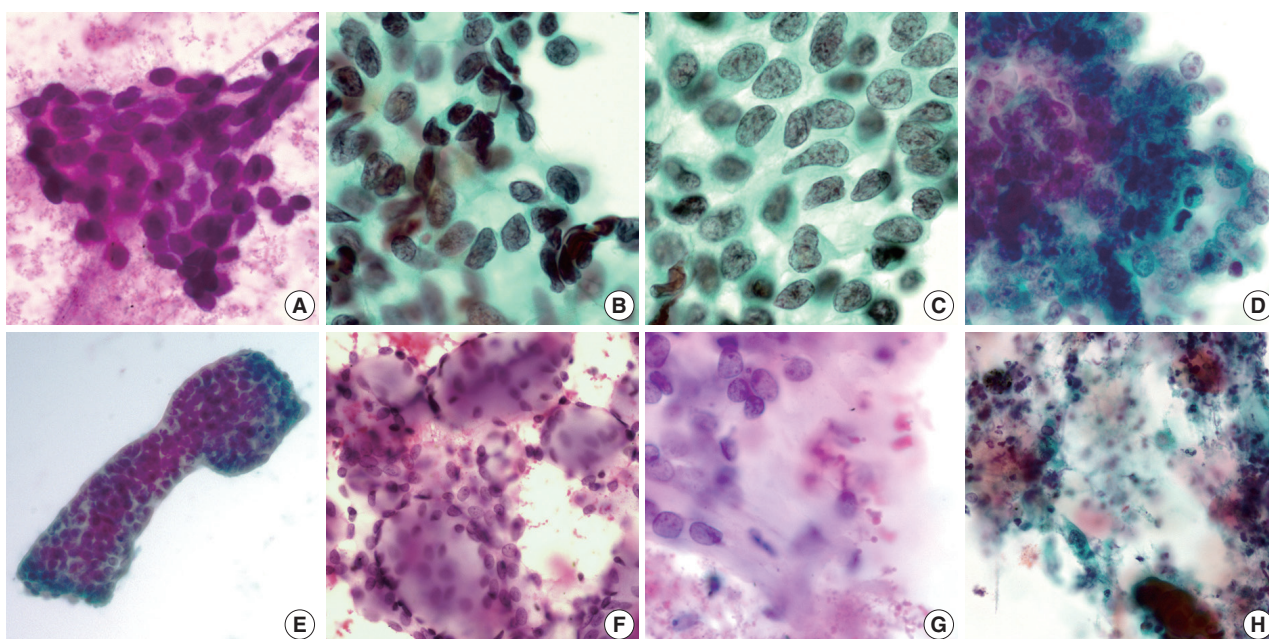


Fig. 1. Cytomorphology of pulmonary adenoid cystic carcinoma. (A) Small cell size, cellular uniformity and hyperchromasia (case 1). (B) Infrequently identified nuclear molding (case 7). (C) Granular cytoplasm and well-defined cell borders (case 7). (D) Distinct nucleoli and sheet formation (case 2). (E) Organoid tumor clusters with smooth border (case 9). (F) Hyaline globules (case 3). (G) Hyaline basement membrane materials (case 3). (H) Necrotic background (case 6).

logic analysis. Besides the fact that they frequently show similar cytomorphology, many primary tumors of the lung share common clinical features. Therefore, differential diagnosis often includes a variety of malignant tumors such as small cell carcinoma, carcinoid tumor and poorly differentiated non-small cell carcinoma. Salivary gland type tumors other than AdCC-pleomorphic adenoma, myoepithelial adenoma/carcinoma, basal cell adenoma/carcinoma and epithelial-myoepithelial carcinoma should also be considered.¹³

Small cell carcinoma is an especially important differential diagnosis to consider because its treatment and prognosis is far different from AdCC. Small cell carcinoma has been thought to be distinguished from AdCC in cytology by nuclear molding and necrosis. However, research has demonstrated the occasional presence of such features in AdCC as well.^{6,11,19} From these reports, pulmonary AdCC often demonstrated small cell size, coarse chromatin¹³ and occasional nuclear molding.¹¹ Chuah *et al.*¹⁰ also demonstrated the diagnostic difficulty of AdCC in bronchial washing by emphasizing the importance of the clean background of AdCC compared to the necrotic background of small cell carcinoma. Kim *et al.*,⁶ who reported a misinterpreted case of AdCC, suggested that lack of apoptotic bodies, nuclear debris, frequent mitoses, and the Azzopardi effect could be distinctive points between AdCC and small cell carcinoma.

In this study, pulmonary AdCC and small cell carcinoma were

well-distinguished from each other when applying the 15 cytomorphological features that we proposed. With the exception of sheet formation, the remaining fourteen features showed statistically significant differences. Cellular uniformity (90%), granular cytoplasm (73%), and organoid cluster formation (100%) were identified as distinguishable features of pulmonary AdCC compared to small cell carcinoma. However, some pulmonary AdCC cases contained cytomorphologic features of small cell carcinoma-coarse chromatin (55%), indistinct nucleolus (55%), occasional molding (70%), and necrotic background (18%). Therefore, one should not depend on a single criterion to conclude the diagnosis in cytology of the pulmonary tumor. Instead, a comprehensive approach using multiple cytomorphological features is recommended. Among the clinical items we investigated, smoking history was the most distinguishable between the pulmonary AdCC group and the small cell carcinoma group. Patients with small cell carcinoma had significant smoking history. Also, the small cell carcinoma cases showed extensive involvement of mediastinal lymph nodes compared to the pulmonary AdCC cases. These clinical presentations could also be helpful for confirmative diagnosis.

Confronting the individual cases of pulmonary AdCC, there were several points that could be confused with small cell carcinoma. Tumor cells of case 1 in Table 1 were small and they had indistinct nucleoli and occasional nuclear molding (in about

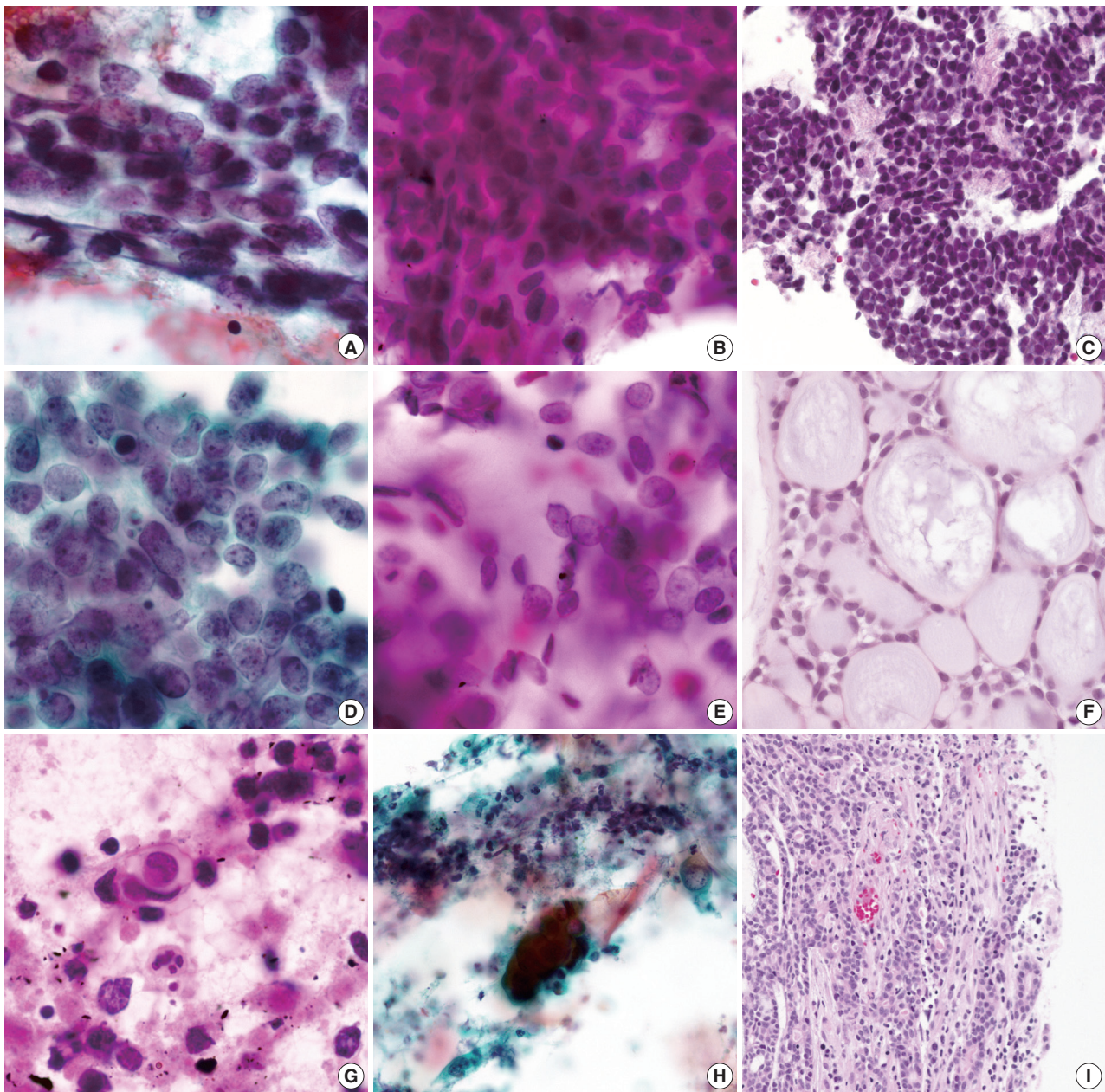


Fig. 2. Cytologic comparison between pulmonary adenoid cystic carcinoma (AdCC) and small cell carcinoma with histologic confirmation. (A) Lack of cellular uniformity in small cell carcinoma. (B) Uniform tumor cells of pulmonary AdCC with occasional nuclear molding (case 1). (C) Biopsy specimen of pulmonary AdCC case 1, which mimicked small cell carcinoma morphology. (D) Coarse chromatin pattern with frequent nuclear molding in small cell carcinoma. (E) Size variation of the tumor cells with fine-stippled to coarse chromatin in pulmonary AdCC (case 3). (F) Biopsy specimen showing typical histology of AdCC (case 3). (G) Extensively necrotic background with frequent single cell necrosis and apoptotic bodies in the small cell carcinoma aspirate. (H) Necrotic background without individual tumor cell necrosis or apoptotic body in pulmonary AdCC (case 6). (I) Surface ulceration identified in the resection specimen of pulmonary AdCC (case 6).

20% of total tumor volume) (Fig. 2B). Although the chromatin pattern was fine-stippled rather than coarse, and granular cytoplasm was identified in some tumor cells, it was difficult to exclude small cell carcinoma straightforwardly (Fig. 2A). Furthermore, only a small portion of the cytology specimens revealed organoid clusters. The biopsy specimen of case 1 also showed

small cell carcinoma-like morphology which was observed in the cytologic slides (Fig. 2C). Recognition of cellular uniformity and focal hyaline basement membrane material was essential in the case. Case 3 in Table 1 consisted of small cells with fine-stippled to coarse chromatin and paucity of granular cytoplasm (Fig. 2E). However, the tumor cells were relatively uniform and lacked

nuclear molding compared to small cell carcinoma. Careful microscopic examination confirmed the diagnosis by identifying organoid clusters with hyaline basement membrane material. A bronchial washing case (case 6 in Table 1) showed a few tumor cells scattered in the necrotic background (Fig. 2H). Although the cell size was slightly larger than small cells and the chromatin pattern was fine rather than coarse, small cell carcinoma was considered in the differential diagnosis due to the necrotic background. However, background necrosis was far more evident in the small cell carcinoma cases, and the individual cell necrosis and the apoptotic bodies were frequently identified (Fig. 2G). The review of histologic slides obtained later by surgical resection revealed ulceration in the surface of the mass with numerous inflammatory cells (Fig. 2I).

We were suspicious of the low frequency of hyaline globules and hyaline basement membrane materials in the pulmonary AdCC cases, as we thought they were stereotypical features of the AdCC. We therefore randomly selected non-pulmonary AdCC cases and concomitantly evaluated them according to the 15 cytomorphic features we identified. Interestingly, small cell size was significantly more common in non-pulmonary AdCC. Compared to the non-pulmonary AdCC cases, pulmonary AdCC was less likely to form diffuse sheets or to have hyaline globules. The lack of hyaline globules may make it difficult to diagnose AdCC, especially when the specimen cellularity is low enough so that architectural information specific for AdCC is not available.

A previous study identified a solid variant of pulmonary AdCC that exhibited tumor cell clusters, which neither formed cylinders/spheres nor were sharply demarcated in cytology.⁸ Two out of 11 cases included in this study showed the solid pattern of growth in biopsy or resection specimens (cases 1 and 2 in Table 1). However, even though the proportion of organoid clusters was relatively small, both cases had the features that favored the diagnosis of AdCC; cellular uniformity, distinct nucleolus (in case 2 only), granular cytoplasm and hyaline basement membrane material (in case 1 only). Furthermore, lack of frequent molding, single cell necrosis and necrotic background precluded the diagnosis of small cell carcinoma.

We recommend using the fifteen diagnostic features not only in the diagnosis of pulmonary AdCC, but also in the cytologic diagnosis of the other AdCC cases. The diagnosis of metastatic AdCC in lymph nodes or other distant organs may not be straightforward because typical architectures such as cribriform or tubular pattern may not be identified in metastatic lesions.¹⁸⁻²³ According to the Yu and Caraway²⁰ who reviewed the FNA findings of metastatic AdCC, five cases (62.5%) had a solid arrange-

ment of tumor cells on FNA slides which made it difficult to diagnose.

In summary, we have identified fifteen cytomorphic features that could be used to successfully distinguish pulmonary AdCC from small cell carcinoma. In this study, we noticed that pulmonary AdCC might be misinterpreted as small cell carcinoma when only a single or a few cytologic features were considered. Therefore, a comprehensive analysis of morphologic features is required in the cytologic diagnosis of pulmonary AdCC.

Conflicts of Interest

No potential conflict of interest relevant to this article was reported.

REFERENCES

1. Inoue H, Iwashita A, Kanegae H, Higuchi K, Fujinaga Y, Matsumoto I. Peripheral pulmonary adenoid cystic carcinoma with substantial submucosal extension to the proximal bronchus. *Thorax* 1991; 46: 147-8.
2. Moran CA, Suster S, Koss MN. Primary adenoid cystic carcinoma of the lung: a clinicopathologic and immunohistochemical study of 16 cases. *Cancer* 1994; 73: 1390-7.
3. Maziak DE, Todd TR, Keshavjee SH, Winton TL, Van Nostrand P, Pearson FG. Adenoid cystic carcinoma of the airway: thirty-two-year experience. *J Thorac Cardiovasc Surg* 1996; 112: 1522-31.
4. Cho YM, Park SY, Lee IC. Cytopathologic features of adenoid cystic of trachea carcinoma: report of 2 cases. *Korean J Cytopathol* 1995; 6: 214-8.
5. Lee JS, Kim JS, Yang BS, Lee MC, Park CS, Juhng SW. Cytopathologic features of primary bronchial adenoid cystic carcinoma: a case report. *Korean J Cytopathol* 1995; 6: 67-70.
6. Kim HJ, Choi S, Kwon J, Kim JY, Park K. Bronchial brushing cytologic finding of primary pulmonary adenoid cystic carcinoma misinterpreted as small cell carcinoma: a case report with literature review. *Korean J Pathol* 2011; 45: 441-4.
7. Qiu S, Nampoothiri MM, Zaharopoulos P, Logroño R. Primary pulmonary adenoid cystic carcinoma: report of a case diagnosed by fine-needle aspiration cytology. *Diagn Cytopathol* 2004; 30: 51-6.
8. Ozkara SK, Turan G. Fine needle aspiration cytopathology of primary solid adenoid cystic carcinoma of the lung: a case report. *Acta Cytol* 2009; 53: 707-10.
9. Segletes LA, Steffee CH, Geisinger KR. Cytology of primary pulmonary mucoepidermoid and adenoid cystic carcinoma: a report of four cases. *Acta Cytol* 1999; 43: 1091-7.
10. Chuah KL, Lim KH, Koh MS, Tan HW, Yap WM. Diagnosis of ade-

- noid cystic carcinoma of the lung by bronchial brushing: a case report. *Acta Cytol* 2007; 51: 563-6.
11. Daneshbod Y, Modjtahedi E, Atefi S, Bedayat GR, Daneshbod K. Exfoliative cytologic findings of primary pulmonary adenoid cystic carcinoma: a report of 2 cases with a review of the cytologic features. *Acta Cytol* 2007; 51: 558-62.
 12. Klijanienko J, Vielh P. Fine-needle sampling of salivary gland lesions. III. Cytologic and histologic correlation of 75 cases of adenoid cystic carcinoma: review and experience at the Institut Curie with emphasis on cytologic pitfalls. *Diagn Cytopathol* 1997; 17: 36-41.
 13. Hara H, Oyama T, Suda K. New criteria for cytologic diagnosis of adenoid cystic carcinoma. *Acta Cytol* 2005; 49: 43-50.
 14. Song IH, Song JS, Sung CO, *et al.* Accuracy of core needle biopsy versus fine needle aspiration cytology for diagnosing salivary gland tumors. *J Pathol Transl Med* 2015; 49: 136-43.
 15. Szyfelbein WM, Ross JS. Carcinoids, atypical carcinoids, and small-cell carcinomas of the lung: differential diagnosis of fine-needle aspiration biopsy specimens. *Diagn Cytopathol* 1988; 4: 1-8.
 16. Delgado PI, Jorda M, Ganjei-Azar P. Small cell carcinoma versus other lung malignancies: diagnosis by fine-needle aspiration cytology. *Cancer* 2000; 90: 279-85.
 17. Lee JS, Hirsh V, Park K, *et al.* Vandetanib Versus placebo in patients with advanced non-small-cell lung cancer after prior therapy with an epidermal growth factor receptor tyrosine kinase inhibitor: a randomized, double-blind phase III trial (ZEPHYR). *J Clin Oncol* 2012; 30: 1114-21.
 18. Anderson RJ, Johnston WW, Szpak CA. Fine needle aspiration of adenoid cystic carcinoma metastatic to the lung: cytologic features and differential diagnosis. *Acta Cytol* 1985; 29: 527-32.
 19. David D, Masineni SN, Giorgadze T. Fine-needle aspiration diagnosis of high grade adenoid cystic carcinoma metastatic to the pancreas. *Diagn Cytopathol* 2015; 43: 117-20.
 20. Yu GH, Caraway NP. Poorly-differentiated adenoid cystic carcinoma: cytologic appearance in fine-needle aspirates of distant metastases. *Diagn Cytopathol* 1996; 15: 296-300.
 21. Mardi K, Kaushal V, Uppal H. Cytodiagnosis of intracranial metastatic adenoid cystic carcinoma: spread from a primary tumor in the lacrimal gland. *J Cytol* 2011; 28: 200-2.
 22. Smith RC, Amy RW. Adenoid cystic carcinoma metastatic to the lung: report of a case diagnosed by fine needle aspiration biopsy cytology. *Acta Cytol* 1985; 29: 533-4.
 23. Park SY, Lee KG. Metastatic adenoid cystic carcinoma of the lung diagnosed by fine needle aspiration biopsy. *Korean J Cytopathol* 1990; 1: 175-8.

Mediastinal Glomus Tumor: A Case Report and Literature Review

Si-Hyong Jang · Hyun Deuk Cho
Ji-Hye Lee · Hyun Ju Lee
Hae Yoen Jung · Kyung-Ju Kim
Sung Sik Cho¹ · Mee-Hye Oh

Departments of Pathology and ¹Radiology,
Soonchunhyang University Cheonan Hospital,
Soonchunhyang University College of Medicine,
Cheonan, Korea

Received: May 6, 2015

Revised: June 12, 2015

Accepted: July 1, 2015

Corresponding Author

Mee-Hye Oh, MD, PhD
Department of Pathology,
Soonchunhyang University Cheonan Hospital,
31 Suncheonhyang 6-gil, Dongnam-gu,
Cheonan 31151, Korea
Tel: +82-41-570-3582
Fax: +82-41-570-3580
E-mail: mhoh0212@hanmail.net

A glomus tumor in the mediastinum is very uncommon, and only five cases have been reported in the English literature. We recently encountered a 21-year-old woman with an asymptomatic mediastinal mass that measured 5.3 × 4.0 cm. Surgical excision was performed, and the tumor was finally diagnosed as mediastinal glomus tumor with an uncertain malignant potential. After reviewing this case and previous reports, we analyzed the clinicopathologic features associated with progression of such a tumor.

Key Words: Glomus tumor; Mediastinum; Neoplasms

Glomus tumors are rare mesenchymal neoplasms that originate from modified smooth muscle cells (glomus body), which help regulate body temperature and control blood pressure.^{1,2} Although these tumors typically develop in the dermis or subcutis in the acral area, they can occur in deep soft tissue or visceral organs including the esophagus, stomach, rectum, kidney, lung, mediastinum, and urinary bladder.^{1,3-6}

Most glomus tumors are benign. Occasionally, these tumors exhibit atypical histologic features such as large size, infiltrative growth pattern, high nuclear grade, increased mitotic activity and atypical mitosis. Such atypical tumors have been known to be associated with local recurrence or distant metastasis.^{4,7} Pathologic classification of glomus tumor has recently been suggested based on various clinicopathologic parameters.⁷

Glomus tumors located in the mediastinum are extremely rare, and only five cases have been reported in the English literature.^{1-3,8,9} We encountered a case of mediastinal glomus tumor in a 21-year-old woman, and reviewed the clinicopathologic characteristics of this case and previous mediastinal glomus tumor cases.

CASE REPORT

A 21-year-old woman was referred to our hospital due to a mediastinal mass that was incidentally detected on a chest X-ray performed during health screening. The patient did not complain of any notable symptoms. Chest computed tomography scan revealed a densely-enhanced, round to oval-shaped mass in the right cardiophrenic angle of the anterior inferior mediastinum. Small tortuous vascular structures were noted near the tumor (Fig. 1A). The patient underwent thoroscopic mediastinal mass excision.

On gross examination, the specimen was a relatively well-demarcated solid mass with a rubbery consistency, measuring 5.3 × 4.0 cm. The cut surface of the tumor was tan yellow and had a nodular appearance without a necrotic or hemorrhagic area (Fig. 1B).

Microscopically, the tumor was enveloped by a variable, thickened fibrous capsule with no evidence of infiltration into adjacent tissue. A solid growth pattern was evident, with prominent vascular structures composed of small- to medium-sized blood ves-

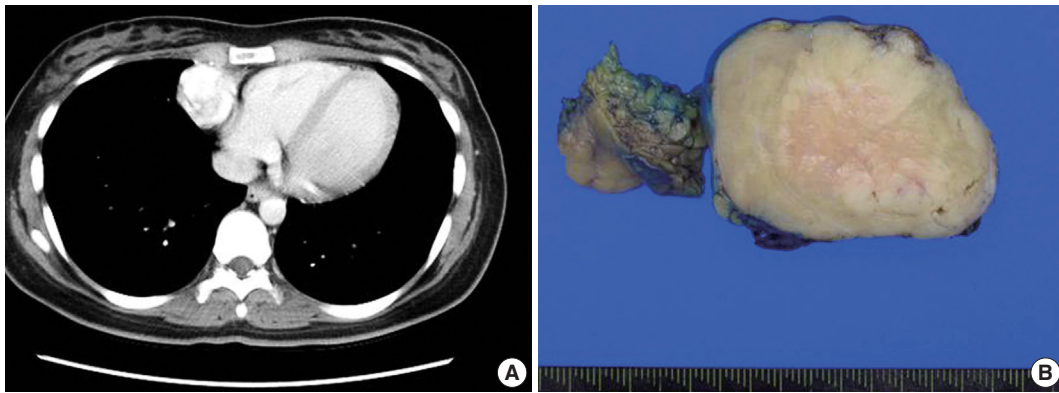


Fig. 1. Radiologic and macroscopic findings. (A) Chest computed tomography reveals a well-demarcated enhanced mass in the anterior inferior mediastinum. (B) Mediastinal mass shows a gray-white homogeneous cut surface with no necrotic or hemorrhagic focus.

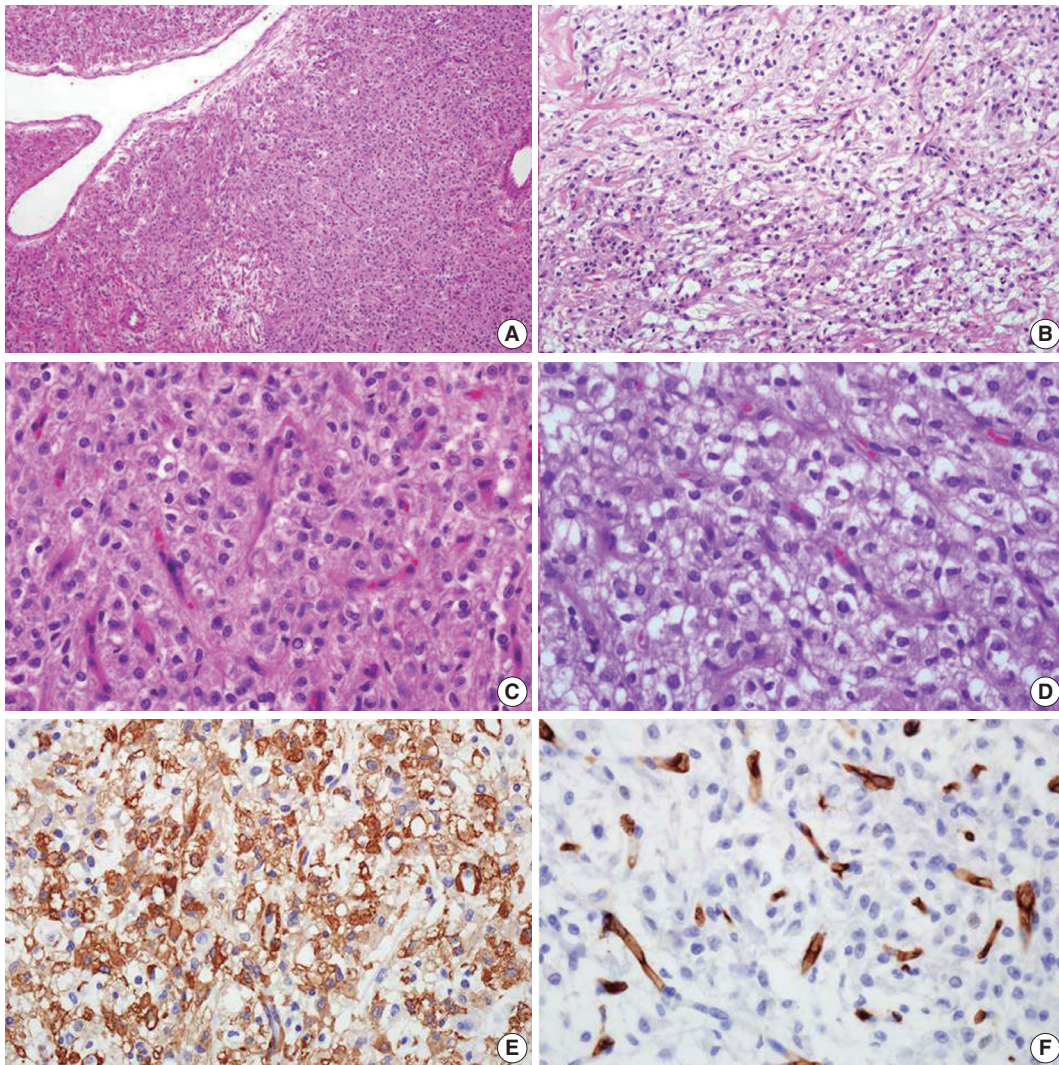


Fig. 2. Macroscopic finding. (A) The tumor displays a sheet-like growth pattern with increased vascularity, and some medium-sized vessels within the tumor has a staghorn appearance. (B) Edematous and myxoid changes are prominent in hypocellular areas. (C, D) Tumor cells have a well-defined cell border and pale to eosinophilic cytoplasm. The nuclei are round and concentrically located with one or two inconspicuous nucleoli. (E) Immunohistochemical staining for smooth muscle actin is positive in tumor cells. (F) CD34 immunohistochemistry is nonreactive in tumor cells.

Table 1. Clinicopathologic data of reported glomus tumor cases of mediastinum

Author	Location	Age (yr)/ Sex	Symptom	Treatment	Clinical result	Follow-up period	Size (cm)	Local invasion	Nuclear grade	Atypical mitosis	Mitotic activity	Diagnosis
Brindley ²	Posterior	29/F	Chest pain	Resection	Free	1 yr	5	No	ND	ND	ND	Glomus tumor
Choi et al. ⁸	Superior	78/F	Dysphagia, dyspnea, hoarseness	Radiation	Died	2 wk	4.5	Extensive	Low	ND	More than 10/10 HPFs	Malignant glomus tumor
Gaertner et al. ¹	Superior	46/F	Pleural effusion, dyspnea	Resection	Free	3 yr	7	Partially	Low	No	Less than 2/10 HPFs	Glomus tumor, locally infiltrative
Bali et al. ³	Posterior inferior	26/F	Lower back pain	Resection	Free	5 yr 4 mo	5	No	High	ND	Scattered	Atypical glomus tumor
Rychlik et al. ⁹	Posterior	59/M	Upper abdominal and chest pain	Resection	Free	1 yr	2	No	Low	ND	ND	Glomus tumor
Present case	Anterior inferior	21/F	No	Resection	Free	7 mo	5.3	No	Low	No	Less than 1/50 HPFs	Glomus tumor of UMP

F, female; ND, not detected; HPF, high power fields; M, male; UMP, uncertain malignant potential.

sels. Medium-sized vessels occasionally appeared with staghorn features and myxoid changes in their walls (Fig. 2A). The tumor displayed both low and high cellular areas. The high cellular areas appeared in vague nodular configuration, and the low cellular area had edematous and myxoid change and was present between high cellular areas (Fig. 2A, B). High-powered examination revealed that the tumor was composed of round epithelioid cells, which had clear to eosinophilic cytoplasm with sharply defined borders. The centrally-located vesicular nuclei were round to polygonal, with a mild convoluted contour of nuclear membranes. One or two small inconspicuous nucleoli were noted. Nuclear pleomorphism was not identified (Fig. 2C, D). Mitotic activity was infrequent, observed in fewer than 1/50 high power fields. Atypical mitosis was not found. Lymphovascular or perineural invasion was not observed. Immunohistochemical staining for smooth muscle actin and vimentin showed diffuse and focal positivity, respectively. Tumor cells were not immunoreactive for CD34, calretinin, cytokeratin, desmin, or neuroendocrine markers, including synaptophysin and chromogranin (Fig. 2E, F). Based on the histology and immunohistochemical results, a pathologic diagnosis of glomus tumor with uncertain malignant potential was made. There was no clinicoradiologic evidence of recurrence or metastasis for seven months after surgery.

DISCUSSION

Glomus tumors are unusual benign smooth muscle neoplasms that comprise fewer than 2% of all soft tissue tumors.^{10,11} These tumors are preferentially located in the subungual area of extremities and have a characteristic clinical triad that includes pain, pinpoint tenderness and hypersensitivity to cold temperatures.¹² Clinically, this type of tumor is usually benign, and malignant cases have rarely been reported.¹³ Additionally, mediastinal glomus tumors, first described in 1949, are extremely rare;² only five cases have been described in the English literature.^{1-3,8,9} This is the sixth case of a glomus tumor in the mediastinum.

The pathologic differential diagnoses of mediastinal glomus tumor include carcinoid tumor, hemangiopericytoma, epithelioid leiomyoma, primitive neuroectodermal tumor, and paraganglioma. Characteristic morphologic features that are helpful for distinguishing these tumors include uniform, round tumor cells with centrally-located nuclei, a well-defined cell membrane and immunohistochemical results that are positive for actin and equivocal or negative for CD34, neuroendocrine markers (chromogranin A, synaptophysin, neuron specific enolase) and CD99.¹

Table 2. Classification of glomus tumor with atypical features⁷

Group	Feature
Malignant glomus tumor	Severe atypia and increased mitotic activity (more than 5/50 HPFs) or presence of atypical mitosis
Glomus tumor of uncertain malignant potential	Superficial location and increased mitotic activity (more than 5/50 HPFs) or large size (more than 2 cm) and/or deep location
Symplastic glomus tumor	Lacks criteria for malignant glomus tumor and severe nuclear atypia
Glomangiomas	Lacks criteria for malignant glomus tumor or glomus tumor of uncertain malignant potential and diffuse growth resembling angiomatosis with prominent glomus component

HPF, high power fields.

A previous article reported that mediastinal glomus tumors tend to have atypical histologic appearance with cytologic pleomorphism and infiltrate into surrounding tissue.¹ However, clinicopathologic features or distinct classification of glomus tumors in the mediastinum or visceral organs have not been established due to their infrequency. We comprehensively reviewed the clinicopathologic data of mediastinal glomus tumors; this data and the current case are presented in Table 1.

Compared with previous cases, our patient was young and did not present with any symptoms. In addition, although previous mediastinal glomus tumors were frequently found in the posterior superior area, this case was noted in an unusual location, the anterior inferior mediastinum. To investigate the clinicopathologic characteristics in malignant mediastinal glomus tumors, we searched for histologic descriptions in former reports. A previous report indicated that, in a fatal mediastinal glomus tumor case,⁸ advanced age, extensive local invasion, and brisk mitotic activity were significant and correlated with poor prognosis in mediastinal glomus tumors.

Glomus tumors with atypical features should be evaluated for variable clinicopathologic features, based on recently-defined classifications. These classifications include tumor location and size, nuclear atypia, and mitosis including atypical ones. The tumors can be categorized into four groups (Table 2).^{4,7} Since glomus tumors that arise in visceral organs, including the mediastinum, can be considered deeply-located tumors, they should be classified as malignant glomus tumor or glomus tumor of uncertain malignant potential. However, only one of six such reported patients died, and the remainder had no evidence of recurrence or metastasis during follow-up. Therefore, we collected and analyzed glomus tumor cases in visceral organs to define and outline characteristics for increased diagnostic accuracy, based on prognosis and adequate treatment.

We described an extremely rare case of mediastinal glomus tumor with no subject symptoms and reviewed the clinicopathologic features of previously reported cases. Considering the unpredictable prognosis of mediastinal glomus tumor, we suggest

the need for histopathologic assessment parameters through collection and observation of glomus tumors that originate in the visceral organs.

Conflicts of Interest

No potential conflict of interest relevant to this article was reported.

Acknowledgments

This work was supported in part by the Soonchunhyang University Research Fund. We appreciate the expert counsel of Jae Ro, MD, PhD, Houston Methodist Hospital.

REFERENCES

- Gaertner EM, Steinberg DM, Huber M, *et al.* Pulmonary and mediastinal glomus tumors: report of five cases including a pulmonary glomangiosarcoma: a clinicopathologic study with literature review. *Am J Surg Pathol* 2000; 24: 1105-14.
- Brindley GV Jr. Glomus tumor of the mediastinum. *J Thorac Surg* 1949; 18: 417-20.
- Bali GS, Hartman DJ, Haight JB, Gibson MK. A rare case of malignant glomus tumor of the esophagus. *Case Rep Oncol Med* 2013; 2013: 287078.
- Folpe AL, Fanburg-Smith JC, Miettinen M, Weiss SW. Atypical and malignant glomus tumors: analysis of 52 cases, with a proposal for the reclassification of glomus tumors. *Am J Surg Pathol* 2001; 25: 1-12.
- Tripodi SA, Rocca BJ, Mourmouras V, Barbanti G, Colecchia M, Ambrosio MR. Benign glomus tumor of the urinary bladder. *Arch Pathol Lab Med* 2013; 137: 1005-8.
- Lamba G, Rafiyath SM, Kaur H, *et al.* Malignant glomus tumor of kidney: the first reported case and review of literature. *Hum Pathol* 2011; 42: 1200-3.
- Goldblum JR, Folpe AL, Weiss SW. *Enzinger and Weiss's soft tissue tumors*. 6th ed. Philadelphia: Saunders/Elsevier, 2014; 749-62.
- Choi YJ, Yang KH, Gang SJ, Kim BK, Kim SM. Malignant glomus tumor originating in the superior mediastinum: an immunohisto-

- chemical and ultrastructural study. *J Korean Med Sci* 1991; 6: 157-63.
9. Rychlik IJ, O'Donnell ME, Davey P, Merard R, McGuigan J. Glomus tumor of the mediastinum. *Asian Cardiovasc Thorac Ann* 2014; 22: 95-7.
 10. Mravic M, LaChaud G, Nguyen A, Scott MA, Dry SM, James AW. Clinical and histopathological diagnosis of glomus tumor: an institutional experience of 138 cases. *Int J Surg Pathol* 2015; 23: 181-8.
 11. Shugart RR, Soule EH, Johnson EW Jr. Glomus tumor. *Surg Gynecol Obstet* 1963; 117: 334-40.
 12. Schiefer TK, Parker WL, Anakwenze OA, Amadio PC, Inwards CY, Spinner RJ. Extradigital glomus tumors: a 20-year experience. *Mayo Clin Proc* 2006; 81: 1337-44.
 13. Hirose T, Hasegawa T, Seki K, *et al.* Atypical glomus tumor in the mediastinum: a case report with immunohistochemical and ultrastructural studies. *Ultrastruct Pathol* 1996; 20: 451-6.

CD30-Positive T-Cell Lymphoproliferative Disease of the Oral Mucosa in Children: A Manifestation of Epstein-Barr Virus-Associated T-Lymphoproliferative Disorder

Mineui Hong · Young Hye Ko¹

Department of Pathology, Hallym University Kangnam Sacred Heart Hospital, Hallym University College of Medicine, Seoul; ¹Department of Pathology, Samsung Medical Center, Sungkyunkwan University School of Medicine, Seoul, Korea

Received: May 14, 2015

Revised: July 10, 2015

Accepted: July 13, 2015

Corresponding Author

Young Hye Ko, MD, PhD
Department of Pathology, Samsung Medical Center, Sungkyunkwan University School of Medicine, 81 Irwon-ro, Gangnam-gu, Seoul 06351, Korea
Tel: +82-2-3410-2762
Fax: +82-2-3410-0025
E-mail: yhko310@skku.edu

Eosinophilic ulcer of the oral mucosa (EUOM) is a very rare, benign, self-limiting ulcerative lesion of the oral cavity of unknown pathogenesis, and belongs to the same spectrum of CD30⁺ T-cell lymphoproliferative disease (LPD) of the oral mucosa. The etiology and pathogenesis of the disease are unknown. We report two cases in children who were initially diagnosed with EUOM and CD30⁺ T-cell LPD, respectively. However, retrospective analysis revealed that a majority of infiltrated atypical T cells were positive for Epstein-Barr virus (EBV). The present cases suggest that the pathogenesis and etiology of EUOM or CD30⁺ T-cell LPD occurring in children are different from those in adults. EUOM or CD30⁺ T-cell LPD in children is a manifestation of EBV-positive T-cell LPD, and should therefore be distinguished from the disease in adults.

Key Words: Eosinophilic ulcer; CD30 positive; Lymphoproliferative disorders; Oral mucosa; Epstein-Barr virus infections; Lymphoreticular

CD30⁺ T-cell lymphoproliferative disease (LPD) of the oral mucosa is uncommon and belongs to the spectrum of mucosal CD30⁺ T-cell LPD, which share pathological and clinical features as follows.¹ CD30⁺ T-cell LPD is an indolent disease and often spontaneously regresses and never appears to progress to systemic disease. The lesion can develop in the gingiva, buccal mucosa, palate, or tongue. It comprises dense infiltrates of CD30⁺ atypical T-cells with polymorphous inflammatory infiltrate in the background, which frequently includes eosinophils. In a number of previous investigations, atypical T-cells were CD3⁺ CD4⁺ CD56⁺ cytotoxic molecules⁺ such as TIA. T-cell receptor (TCR) gene rearrangement is clonal in the majority of cases,² but in some cases it is polyclonal.^{3,4} Eosinophilic ulcer of the oral mucosa (EUOM) which is one of the differential diagnoses of CD30⁺ T-cell LPD is a very rare, benign, self-limited, ulcerative lesion of the oral cavity of unknown pathogenesis. EUOM has been reported under various synonyms, including traumatic ulcerative granuloma with stromal eosinophilia, traumatic granuloma, traumatic eosinophilic granuloma, and eosinophilic gran-

uloma of the tongue.⁵⁻¹⁰ EUOM occurs mainly in adults, but shows two age peaks: during the first two years of life and between the sixth and seventh decades.¹¹ The etiology of EUOM is unknown. Several reports proposed that some viral or toxic agents may play a role in the development of EUOM or that trauma is a contributing factor.⁵ Evidence that has accumulated mostly over the past decade suggests that EUOM and CD30⁺ T-cell LPD are closely related and that EUOM can be included within the spectrum of CD30⁺ T-cell LPD.^{1,2,6-9,11} In addition, the Epstein-Barr virus (EBV) status of these diseases has not been defined yet. Herein, we report two cases of CD30⁺ T-cell LPD or EUOM in children, which revealed clonal proliferation of T-cells harboring EBV.

CASE REPORT

Case 1

A 13-year-old boy was referred to our hospital because of a two-week history of a painful 4 cm ulcer on his left lower gingiva. The

sharply demarcated ulcer developed spontaneously without mechanical irritation. Before admission, he had suffered from recurrent stomatitis and had high fever, night sweats, and diarrhea. He was treated with antibiotics and an antipyretic, but the ill-

ness was persistent. On physical examination, he appeared acutely ill. The ulcer along the buccal gingiva was linear with a sharp erythematous margin, and was covered with a purulent exudate (Fig. 1A). He was diagnosed with EUOM before the referral, and

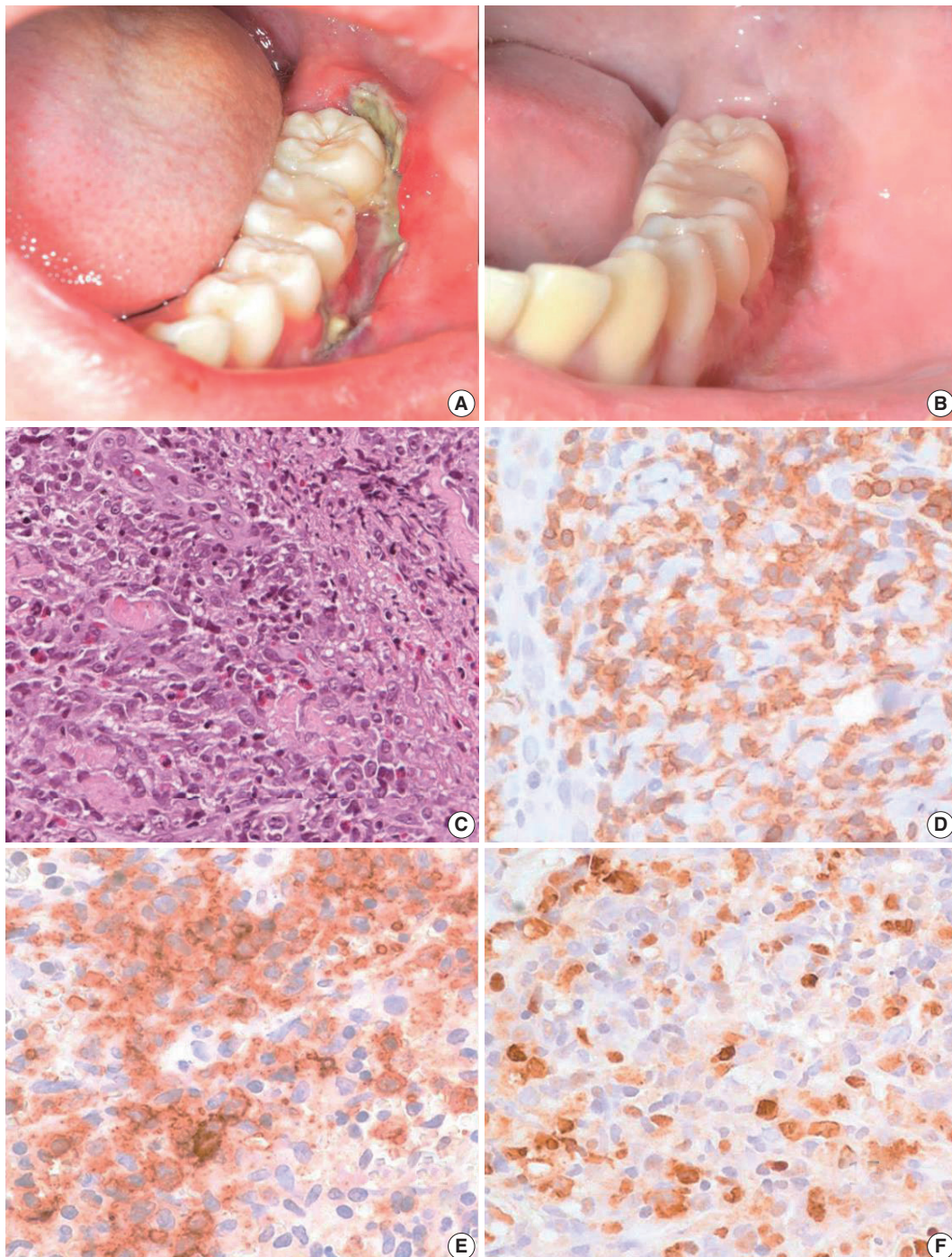


Fig. 1. Clinical finding and histopathologic findings of the oral lesion in case 1. A sharply demarcated linear ulcer was seen at the left lower gingiva (A), which was completely healed 10 days after diagnosis (B). (C) Histologically, infiltration of large atypical cells with many eosinophils was found. (D) CD3 staining highlights large T-blasts. These cells are also stained with CD30 (E) and Epstein-Barr virus (EBV) by EBV-encoded RNA *in situ* hybridization (F).

the pathology slide was reviewed by the authors.

On retrospective review, biopsy revealed diffuse infiltration of large atypical CD3⁺ T-cells intermixed with numerous eosinophils and small lymphocytes in the submucosa and soft tissue with necrosis. These cells were CD3⁺, CD30⁺, and CD56⁺. Some small or large lymphocytes were positive for CD4, TCRβF1, and granzyme B. EBV-encoded RNA (EBER) was detected in many large atypical cells by *in situ* hybridization (Fig. 1C–F). TCRγ gene rearrangement study revealed monoclonality (Fig. 2A). Epstein-Barr (EB) viral load in blood was elevated. The diagnosis was revised to EBV-positive T-cell LPD. He was treated with chemotherapy with 106B induction (prednisolone, cyclophosphamide, daunorubicin, vincristine, and L-asparaginase). After 10 days from the diagnosis, the ulcer was resolved. During the 21 months of follow-up period, the oral ulcer showed a wax and wane pattern without further treatment. The patient was quite well; however, EB viral load was persistently high with 34.5 copies/μL in whole blood (normal range up to 1.02 copies/μL) at the last visit (Fig. 2B).

Case 2

An 11-year-old girl was admitted with a 20-day history of buccal abscess. She had suffered from frequent infections since infancy, such as pneumonia, bronchiolitis, and acute gastroenteritis. She also suffered from a two-year history of recurrent fever and oral ulcer. The oral ulcer would develop every two months and spontaneously regress. Two years earlier, a biopsy of the oral ulcer was conducted at another hospital, and was diagnosed as chronic inflammation. Before admission, she showed a buccal abscess and submandibular lymphadenopathy. At admission, there was a 0.3 cm oral ulcer on her left inferior gingiva and broad ulcerative lesion on her palate. Complete blood count was within normal range with a normal T-cell subset. Blood chemistry was within normal limits except for a slightly increased alkaline phosphatase (125 U/L, normal range 42–98 U/L). T lymphocyte proliferative activity in response to mitogens (phytohemagglutinin and concanavalin A) was preserved. A nitroblue-tetrazolium test to exclude chronic granulomatous disease was negative. A biopsy from the buccal ulcer showed mucosal ulcer-

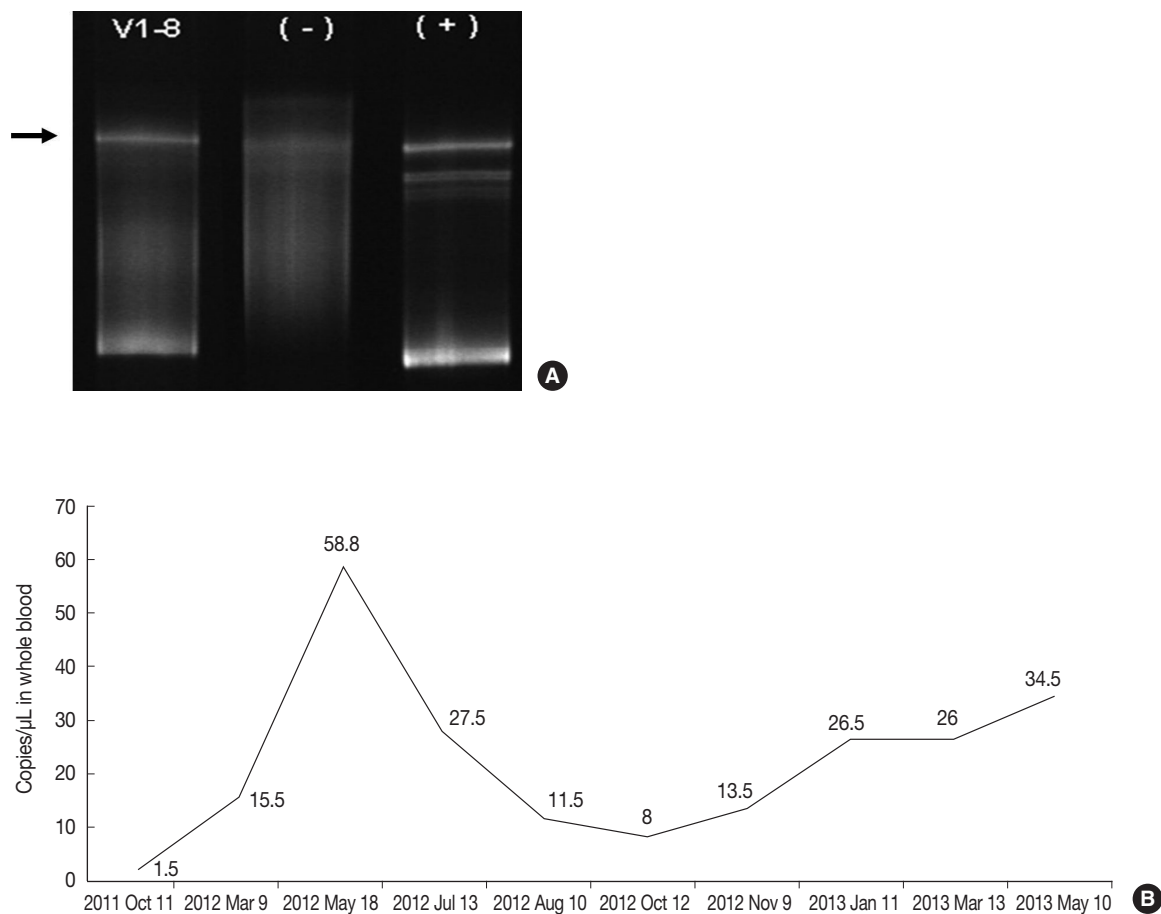


Fig. 2. (A) TCRγ gene rearrangement in case 1 showed a monoclonal band. (B) Epstein-Barr viral load analyzed in blood was persistently elevated in case 1 up to 58.8 copies/μL for two years until last follow up.

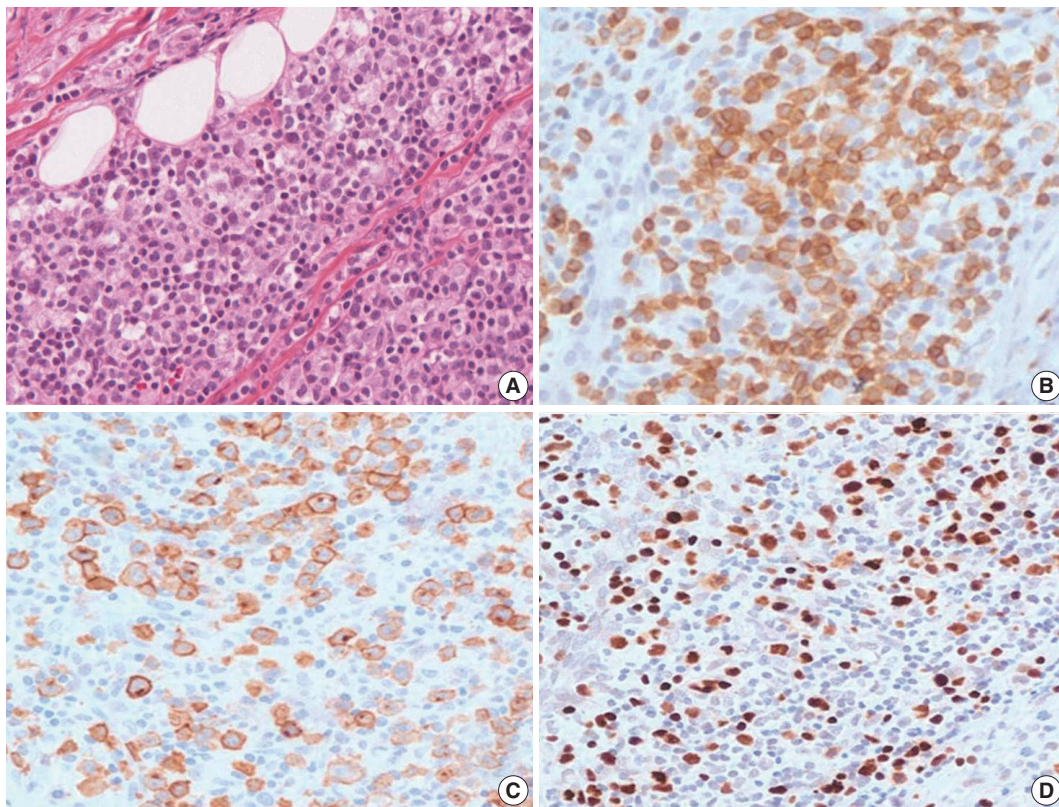


Fig. 3. Histopathologic findings of oral lesion in case 2. (A) Large cells are scattered among small lymphocytes. (B) These cells are positive for CD3. (C) CD30 were positive in the cytoplasmic membrane and perinuclear zone of large atypical lymphocytes. (D) Large cells are also positive for Epstein-Barr virus-encoded RNA *in situ* hybridization.

ation with marked inflammatory cell infiltration including eosinophils. The ulcerated mucosa was covered by fibrinopurulent exudate. The submucosa and adjacent skeletal muscle showed diffuse or patchy infiltration of mixed small, medium, and large lymphocytes (Fig. 3A). These lymphocytes were CD3⁺, which highlighted the irregular nuclear contour of atypical T cells (Fig. 3B). CD30 was positive in the cytoplasmic membrane and perinuclear zone of large atypical lymphocytes (Fig. 3C). Anaplastic lymphoma kinase (ALK) protein was negative. Under the diagnosis of CD30⁺ T-cell LPD, a subset of ALK-negative anaplastic large cell lymphoma, the patient was treated with chemotherapy with methotrexate and cyclophosphamide. After 15 months of chemotherapy, the patient was stable without disease progression. However, on retrospective review of the specimen, the diagnosis was revised as EBV-positive T-cell LPD, most likely chronic active EBV (CAEBV) infection because of EBV positivity in the majority of the small to large atypical cells (Fig. 3D).

DISCUSSION

One of the main differential diagnoses of CD30⁺ T-LPD of

the oral cavity is EUOM. EUOM is characterized by mucosal ulceration with an underlying extensive inflammatory infiltrate consisting of B and T lymphocytes, macrophages, abundant eosinophils, and large atypical mononuclear cells of variable proportion. Atypical lymphoid infiltration and CD30 positivity can be seen to some extent, in 41% to 70% of cases.^{1,6-8,10} Monoclonal T-cell proliferation was reported in 12 of 48 cases analyzed.^{1,7,8,10} However, despite the presence of CD30 expression or T-cell monoclonality, the prognosis of EUOM is known to be excellent. Based on the similarity of clinicopathologic features between EUOM and mucosal CD30⁺ T-cell LPD, at least a subset of EUOM might be CD30⁺ T-cell LPD of the oral mucosa. In EUOM or CD30⁺ T-cell LPD, EBV status was unknown because it is usually not examined in routine diagnosis. So far, there are only two reports of EBV status. Agarwal *et al.*¹ examined three adult patients with oral CD30⁺ T-cell LPD by EBER *in situ* hybridization and reported no association between EBV and CD30⁺ T-cell LPD. Abdel-Naser *et al.*¹¹ first demonstrated the association between EBV and EUOM in a 12-year-old boy with an eosinophilic oral ulcer. EBV latent membrane protein was expressed in coexistence with CD30⁺ T lymphocytes. Epstein-Barr nucle-

ar antigen 2 or Zebra antigen was negative. Gene rearrangement studies revealed polyclonal B cells and oligoclonal T cells.¹¹ Notably, the patient reported by Abdel-Naser *et al.*¹¹ and our two patients were children. After primary infection of EBV, most children will completely recover; however, some children can be rarely complicated by severe or persistent infections such as acute hemophagocytic lymphohistiocytosis, systemic T-cell LPD, or CAEBV infection.¹²⁻¹⁴ CAEBV infection mainly involves T or natural killer (NK) cells and is accompanied by varying degrees of lymphoproliferation, which may progress from polyclonal lymphoproliferation to monoclonal disease.¹⁵ Usually, systemic symptoms such as fever persist for more than six months with increased EB viral load in blood or tissues. Although the most frequent symptoms include organomegaly, anemia, and thrombocytopenia, patients often present with uncommon clinical findings such as coronary aneurysms, central nervous system involvement, bowel perforation, or Behçet-like orogenital ulcer.¹⁶ The clinical course is variable and depends on the immune response of the individuals. Some patients have a prolonged and indolent disease course, whereas half the patients die of hemophagocytic syndrome or aggressive NK cell leukemia/lymphoma.¹⁵ One of our patients showed persistently elevated EB viral load in the blood and infiltration of clonal EBV-positive T-cells in an oral ulcerative lesion. We did not examine EB viral load in the blood of the case 2 because this was a retrospective study. Persistent elevation of EB viral load in the blood of the case 1 with monoclonality of infiltrated CD30⁺ cells suggest that the oral ulcer of these two patients is a manifestation of EBV-associated T-cell LPD, which is clinically consistent with an indolent form of CAEBV infection.

An important differential diagnosis is EBV-positive mucocutaneous ulcer, which is part of the spectrum of age-related EBV-positive LPD. According to Dojcinov *et al.*,¹⁷ the median age of patients was 77 years. In addition, EBV-infected large blasts were mainly B-cells with CD20 expression. The present cases are distinct from EBV-positive mucocutaneous ulcer in their EBV positivity in T-cells and the young age of the patients.

In conclusion, our cases suggest that the pathogenesis and etiology of so-called "oral eosinophilic ulcer" or CD30⁺ T-cell LPD occurring in children are different from the disease in adults. EUOM and CD30⁺ T-cell LPD in children is a manifestation of EBV-positive T-cell LPD, and therefore should be distinguished from those of adults. Examination of EBV status in more cases of children and adult patients would provide more convincing data to support our observations.

Conflicts of Interest

No potential conflict of interest relevant to this article was reported.

REFERENCES

1. Agarwal M, Shenjere P, Blewitt RW, *et al.* CD30-positive T-cell lymphoproliferative disorder of the oral mucosa: an indolent lesion: report of 4 cases. *Int J Surg Pathol* 2008; 16: 286-90.
2. Sciallis AP, Law ME, Inwards DJ, *et al.* Mucosal CD30-positive T-cell lymphoproliferations of the head and neck show a clinicopathologic spectrum similar to cutaneous CD30-positive T-cell lymphoproliferative disorders. *Mod Pathol* 2012; 25: 983-92.
3. Wang W, Cai Y, Sheng W, Lu H, Li X. The spectrum of primary mucosal CD30-positive T-cell lymphoproliferative disorders of the head and neck. *Oral Surg Oral Med Oral Pathol Oral Radiol* 2014; 117: 96-104.
4. Erős N, Marschalkó M, Lőrincz A, *et al.* CD30-positive anaplastic large T-cell lymphoma of the tongue. *J Eur Acad Dermatol Venereol* 2009; 23: 231-2.
5. Tang TT, Glicklich M, Hodach AE, Oechler HW, McCreddie SR. Ulcerative eosinophilic granuloma of the tongue: a light- and electron-microscopic study. *Am J Clin Pathol* 1981; 75: 420-5.
6. Ficarra G, Prignano F, Romagnoli P. Traumatic eosinophilic granuloma of the oral mucosa: a CD30+(Ki-1) lymphoproliferative disorder? *Oral Oncol* 1997; 33: 375-9.
7. Alobeid B, Pan LX, Milligan L, Budel L, Frizzera G. Eosinophil-rich CD30+ lymphoproliferative disorder of the oral mucosa: a form of "traumatic eosinophilic granuloma". *Am J Clin Pathol* 2004; 121: 43-50.
8. Salisbury CL, Budnick SD, Li S. T-cell receptor gene rearrangement and CD30 immunoreactivity in traumatic ulcerative granuloma with stromal eosinophilia of the oral cavity. *Am J Clin Pathol* 2009; 132: 722-7.
9. Segura S, Romero D, Mascaró JM Jr, Colomo L, Ferrando J, Estrach T. Eosinophilic ulcer of the oral mucosa: another histological simulator of CD30+ lymphoproliferative disorders. *Br J Dermatol* 2006; 155: 460-3.
10. Hirshberg A, Amariglio N, Akrisch S, *et al.* Traumatic ulcerative granuloma with stromal eosinophilia: a reactive lesion of the oral mucosa. *Am J Clin Pathol* 2006; 126: 522-9.
11. Abdel-Naser MB, Tsatsou F, Hippe S, *et al.* Oral eosinophilic ulcer, an Epstein-Barr virus-associated CD30+ lymphoproliferation? *Dermatology* 2011; 222: 113-8.
12. Cho EY, Kim KH, Kim WS, Yoo KH, Koo HH, Ko YH. The spec-

- trum of Epstein-Barr virus-associated lymphoproliferative disease in Korea: incidence of disease entities by age groups. *J Korean Med Sci* 2008; 23: 185-92.
13. Wang RC, Chang ST, Hsieh YC, *et al.* Spectrum of Epstein-Barr virus-associated T-cell lymphoproliferative disorder in adolescents and young adults in Taiwan. *Int J Clin Exp Pathol* 2014; 7: 2430-7.
 14. Park S, Ko YH. Epstein-Barr virus-associated T/natural killer-cell lymphoproliferative disorders. *J Dermatol* 2014; 41: 29-39.
 15. Ohshima K, Kimura H, Yoshino T, *et al.* Proposed categorization of pathological states of EBV-associated T/natural killer-cell lymphoproliferative disorder (LPD) in children and young adults: overlap with chronic active EBV infection and infantile fulminant EBV T-LPD. *Pathol Int* 2008; 58: 209-17.
 16. Park BM, Ahn JS, Lee JB, Won YH, Yun SJ. Chronic active Epstein-Barr virus infection-associated hydroa vacciniforme-like eruption and Behcet's-like orogenital ulcers. *Dermatology* 2013; 226: 212-6.
 17. Dojcinov SD, Venkataraman G, Raffeld M, Pittaluga S, Jaffe ES. EBV positive mucocutaneous ulcer: a study of 26 cases associated with various sources of immunosuppression. *Am J Surg Pathol* 2010; 34: 405-17.

Intrahepatic Cholangiocarcinoma with Ductal Plate Malformation-like Feature Associated with Bile Duct Adenoma

Ah-Young Kwon · Hye Jin Lee · Hee Jung An · Haeyoun Kang · Jin-Hyung Heo · Gwangil Kim

Department of Pathology, CHA Bundang Medical Center, CHA University, Seongnam, Korea

Intrahepatic cholangiocarcinoma (ICC) is a malignant tumor with biliary epithelial differentiation. Malignant transformation of von Meyenburg complex (VMC) to ICC has been reported,^{1,2} and a new subtype of ICC with ductal plate malformation (DPM) pattern has been suggested.³ However, bile duct adenoma (BDA) is a rare entity and is not as well known as DPM. Moreover, it has not been determined whether BDA is a risk factor of ICC. We present a rare case of ICC with DPM-like features associated with BDA.

CASE REPORT

The publication of the case information and materials was approved by the Institutional Review Board of CHA Bundang Medical Center, CHA University.

A 34-year-old female patient was referred for further evaluation of a small hepatic nodule found on a regular health check-up. She did not have any remarkable medical history associated with liver disease. On magnetic resonance imaging, a 2-cm-sized mass was present in liver segment 4, showing high signal on T1- and low signal on T2-weighted images (Fig. 1A).

The patient underwent hepatic segmentectomy. The liver showed a relatively well-demarcated, subcapsular (5 mm from the capsule), nonencapsulated, solid, rubbery, and pale brown mass. It was multilobulated with a central fibrous scar (Fig. 1B).

Histologically, the nodule was composed of three distinct ar-

eas. First, many compact, small, tubular structures lined by single cuboidal to low columnar epithelial cells were present without bile or dilated ducts. Nuclei were small and uniform without any mitotic activity, which was compatible with BDA containing portal tracts (Fig. 2A). Second, the central area showed DPM-like features, having irregularly dilated ductal structures lined by low columnar neoplastic epithelial cells with mild pleomorphism within fibrous stroma (Fig. 2B). Third, the opposite side of the BDA showed ICC. Columnar to cuboidal epithelial cells forming fused glandular structures with nuclear anaplasia and frequent mitoses were present (Fig. 2C). There were transitional areas from BDA to ICC (Fig. 2D).

On immunohistochemistry, cytokeratin (CK) 7, CK19, and epithelial cellular adhesion molecule (EpCAM) were positive, and monoclonal carcinoembryonic antigen (CEA), CD117, p53, and hepatocyte antigen were negative in all three areas. The ICC area showed diffuse positivity for polyclonal CEA; in contrast, the BDA and DPM-like areas showed apical reactivity only. Epithelial membrane antigen was negative in the BDA area, apically reactive in the DPM-like area, and strongly reactive in the ICC area. NCAM was positive in the ICC area, focally positive in the DPM area, but negative in the BDA area. The Ki-67 labeling index was variable, with values of 1%–2% in the BDA area, 10%–20% in the DPM-like area, and 40%–50% in the ICC area (Table 1, Fig. 3).

The remaining parenchyme did not show VMC or DPM features. No recurrence or metastasis was observed at a 28-month follow-up.

DISCUSSION

Some benign hepatic biliary lesions, such as VMC or bile duct

Corresponding Author

Gwangil Kim, MD

Department of Pathology, CHA Bundang Medical Center, CHA University, 59 Yatap-ro, Bundang-gu, Seongnam 13496, Korea

Tel: +82-31-780-5452, Fax: +82-31-780-5476, E-mail: blacknw@cha.ac.kr

Received: March 24, 2014 Revised: May 10, 2015

Accepted: June 19, 2015

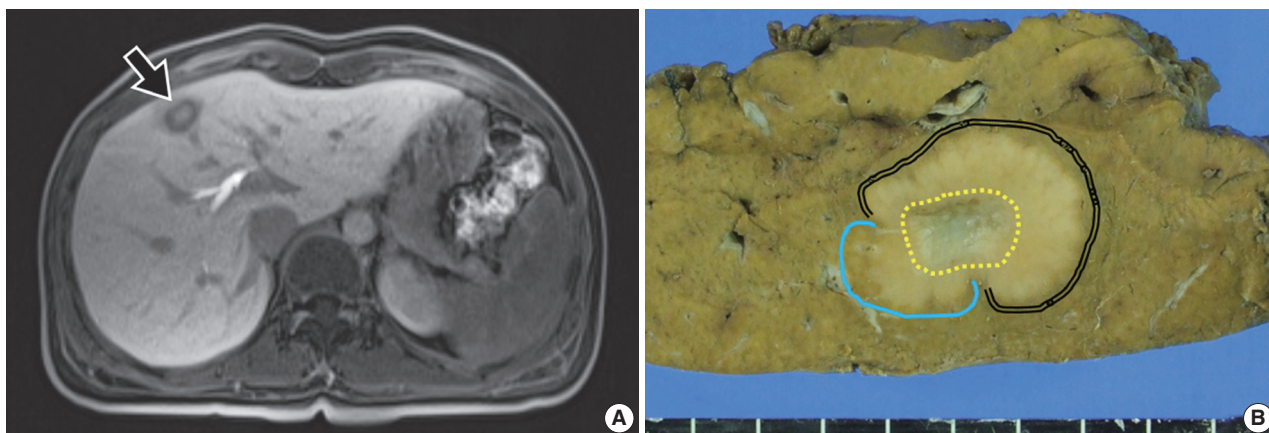


Fig. 1. Radiologic and gross findings. (A) Magnetic resonance imaging of the liver reveals a 2-cm target appearance lesion (arrow) in segment 4. On a T1-weighted image, the central portion shows low signal intensity (SI), and the peripheral zone shows intermediate to slightly high SI. (B) Grossly, the tumor is a relatively well-defined, solid, pale brown mass with a multinodular margin and central fibrous scar. The tumor has three areas: double line of right upper area, cholangiocarcinoma; dotted central circle, dilated ducts with fibrous stroma; and line of left lower area, bile duct adenoma.

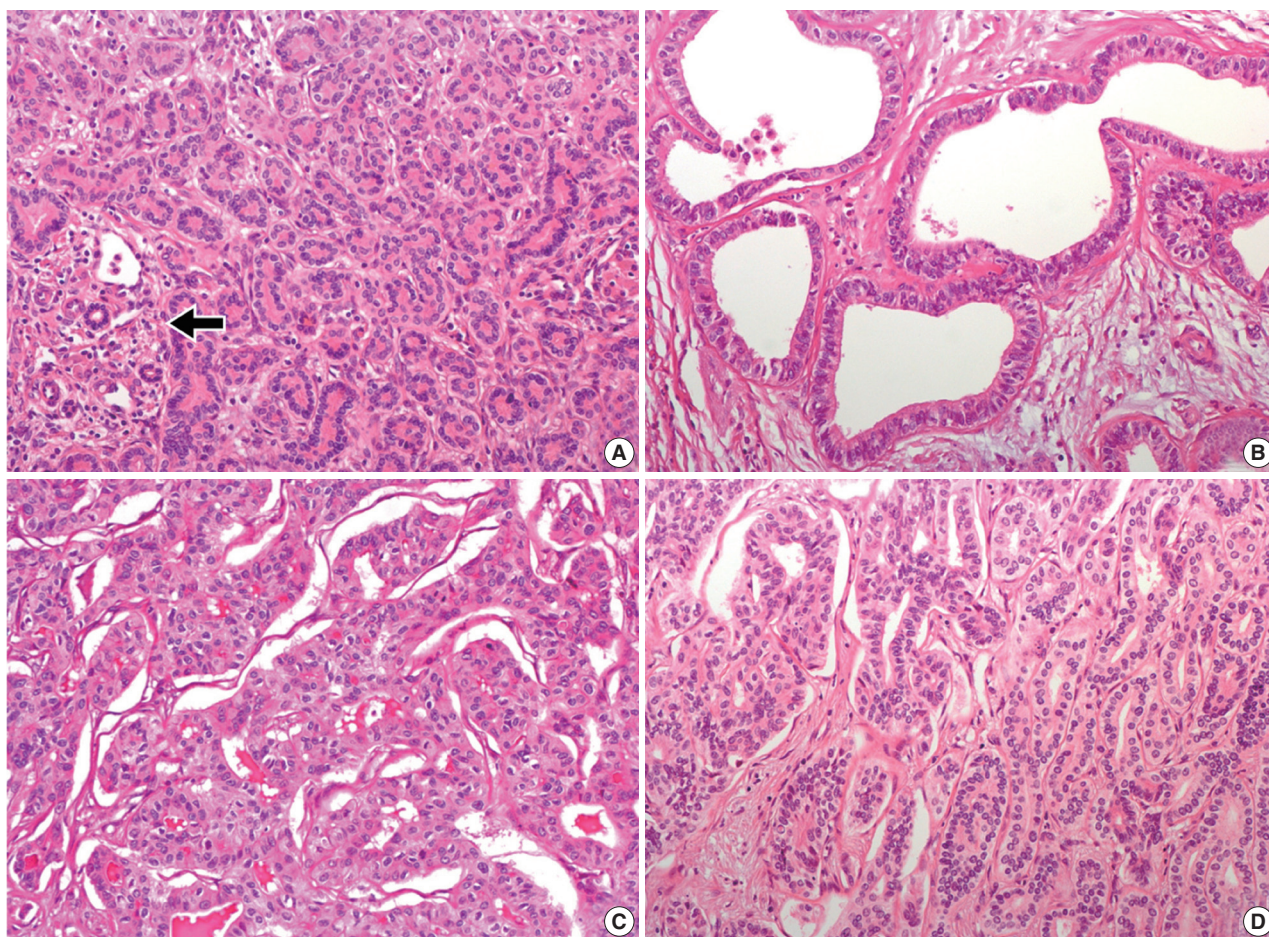


Fig. 2. Microscopic findings of the tumor. (A) One peripheral portion shows highly packed ducts with bland looking nuclei; bile duct adenoma containing portal tracts (arrow). (B) Central area reveals irregularly dilated glandular structures within fibrous stroma, resembling features of ductal plate malformation. (C) In the other peripheral lesion, fused and cribriform glands infiltrate into the stroma. The nuclei are atypical and show brisk mitotic activity; cholangiocarcinoma. (D) The tumor shows a transitional area between bile duct adenoma (right) and cholangiocarcinoma (left). Bland uniform ductal structures become irregular and anastomosing.

adenofibroma, are known candidate precursors of ICC.⁴ VMC is a congenital anomaly of biliary cells forming a hepatic tumor-like lesion.⁵ Intrahepatic cholangiocarcinoma arising in VMC

has been observed since 1961.^{2,6} According to the ductal plate hypothesis proposed in 2011,⁷ VMC is implicated in DPM as a developmental anomaly of fetal biliary cells (ductal plate). Re-

Table 1. Immunohistochemical stain of tumor

Antigen	Source, clone	BDA area	DPM area	ICC area
CK7	Neomarker, OV-TL 12/30	P	P	P
CK19	Neomarker, A53-B/A2.26	P	P	P
Polyclonal CEA	Neomarker, CEA Ab-2	P (apical)	P (apical)	P (membranous)
Monoclonal CEA	Neomarker, COL1	N	N	N
EpCAM	Novocastra, VU-1D9	P	P	P
EMA	Cell MARQUE, E29	N	P (apical)	P (membranous)
NCAM (CD56)	Roche, 123C3	N	P (focal)	P
CD117 (c-Kit)	DAKO, rabbit polyclonal	N	N	N
p53	DAKO, DO-7	N	N	N
Hepatocyte	DAKO, OCH1E5	N	N	N
Ki-67 (%)	Neomarker, SP6	1–2	10–20	40–50

BDA, bile duct adenoma; DPM, ductal plate malformation; ICC, intrahepatic cholangiocarcinoma; CK, cytokeratin; P, positive; CEA, carcinoembryonic antigen; N, negative; EMA, epithelial membrane antigen.

Table 2. Cases of cholangiocarcinoma associated with bile duct adenoma

Reference	Year	Sex/Age (yr)	Location	Size (cm)	Operation	Histology	Associated liver disease
Hasebe <i>et al.</i> ⁸	1995	M/59	S4	2.2	Partial resection	ICC with BDA and VMC	No
Takahashi <i>et al.</i> ¹⁰	2010	M/76	S6	3	Resection	ICC with BDA and VMC	No
Pinho <i>et al.</i> ⁹	2012	F/60	S5	3.83	Liver biopsy (at the age of 58) Right hepatectomy	BDA ICC	No
Present case	2015	F/36	S4	2	Segmentectomy	ICC with DPM pattern associated with BDA	No

ICC, intrahepatic cholangiocarcinoma; BDA, bile duct adenoma; VMC, von Meyenburg complex; DPM, ductal plate malformation.

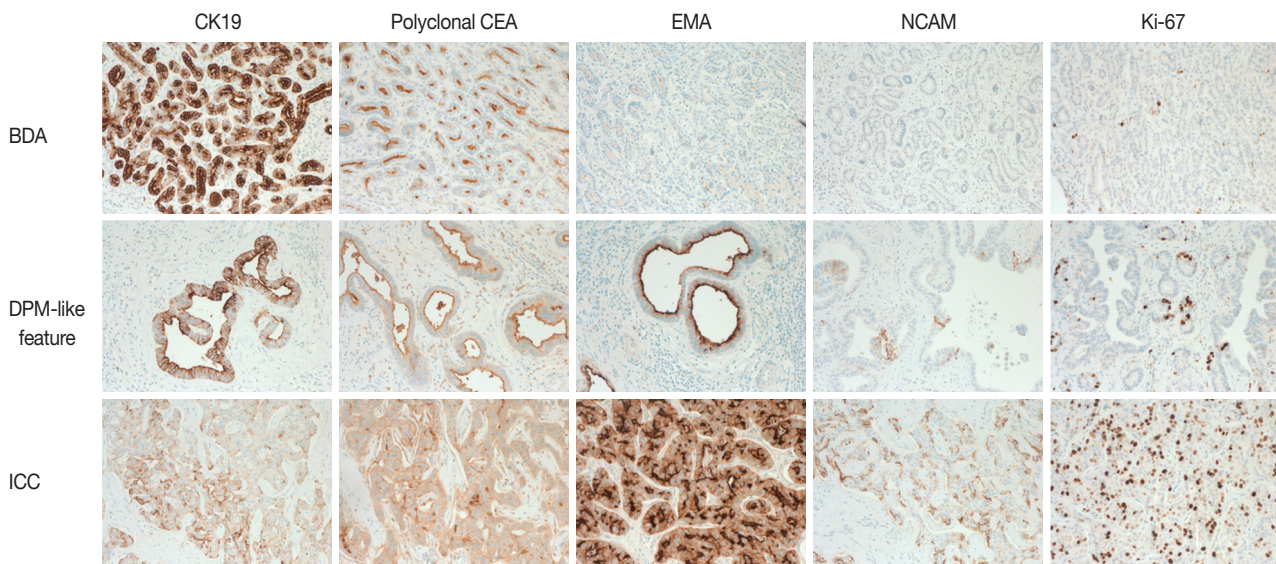


Fig. 3. Immunohistochemical staining patterns in three areas. Cytokeratin 19 (CK19) and polyclonal carcinoembryonic antigen (CEA) are positive in all areas, but intensity and location are different. Epithelial membrane antigen (EMA) and NCAM are negative in the bile duct adenoma (BDA) area, weakly positive in the ductal plate malformation (DPM) area, and positive in the cholangiocarcinoma (ICC) area. The Ki-67 labeling index differs in the different areas, from 1%–2% in BDA to 40%–50% in the cholangiocarcinoma area.

cently, cases of ICC with VMC features in a large proportion of the tumor are reported as ICC with predominant DPM pattern (ICC-DPM), a new subtype of ICC.³

In the present case, the tumor showed three histologically distinct areas of BDA, DPM, and ICC, and their proportions were 30%, 20%, and 50%, respectively.

BDA is a rare solitary intrahepatic lesion that consists of many small, uniform ducts with benign cuboidal cells and a narrow lumen. The BDA area in the present case was typical and localized to one side. Although BDA can be confused with bile ductular carcinoma foci of ICC-DPM, the latter show malignant epithelium and similar immunoreactivity to ICC-DPM. In contrast to VMC, BDA is not regarded as a precursor of ICC because ICC with BDA has been reported in only three cases (Table 2).⁸⁻¹⁰

DPM-like areas in our case revealed irregularly dilated glands within fibrous stroma, resembling VMC. The neoplastic columnar cells were different from typical VMC. This DPM-like feature might be a part of ICC-DPM or represent a transitional area between BDA and ICC. There were several unique points in the present DPM-like features that differ from the previously reported ICC-DPM. First, the typical irregular protrusions and bridging structures were not prominent in the DPM-like area in the present case. Second, there was no obvious stromal invasion in this area. Third, ICC and BDA in this case were distinguishable from the DPM-like area grossly, histologically, and immunohistochemically (especially with respect to CEA, EpCAM, NCAM, and Ki-67).³

The results of immunohistochemical staining of each area corresponded to the histological diagnosis. Intriguingly, NCAM was expressed in ICC and focally in the DPM-like area. This result supports the previous suggestion that ICC with DPM features is a subtype of hepatocellular-cholangiocarcinoma with stem cell features.⁵

In summary, we present a case of ICC with DPM-like features associated with BDA. Although the etiologic relationship between ICC and BDA or DPM needs further study, the possibility of BDA as a precursor of ICC is presented. Such a situation should be considered when BDA is found on a needle biopsy.

Conflicts of Interest

No potential conflict of interest relevant to this article was reported.

REFERENCES

- Jain D, Nayak NC, Saigal S. Hepatocellular carcinoma arising in association with von-Meyenburg's complexes: an incidental finding or precursor lesions? A clinicopathologic study of 4 cases. *Ann Diagn Pathol* 2010; 14: 317-20.
- Xu AM, Xian ZH, Zhang SH, Chen XF. Intrahepatic cholangiocarcinoma arising in multiple bile duct hamartomas: report of two cases and review of the literature. *Eur J Gastroenterol Hepatol* 2009; 21: 580-4.
- Nakanuma Y, Sato Y, Ikeda H, et al. Intrahepatic cholangiocarcinoma with predominant "ductal plate malformation" pattern: a new subtype. *Am J Surg Pathol* 2012; 36: 1629-35.
- Nakanuma Y, Tsutsui A, Ren XS, Harada K, Sato Y, Sasaki M. What are the precursor and early lesions of peripheral intrahepatic cholangiocarcinoma? *Int J Hepatol* 2014; 2014: 805973.
- Terada T. Combined hepatocellular-cholangiocarcinoma with stem cell features, ductal plate malformation subtype: a case report and proposal of a new subtype. *Int J Clin Exp Pathol* 2013; 6: 737-48.
- Lindgren AG, Hansson G, Nilsson LA. Primary carcinoma arising in congenital liver in conjunction with miliary cholangiomatosis: report of case. *Acta Pathol Microbiol Scand* 1961; 52: 343-8.
- Desmet VJ. Ductal plates in hepatic ductular reactions. Hypothesis and implications. III. Implications for liver pathology. *Virchows Arch* 2011; 458: 271-9.
- Hasebe T, Sakamoto M, Mukai K, et al. Cholangiocarcinoma arising in bile duct adenoma with focal area of bile duct hamartoma. *Virchows Arch* 1995; 426: 209-13.
- Pinho AC, Melo RB, Oliveira M, et al. Adenoma-carcinoma sequence in intrahepatic cholangiocarcinoma. *Int J Surg Case Rep* 2012; 3: 131-3.
- Takahashi S, Takada K, Kawano Y, et al. Cholangiocarcinoma with bile duct adenoma and hamartoma-like lesion in the bile duct. *Nihon Shokakibyo Gakkai Zasshi* 2010; 107: 461-9.

Apocrine Carcinoma of the Axilla Associated with Extramammary Paget's Disease: A Case Report and Review of the Literature

Hye Ra Jung · Sun Young Kwon · Daegu Son¹

Departments of Pathology and ¹Plastic Surgery, Keimyung University School of Medicine, Daegu, Korea

Paget's disease has traditionally been divided into mammary and extramammary. Extramammary Paget's disease (EMPD) most commonly affects the anogenital area, though it can rarely affect the axillae, in which apocrine glands are normally encountered.¹ Herein, we report a rare case of apocrine carcinoma associated with EMPD of the axilla with review of the relevant literature.

CASE REPORT

The publication of the case information and materials was approved by the Institutional Review Board of Keimyung University Dongsan Medical Center.

A 77-year-old man was referred with a 3-month history of an erythematous, hyperkeratotic, and inflamed eczematous patch with focal desquamation and itching sensation in the left axilla. Examination of the left axilla showed a discrete red patch with irregular margins and exudative surface, measuring 5×3 cm. No fungal hyphae were noted on the KOH test. Histological examination of a punch biopsy showed round, pale malignant cells scattered individually and in groups throughout the epidermis, particularly in the basal layer. Also, a focal intradermal invasive lesion was noted. The patient was treated with wide excision with margins up to 2 cm. The cut surface of the resected specimen showed a round, pale, tan to white and solid subcutaneous mass, measuring 0.8 cm in diameter. The mass was

attached to the overlying skin. Histologically, the subcutaneous mass consisted of large, round to polygonal cells with abundant eosinophilic cytoplasm, indicative of apocrine carcinoma. Some sweat glands in the dermis were filled with malignant cells, similar to those in the subcutaneous mass. These cells also involved the epidermis and showed a typical pagetoid spread. The infiltrative and intraepithelial tumor cells stained positive with periodic acid Schiff and showed strong positive immunohistochemical staining for cytokeratin 7 (CK7) and HER2, confirming the diagnosis of invasive apocrine carcinoma with EMPD (Fig. 1). The tumor cells showed focal and weak positivity for anti-gross cystic disease fluid protein-15 (GCDFP-15) and were negative for GATA-3, estrogen receptor, and progesterone receptor.

Based on these results, the patient was evaluated for evidence of breast cancer to rule out metastatic apocrine carcinoma from the breast. Chest radiograph and breast ultrasonogram showed no definite lesion. After 6 months of follow-up, the patient is healthy and free of symptoms.

DISCUSSION

Paget's disease is an intraepithelial neoplastic lesion involving Paget cells, which are regarded as apocrine origin because of their immunohistochemical characteristics; positive staining for carcinoembryonic antigen, GCDFP-15, and CK7.²

In rare cases, Paget's disease co-exists with underlying invasive apocrine carcinoma. EMPD with underlying invasive apocrine carcinoma in the axilla is rarer. Morgan *et al.*³ reported a case of axillary EMPD with underlying apocrine carcinoma. They reported that 45.5% (5/11) of previously reported axillary EMPDs were associated with an underlying carcinoma.³ Chiu *et*

Corresponding Author

Hye Ra Jung, MD
Department of Pathology, Keimyung University School of Medicine, 56 Dalseong-ro, Jung-gu, Daegu 41931, Korea
Tel: +82-53-580-3826, Fax: +82-53-250-7211, E-mail: junghr0519@dsmc.or.kr

Received: May 7, 2015 Revised: June 18, 2015

Accepted: June 22, 2015

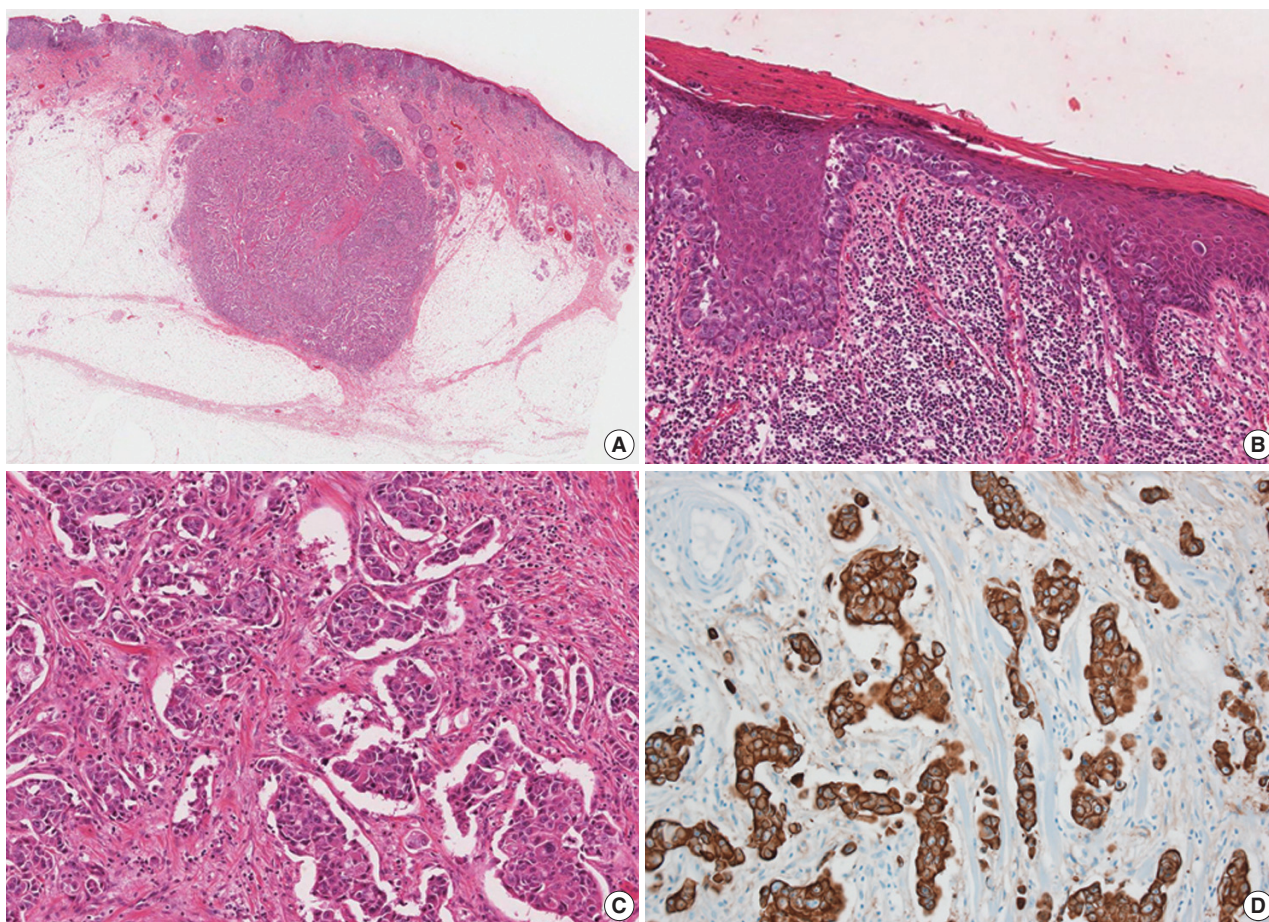


Fig. 1. (A) Slide scan of the left axillary lesion shows a round mass in the subcutaneous tissue. (B) Large tumor cells with abundant cytoplasm show a pagetoid spread pattern in the epidermis. (C) Tumor cells with abundant eosinophilic cytoplasm infiltrating the dermis. (D) Tumor cells showing diffuse strong positive staining for cytokeratin 7.

*al.*⁴ reported seven cases of EMPD in the unilateral axilla, with only one patient having underlying axillary carcinoma (14.3%).

Wilkinson and Brown⁵ classified vulvar EMPD into intraepithelial Paget's disease, intraepithelial Paget's disease with invasion (IP), and intraepithelial Paget's disease with underlying adenocarcinoma (IEPUA). Based on Wilkinson and Brown's classification, the present case was thought to be IEPUA. In other studies of EMPD in the vulvar region, IEPUA represents between 2% and 37% of all cases.⁶⁻⁹ Kodama *et al.*⁸ reported a recurrence rate of 79.8% and a survival rate of 27.7% for patients with IEPUA. Parker *et al.*⁹ have similarly reported poor prognosis for patients with IP and IEPUA.⁷ However, in the report of Chiu *et al.*,⁴ no patient experienced recurrence after surgery (mean time of follow-up, 65.7 months) even in the cases of underlying malignancy (i.e., at least IP or IEPUA). All patients in their study underwent local wide excision with margins up to 2–3 cm. The authors offer that the low recurrence rate of patients in their study might be a result of the clear anatomy of

the axillary region compared with that of the anogenital area, the early stages of their cases, and the limited follow-up.

When apocrine carcinoma is present in the axilla, metastasis from breast apocrine carcinoma or primary breast cancer in ectopic mammary tissue must be ruled out. Immunohistochemistry is not helpful in differentiating these options.¹⁰ In apocrine carcinoma of ectopic mammary tissue, remaining ectopic mammary tissue is present in the sample. To exclude the possibility of metastatic mammary apocrine carcinoma, additional breast examination and radiologic work-up are needed. In the present case, there was no evidence of apocrine carcinoma arising in ectopic mammary tissue or of metastatic mammary apocrine carcinoma.

We report a rare case of EMPD with underlying invasive apocrine carcinoma in the axilla in order to increase awareness of EMPD in the axilla and to highlight its association at this site with adjacent underlying apocrine carcinoma.

Conflicts of Interest

No potential conflict of interest relevant to this article was reported.

REFERENCES

1. Elder DE, Elenitsas R, Johnson BL Jr, Murphy GF, Xu G. *Lever's histopathology of the skin*. Philadelphia: Lippincott Williams & Wilkins, 2009.
2. Merot Y, Mazoujian G, Pinkus G, Momtaz TK, Murphy GF. Extramammary Paget's disease of the perianal and perineal regions: evidence of apocrine derivation. *Arch Dermatol* 1985; 121: 750-2.
3. Morgan JM, Carmichael AJ, Ritchie C. Extramammary Paget's disease of the axilla with an underlying apocrine carcinoma. *Acta Derm Venereol* 1996; 76: 173-4.
4. Chiu CS, Yang CH, Chen CH. Extramammary Paget's disease of the unilateral axilla: a review of seven cases in a 20-year experience. *Int J Dermatol* 2011; 50: 157-60.
5. Wilkinson EJ, Brown HM. Vulvar Paget disease of urothelial origin: a report of three cases and a proposed classification of vulvar Paget disease. *Hum Pathol* 2002; 33: 549-54.
6. Shaco-Levy R, Bean SM, Vollmer RT, *et al*. Paget disease of the vulva: a histologic study of 56 cases correlating pathologic features and disease course. *Int J Gynecol Pathol* 2010; 29: 69-78.
7. Jones IS, Crandon A, Sanday K. Paget's disease of the vulva: diagnosis and follow-up key to management; a retrospective study of 50 cases from Queensland. *Gynecol Oncol* 2011; 122: 42-4.
8. Kodama S, Kaneko T, Saito M, Yoshiya N, Honma S, Tanaka K. A clinicopathologic study of 30 patients with Paget's disease of the vulva. *Gynecol Oncol* 1995; 56: 63-70.
9. Parker LP, Parker JR, Bodurka-Bervers D, *et al*. Paget's disease of the vulva: pathology, pattern of involvement, and prognosis. *Gynecol Oncol* 2000; 77: 183-9.
10. Toledo-Pastrana T, Llombart-Cussac B, Traves-Zapata V, *et al*. Case report: differential diagnosis between primary cutaneous apocrine adenocarcinoma versus extramammary or metastatic breast adenocarcinoma. *Am J Dermatopathol* 2014; 36: e175-8.

Erratum: WHO Grade IV Gliofibroma: A Grading Label Denoting Malignancy for an Otherwise Commonly Misinterpreted Neoplasm

Paola A. Escalante Abril · Miguel Fdo. Salazar · Nubia L. López García · Mónica N. Madrazo Moya ·
Yadir U. Zamora Guerra · Yadira Gandhi Mata Mendoza · Erick Gómez Apo · Laura G. Chávez Macías

Pathology Unit, Neuropathology Service, Mexico General Hospital, Mexico City, Mexico

To the Editor:

We found errors in our published article.

Escalante Abril PA, Salazar MF, López García NL, Madrazo Moya MN, Zamora Guerra YU, Mata Mendoza YG, Gómez Apo E, Chávez Macías LG. WHO grade IV gliofibroma: a grading label denoting malignancy for an otherwise commonly misinterpreted neoplasm. *J Pathol Transl Med* 2015; 49(4): 325-30. <http://dx.doi.org/10.4132/jptm.2015.05.20>.

Page 328, Table 1.

The phrases “Mortality rate (cases with available data) (5/8) = 62.5%” and “Overall mortality rate (cases with available data) (7/10) = 70.0%” of the Table 1 should read “Mortality rate (cases with available data) (3/8) = 37.5%” and “Overall mortality rate (cases with available data) (5/10) = 50.0%”, respectively.

Page 328, left column.

The sentence “However, when considering the lethality of the high-grade-only subset, this value increases to 70% or even 100% in cases with an accompanying glioblastoma component (Table 1).⁸⁻¹³” on page 328 should read “**However, when considering the lethality in the sole high-grade subset, this value increases up to roughly 40% or even 100% in those instances with an accompanying glioblastoma component (Table 1).**⁸⁻¹³”

Page 329, left column.

The sentence “As shown in our case and previously advised by other authors, gliofibroma prognosis is greatly influenced by the degree of anaplasia of the glial component” on page 329 should read “**As shown in our case and previously advised by some authors, gliofibroma prognosis is, indeed, influenced by the degree of anaplasia of the glial component.**”

We apologize for the inconvenience caused by these errors.